AFAPL-TR-77-2

INTEGRAL, LOW-COST, HIGH-TEMPERATURE TURBINE FEASIBILITY
DEMONSTRATOR (SMALL LAMINATED AXIAL TURBINE PROGRAM)

AIRESEARCH MANUFACTURING COMPANY OF ARIZONA
A DIVISION OF THE GARRETT CORPORATION
402 S. 36TH STREET, P.O. BOX 5217
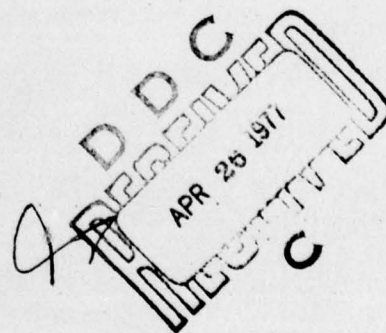PHOENIX, ARIZONA 85010

February 1977

TECHNICAL REPORT AFAPL-TR-77-2

Final Report for Period March 1974 to September 1976

Approved for public release; distribution unlimited

AIR FORCE AERO PROPULSION LABORATORY
AIR FORCE WRIGHT AERONAUTICAL LABORATORIES
AIR FORCE SYSTEMS COMMAND
WRIGHT-PATTERSON AIR FORCE BASE, OHIO 45433

NOTICE

NOTICE

When Government drawings, specifications, or other data are used for any purpose other than in connection with a definitely related Government procurement operation, the United States Government therby incurs no responsibility nor any obligation whatsoever; and the fact that the Government may have formulated, furnished, or in any way supplied the said drawings, specifications, or other data, is not to be regarded by implication or otherwise as in any manner licensing the holder or any other person or corporation, or conveying any rights or permission to manufacture, use, or sell any patented invention that may in any way be related thereto.
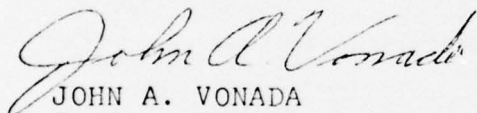
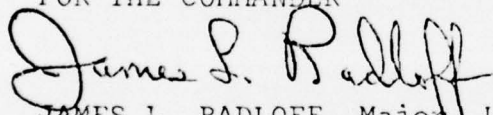This report has been reviewed by the Information Office, ASD/OIP, and is releasable to the National Technical Information Service (NTIS). At NTIS, it will be available to the general public, including foreign nations.

This technical report has been reviewed and is approved for publication.

JOHN A. VONADA
Project Engineer

FOR THE COMMANDER

JAMES L. RADLOFF, Major, USAF
Chief, Components Branch

REPORT DOCUMENTATION PAGE		READ INSTRUCTIONS BEFORE COMPLETING FORM
1. REPORT NUMBER AFAPL-TR-77-2	2. GOVT ACCESSION NO.	3. RECIPIENT'S CATALOG NUMBER
4. TITLE (and Subtitle) Integral, Low-Cost, High-Temperature Turbine Feasibility Demonstrator (Small Laminated Axial Turbine Program)		5. TYPE OF REPORT & PERIOD COVERED Final Report, Mar 74 - Sep 76,
		6. PERFORMING ORG. REPORT NUMBER 74-210841(29)
7. AUTHOR(s) D. G. Furst, R. W. Vershure, J. A. Pyne J. J. Clark		8. CONTRACT OR GRANT NUMBER(s) F33615-74-C-2034
9. PERFORMING ORGANIZATION NAME AND ADDRESS Garrett Corporation AiResearch Manufacturing Co. of Arizona Phoenix, Arizona 85034		10. PROGRAM ELEMENT, PROJECT, TASK AREA A WORK UNIT NUMBERS Project No. 3066
11. CONTROLLING OFFICE NAME AND ADDRESS Air Force Aero Propulsion Laboratory Air Force Systems Command Wright-Patterson AFB, Ohio 45433		12. REPORT DATE February 1977
		13. NUMBER OF PAGES 192
14. MONITORING AGENCY NAME & ADDRESS(if different from Controlling Office)		15. SECURITY CLASS. (of this report) Unclassified
		15a. DECLASSIFICATION/DOWNGRADING SCHEDULE

16. DISTRIBUTION STATEMENT (of this Report)

Approved for public release; distribution unlimited

17. DISTRIBUTION STATEMENT (of the abstract entered in Block 20, if different from Report)

18. SUPPLEMENTARY NOTES

19. KEY WORDS (Continue on reverse side if necessary and identify by block number)

Laminated
Axial Turbine
Turbofan Engine
Waspaloy

20. ABSTRACT (Continue on reverse side if necessary and identify by block number)

The Integral Low-Cost, High-Temperature Turbine Feasibility Demonstrator Program was conducted to establish the feasibility of constructing a small, integral, cooled turbine using photo-etched laminates bonded together to form a complete wheel. A turbine design was established utilizing a cooling scheme compatible with operation at 2600°F. Methods were established for making the laminate photoetch tooling with the use of ⟶ next page
(Contd)

DD FORM 1473 EDITION OF 1 NOV 65 IS OBSOLETE
1 JAN 73

cont

computer graphic design techniques. Photoetching and bonding parameters were optimized through the use of small bonded stacks. The photoetch and bonding methods were further optimized by bonding full-size wheel blanks, and the successful construction of a complete integral, cooled, laminated turbine. The wheel integrity was established by subjecting it to a 115-percent design speed spinpit test. It is recommended that this method of turbine construction be further developed because of the great potential for both cost-reduction and achieving high operating temperature capability through this approach.

PREFACE

THIS PAGE INTENTIONALLY LEFT BLANK

TABLE OF CONTENTS

v

TABLE OF CONTENTS (Contd)

LIST OF ILLUSTRATIONS

LIST OF ILLUSTRATIONS (Contd)

LIST OF ILLUSTRATIONS (Contd)

LIST OF ILLUSTRATIONS (Contd)

LIST OF ILLUSTRATIONS (Contd)

LIST OF ILLUSTRATIONS (Contd)

LIST OF ILLUSTRATIONS (Contd)

LIST OF TABLES

SECTION I
INTRODUCTION

This final report has been prepared by the AiResearch Manufacturing Company of Arizona, a Division of The Garrett Corporation, and submitted to the U.S. Air Force Systems Command, Aero Propulsion Laboratory. The report covers the Integral, Low-Cost, High-Temperature Turbine Feasibility Demonstrator Program (Small Laminated Axial Turbine Program), which was conducted under Air Force Aero Propulsion Laboratory Contract No. F33615-74-C-2034. This 31-month program was a manufacturing study and evaluation of an air-cooled laminated axial turbine rotor design. The program included design, fabrication, and cold spin-pit test of an air-cooled, laminated, (high-pressure) turbine wheel derived from the AiResearch Model TFE731-3 Engine.

The outstanding technical manufacturing problem that limits the achievement of high operating temperatures in small gas turbines has been the inability to provide internal passages for effective cooling of turbine components without an associated high cost of production. A manufacturing technique that can provide the required complex internal passages, and allow more effective cooling schemes for this class of turbine is the lamination concept. This concept permits utilization of combined impingement, convective, and film-cooling techniques in small turbines of either radial or axial configuration. The cooled laminated turbine is produced from numerous thin laminates that are bonded together. Complex internal cooling passages are formed from a combination of laminate configurations that are initially photo-etched from sheet material. When properly stacked and bonded, the resulting component is finish-machined to provide the desired aerodynamic and structural configuration. The concept is applicable to turbine stators, shrouds, and rotors (either axial or radial). Axial rotors can be produced with either integral or inserted blades.

An AiResearch-funded research and development program started in 1970 demonstrated the feasibility of the laminated turbine concept through the manufacture of a radial-flow turbine rotor from Waspaloy sheet material. A Waspaloy wheel of this configuration was successfully spin-tested at room temperature with speeds up to 70,200 rpm (1900 feet-per-second tip speed).

With the feasibility of the manufacturing concept having thus been established, the program requirement was for the further development of the photoetching process, bonding parameters and alloys, and finish-machining procedures leading to the production of an air-cooled laminated turbine rotor that would permit a subsequent high-temperature test evaluation.

Successful completion of the program could lead to lower engine costs per pound of output power due to lower component costs, increased operating temperature capability, reduced fuel consumption, and increased power density (and hence weight reductions) from gas turbine propulsion engines and auxiliary power systems. Preliminary cost analysis, based on a 7.5-inch diameter turbine wheel, indicated that a 2400°F integral, cooled, laminated turbine would have a 35-percent lower production cost than a conventional inserted-blade turbine wheel. A more recent cost comparison of the 11.13-inch diameter laminated, cooled, axial-flow turbine with the existing production TFE731-3 inserted-blade turbine wheel indicates a 50-percent cost savings in production for the integral laminated configuration.

This program included design and manufacturing studies. The design study considered possible axial wheel configurations, various cooling schemes, and design of manufacturing tooling and equipment. The manufacturing study included evaluation of processes for photo-etching Waspaloy laminates, bonding processes, bond alloys, and evaluation of small test stacks and one large stack (simulating the thermal mass and dimensions of a full-size wheel). The manufacturing study also included mechanical property testing of the test stacks, and definition of the final process and materials to be used. After the study phases were completed, one full-scale laminated axial turbine wheel was bonded. The wheel was completely machined, and an evaluation and test phase including cold spin-pit testing was performed for the purpose of establishing the integrity of the turbine wheel.

In March, 1974, AiResearch Manufacturing Company of Arizona
initiated a program for the United States Air Force Aero Propulsion Laboratory to prove the feasibility of manufacturing a
small, integral, cooled, axial turbine wheel using a laminated
construction concept. The cooled laminated turbine was produced
from numerous thin laminates that were bonded together. Complex
internal cooling passages were formed from a combination of
laminate configurations that are initially photoetched from
sheet material. Additional objectives of the program were to:

o   Utilize a complex cooling configuration design
    that will be compatible with operation up to
    2600°F.

o   Further develop the photoetching, bonding
    parameters, and finish machining procedures to
    permit manufacture of the laminated axial
    turbine wheel.

o   Design and fabricate a laminated turbine wheel
    using the established procedures.

o   Evaluate the wheel material properties and
    bond-joint characteristics.

o   Prove the wheel integrity utilizing overspeed
    test procedures.

Figure 1 is a flow chart of the Small Laminated Turbine
Program.

1.   DESIGN

The AiResearch Model TFE731-3 high-pressure turbine wheel
(see Figure 2) was selected as the baseline design to be
modified for the integral laminated wheel concept. The TFE731-3
turbine is a conventional cooled turbine utilizing a forged
disk and inserted cast cored blades. The design effort consisted
of the study, analysis, detail design, and tooling design of a
laminated, integral, cooled axial turbine. The most significant
activities were:

o   The study of three cooling concepts with the most
    complex design compatible with operation up to 2600°F
    being selected for detail design. The selected
    cooling concept, as seen in Figure 3, utilizes
    impingement cooling of the leading edge with film-
    discharge slots, convection cooling of a two-passage
    center section, and convection cooling with trailing-
    edge center discharge in the trailing-edge section.
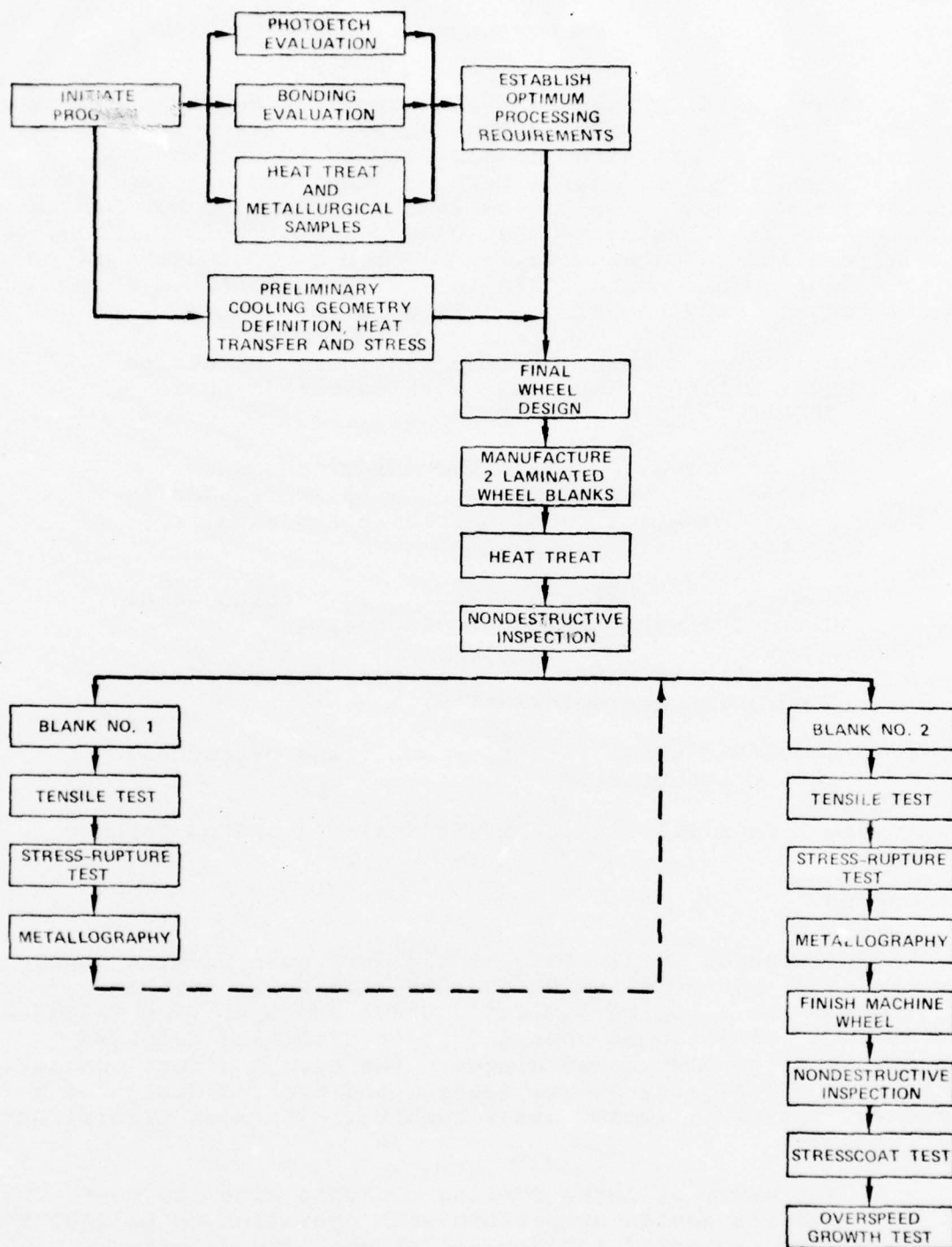
Figure 1. Flow Chart of the Small Laminated Turbine Wheel Program.

4
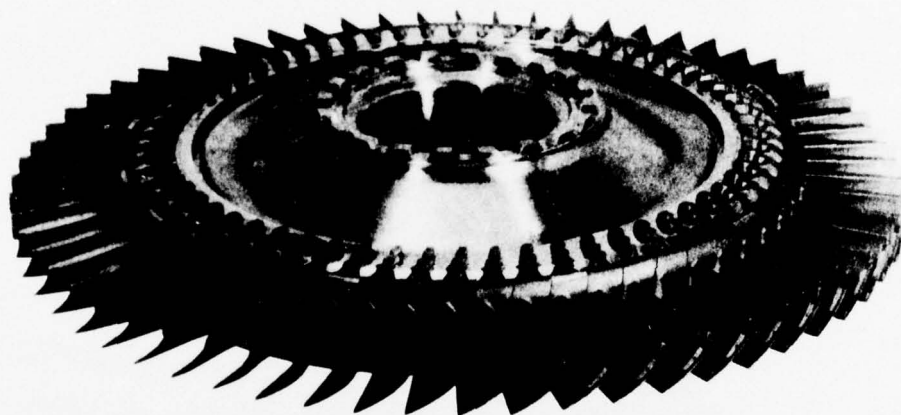
Figure 2. AiResearch Model TFE731-3 Cooled Turbine Wheel
with Inserted Blades.
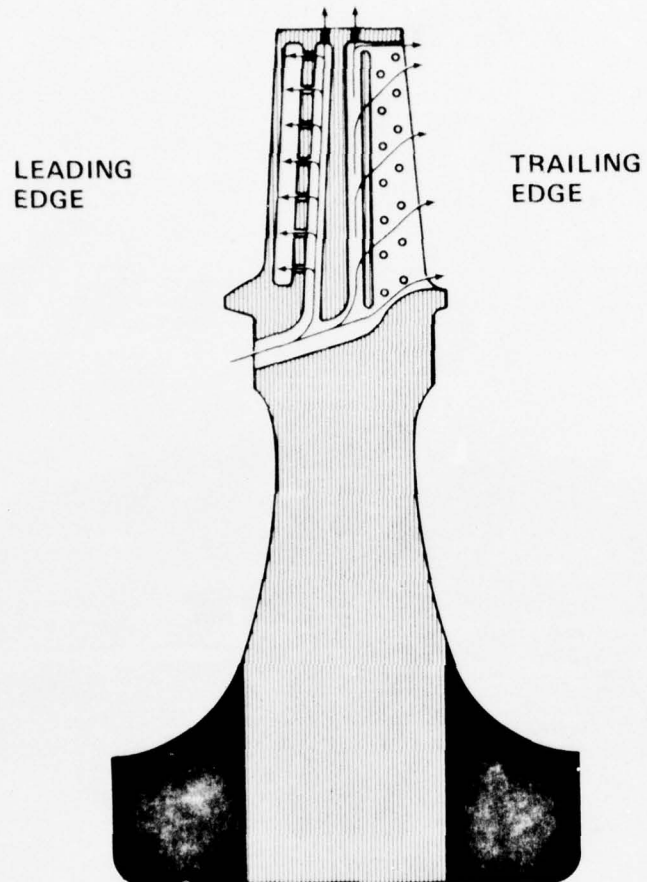
Figure 3. Cooling Concept Selected for Final Detail Design of the Laminated Axial Turbine Wheel.

o   The final design utilizing a total of sixty-two
    0.010- and 0.020-inch Waspaloy laminates, each
    with a different photoetched cooling passage.

o   The accomplishment of the thermal and stress analysis,
    and the successful attainment of the temperature and
    life goals as shown in Table 1.

o   The development of very accurate computer graphics
    design techniques to automatically make tooling
    plots for each of the laminate configurations.
    Photoetch tools were simply made from these master
    tooling plots by lithography techniques. In
    addition to improving the accuracy of the tooling
    and the resulting photoetched parts, the previously
    required tooling lead time was reduced by more
    than half.

o   The completion of estimates of the preliminary
    production costs,which indicated that the turbine
    could be fabricated for one-half that of the con-
    ventional inserted blade TFE731-3 turbine.

TABLE 1.   TEMPERATURE AND LIFE PREDICTIONS
           FOR THE LAMINATED TURBINE WHEEL.

Turbine Material	Temperature (°F)	Life at Temperature (Hours)
Waspaloy	2320	20
Astroloy	2530	20
AF2-1DA	2600	29

2.   MANUFACTURING METHODS

The manufacturing methods task consisted of optimizing the photoetching and bonding parameters to an extent that would permit fabrication of an integral-cooled laminated turbine wheel. The most notable contributions to the program realized during this task were:

o   The definition of the preferred activated-diffusion bonding (ADB) alloy composition.

o   The development of high-quality bonding tape permitting more uniform, yet cost effective, bond-alloy application.

o   The optimization of the bonding pressure, tempera-ture cycle, and load for small stacks.

o   The definition of the photoetch acid bath chemistry and life.

o   The optimization of the photoetch process procedure and the associated process quality control.

o   The establishment of a sheet stock cleaning proce-dure for Waspaloy that would allow high-quality photoetch parts to be produced (see Figures 4 and 5).

o   The development of a full-scale wheel bonding tool.

o   The development of a full-scale wheel bonding method.

o   The determination of the critical bonding transient thermal cycle requirements.

o   The development of an ultrasonic nondestructive testing method to verify the soundness of bonds in the turbine disk.

o   The successful bonding and machining of an integrally-cooled laminated turbine wheel as shown in Figure 6.

3.   EVALUATION AND TESTING

Evaluation and testing was conducted on the finish-machined integrally-cooled laminated turbine to verify its integrity. The tests consisted of:

o   Stress analysis using the latest design information in order to establish the predicted overspeed and
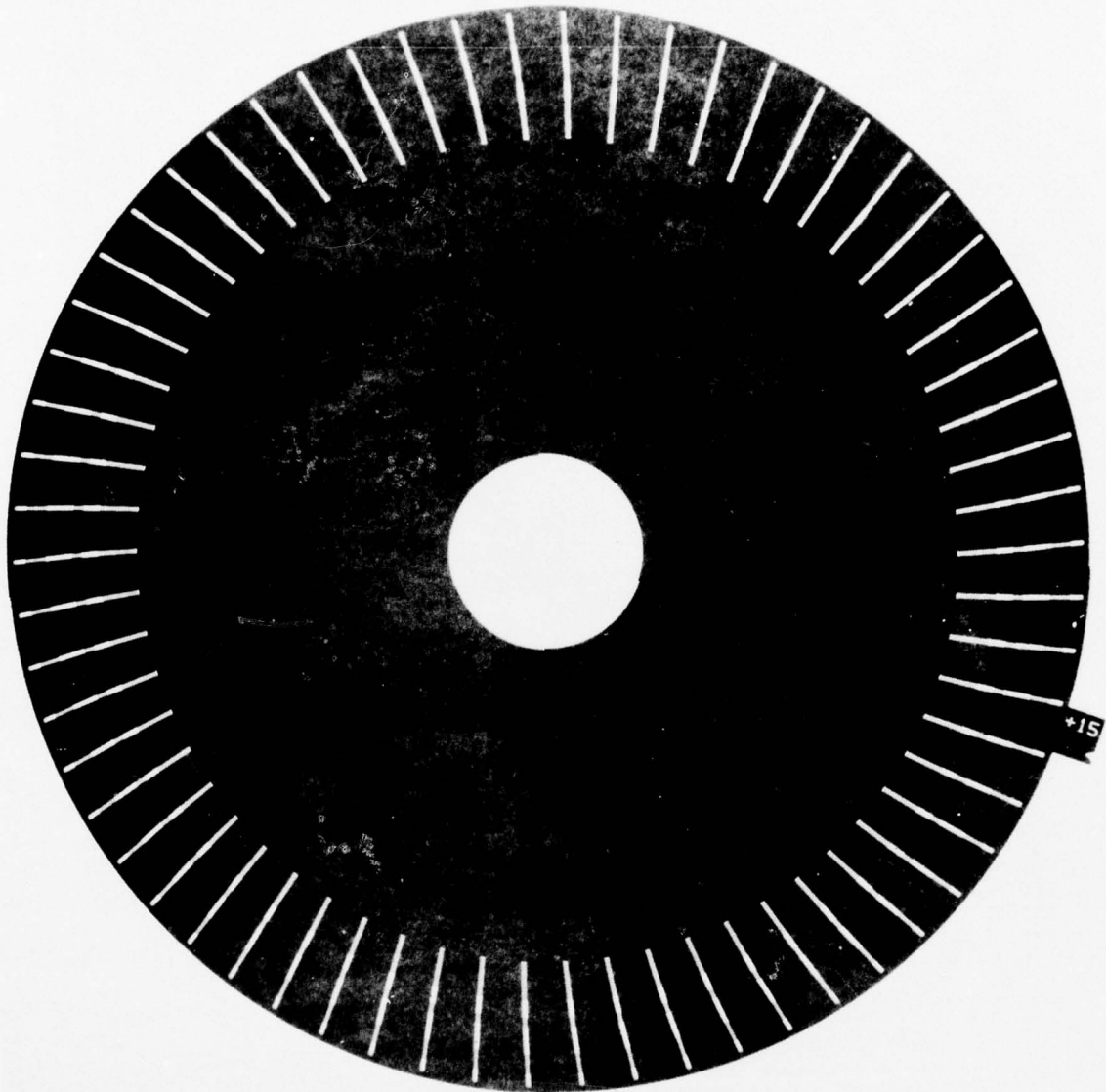
Figure 4.   Completed Final Wheel Blank Laminate
Showing Cooling Passages

9

Figure 5.   Completed Final Wheel Blank Laminate Showing
Center Section Convection Cooling Passages.
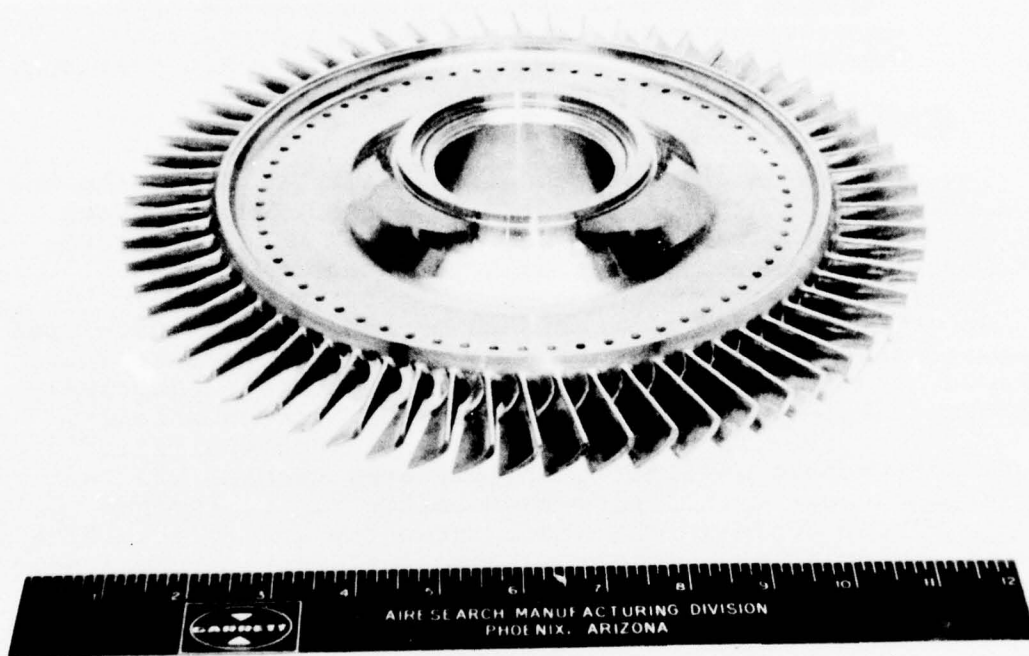
Figure 6. Fully-Machined Laminated Axial
Turbine Wheel.

burst margin of the wheel. The predicted burst
margin is 1.26.

o   Stresscoat testing to determine the relative
     stress levels in the disk and blades.

o   A series of overspeed and growth check tests
     up to 115-percent speed. No evidence was seen
     of any cracking in the bonded lamination joints.
     The maximum bore growth of 0.042 percent was
     somewhat less than that of another AiResearch
     uncooled integral turbine wheel in production
     for long life commercial and military applications.

4.   CONCLUSIONS

The program established the feasibility of designing and
manufacturing an integrally-cooled laminated turbine wheel
incorporating complex cooling passages. It was also proven
that the turbine wheel possessed good integrity.

It is recommended that this concept be further developed
incorporating more advanced bonding processes and materials
developed under United States Air Force Materials Laboratory
Contract F33615-75-C-5211. Heat-transfer testing should be
conducted in order to correlate predicted characteristics with
actual test results. Testing of laminated turbine wheels
should be conducted in a high-temperature rig to further
establish confidence in the wheel integrity, and to determine
life characteristics. This should be followed by redesign of
the turbine rotor, and testing in a gas generator or turbine
engine.

SECTION III
DESIGN

1. GENERAL APPROACH

The laminated approach is believed to provide the most cost-effective method for fabricating a cooled, axial-flow, integral turbine wheel when the cooling scheme effectiveness is comparable with that of a separately bladed disk. With this fabrication technique, photochemical machining (PCM), or photo-etching, is the most straightforward and cost-effective method of producing stress-free, intricately shaped laminations from the required high-strength superalloy sheet. Following PCM, an activated-diffusion-bonding (ADB) type of process is used to join the individual laminations to form the wheel shape, since only low-bond pressures are required for producing high-strength joints. Following wheel bonding, the process sequence is completed by post-bond diffusion, final heat treatments, wheel inspection, and machining. Figure 7 is a flow diagram of the design and manufacturing method used in fabricating a cooled axial turbine wheel of laminated and bonded construction.

2. BASELINE TURBINE

The baseline axial-flow turbine wheel design chosen for the AFAPL Low-Cost, High-Temperature Turbine Feasibility Demonstrator Program (Small Laminated Axial Turbine Program) was the AiResearch Model TFE731-3 Engine high-pressure turbine rotor. The TFE731-3 Engine requires an air-cooled configuration for the high-pressure turbine. The conventional design consists of 62 separately cast blades attached to a forged disk. The blades contain cooling passages, and the disk is externally cooled. This 11.13-inch diameter turbine has a design speed of 29,692 rpm.

The Model TFE731-3 Turbofan Engine (shown in Figure 8) is a 2.7-bypass-ratio, two-spool, geared-front-fan engine rated at 3700-pounds thrust at sea-level, standard-day takeoff conditions; and 817-pounds thrust at maximum cruise, 40,000-feet altitude, standard-day, 0.8 Mach number. Corresponding thrust-specific-fuel-consumption values of 0.506 and 0.818, respectively, reflect the excellent fuel economy of this engine.

The single-stage air-cooled high-pressure (HP) axial turbine of the Model TFE731-3 has a maximum operating inlet temperature of 1935°F (average). This is a modest operating condition for air-cooled turbines, since larger engines in commercial service operate to 2400°F. Also, as explained below, further conservatism exists because the TFE731-3 HP turbine was designed for temperatures well in excess of 1935°F in order to permit further engine growth without significant HP turbine redesign. Actual operating metal temperatures of the turbine parts, which is a

13
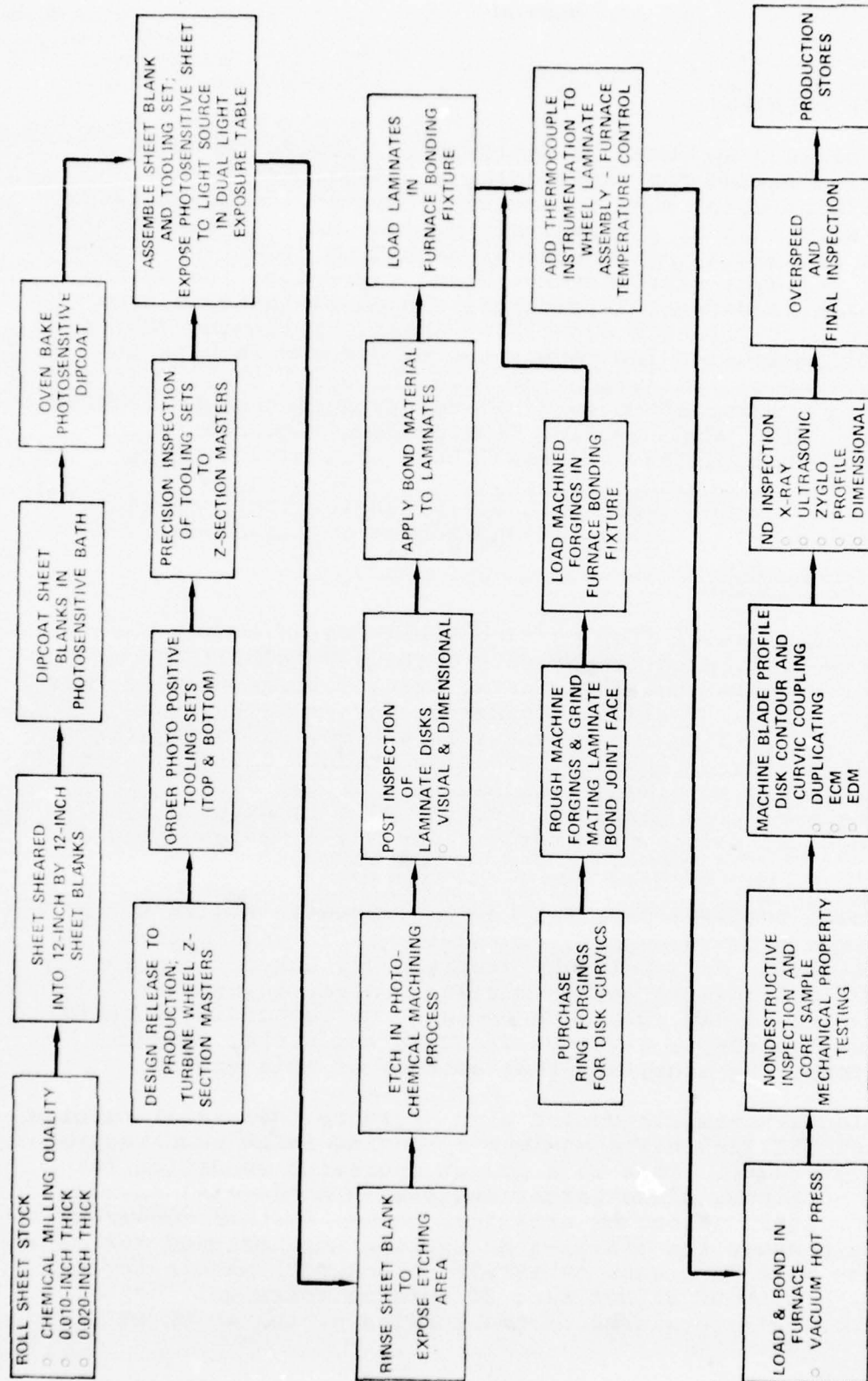
Figure 7. Flow Diagram of the Production Manufacturing Method for a Cooled Axial Turbine Wheel.

HIGH-PRESSURE TURBINE ROTOR
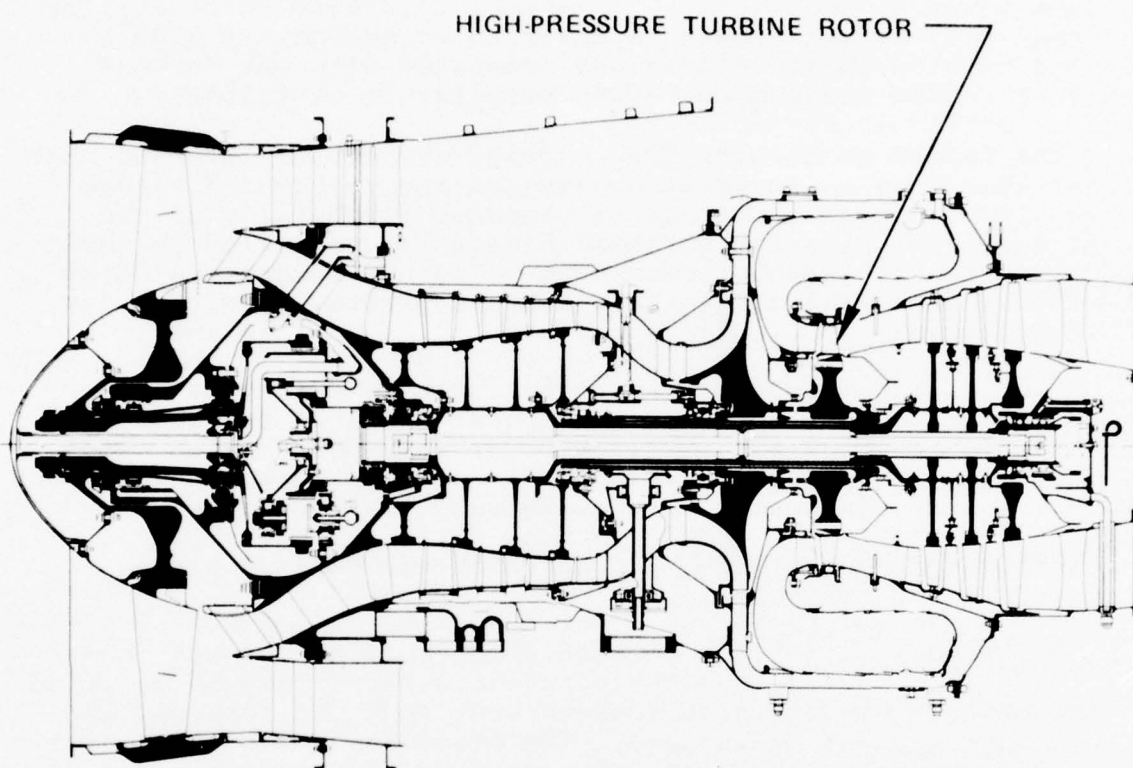
Figure 8. AiResearch Model TFE731-3 Turbofan Engine.

MP-56472

significant determinant of life, are less for the TFE731-3 than for the uncooled TFE731-2.

The design-life criteria for the TFE731-3 HP turbine included the assumptions of an average turbine inlet temperature (TIT) of 2000°F concurrent with a maximum stress environment and minimum material properties. A minimum 10,000-start capability was required, as was growth capacity to accommodate a 2100°F average turbine inlet temperature (compared with the current TFE731-3 Engine maximum operating temperature of 1935°F).

The forged HP turbine disk carries air-cooled inserted cast blades (Figure 9). Internal cooling of the unshrouded blades is provided through three radial passages discharging at the blade tip. Air-metering to these blades is controlled by individual orifices at each blade shank. The stationary casing at the tip is segmented to minimize thermal growth, providing for minimum running tip clearance and high turbine efficiency.

Cooling air from the HP turbine rotor is extracted from downstream of the HP compressor diffuser ahead of the deswirl vanes (refer to Figure 10). It then travels down the backside of the outer transition liner, and is taken on board the HP front seal plate through small orifices between the two labyrinth seals. The front seal plate provides for axial blade retention, and forms a pumping cavity through which the cooling air is directed to the blade shank.

Air enters each blade through a controlling forward shank orifice. This orifice and the tip configuration may be modified to accommodate higher inlet temperatures, but the internal configuration need not be changed. The blade is divided internally into three separate cavities. The forward cavity discharges at the tip on the suction side, with the other two cavities discharging to the pressure side of the blade, as shown in Figure 9. Pin-fins are used to improve heat-transfer characteristics in the trailing-edge cavity. The larger central cavity employs pin-fins to increase flow resistance, reducing the flow to this cavity, and encouraging flow in the leading and trailing edges.

3. PRELIMINARY DESIGN

a. Blade Preliminary Design

This program was a manufacturing study of an integral cooled, laminated, Waspaloy wheel. The cooling scheme was to be suitable for operation at turbine inlet temperatures up to 2600°F with compromises as required to favor the laminated process. Compromises that were investigated included cooling scheme simplicity with material changes to achieve 2600°F capability, modified blade chord, increased blade thickness, and reduced number of blades. An additional requirement during the preliminary design phase of the program was the consideration of two cooling schemes. All of these factors were considered

16

COOLING AIR DISCHARGE

CENTER CAVITY

TRAILING-EDGE CAVITY

LEADING-EDGE CAVITY

BLADE MATERIAL IN-100

COOLING AIR INLET
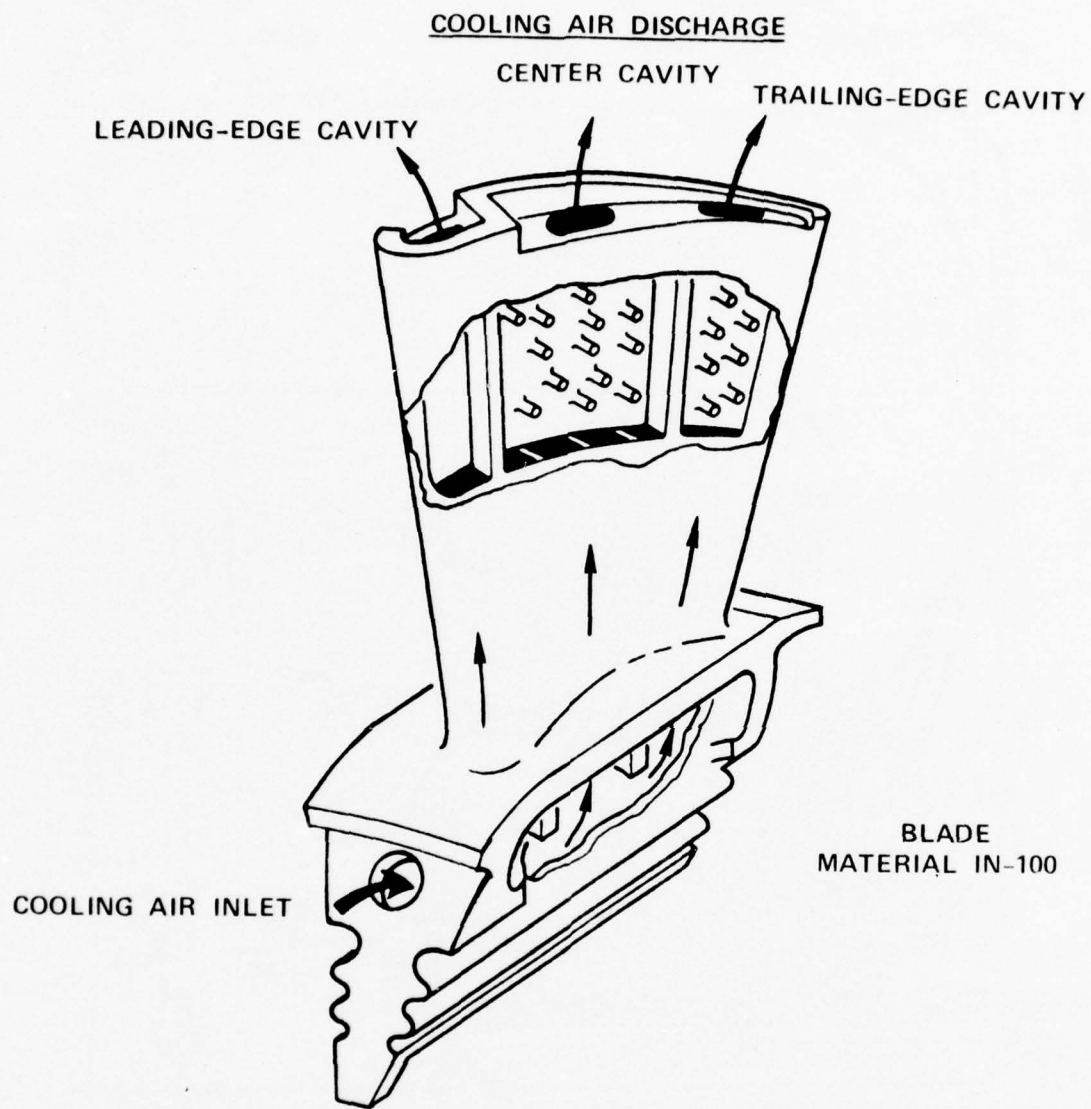
Figure 9.   Air-Cooled TFE731-3 High-Pressure Turbine Blade.

17
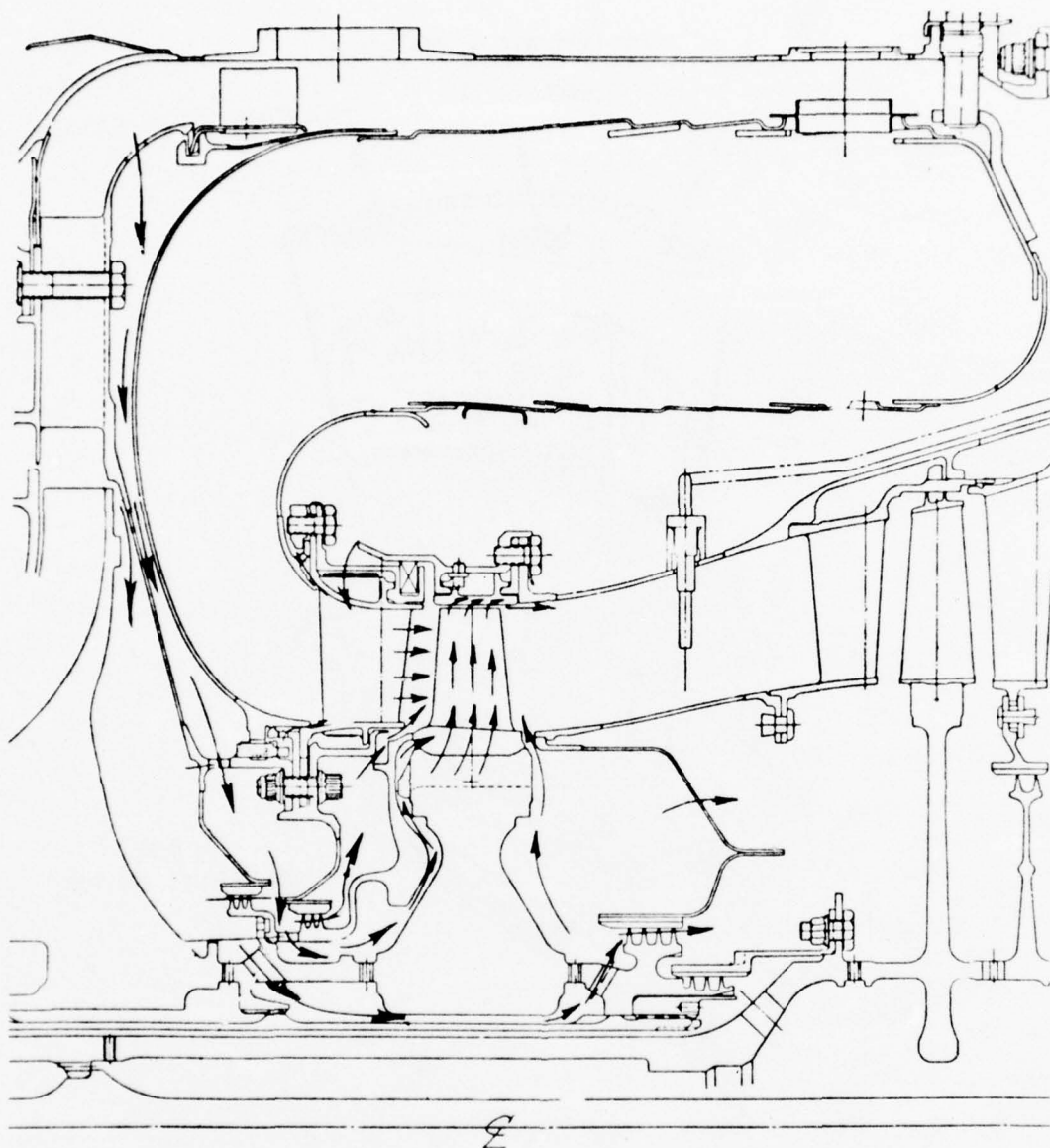
Figure 10.   TFE731-3 Secondary Cooling Airflow System

18

in varying degrees during the preliminary design phase of the program.

The first cooling scheme considered was a three-passage, single-pass, radial-outflow configuration. That scheme was selected on the basis of simplicity. Analyses indicated an upper turbine inlet temperature limit of approximately 2200°F with relatively short life. Although the inlet temperature limit and/or the life could be increased by switching to a better material, this design was judged to be marginal, and a higher capability cooling scheme was a preferable approach to satisfy the 2600°F representative cooling scheme requirements of the program.

A single-passage, three-pass scheme was investigated and had somewhat lower operating temperature limits than the three-passage, single-pass scheme; however, in the region where both schemes are satisfactory, the three-pass scheme has somewhat lower coolant flow requirements. A three-pass, two-passage, tip and trailing-edge discharge scheme is shown schematically in Figure 11.

This scheme has high-cooling capability and is typical of one of AiResearch's cooled-blade configurations; however, it can be cast. It was judged more advantageous to consider a cooling scheme with an even higher cooling capability, and that did not need to be cast. This approach would permit attainment of the 2600°F objective, and would demonstrate the unique capability of the laminated fabrication process to provide complex cooling schemes.

A number of variations were considered with these objectives in mind. The leading edge should be impingement cooled, and the trailing edge should be cooled with internal passages that discharge through the trailing edge. The trailing edge could also be film cooled, but some loss of coolant flow control, and a compensatory higher coolant flow rate, was anticipated with trailing-edge film-cooling protection. The center-body region of the blade would be cooled with the leading- and trailing-edge coolant, except near the blade tip where some center-body flow would be required. The resulting cooling scheme is shown schematically in Figure 12, and the overall wheel design approach is shown in Figure 3. As illustrated, the photoetched laminate process allows the incorporation of a sophisticated high-effectiveness cooling scheme, even in a small turbine (11.13-inches in diameter). The high-effectiveness cooling scheme incorporates impingement and film cooling in the leading edge, convection cooling in the center section, and convective-cooling trailing-edge discharge.

19
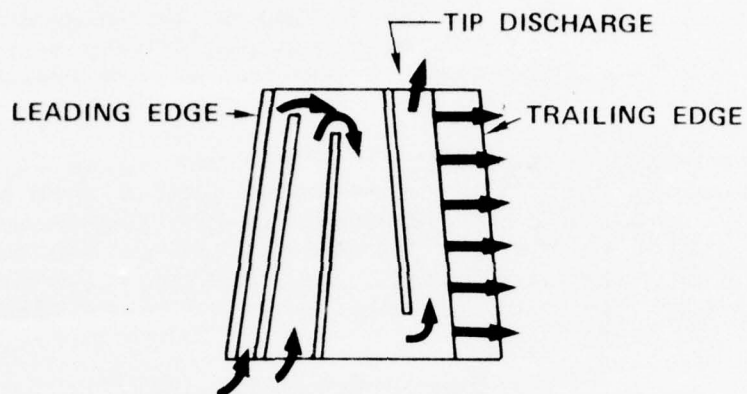
Figure 11. Three-Pass, Two-Passage, Tip and Trailing-Edge
Discharge Cooling Scheme for the TFE731-3
Laminated Turbine Wheel.
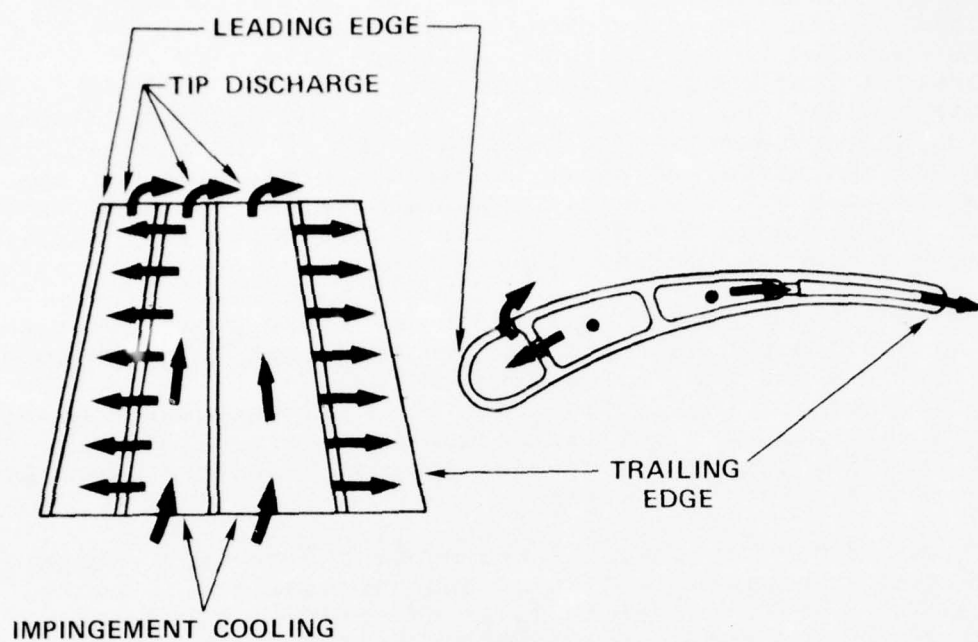
Figure 12. Impingement-Cooled Leading-Edge, Tip, and
            Trailing-Edge Discharge Cooling Scheme for
            the TFE731-3 Laminated Turbine Wheel.

The center body region would have internal fins, probably of the pin-fin variety. Coolant air flows radially outward in the center-body region, which also serves as a manifold for both the leading and trailing edges. Some of the coolant discharges at the blade tip in the center-body region to both cool this region, and also to provide dust holes to eliminate any dirt in the passages that could cause blockage problems. Coolant impinges against the leading edge, turns, and flows to discharge slots on the pressure and/or suction sides of the blade. Near the tip of the blade, there may be insufficient room for the coolant to turn and discharge on the sidewalls. In this region of the leading edge, the coolant will flow radially outward, and discharge at the tip of the leading edge.

The only compromise required on the blade profile was the trailing-edge thickness. The trailing edge was cut back to a thickness of 0.060 inch to permit all passages to be made by the laminated process, thus eliminating any coolant passage machining. To maintain the same mainstream flow-rate throat area and vector diagram, the blade row was closed 1.5 degrees from the current TFE731-3 configuration.

A preliminary estimate of the coolant flow requirements for 2600°F operation was 5 percent of the throughflow. Detailed calculations were required to solve the heat-transfer, flow-distribution, and stress problems for this design. The features of this design included all of the requirements for high-cooling capability, and it was on that basis that the concept was selected for detailed design.

b.   Disk Preliminary Design

The preliminary design of the cooled, laminated, axial turbine disk (for the AiResearch Model TFE731-3 Engine) was conducted, and since the basic laminated Waspaloy mechanical properties were not available, the turbine disk was designed as if the material were isotropic and homogeneous (Waspaloy, Condition A).

The turbine disk was analyzed under three loading conditions:

(1)   Centrifugal loading at 29,692 rpm

(2)   Thermal gradient in the radial direction

(3)   Thermal gradient in the axial direction

Figure 13 shows the preliminary disk configuration. Figures 14, 15, and 16 illustrate the displacement and stress distributions at 29,692 rpm. It should be noted that the radial and tangential stress distributions across the disk web are quite uniform. It indicates that the blade loads are dispersed into the disk directly by means of radial and tangential stresses so that the shearing stress is minimized, and not a significant factor.

Thermal stresses were studied with arbitrary thermal gradients. The results indicate that every 100°F of temperature difference between bore and rim will add approximately 10,000-psi tensile stress to the bore. However, 100°F of axial temperature difference across the disk does not add any significant thermal stress to the disk.

Table 2 summarizes the maximum stresses of the disk at 29,692 rpm, and the burst margin at room-temperature conditions.

TABLE 2.   DISK STRESS RESULTS.

Average Tangential Stress	–	60.9 ksi
Maximum Tangential Bore Stress	–	94.0 ksi
Maximum Radial Stress at Web	45.3 ksi	
Maximum Shear Stress	–	23.5 ksi
Burst Margin (Cold)*	–	1.35

*Burst Margin $= \sqrt{\left(\dfrac{0.84 \times \text{ultimate strength}}{\text{Average Tangential Stress}}\right)}$; where

ultimate strength at 29,692 rpm = 140 ksi; and
the estimated minimum bond shear strength = 40 ksi.

4.   DETAIL DESIGN

a.   Blade Detail Design

The design objectives for the high-temperature laminated blade had to satisfy specific requirements. These included engine operating conditions, either hypothetical, or taken from data gathered on an existing engine with growth potential suitable for higher turbine temperatures. The blade life and the type of service conditions used to calculate life are a prime requirement. In this regard, the blade profile, aerodynamic design, turbine inlet temperature profile, wheel design speed, and fluid pressure levels were taken from the TFE731-3 design for the laminated axial turbine rotor design. Major departures in similarity with the TFE731-3 were the average turbine inlet temperature level (targeted for 2600°F), integral blade and disk instead of firtree attachment, increased complexity in the blade internal passages, and an increase in cooling flow to sustain the higher-temperature level. The blade life requirement was targeted for 20 hours with two-percent creep life at steady-state maximum turbine inlet temperature conditions.

COOLING
AIR PASSAGE
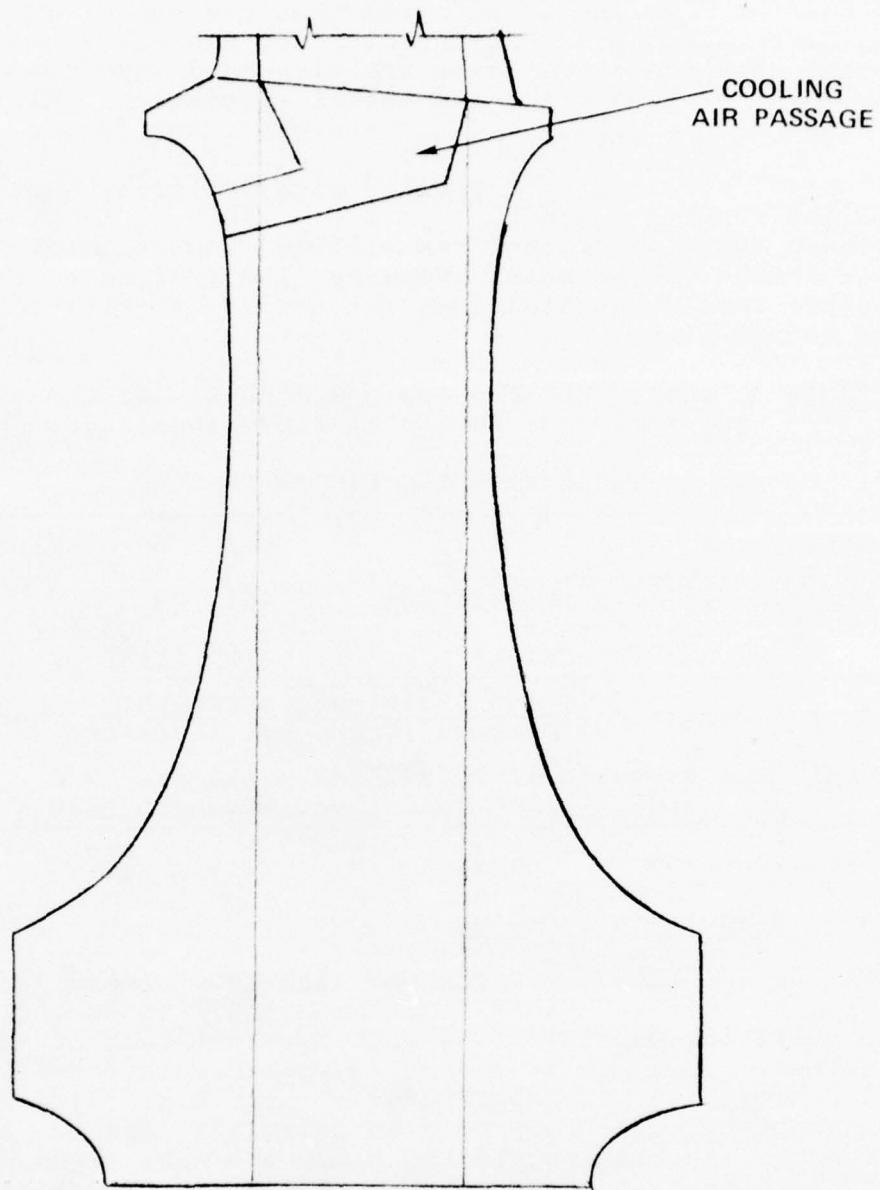
Figure 13. Preliminary Laminated Turbine Disk Geometry.

24
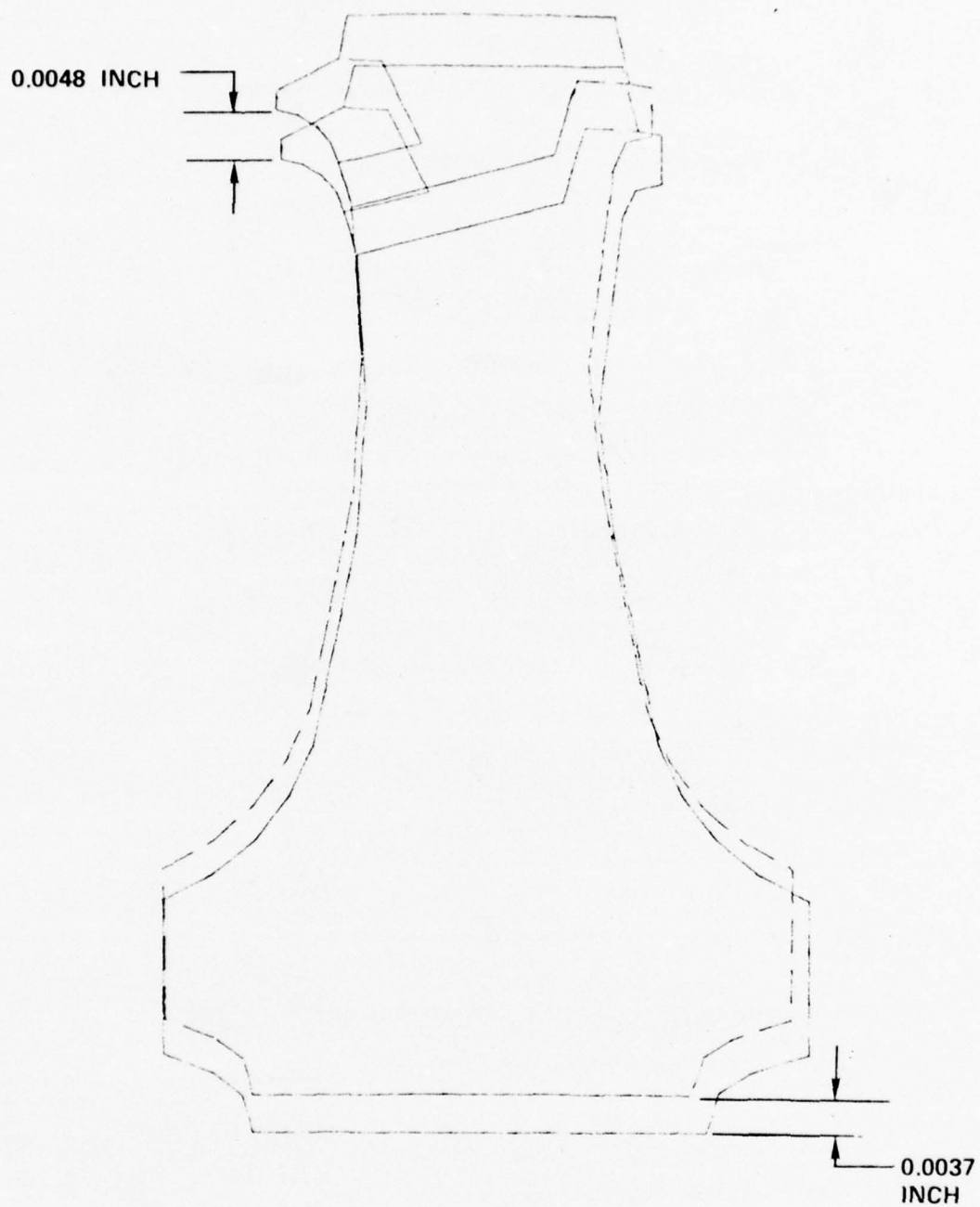
Figure 14.   Laminated Turbine Disk Magnified Displacement Due to Centrifugal Loading Only (29,692 RPM).
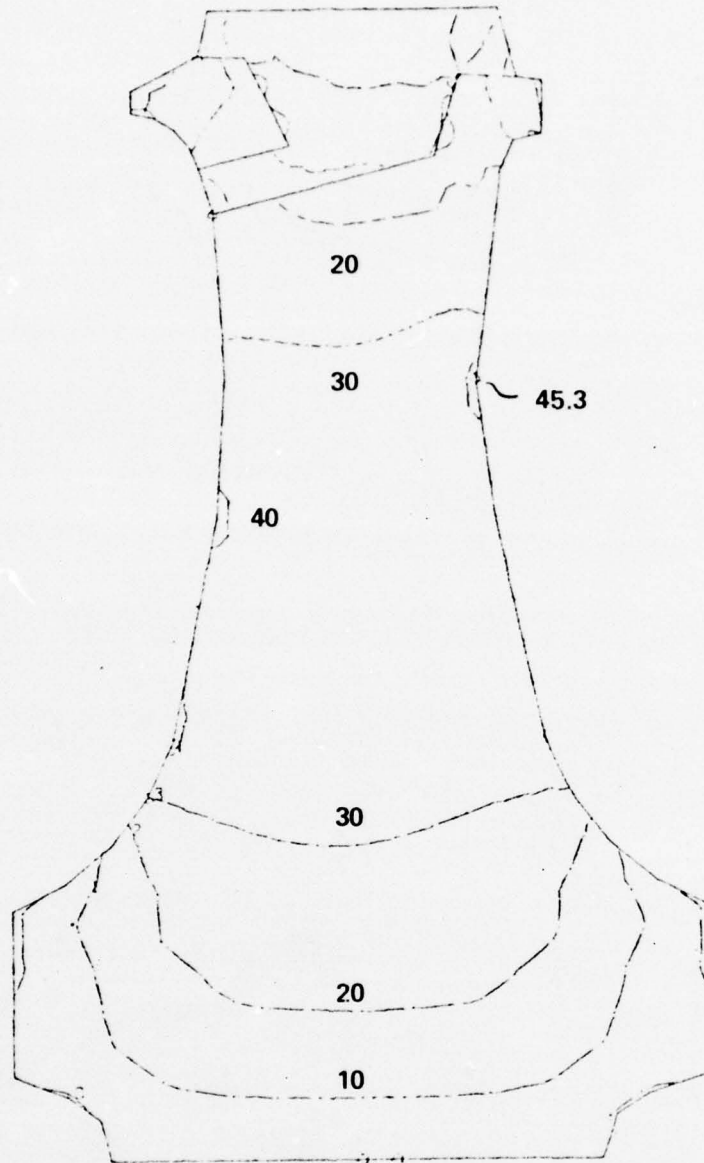
Figure 15.   Laminated Turbine Disk Radial Stress
             Distribution (KSI) Due to Centrifugal
             Loading Only (29,692 RPM).
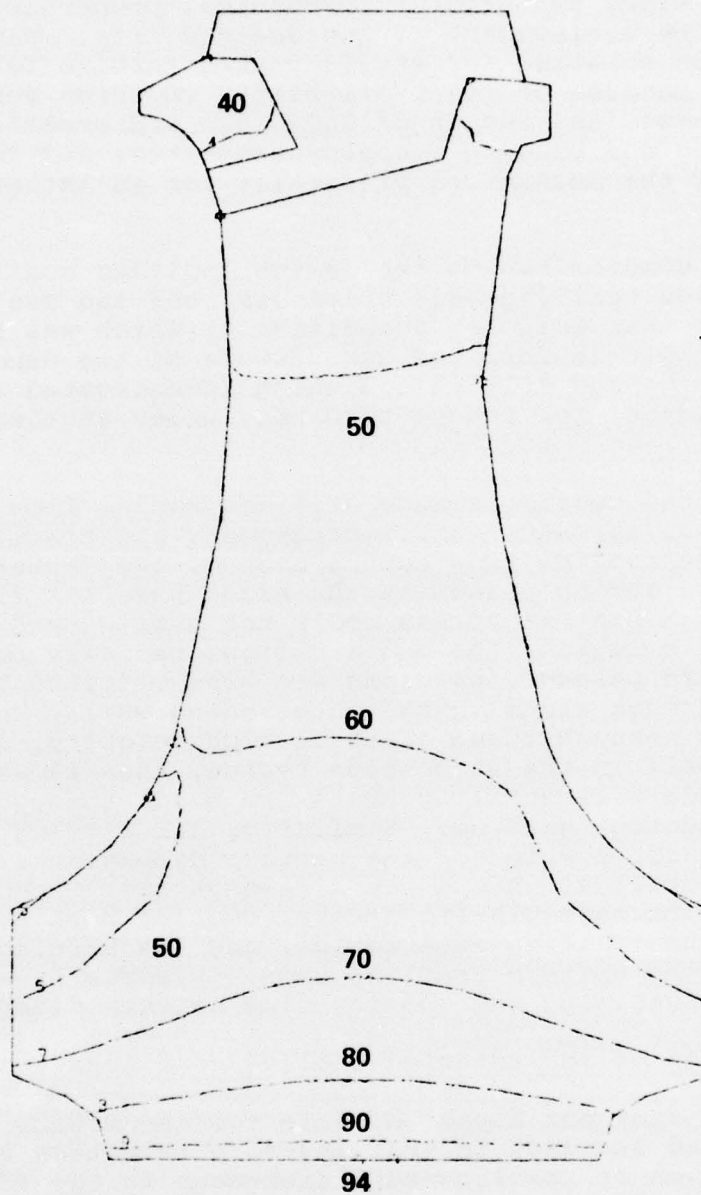
Figure 16. Laminated Turbine Disk Tangential Stress
Distribution (KSI) Due to Centrifugal Loading
Only (29,692 RPM).

The selection of a blade material was an important design consideration since satisfactory mechanical properties are critical for the achievement of the desired life. Waspaloy Condition A was selected for the laminated turbine feasibility demonstration because of its availability in sheet form of the desired thickness, the amount of knowledge and experience concerning etching and bonding Waspaloy laminates, and the general suitability of the mechanical properties for an integral disk and blade design.

Possible compromises to the design included modified blade chord, increased trailing-edge thickness, and the use of a material other than Waspaloy (Condition A) which was readily available in laminate form for manufacture of the demonstrator wheels. Astroloy and AF2-1DA are being investigated as possible material candidates for future turbines, under another Air Force contract.

The selected cooling scheme utilizes radial flow with heat-transfer surface augmentation, impingement, and trailing-edge discharge. The cooling flow enters each of two centerbody passages from a common plenum at the blade base, and flowing radially through pin-fin arrays, cools the suction and pressure surfaces in this region. As the air flows radially outward in the more forward passage, portions are bled off into a leading-edge cavity through slots in the intervening wall. The cooling air discharges through these slots at high velocity, and impinges on the blade wall in the stagnation region, then flows aft on the suction side wall until it exits the blade through film slots in the suction surface. Similarly, air flowing radially outward in the aft portion of the centerbody passages is distributed through orifices into a trailing-edge slot through which it travels aft through pin-fin arrays, cooling both surfaces of the blade in the trailing-edge region, and discharging into the mainstream at the extreme trailing edge. Figures 17 and 18 will aid in visualizing the cooling flow pattern described.

(1)   Impact of the selected cooling configuration

The most prominent impact of this cooling scheme selection was the required increase in trailing-edge thickness to permit the incorporation of trailing-edge discharge in the TFE731-3 HP turbine blade profile. The laminate thickness and orientation required the use of a 0.060-inch minimum trailing-edge thickness to maintain adequate slot area. It was necessary to utilize 0.010-inch thick laminates over the entire trailing-edge region to ensure adequate slot area instead of the 0.020-inch thick stock used in the center section of the blade. The 0.060-inch minimum thickness was achieved by cutting back on the blade chord length, but this, in turn, necessitated rotating the blade row closed 1.5 degrees from the latest TFE731-3 design in order to maintain the desired throat area and turbine vector diagrams. The aerodynamic effects of rotating and shortening the blade were

28

RADIUS = 4.0035
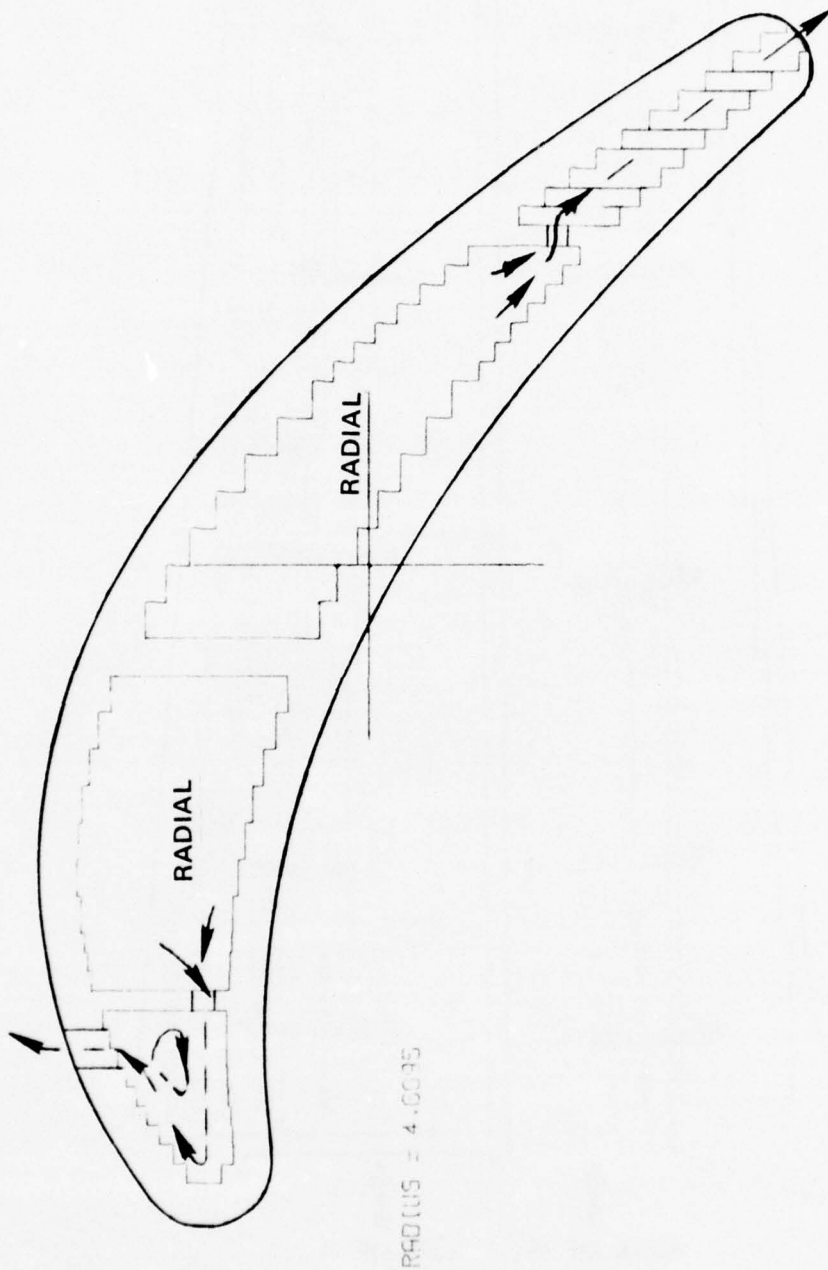
Figure 17. Laminated Blade Chordwise Flow Patterns.

NOTE:

0.XXX - FRACTIONS
OF TOTAL PASSAGE
INLET FLOW
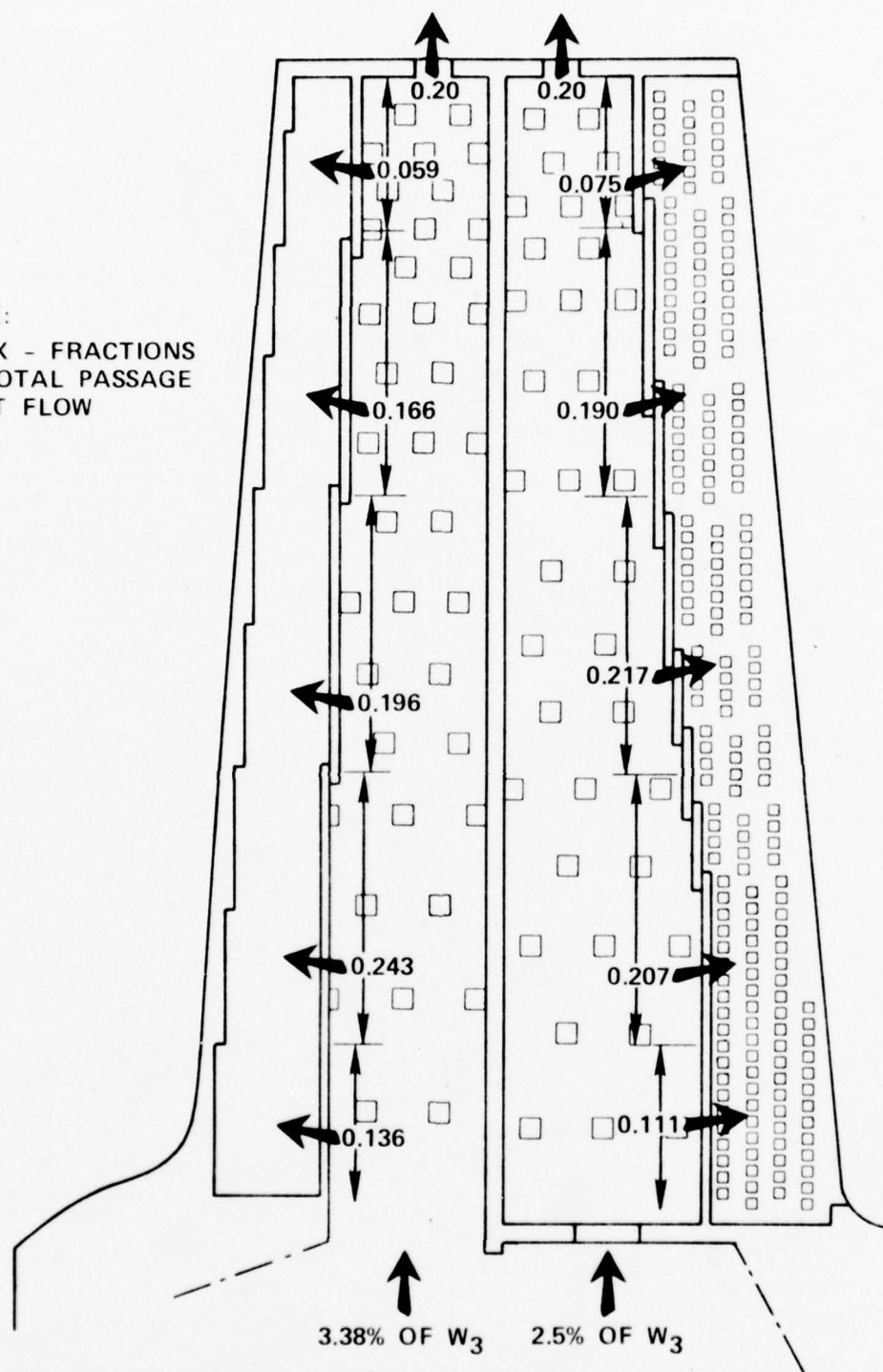
TOTAL COOLANT FLOW = 5.88 PERCENT OF COMPRESSOR FLOW (W_3)

Figure 18. Laminated Blade Cooling-Flow Split and
Radial Distribution.

30

examined to predict variations in the surface velocity diagrams for the new configuration versus the TFE731-3 design. Alterations of the loading diagrams at all radial stations were significant for the laminated blade. Qualitatively, the greatest change was an increase in suction- and pressure-side velocities over the aft-half of the blade chord.

A secondary impact of this cooling scheme selection was the necessity for placement of three radially continuous walls spanning the blade cross section from suction to pressure surfaces. The location of these walls would simultaneously determine flow areas, and influence the stress distribution in the blade. These walls would also be subject to thermal gradients and stresses due to thickness, location, and thermal boundary conditions.

The factors that were initially considered in determining the cross-section geometry for the given aerodynamic profile were the cooling-passage areas and the blade-metal areas at various radial stations. In the high-temperature laminated blade, the location of these divider walls determines the flow area split between the two centerbody radial passages, and the leading- and trailing-edge cavities. The metal area at any radius, or taper ratio, determines the total-flow area for all cavities at that radius. The most forward divider wall, or impingement plate, was located from considerations of impingement heat-transfer performance as determined by probable slot height and distance to the leading-edge stagnation region. The other divider walls were located to yield smoothly converging flow areas, when viewed from the base to the tip of the blade. The intent was to keep coolant velocity in the center passages up as the flow decreases from distributed bleed.

The blade-wall taper ratio was determined by considering the stresses generated due to radial centrifugal loading only. It was determined that an area 1.33 times the 1/4-section area was required at the base section (radius = 4.295). The selection of blade-wall thicknesses at stations outboard of the 1/4 section was based upon manufacturing tolerance considerations and blade design experience.

The turbine inlet temperature profile selected was determined from TFE731-2 engine testing. This profile has a peak local temperature that is 125°F above the radially integrated average, and it occurs at the 1/4 section of the blade. Figure 19 illustrates this profile. To simplify analysis of the design, the 1/4 section was taken as the critical section for purposes of detailed thermal, stress, and creep-life calculations. High metal temperatures and loads on this section will make it life limiting for the blade.

31
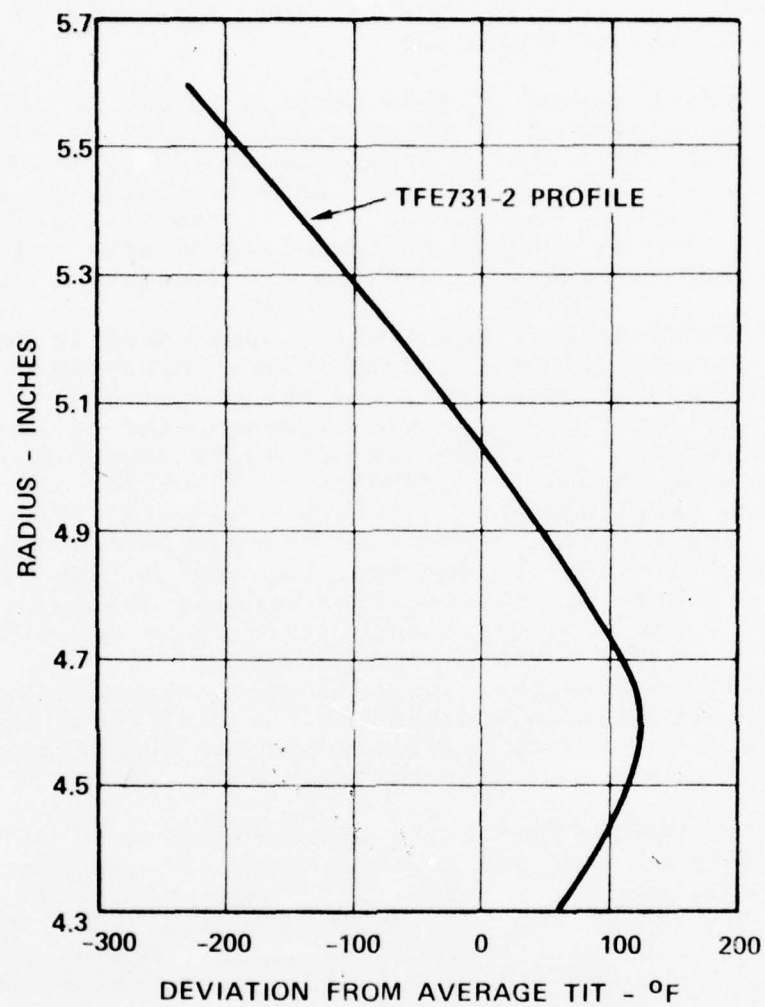
Figure 19.   High-Temperature Laminated Turbine Blade
            Inlet Temperature Profile.

(2) Cooling system design

        The external heat-transfer boundary conditions (the
blade external adiabatic wall temperatures, turbulent and laminar
heat-transfer coefficients, and surface static-pressure dis-
tributions) were computed at the design target level of a 2600°F
average turbine inlet temperature ($T_{4_{AVG}}$). The blade relative
total pressure, as well as all other pressure levels in this
design, were compatible with TFE731-3 cycle design point values.
The surface velocity ratios used in these calculations included
the effects of rotating the blade and cutting back the trailing
edge as previously discussed. The tangential and axial gas
loading on a blade section were also computed for later use in
the stress analysis. Figures 20[(a) through (e)] and 21[(a)
through (e)] show the results of these calculations at various
sections of the blade.

        The stagnation region of this blade has typically high
external heat-transfer coefficients in combination with unusually
high adiabatic wall temperatures for small engine turbine blades
with relatively sharp leading-edge radii. The leading edge
can only be cooled by the generation of equally high convective
heat-transfer rates on the wall inner surface. The best method
for achieving these high cooling rates, in a fashion that makes
them proportional to the local external heat-transfer coeffi-
cients, was by impingement. Items critical to successful
impingement design are the cooling-jet stagnation location on
the wall inner surface, and geometric factors such as impingement
slot height, gap distance from slot to wall, and leading-edge
inner radius.

        Blade curvature and the laminate design restriction (slots
may only be normal to the surface of a laminate) force the place-
ment of the impingement slot to be close to the pressure wall in
order to impinge directly on the leading-edge stagnation point.
A high-velocity jet flowing near the pressure-side wall prevents
any possibilities of partial or complete film discharge onto the
pressure surface. Suction-side gill-position discharge was the
logical choice, and was desirable for two reasons. First, the
flow of cooling air aft along the rough suction wall after
impingement is desirable for heat-transfer performance. The
second was the consideration of mainstream static pressure at
the film discharge locations for pressure- or suction-side
slots. An isobaric plot for the suction surface revealed that
the maximum radial static-pressure variation was approximately 7
psi; whereas, the pressure-surface static-pressure variation was
on the order of 15 psi. Minimizing the film-slot discharge pres-
sure variation was beneficial to achieving the proper radial
distribution of cooling flow within the leading-edge cavity.
From this standpoint, suction-surface discharge was much
preferred. In regards to the selection of single-side film
discharge, it should also be pointed out that the magnitude of
surface static pressure differs substantially from suction side

33
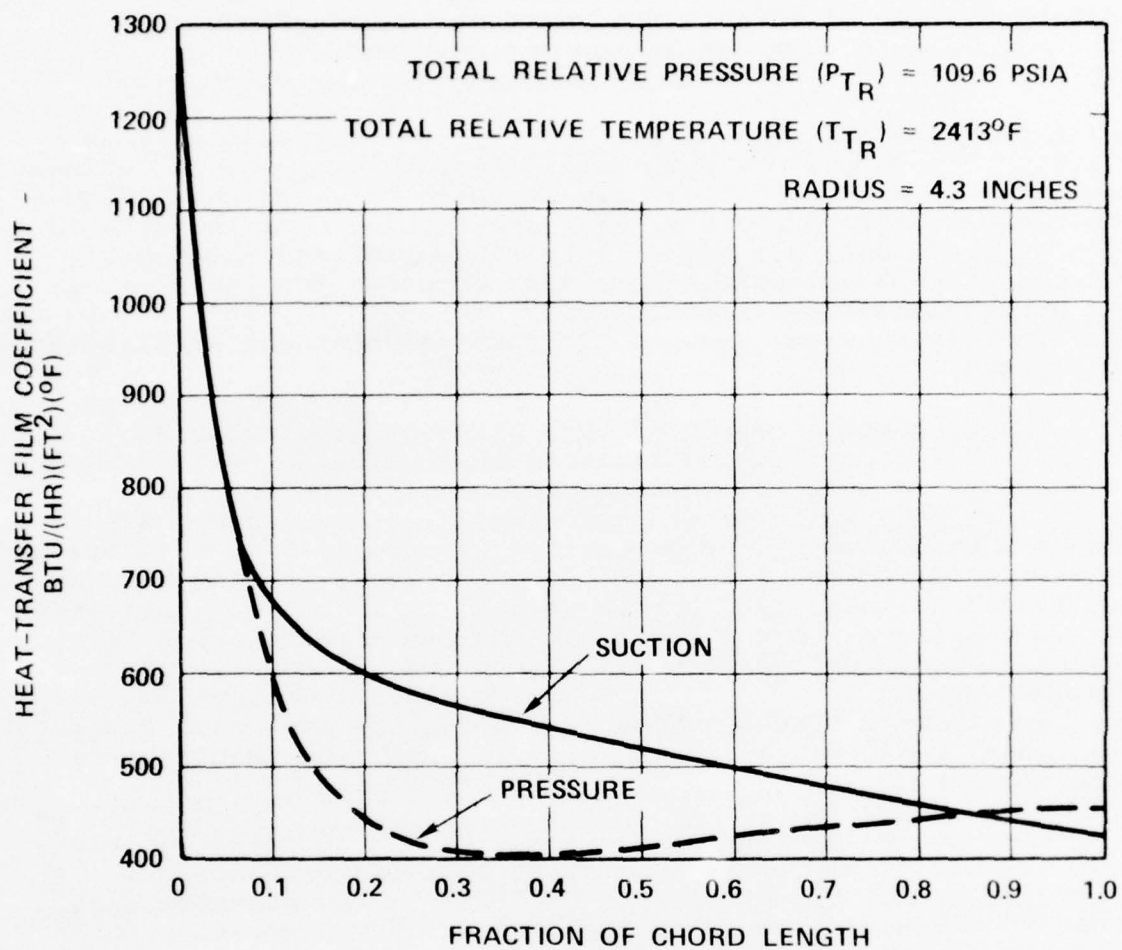
Figure 20. (a) High-Temperature Laminated Blade
Turbulent Heat-Transfer Coefficients
for Five Sections. (TIT Average
= 2600°F, and $P_{T_{IN}}$ = 152.5 PSIA).
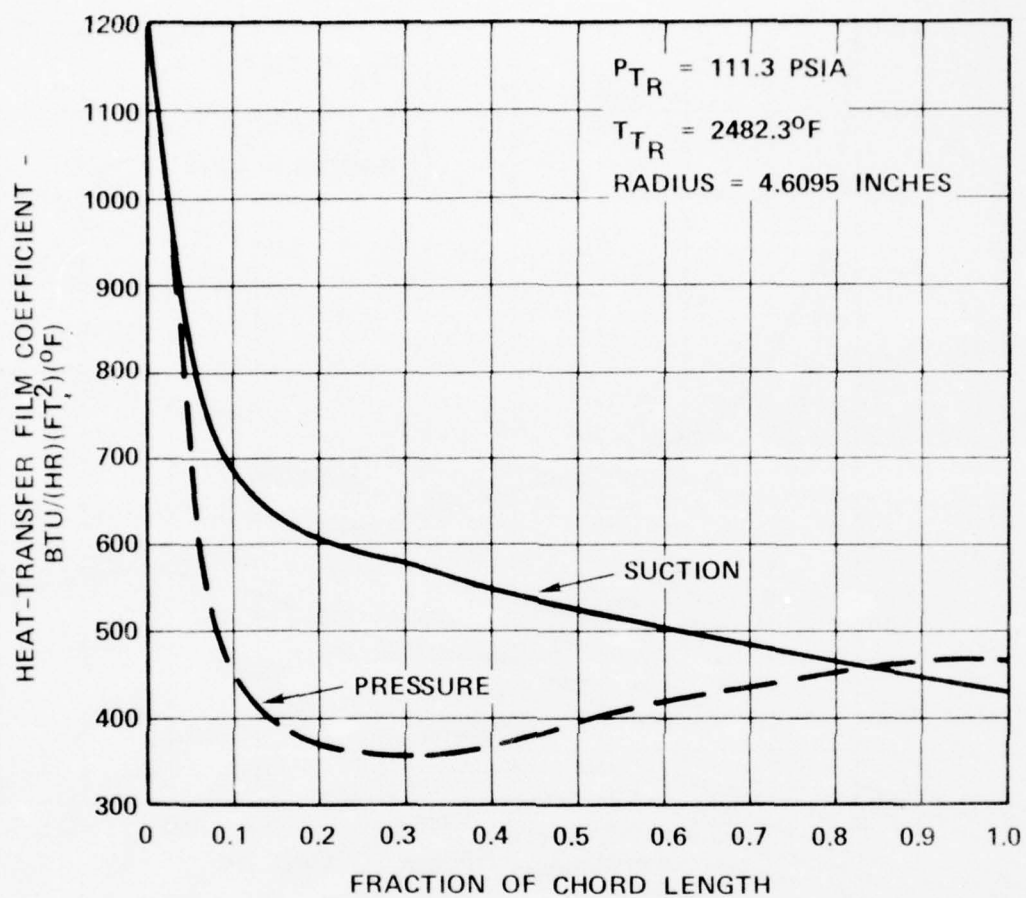
Figure 20.   Continued (b)
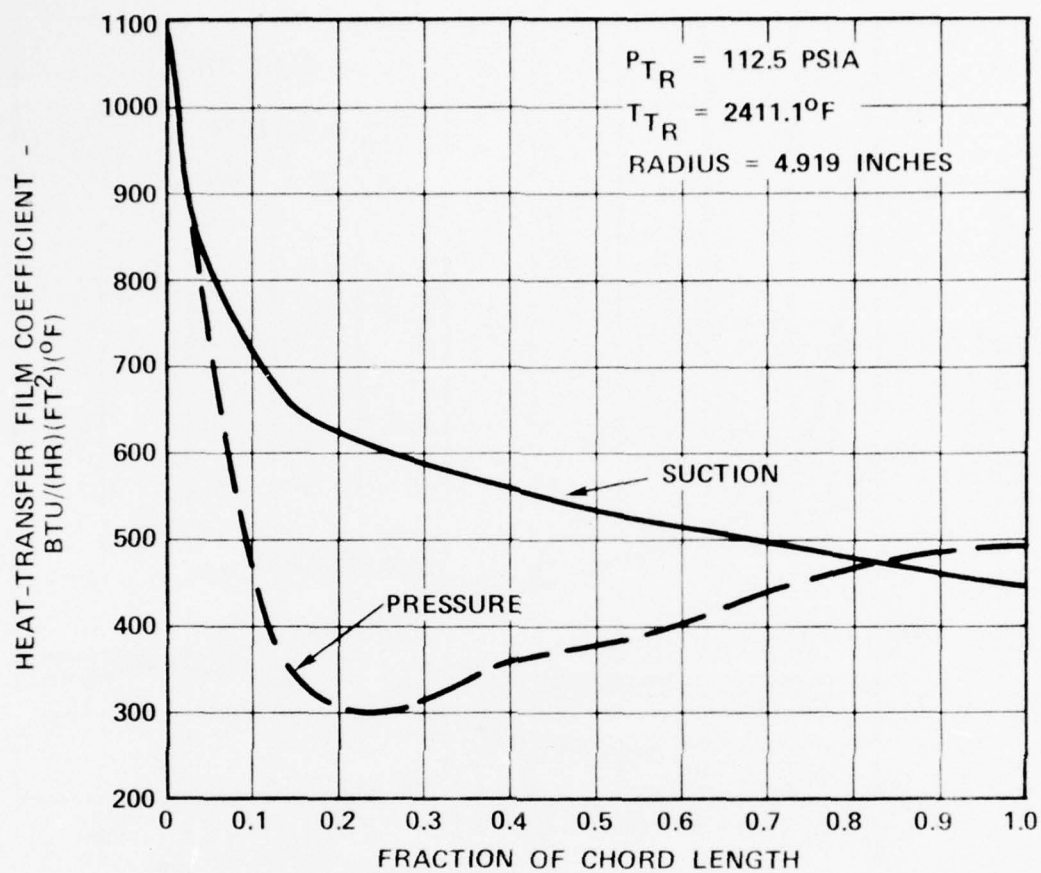
Figure 20.   Continued (c)
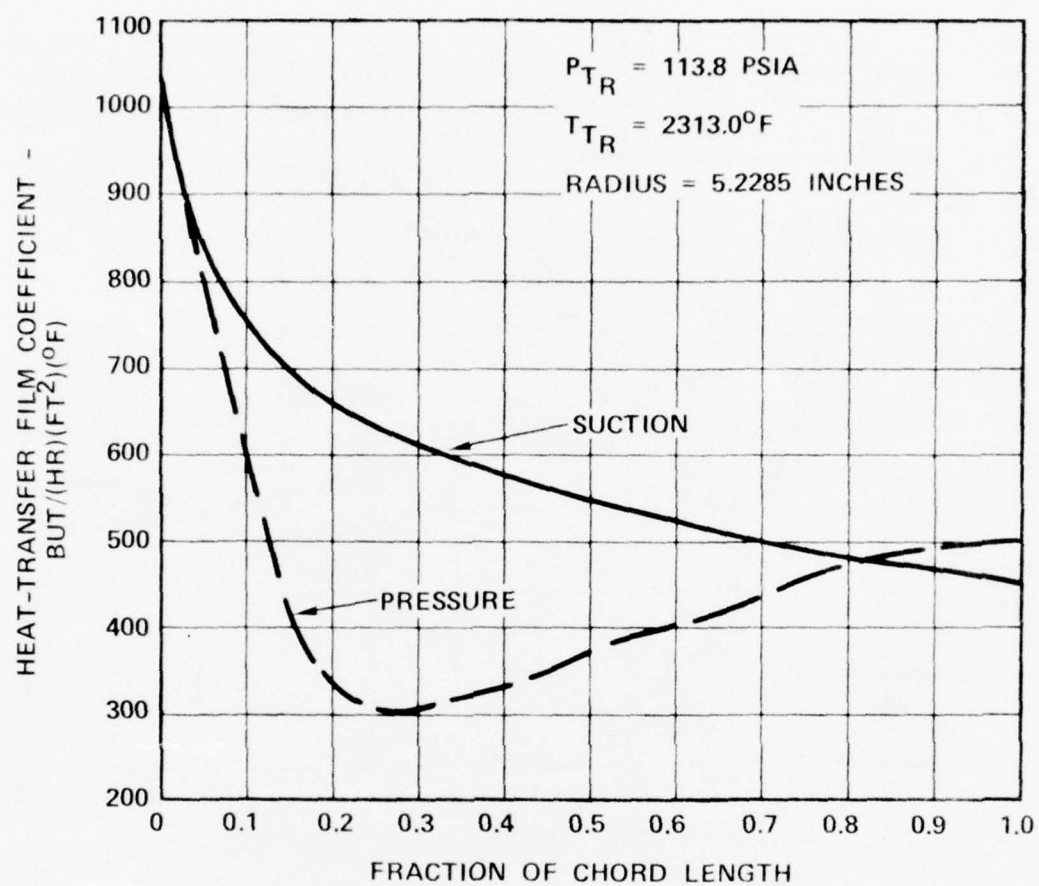
Figure 20. Continued (d)

37
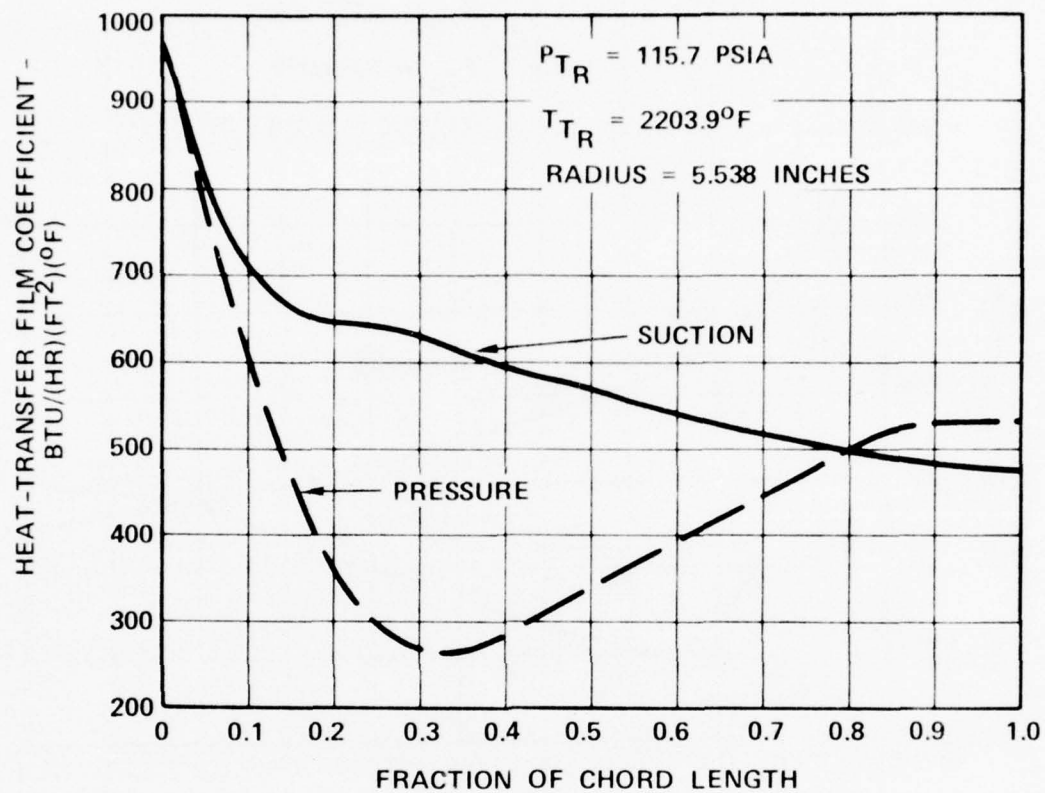
Figure 20. Concluded (e)

38
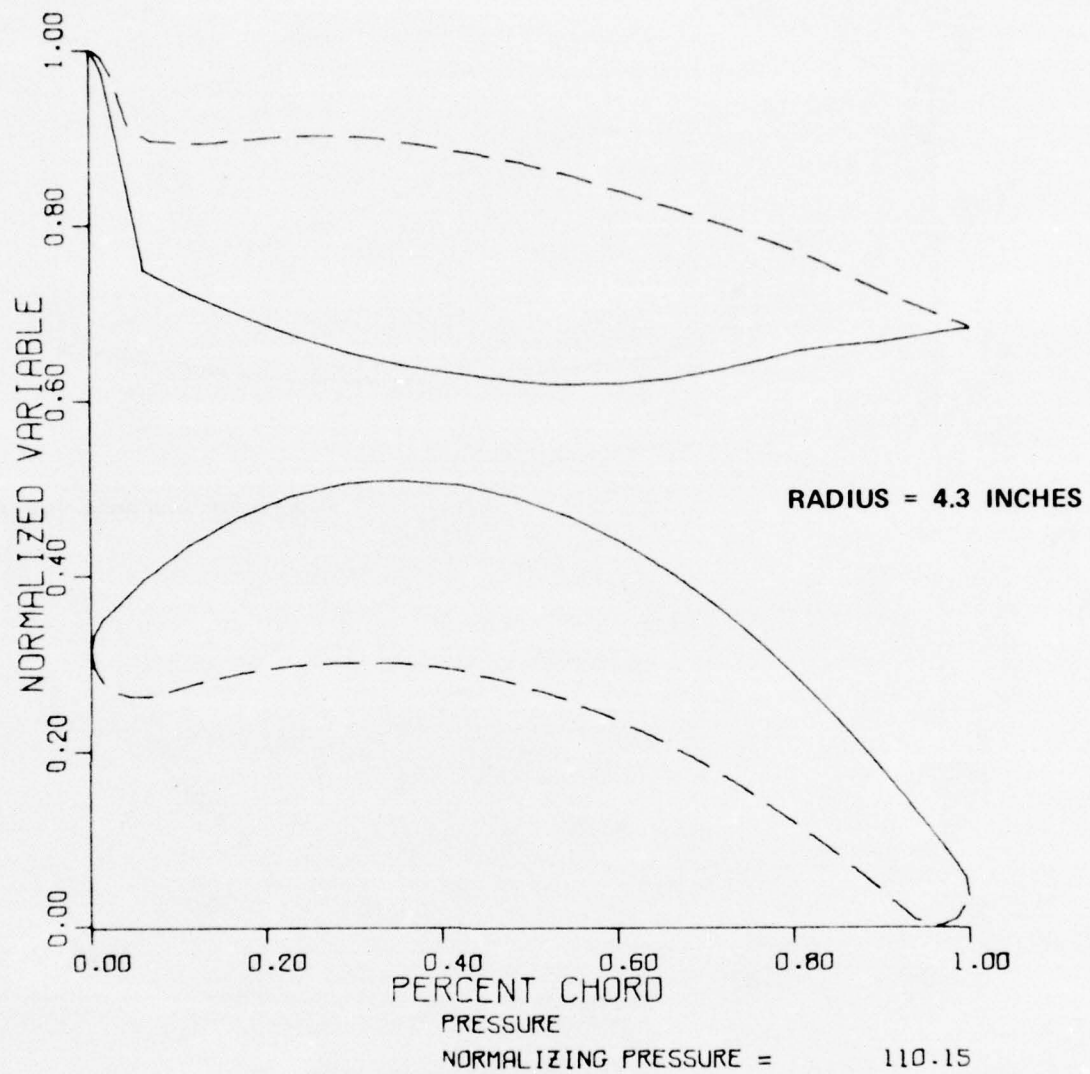
Figure 21. (a) High-Temperature Laminated Blade-Surface
Static Pressures for Five Sections. (TIT
Average = 2600°F, and $P_{T_{IN}}$ = 152.5 PSIA)

39

Figure 21.   Continued (b)

RADIUS = 4.919 INCHES

NORMALIZED VARIABLE

PERCENT CHORD

PRESSURE

NORMALIZING PRESSURE =   112.59
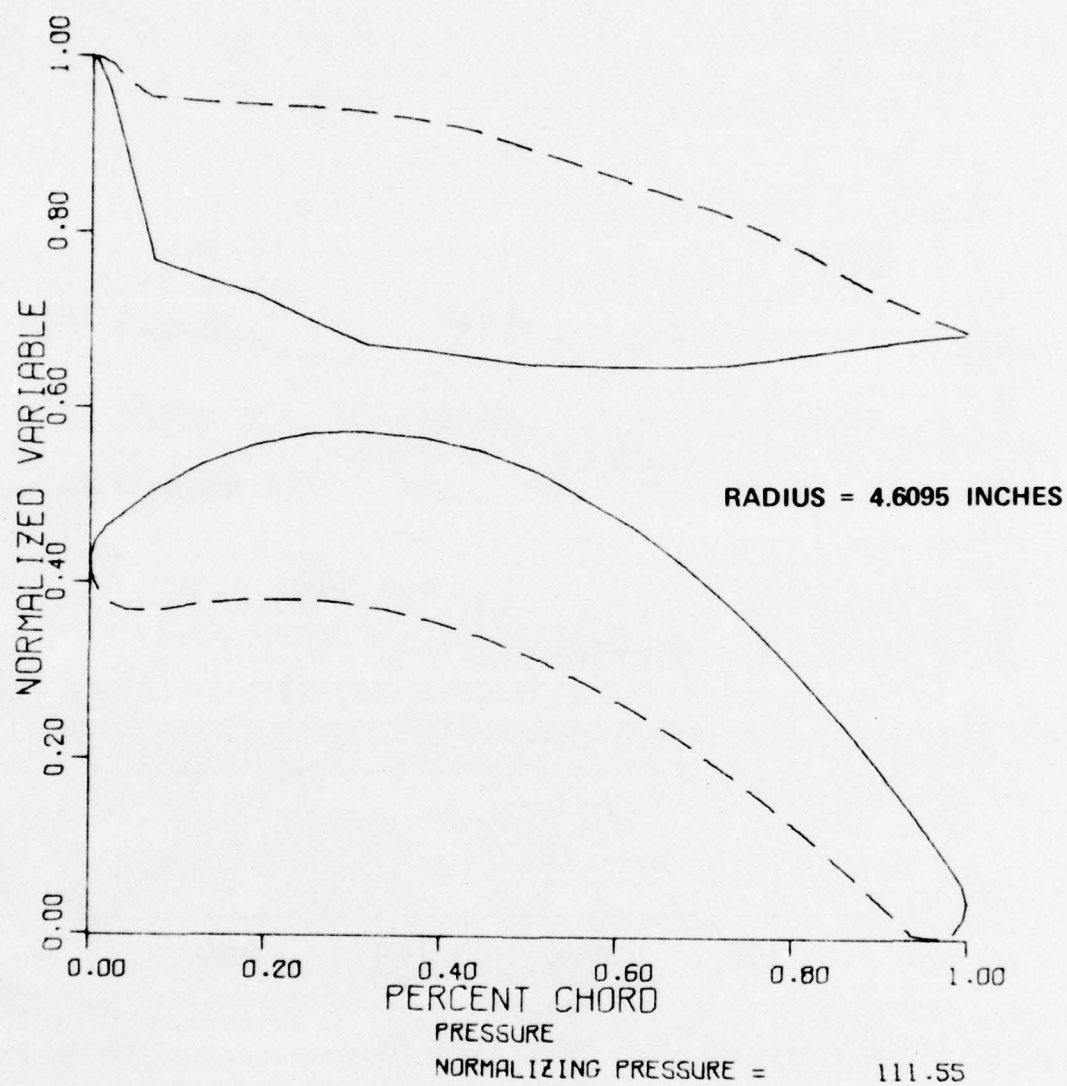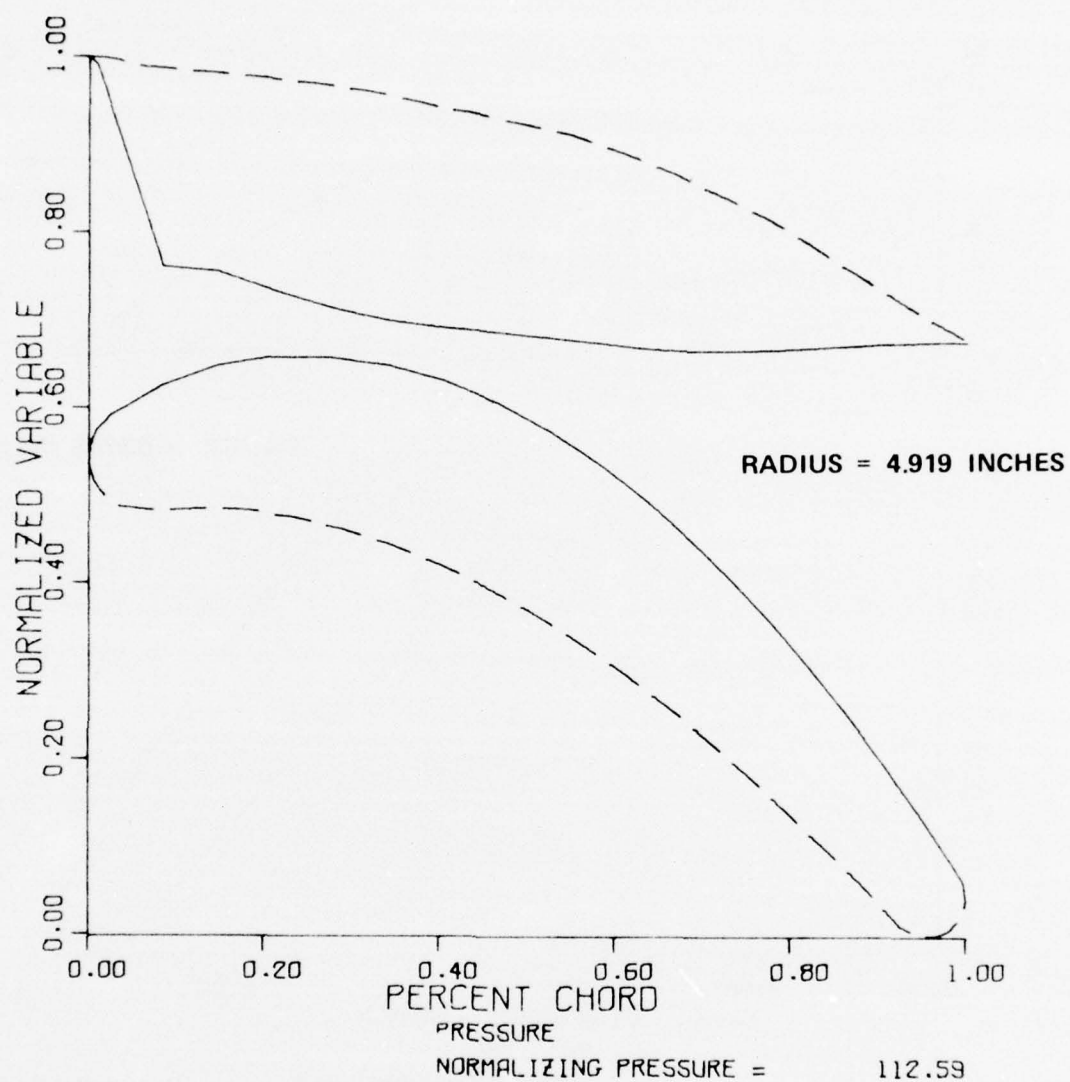
Figure 21.   Continued (c)

41
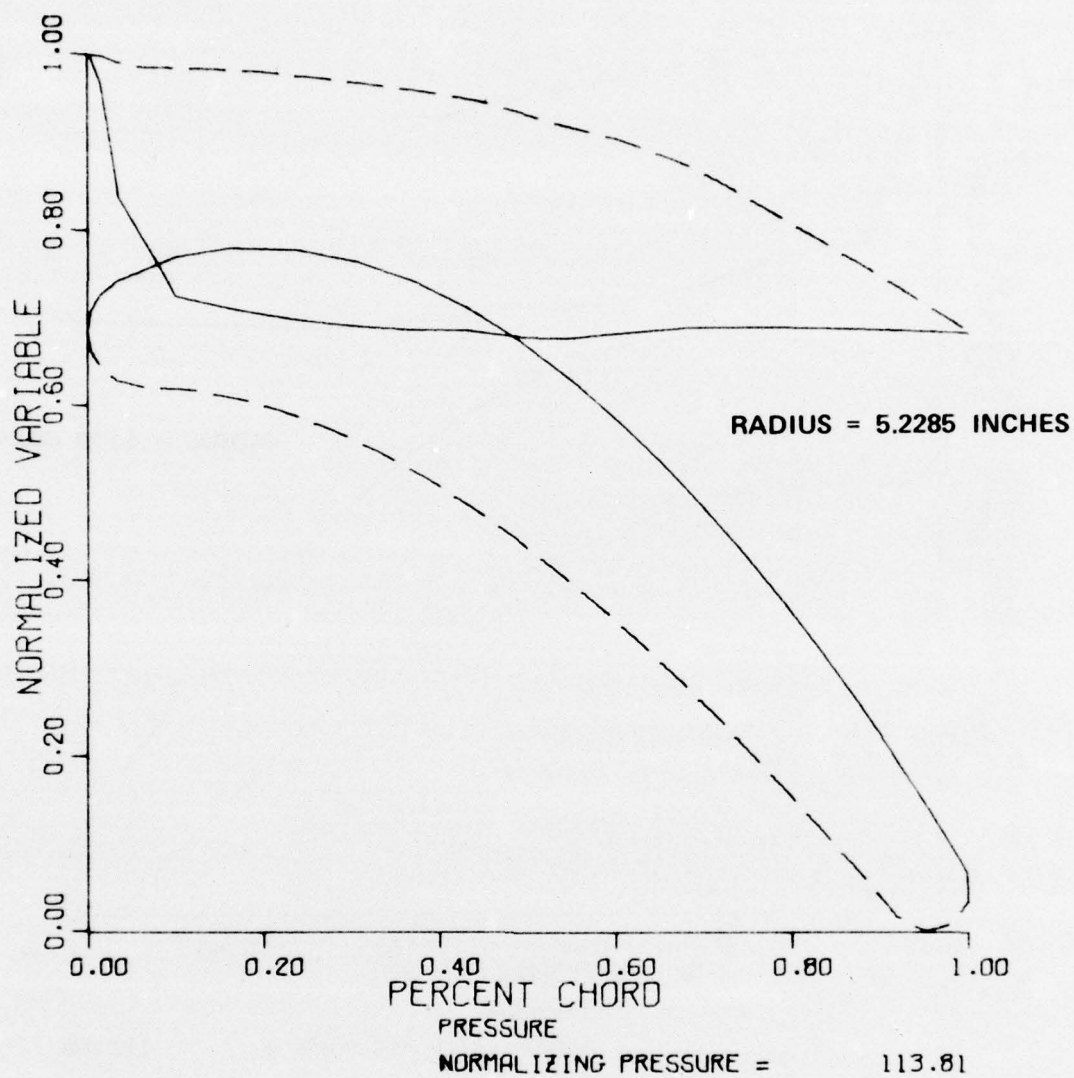
Figure 21. Continued (d)
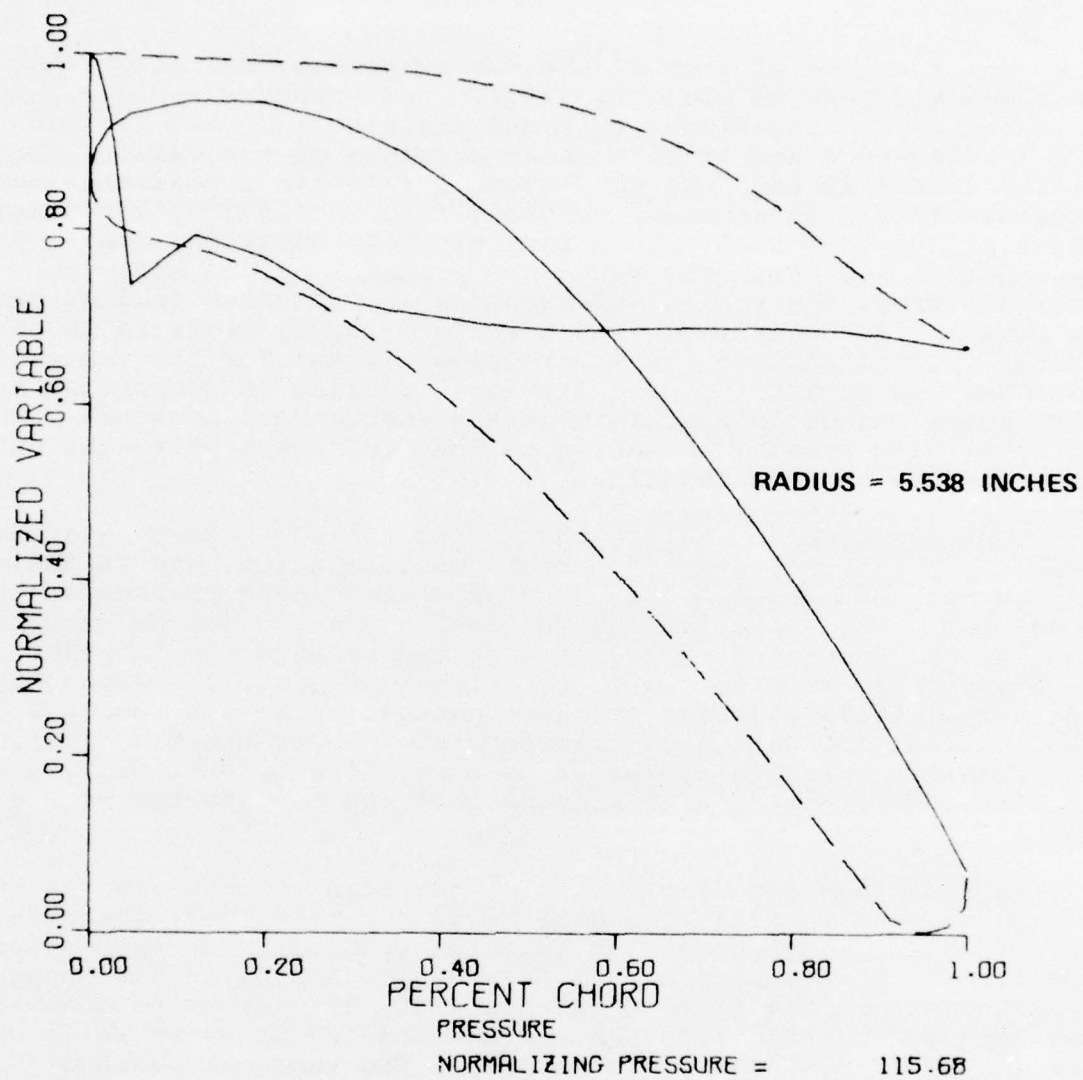
Figure 21.   Concluded (e)

to pressure side in the gill region of the blade. It would be extremely difficult to balance the flow discharging on both surfaces.

The function of each of the two centerbody radial cooling passages was both to cool the suction and pressure surfaces, and to serve as cooling flow supply and distribution channels for the leading-edge and trailing-edge portions of the blade. The design intent in each was to provide a relatively constant fluid pressure to aid in controlling bleed into the leading-edge cavity and trailing-edge slot from hub to tip. In addition, since impingement heat-transfer rates are proportional to slot-jet pressure drop, the radial variation in leading-edge cooling can be more easily controlled with a uniform supply pressure in the center-forward passage. Another design intent for the centerbody passages was to provide adequate local cooling in proportion to the radial change in heat load on the suction and pressure surfaces with special attention to the tip region where the net coolant-flow rate is relatively low.

Options open to achieve these aims include passage entrance and exit orificing, pin-fin pattern specification, and variations in the net through-flow that discharges from each passage at the blade tip. Radial variations in pin-fin spacing can be used to control the frictional pressure drop and balance the increases in fluid-pressure drop due to rotational pumping, thereby achieving a relatively constant pressure passage. Pin-fin spacings also control the wall heat-transfer rate. Near the blade tip, the remaining passage flow will be controlled by exit orificing so that sufficient flow remains to cool the top quarter of the blade.

A trailing-edge discharge slot has been incorporated in this design to achieve effective cooling of the relatively inaccessible trailing-edge region at the high turbine inlet temperatures specified. Consideration must be given to achieving the proper radial distribution of flow in this slot, as well as to generating adequate cooling rates on the suction and pressure walls with the available flow and pressure drop. The inherent passage roughness of the laminated design in the chordwise-flow direction will increase the heat transfer and friction factor. Pin-fin arrays are particularly useful in a slot of this geometry to increase the heat-transfer rate if sufficient pressure drop is available.

Initial heat-transfer calculations for the high-temperature laminated blade indicated an approximate cooling flow requirement of 5 to 6 percent of compressor discharge flow for attainment of the required turbine inlet temperature using a relatively complex cooling scheme. The figure of 5-percent total cooling flow was selected as a starting point for this design, with an even split of 2.5 percent to the forward and aft halves of the blade chord through the center-forward and center-aft coolant passages, respectively.

The variation in leading- and trailing-edge cooling flow requirements with radius was estimated initially with the intention of adjusting the distribution following detailed thermal analysis at each of the five primary blade sections being considered from blade base to blade tip. The approach used to determine the initial radial cooling flow distribution was to make the leading-edge impingement flow and trailing-edge slot flow proportional to the local gas-heat load at a given radius. The variation in heat load was calculated assuming the desirability of a uniform bulk-metal temperature from hub to tip at the leading and trailing edges. The magnitude of the assumed metal temperature in each case was typical of a high-temperature blade design. The radial variation in heat load was, therefore, a function of the turbine inlet temperature profile, the blade aerodynamics that determined the gas-side heat-transfer rates at various radial stations, and the blade geometry that determines the metal areas that must be cooled. The fraction of the total cooling flow needed to cool each spanwise section of the blade was made directly proportional to the relative heat load on that section. A net through-flow fraction of 0.20 in each of the centerbody passages was assumed to be adequate for convectively cooling the centerbody-tip region of the blade. Figure 18 shows the cooling distribution breakdown used for all flow-analysis and heat-transfer calculations.

Compressible flow analysis of the two centerbody cavities was performed for the variable-passage flow experienced in this design. The entire passage was modeled for analysis including inlet and exit orifices, and variable spacing pin fins. Heat transfer between the coolant and passage walls was considered, and all boundary conditions required for a thermal analysis of the blade section at any radius of interest were computed.

The coolant supply pressure at the base of the blade selected for this design was compatible with the TFE731-3 cycle design-point pressures. In the initial calculations, a value of 110 psia was used, since this is approximately the blade-shank-cavity pressure in the current TFE731-3 HP turbine blade. Later evaluation of the leading-edge cooling requirements raised this pressure to 130 psia, which is a reasonable estimate of the attainable blade shank pressure for a modified coolant delivery system in the TFE731-3 with coolant-flow rates increased to 5 or 6 percent.

The static pressures on the blade tip were required to enable the design of tip discharge orifices to flow the desired amount of coolant air in both the center-forward and center-aft cooling passages. The pressures were determined from data measured on a TFE731-3 Engine using Kulite pressure probes. Since the laminated blade does not have a squealer tip, the pressure was taken as the average of pressure-surface and suction-surface measurement values for the tested TFE731-3 blade with a 0.020-inch squealer tip. Kulite probe test data had been related to the tested turbine inlet total pressure, and

45

hence, static pressures could be determined for the laminated blade from the design turbine inlet total pressure. The discharge locations in the laminated blade differ somewhat from those for the three-passage TFE731-3 blade design, thus tip pressures, were determined by plotting the test data against relative chord position.

The design effort in both centerbody passages was aimed at selecting pin-fin spacings that would simultaneously yield appropriate heat-transfer rates on the suction and pressure walls, and also produce a constant pressure passage by balancing friction pressure drop with rotational pumping. The laminated fabrication technique establishes some pin-fin pattern design conditions. First, the pin size is determined by the laminate thickness, which in this blade was 0.020 inch in the centerbody region. Second, the pin center-to-center axial spacing must be an even multiple of the laminate thickness. In a small passage, this prevents uniform distribution of pins across the flow path in many cases. A third criteria is the orientation of the pins which must, of course, be parallel to the laminations. Being most apparent in the center-aft cavity, maximum fin effectiveness cannot be achieved as would be possible with shorter pins running normal to the passage walls. The pins are also of square cross section, which, while probably producing higher heat-transfer rates, makes the use of existing correlations for normal pin fins more of an approximation.

The final design in both passages uses 0.020-inch square pins on both 0.080-inch or 0.060-inch center-to-center transverse spacing, with variable longitudinal or flow direction spacing. The spacing, in general, is quite loose at the base of the blade where radial flow is quite high and becomes tightly packed near the tip to keep wall temperatures down with lower flow rates. The coolant temperature at the base of the blade was designed to remain consistent with the design of TFE731-3 HP turbine blade (1000°F). Coolant temperature rise in the center-forward passage is a total of 330°F for the final blade design flow of 5.88 percent of W_3 at an average TIT of 2600°F. The corresponding coolant temperature rise in the center-aft passage is about 475°F. The desire to maintain constant pressure passages was compromised in the last one third of the blade span since it was necessary to design sufficient pin-fin pressure drop to keep heat-transfer rates up, and wall temperatures within a reasonable range.

The high-cooling requirements of the leading-edge region necessitated raising the coolant inlet pressure at the base of the blade to 130 psia, and the coolant flow in the center forward passage from 2.5 to 3.38 percent of W_3. However, the increased pressure was not desirable in the center-aft passage, and therefore, an inlet orifice was incorporated to produce the desired passage pressure. The desired flow split between the center-forward and center-aft passages is controlled, in part, by the tip-discharge orifices of each passage.

46

The critical section, at R = 4.6095 or one-fourth of the blade span, was modeled in detail to determine the temperature and stress distributions and creep life. The heat-transfer design effort in the leading-edge region was concentrated on this section with the intention of later duplicating these calculations in less detail at all other radii to arrive at a total design. Treatment of critical section heat-transfer and flow design independently of neighboring sections of the blade was possible, since all flow within the leading-edge cavity is intended to be strictly chordwise. Film-slot and impingement-slot design flows were compatible so that radial crossflow could be held to a minimum.

Leading-edge impingement heat-transfer correlations were taken from AiResearch sponsored experimental studies at Arizona State University. The correlations used were compatible with the laminated blade leading-edge geometry (in that they accounted for the sharp leading-edge concavity) and were based upon the physical parameters of slot height, slot-to-stagnation point distance, impingement-cooled surface length, and cavity width at the impingement slot. Since crossflow was to be minimized by design intent, its effect in degrading heat-transfer rates was not considered.

Visualizing the leading-edge cavity flow pattern (see Figure 17) the coolant jet discharges from the impingement slot at a high velocity, and flows forward towards the stagnation point. It is constrained to flow along the pressure-side wall by spent coolant that is traveling in the opposite direction on the suction wall and in the central part of the cavity. After impinging near the stagnation point, the spent coolant turns and flows aft on the rough suction-wall inner surface and then discharges through the film slots into the mainstream.

The initial impingement configuration calculated for the 2.5-percent cooling flow in the forward half of the blade chord utilized an available pressure drop from the center-forward passage to the suction-side static pressure of 28.4 psi. The film-coolant discharge flow area was determined by assuming a width of two 0.011-inch laminate thicknesses, and a length in the radial direction that was a maximum of two-thirds of the blade length in that portion of the blade being considered. The film-slot flow coefficient was calculated to account for the depressing effects of high-mainstream crossflow momentum. The impingement-slot length in the radial direction was set at 80 percent of the available length, and the slot height, which is critical to heat-transfer performance, was calculated to utilize the maximum pressure drop possible and generate high heat-transfer coefficients.

When the initial heat-transfer design and critical blade section thermal analysis were completed, the leading-edge temperatures were found to be too high. This resulted in adverse temperature gradients in the cross section, and very low creep life. Efforts were then made to optimize the leading-edge cooling for the existing impingement-wall position, and hence, the existing passage-flow area splits in the blade. The high leading-edge temperatures were caused by a number of factors that are listed below:

o   The sharp leading-edge radius of this small blade is not suitable for extremely high turbine inlet temperatures since the inside-surface area to outside-surface area match is very disadvantageous. Cooling requirements at the stagnation point are extremely high, and impingement cooling is hindered by penetration problems. In any application of the laminated design, the aerodynamic design would of course be modified for a more blunt leading edge to be compatible with the 2600°F design requirement.

o   The impingement-slot location, as dictated by the laminated configuration, forces the choice of single-side coolant discharge. Flow rates are high enough that a substantial pressure drop is required across the available film-slot area leaving a less than desirable pressure drop across the impingement slot.

o   The original location of the impingement wall was not optimized, and shifting it forward may be beneficial if the proper flow distribution can be maintained.

The studies made of the leading-edge cooling problem include increases in the film-discharge slot area, variation of the impingement-slot height, and changes in the flow rate. These geometric changes proved to have either no or small beneficial effect. The most successful design alteration made was an increase in the center-forward cavity coolant-supply pressure to 130 psia at the critical section radius. This increased the available total pressure drop to 47.4 psi so that by holding the slot areas constant and allowing the flow rate to increase from 2.5 percent to almost 3.4 percent in the forward half of the blade chord, the leading-edge bulk-metal temperature decreased substantially, and the blade creep life was increased.

The final design selected for the leading edge at the critical section employs an impingement slot that is 0.0133-inch high and covers 80 percent of the blade radial height in this region. The total film-slot dimensions remain the same as previously mentioned--two laminate thicknesses by two thirds of the blade height. Detailed thermal analysis indicates a peak-edge surface-metal temperature of 1880°F, and a bulk-metal temperature of 1830°F for the 2600°F average turbine inlet temperature.

The increase in friction factor and heat transfer for the rough-surface trailing-edge slot over a smooth duct was calculated. These calculations predict a 25-percent increase in friction factor, and an 88-percent increase in Stanton Number for chordwise flow through the slot at the critical section using 2.5 percent of W3 in the aft half of the blade chord. Despite increases in friction factor, there is abundant pressure drop available from the center-aft passage to the extreme trailing edge. The magnitude of pressure drop was such as to require substantial orificing in the wall between the center-aft cavity and the trailing-edge slot to keep the flow down to required levels. The small area high-velocity orifices in combination with a relatively short trailing-edge slot in the flow direction would inhibit the formation of a smooth, uniform, radial distribution of flow prior to discharge from the slot. This factor, in addition to the obvious heat-transfer benefits, made the incorporation of pin fins desirable.

Examination of the characteristic heat-transfer promotion methods, and the pressure drop of various attainable pin-fin arrays led to the selection of design specifications of 0.011-inch square pins (a single laminate thickness) with transverse and longitudinal center-to-center spacing of 0.020 inch and 0.030 inch, respectively. The heat-transfer coefficients generated with this array are greater than twice that of the rough-passage values with the same flow rate. The physical dimensions of the slot are such that from three to four rows of pins may be placed in the flow direction. This orificing consists of slots that are 0.010- to 0.012-inch high, and cover a high percentage of the available blade length.

Heat-transfer design calculations at the critical section for all flow cavities was performed in detail to develop boundary conditions for the thermal analysis, and following that, stress and creep analysis of that section. The flow design of other sections of the blade, both above and below the one-quarter span section, was completed after life analysis of the critical section was accomplished. Flow rates in all coolant passages had been established as explained previously, and other aspects of the geometry had been determined except for impingement-slot, film-slot, and trailing-edge orifice sizes. These details were determined from a flow-distribution standpoint, keeping the general pressure-drop relationships existing

at the critical section, but without any thermal calculations to
determine blade-metal temperatures. It was assumed that in
setting flow rate proportional to thermal loading at any radius,
and by designing for pressure splits similar to the critical
section, the resultant thermal boundary conditions would yield
metal temperatures close to those at the critical section.

Below the critical section and at the pitch section of the
blade, the film-slot area was set at the maximum of two laminates
wide by two-thirds of the blade length in that section, and the
impingement-slot width was thereby determined by the remaining
pressure drop. Towards the tip of the blade, the impingement-slot
width was set at a minimum value of 0.010 inch, and the film-slot
area was determined by the remaining pressure drop. Smaller slot
heights and higher jet velocities near the tip may partially
compensate for higher coolant temperatures. Trailing-edge
orificing was calculated at all sections strictly from pressure-
drop considerations with the pin-fin array identical to that at
the critical section. The cooling effectiveness of the final
design, as shown in Figure 22, is very comparable to that
achieved by advanced inserted-blade cooling methods.

(3) Blade loading analysis

The gas-pressure loads were computed on the blade at all
sections resulting from static-pressure differentials between
pressure and suction surfaces. These gas loads are used to
calculate mechanical loading on any section of the blade due to
centrifugal forces and gas loads. The results of the loading
calculations include section-area properties, especially the
center-of-area and center-of-mass locations with respect to the
stacking axis, radial load, tangential load, and axial movements
generated on the critical section about the stacking axis by the
combined forces mentioned. These entities are used to determine
the steady-state-stress distribution, and the creep life of the
blade.

The high-temperature laminated blade was analyzed using five
sections from base to tip to describe the internal and external
profile. The pin fins were included in center passages and
trailing-edge slots. The rotational speed used for this turbine
was 29,692 rpm, which is the design-point speed of the TFE731-3
high-pressure turbine wheel.

It is desirable in most turbine blade designs to lean the
blade from root to tip in the direction of rotation so that the
straightening effect of centrifugal forces will balance the gas-
bending loads exerted on the blade. The blade lean angle must
be determined by varying the angle over a range, and calcul-
ating its effect upon creep life. By plotting creep life versus
lean angle, or tip offset, an optimum angle can be determined
that maximizes creep life because of the mechanical stress dis-
tribution imposed on the critical section of the blade by changes
in centrifugal loading. In this design effort, only lean in the

50
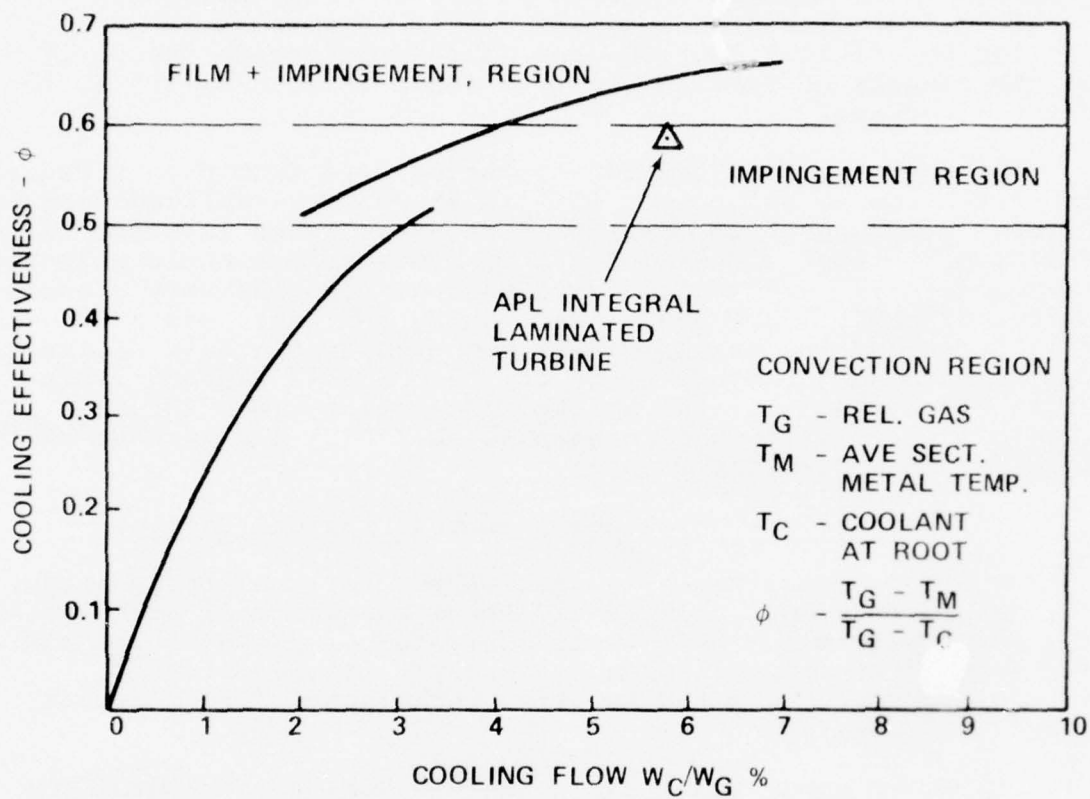
Figure 22.   Laminated Turbine Blade Airfoil
            Cooling Effectiveness.

tangential direction was considered since lean variations in the
axial direction would require extensive changes in the laminate
definitions that had been established at the time. The lean an-
gle for this blade was taken as the angle between the stacking
axis, which is a radial line, and a straight line drawn in such
a manner as to minimize moments at the critical section. This
straight line passes through the center of mass at the one-
quarter or critical section, and is faired through the positions
of the centers of mass at sections above it when viewed in the
axial direction.

Lean angles selected for the study were from 0 to 5 degrees.
The variation in calculated life is shown in normalized form in
Figure 23, where it is apparent that an increase in creep life (a
factor of three) is obtained at the optimum lean angle selected
(3.3 degrees). The angle of 3.3 degrees compares very closely
with the TFE731-3 HPT blade lean angle, but there was a tangen-
tial offset of the stacking axis required at the base of the
laminated blade from the blade of the TFE731-3 design. This
offset is a result of the shifts in center of mass for the
laminated blade from the three-passage TFE731-3 blade due to
internal configuration changes.

(4) Blade-life calculation at the critical section

A single nodal network model serves for the steady-state
thermal, stress, and creep analysis of the critical section.
The model set up for this blade consisted of 268 elements and
366 nodes, the complexity being a result of the irregular
internal geometry and the modeling technique. This model is
shown in Figure 24.

External conditions, the adiabatic-wall temperature, and
heat-transfer coefficients were discussed previously. In the
center coolant passages, the heat-transfer coefficients promoted
by pin-fin arrays, and the coolant temperature accounting for
heat pickup were computed. In the leading-edge cavity, impinge-
ment heat-transfer rates were calculated at local positions on
the suction wall and at the stagnation region. On the pressure-
wall, laminar flat-plate heat-transfer was considered as the
best approximation to the local flow behavior. A coolant
temperature was determined by heat-exchanger considerations. In
the trailing-edge slot, an average heat-transfer coefficient
with pin-fins was determined, and an effective coolant tempera-
ture was calculated from heat-exchanger considerations.

A steady-state two-dimensional thermal solution was computed
at an average turbine inlet temperature of 2600°F. Radiation
between suction and pressure walls was considered in the
analysis. The resulting temperature distribution is shown in
Figure 25. The major design difficulties, that are apparent
from this figure include the high leading-edge bulk-metal tem-
perature, the temperature difference from the leading edge to

52
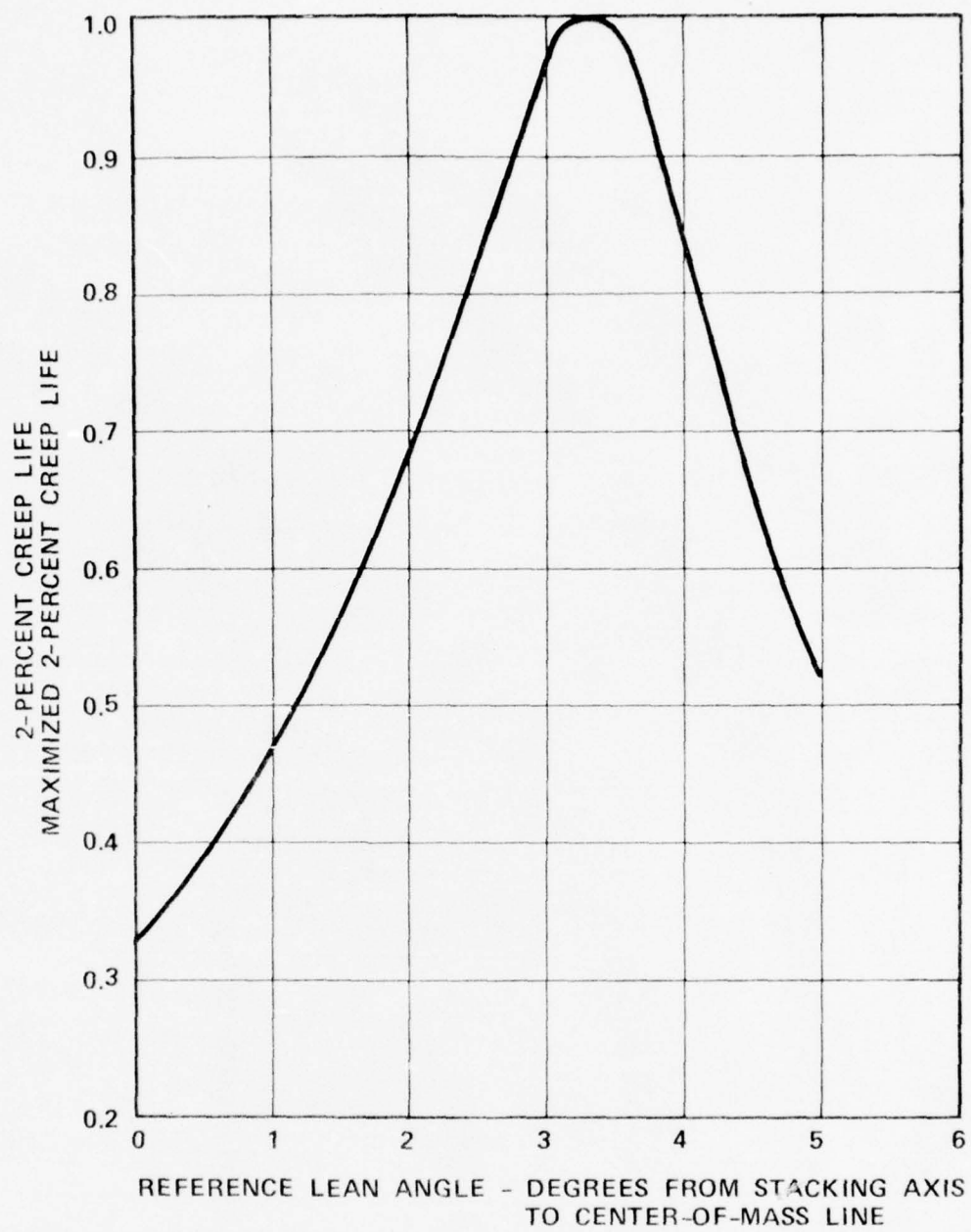
Figure 23.   Laminated Turbine Blade Lean Angle
             Creep-Life Optimization.

ELEMENTS

NODES

RADIUS = 4.6095 INCHES

Figure 24. Laminated Turbine Blade Critical Section Grid Model.
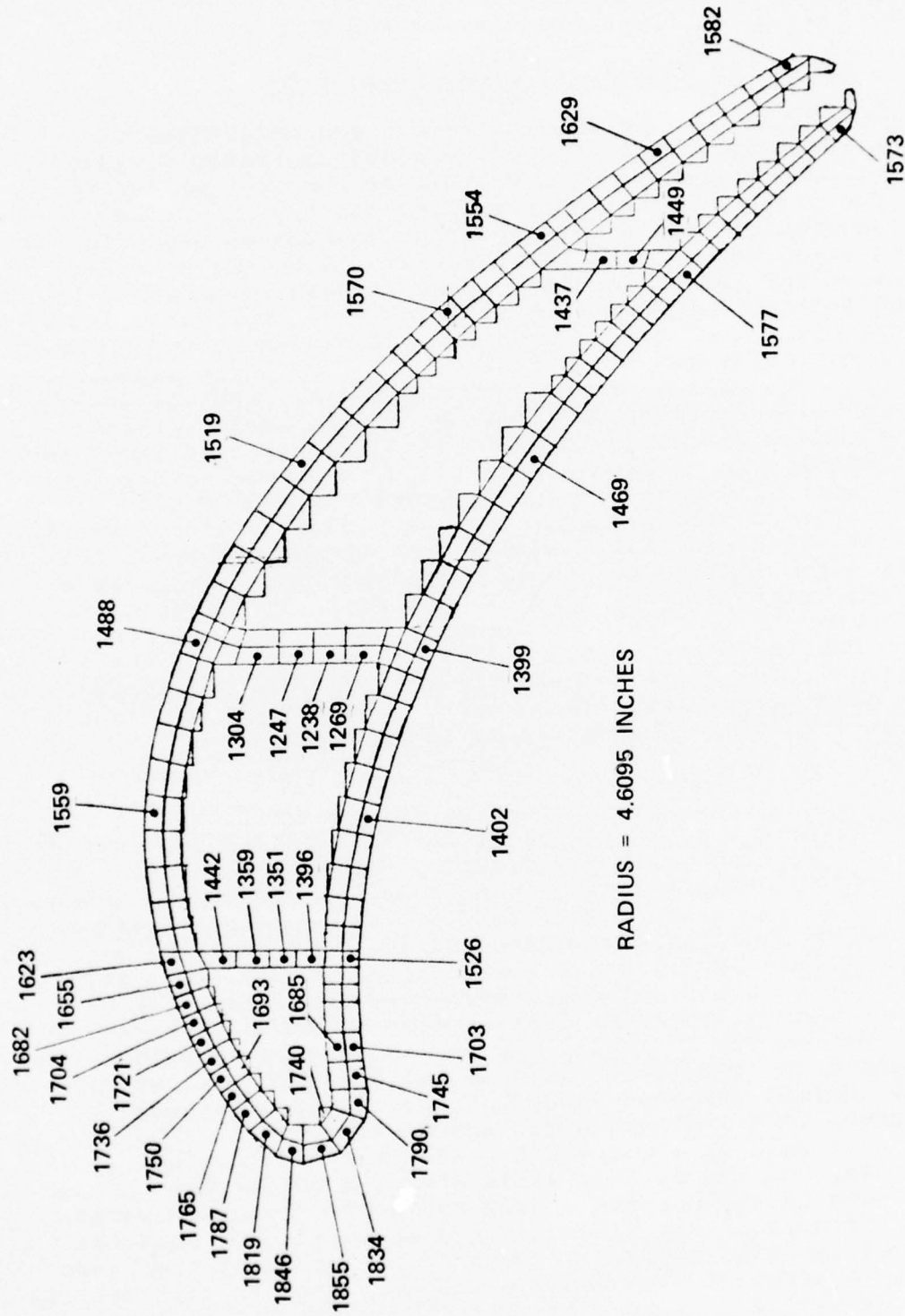
Figure 25. Laminated Turbine Blade Critical Section Steady-State Temperature Distribution (TIT Average = 2600°F, and $W_{coolant}$ = 5.9 Percent).

RADIUS = 4.6095 INCHES

the cold-pressure side at mid chord, the temperature difference between suction and pressure walls at the center-forward passage location, and the cold-passage divider walls.

(5) Laminated Waspaloy-A creep properties

A great deal of experimental effort was undertaken to determine the degree that diffusion-bonded laminated Waspaloy-A mechanical properties differ from that of the wrought parent alloy. The property of primary interest in the analytical phase of design of this high-temperature laminated blade is the 2-percent creep strength of the material. A 2-percent creep design curve for the laminated turbine of Waspaloy-A was developed from a limited amount of AiResearch test data, and from consideration of the parent material stress-rupture properties. This curve is representative of minus three sigma minimum property values of the parent material, and was considered to be appropriate for laminated construction. Since that time, additional detailed stress-rupture data on laminate-sheet stacks has been taken using the best bonding techniques found to date. The test results indicate the equivalence of average stress-rupture properties of the wrought parent material, and the laminated material loaded in the direction parallel to the laminates. For loading tranverse to the laminate direction the stress-rupture property is slightly degraded, but remains above minimum values in the small data sample taken. It was concluded from this limited stress-rupture data on the laminated sheet that the 2-percent creep curve previously selected was appropriate for use as a minimum property design curve. The 2-percent creep design curve and the substantiating new data are shown in Figure 26.

The steady-state stress solution for the critical section was computed with the completion of the two-dimensional thermal analysis of the blade critical section, and the calculated radial load and moments acting on this section due to gas-bending loads and centrifugal loading. This program combines thermal stresses and mechanically generated stresses to describe a steady-state two-dimensional uniaxial stress field. The stress distribution for the final blade design at an average TIT of 2600°F, and with 5.9-percent cooling flow is shown in Figure 27. The high compressive stress at the leading-edge stagnation region, and high tensile stresses in the pressure wall at mid chord are thermal stresses caused by the high leading-edge temperatures, cold-pressure side, and divider walls. The pressure-side wall is about 450°F colder than the extreme leading edge, and the divider walls are even colder due to high cooling rates in the pin-fin arrays and poor conduction paths from the surfaces of the blade. These walls act as, what has been termed, a "cold bridge" between hotter areas of the blade, and are in a state of high tensile stress. This is particularly true in the center-divider wall where the maximum overall blade stress occurs. Stresses in the aft half of the blade chord are

56

Figure 26. Laminate Waspaloy-A 2-Percent
Creep Design Curve.

The figure shows a log-linear plot with STRESS - KSI on the vertical axis (ranging from 4 to 100) and LARSEN MILLER PARAMETER* on the horizontal axis (ranging from 38 to 52). The plot contains the following labeled curves and data points:

- AVERAGE STRESS RUPTURE
- TRANSVERSE LOADING WASPALOY LAMINATE STAGE TESTS
- LONGITUDINAL LOADING
- AVERAGE 2-PERCENT CREEP DATA FROM AIRESEARCH RADIAL FORGINGS
- 2-PERCENT CREEP DESIGN CURVE (-3σ MINIMUM)

$$*LMP = (T+460)(20\ LOG_{10}t)(10^{-3})$$

RADIUS = 4.6045 INCHES

Figure 27. Laminated Turbine Blade Critical Section Steady-State Stress Distribution (TIT Average = 2600°F, and $W_{Coolant}$ = 5.9 Percent).

58

moderate to low in both pressure and suction walls, and the low temperatures produced by high trailing-edge cooling rates make the creep life fairly high.

In examining the stress distributions, as shown on Figure 27, it should be noted that there was no opportunity to determine the effects of divider-wall location and thickness on stress levels, and no opportunity to change or optimize the original blade-metal-taper ratio to reduce steady-state stresses. The most significant factor in the high stress levels is the hot leading edge, but geometric variations might provide for a better distribution of stresses through the blade cross section.

In addition to the steady-state stress calculation, a creep analysis of the blade was also performed. The critical section creep behavior occurs over a finite radial length of the blade, and the blade-stress distribution is recalculated after each increment of creep strain using the steady-state temperature distribution. Calculated creep strains and stress values are continued until some element in the blade reaches the creep-strain limit of 2 percent.

The 2-percent creep life of the final design at an average TIT of 2600°F with a 5.9-percent cooling flow is calculated as 10.2 hours. The failure or maximum strain location is in the impingement wall. Figures 27 and 28 show the pertinent results for this analysis. Although the failure location is in an area that might be considered noncritical to the part integrity, it can be seen from the creep distribution at 10.2 hours that creep strains approaching 2 percent are also present along the entire suction side, leading-edge wall, and on the pressure side below the impingement wall also. The stress distribution at 10.2 hours is also shown in Figure 28. The peak steady-state tensile stress in the center-passage divider has fallen from 130 ksi to 84 ksi, and the strain at this location is 1.6 percent. The leading-edge steady-state compressive stress has become tensile due to strain relief during the initial creep period, an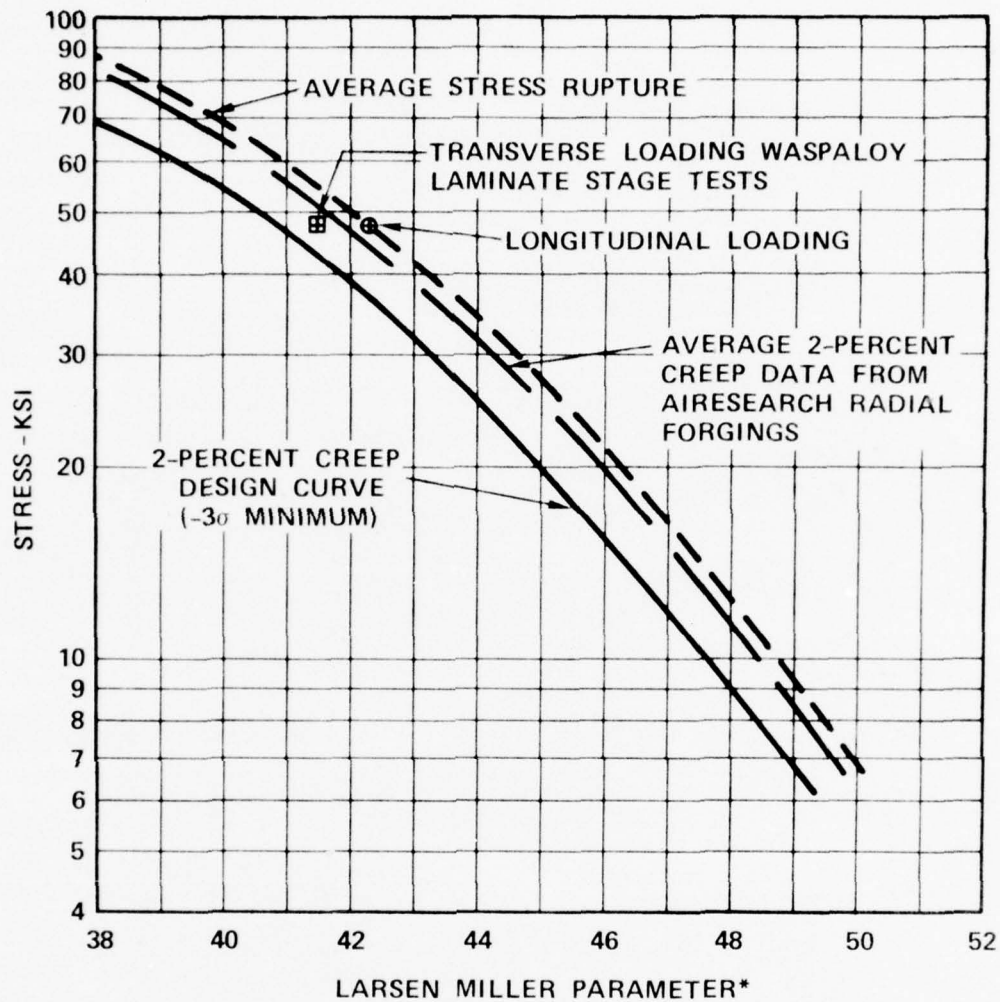d the creep strain at 10.2 hours is 1.7 percent. The creep strains for compression and tension are added algebraically to determine a final value. In general, the high tensile stresses along the pressure wall at mid chord have decreased substantially at 10.2 hours, and on the suction wall, the outer-fiber stresses have risen significantly.

The calculated 2-percent creep life of 10.2 hours is adjusted by normal practice to a reportable life figure. The method used to determine the reportable life determines a life with a 95-percent confidence level based upon variables in the calculations and experience in predicting turbine blade life. The difference between calculated life and reportable life increases as their absolute magnitudes decrease. This design, therefore, has a 95-percent probability of a successful life of 1 hour, at 2600°F average TIT, and with a 5.9-percent W_3 coolant flow rate.

59
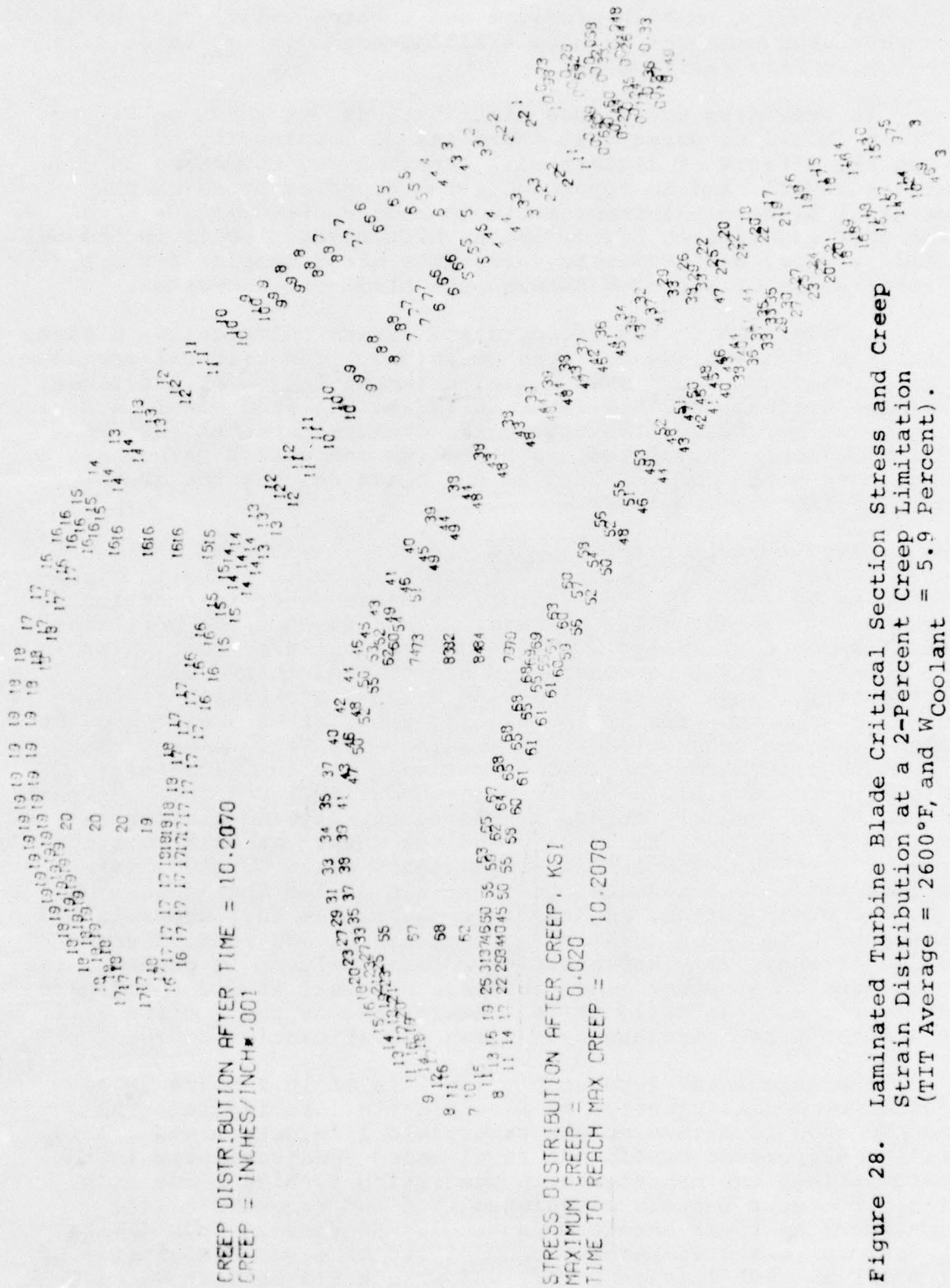
Figure 28. Laminated Turbine Blade Critical Section Stress and Creep Strain Distribution at a 2-Percent Creep Limitation (TIT Average = 2600°F, and W Coolant = 5.9 Percent).

60

The relatively short life determined for the final blade design at a 2600°F average TIT makes it desirable to predict the effect of reduced inlet temperature levels on creep life. Changes in the analysis are only in the thermal boundary conditions with the coolant flow level maintained at 5.9-percent W_3. External gas side-boundary conditions were determined for selected TIT levels at the critical section for the nodal network analysis, and below the critical section to account for the effect on coolant temperature increase along radial passages. Coolant temperature rise in the center passages was computed, and heat-exchanger calculations were performed to determine the remaining internal thermal-boundary conditions. Temperatures of 2200°F and 2400°F were selected as the points of average turbine inlet temperature, from which the variation in creep life could be determined.

Results of the analyses indicate substantial decreases in leading-edge metal temperature (approximately 110°F for each 200°F decrease in average turbine inlet temperature), but they are accompanied by decreases in pressure-wall and passage-divider-wall temperatures. The effect is a moderate decrease in thermal gradient throughout the section, and thereby reductions in stress levels at the leading edge and the cold-pressure side wall. Thus, life increases with the major factor being the decrease in metal-temperature level rather than better distribution of temperature and relief of thermal stresses. The resulting 2-percent creep life versus average turbine inlet temperature is shown in Figure 29 for the final blade design in terms of as-calculated life and reportable life, with the 95-percent confidence level. The results shown in Figure 29 are summarized in Table 3.

TABLE 3.   SUMMARY OF HIGH-TEMPERATURE LAMINATED BLADE
          2-PERCENT CREEP LIFE VERSUS AVERAGE TURBINE
          INLET TEMPERATURE DATA.

Turbine Material	Temperature (°F)	Life at Temperature (Hours)
Waspaloy	2320	20
Astroloy	2530	20
AF2-1DA	2600	29
Total wheel life would of course be considerably longer, depending on the duty cycle for the particular application.		

5.   FINAL LAMINATE DEFINITION

A dimensional feature size and positional tolerance investigation was performed to establish blade-wall thickness and

61
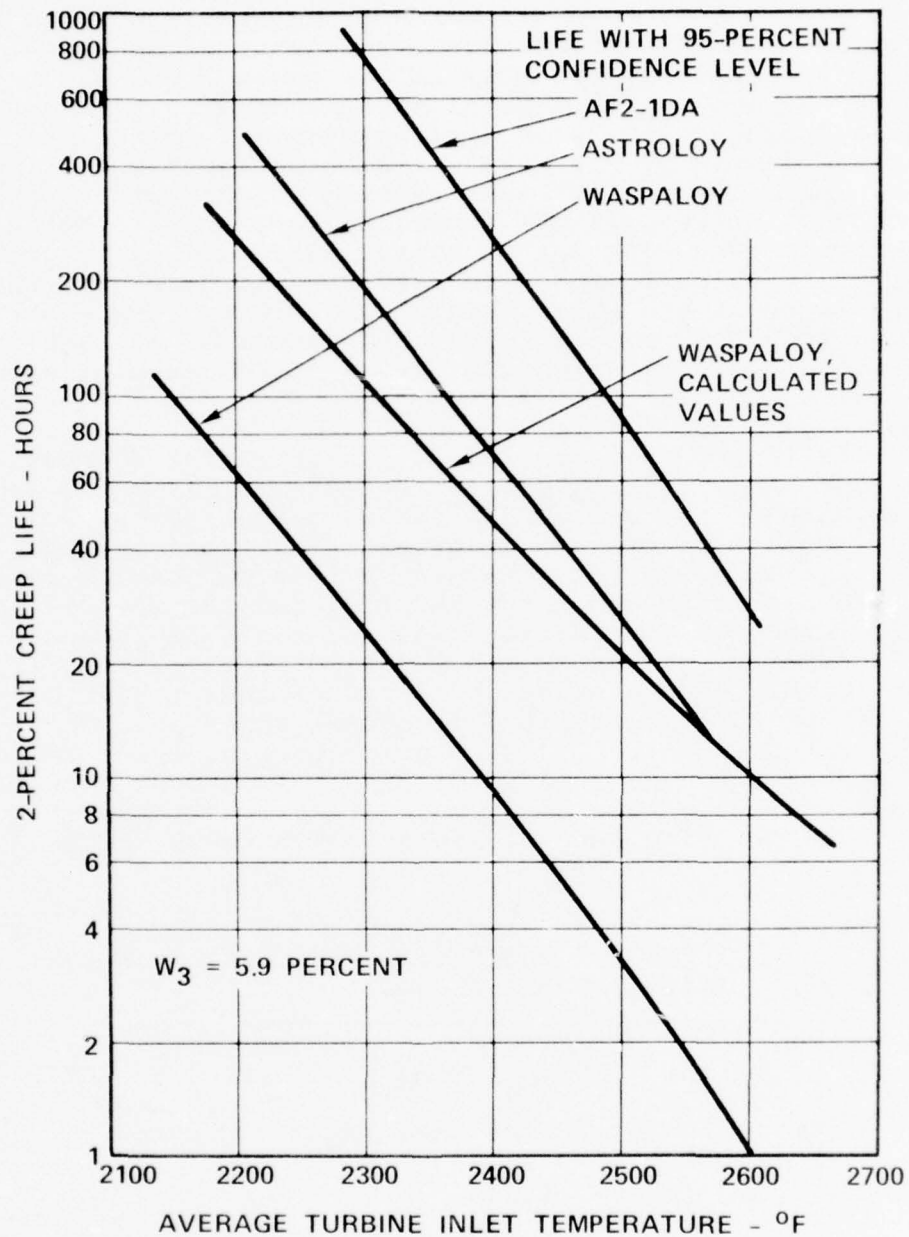
Figure 29. Laminate Turbine Blade Critical Section
(R = 4.6095 Inches) 2-Percent Creep Life
Versus Average Turbine Inlet Temperature.

cooling flow path area for the prototype wheel blank. The wheel tolerance investigation was established based on then current laminate detail drawing methods. The method that was first tried for this program follows:

o   All layout line work width is 0.010 inch, maximum line width is 0.015 inch.

		Line Tolerance		Actual Tolerance
o	Layout of 10X size passages	$\pm$0.005	=	0.0005
o	Final wheel must consider more than one passage master	$\pm$0.005	=	0.0005
o	Layout of 10X size targets	$\pm$0.0025	=	0.00025
o	Layout of 4X size (grid and tooling targets)	$\pm$0.0025	=	0.0006
o	Artwork using 10X size layout and incorporating etch factor	$\pm$0.005	=	$\pm$0.0005
o	Photo reduction (twice 10X to 4X to full size)	$\pm$0.0005	=	0.001
o	Positioning of 4X size positive on grid	$\pm$0.005	=	0.00125
o	Etching (variance) process (0.020 thickness)	$\pm$0.002	=	0.002
o	Fixture (tooling) lamination positioning	$\pm$0.002	=	0.002
o	Blade contour	$\pm$0.003	=	0.003
o	Blade position	$\pm$0.0025	=	0.0025
	Total		=	$\pm$0.0141

Probable Tolerance Stack = T_s = 1.3 $\sqrt{T_1^2 + T_2^2 + T_n^2}$

$$T_s = \pm 0.00675$$

After the wheel tolerance investigation was completed, a large tolerance control laminate blank was detail designed. The primary purpose of this blank was to investigate the dimensional characteristics of a large laminated blank by detail preinspection and post inspection of representative air-passage

63

features. Also, the blank was sized to the TFE731-3 wheel
envelope (11.32-inch diameter by 2.5-inches wide), and therefore
allowed an early assessment of the etching and bonding process.
The bonding furnace tooling for this blank was detailed, and
this tooling was used for manufacture of the prototype wheel
blank.

The laminated airflow passage stack (2 inches by 1.5 inches
by 2.4 inches) was detailed, and the photographic tooling masters
and etching tooling was completed. The airflow stack has
various representative turbine blade cooling-flow passage shapes
that were airflow tested to establish the pressure-drop charac-
teristics. The results are discussed in Section IV of this
report.

The detail design effort was reviewed to ensure that the
final 1:1 film tooling masters were being produced to adequate
dimensional tolerances. The inspection results revealed +0.0017-
circumferential and 0.0034-radial shift. At that point, a
redirection of the method of detail design of the cooling
passages was initiated in order to ensure a reduction in toler-
ances related to the tooling. The new method, utilizing computer
aided design techniques, included definitions of the cooling
passages by straight-line elements that used an x/y digitized-
coordinate system at each Z-section. The coordinates were fed
into an Auto-Trol mini-computer, and reproduced graphically as a
final check prior to tape input into a Gerber Automatic plotting
table with an optical exposure head. The final 1:1 size
Z-section tooling master is automatically plotted on a photo-
sensitive glass plate to a tolerance of +0.001 inch or less.
Mylar photopositives are made of the final tooling for each of
the laminates. Figure 30 is an example of one of the master
tools generated by this automatic graphics method. The benefits
to this design method are:

o   Substantially increased accuracy.

o   More consistent photoetching since the optically
     generated line width is precise (+0.0005) com-
     pared to a hand-drawn line photo-reduced to size.

o   Faster turnaround time

As a final check of the cooling-passage minimum size, a
special 0.010-inch thickness photoetched Waspaloy specimen was
made with various hole and pin sizes. Figure 31 shows the three
specimens that were optically inspected after etching, and Figure
32 shows an enlarged view of one of the specimens. The inspec-
tion results are given in Figure 33 and Table 4. Note the
number 1A hole did not etch through, and the tooling line width
(A = 0.004) produced the greatest variation in sidewall shape
(i.e., variation between C and H, and between CW and HW).
Therefore, the smallest line width that can produce consistent

64
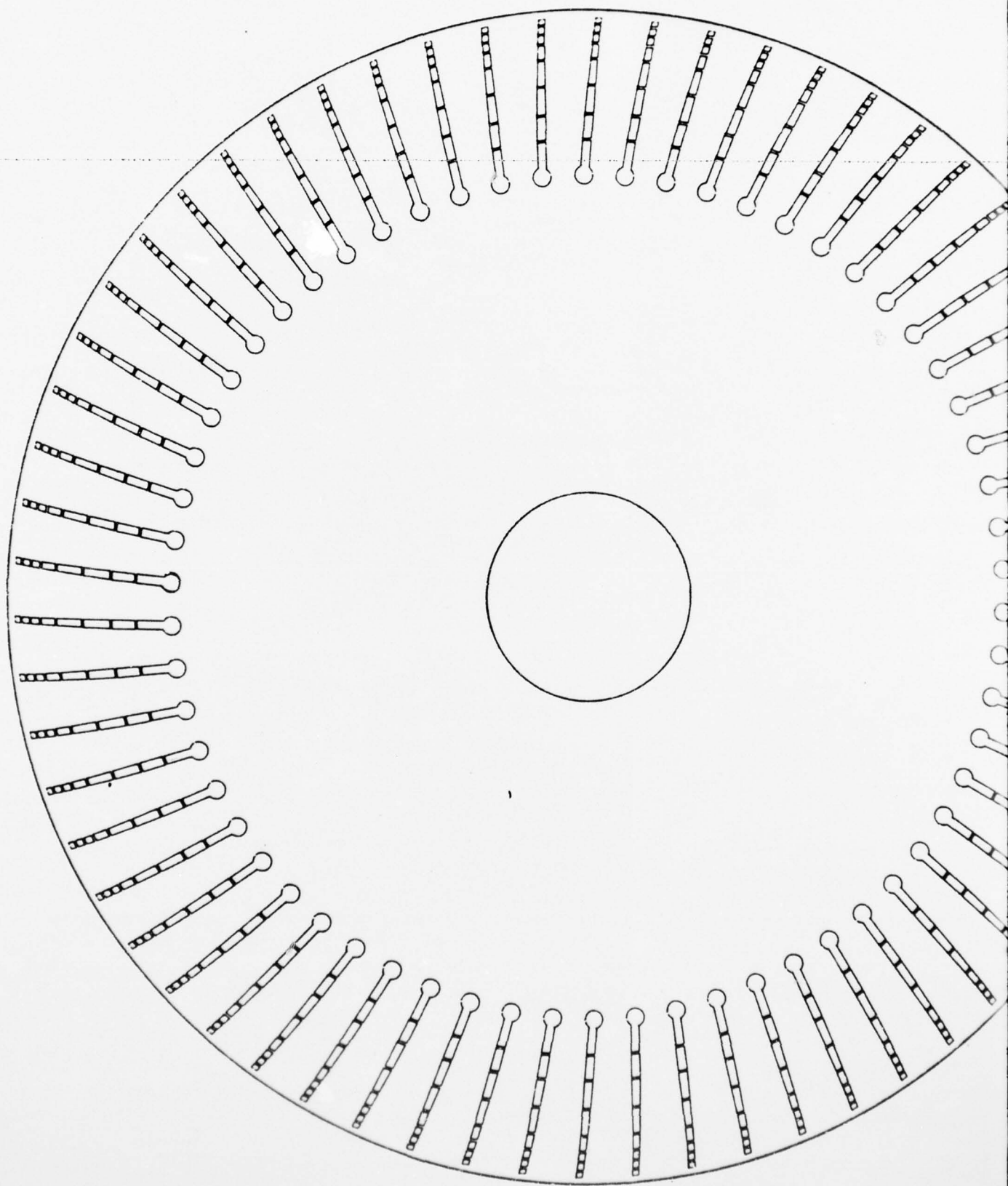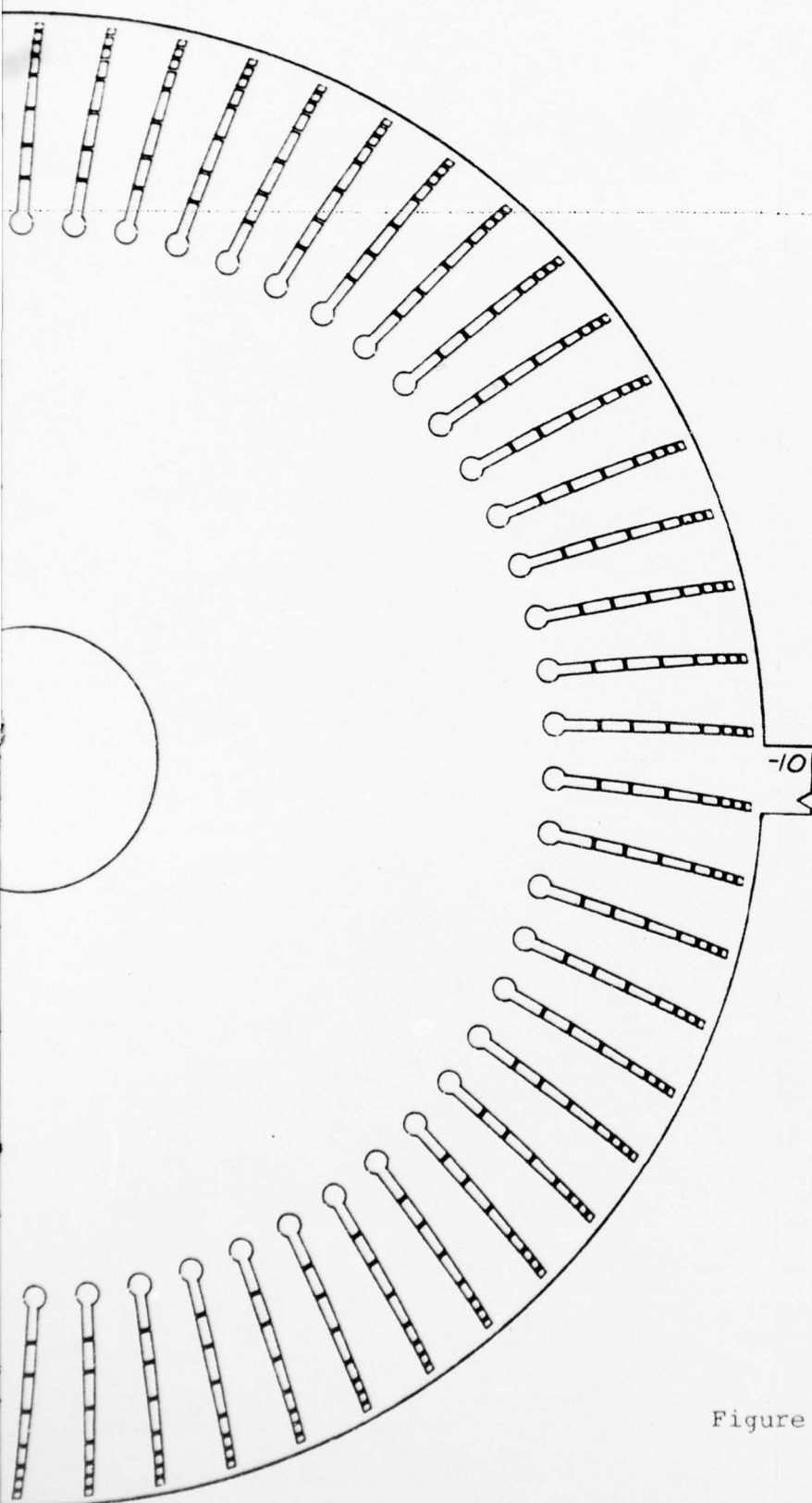
Figure 30.   Example of Master Tool Generated
by Automatic Graphic Method.
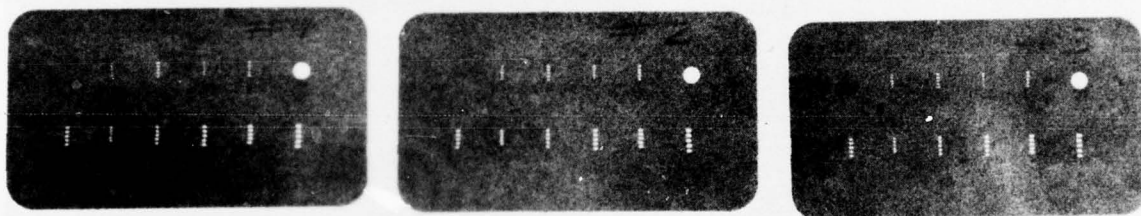
Figure 31.   Sheet Specimens with Etched Holes for
            Determining Minimum Hole Size for the
            Waspaloy Laminate Sheets.

67
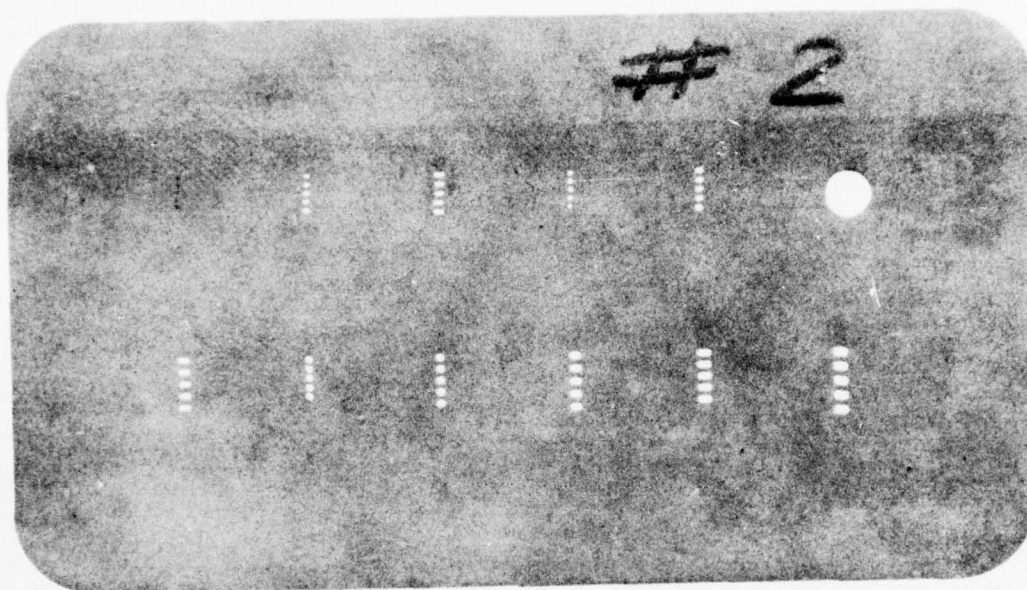
Figure 32.   Specimen of Etching Evaluation for Hole Size
for the Waspaloy Laminate Sheets.

DIMENSIONS (D)

HW = HOLE WIDTH
CW = CAVITY WIDTH
C = CAVITY HEIGHT
H. = HOLE HEIGHT
P = PIN SPACING

TOOLING
LINE
WIDTH
A = 0.004
B = 0.007
C = 0.010
D = 0.014

0.010 X 0.010   PIN 0.010

0.010 X 0.020   PIN 0.014

0.010 X 0.03   PIN 0.016

0.013 X 0.013   PIN 0.010

0.013 X 0.02   PIN 0.013

0.125 GAUGE HOLE

0.020 X 0.036   PIN 0.020

0.016 X 0.036   PIN 0.016

0.016 X 0.03   PIN 0.020

0.016 X 0.02   PIN 0.016

0.016 X 0.016   PIN 0.010

0.013 X 0.03   PIN 0.020

1A   2A   3A   4B   5B

6B   7C   8C   9C   10C   11C
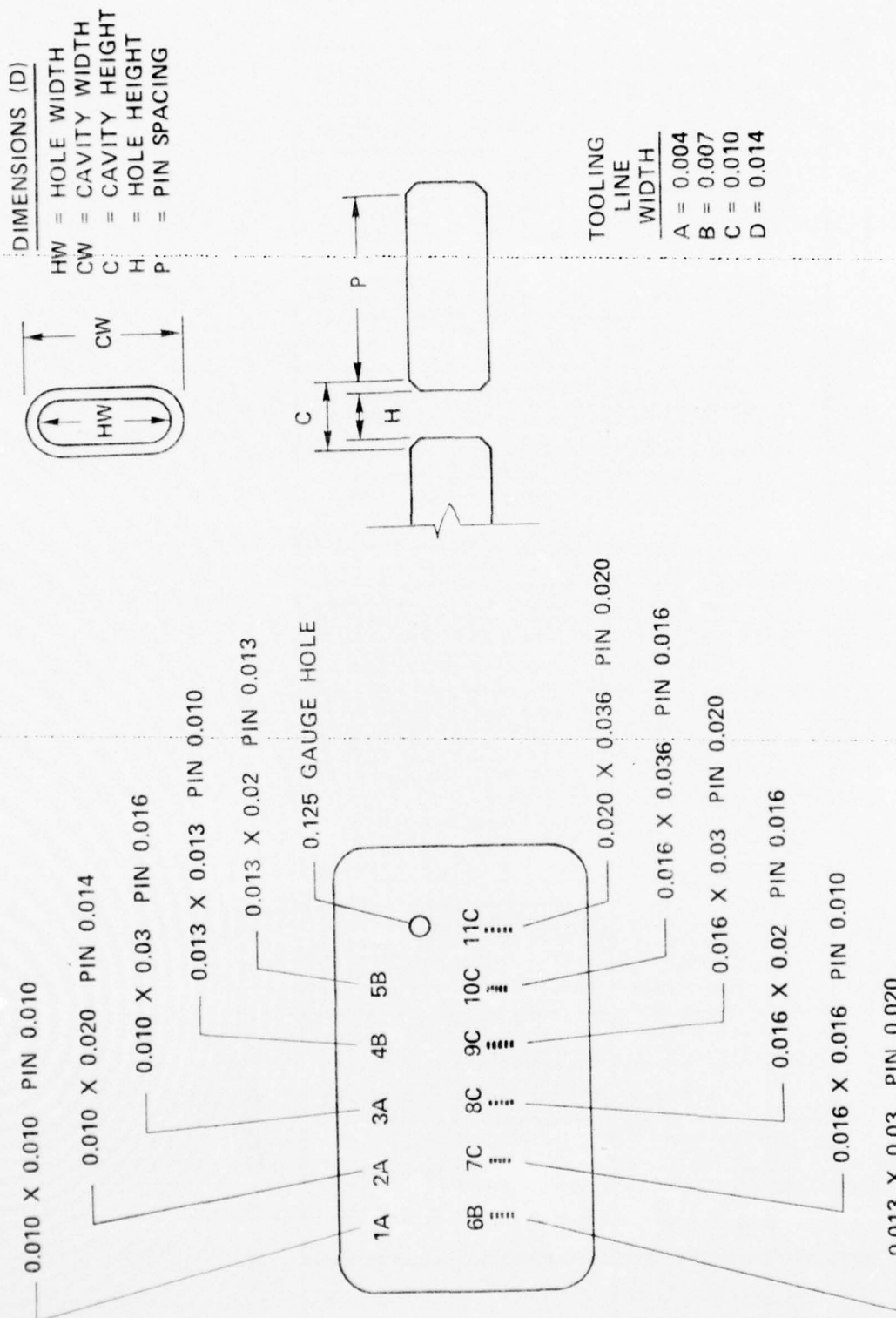
Figure 33.   Layout of Cooling Passage Inspection Test Laminate Sheets.

69

TABLE 4. COOLING PASSAGE INSPECTION TEST RESULTS.

Sheet No.	(D)*	SPECIMEN NUMBER										
		1	2	3	4	5	6	7	8	9	10	11
1	C	C=0.009	0.011	0.011	0.012	0.015	0.014	0.017	0.013	0.018	0.019	0.023
	H	H-	0.008	0.008	0.009	0.011	0.014	0.015	0.013	0.018	0.019	0.023
	P	Not	0.013	0.015	0.010	0.011	0.018	0.008	0.014	0.017	0.014	0.018
	CW	Thru	0.017	0.029	0.012	0.020	0.030	0.017	0.023	0.034	0.037	0.038
	HW		0.014	0.023	0.009	0.018	0.030	0.015	0.021	0.030	0.035	0.038
2	C	C=0.008	0.011	0.012	0.014	0.015	0.014	0.018	0.018	0.019	0.018	0.023
	H	H-	0.009	0.008	0.011	0.014	0.014	0.016	0.017	0.018	0.017	0.021
	P	Not	0.012	0.016	0.011	0.012	0.019	0.008	0.014	0.017	0.015	0.018
	CW	Thru	0.017	0.028	0.014	0.020	0.030	0.018	0.022	0.031	0.038	0.038
	HW		0.015	0.024	0.011	0.018	0.029	0.016	0.021	0.031	0.032	0.032
3	C	C=0.009	0.011	0.009	0.013	0.013	0.015	0.016	0.018	0.019	0.018	0.020
	H	H-	0.007	0.008	0.008	0.012	0.014	0.015	0.016	0.018	0.018	0.020
	P	Not	0.013	0.015	0.010	0.014	0.019	0.010	0.014	0.018	0.015	0.020
	CW	Thru	0.018	0.023	0.013	0.020	0.030	0.016	0.021	0.031	0.036	0.037
	HW		0.014	0.023	0.008	0.018	0.029	0.015	0.021	0.030	0.036	0.037

*(D) - Refer to Figure 33.

results is B (0.007 inch), and this, coupled with the number 6 hole size (0.013 inch by 0.030 inch), defined the minimum size hole that can be etched accurately in 0.010-inch Waspaloy sheet stock. The 0.020-inch Waspaloy sheet used in the detail design has relatively large passages, and a consistent etching was achieved with an 0.018-inch line width.

The testing and investigations assisted in defining two design rules:

o   First, the line width must be constant for a given material and thickness on any single lamination.

o   Second, the smallest hole in a given design etches more consistently if a ratio of 1:1:3 or greater is maintained for the dimensions of material thickness, narrowest hole dimension, and longest hole dimension.

The final rotor detail design is shown in Figure 34 [(a) through (d)].

The design utilizes a total of 62 laminates, 24 of which are of 0.020-inch sheet stock and 38 of 0.010-inch sheet stock. Each of these laminates has a different cooling passage definition to enable the properly stacked laminates to have the desired blade and disk internal cooling passage arrangement. The laminates are sandwiched between two solid end plates of Waspaloy to form the remainder of the turbine disk. The external blade and disk shape is designed to be machined after bonding of the wheel elements.
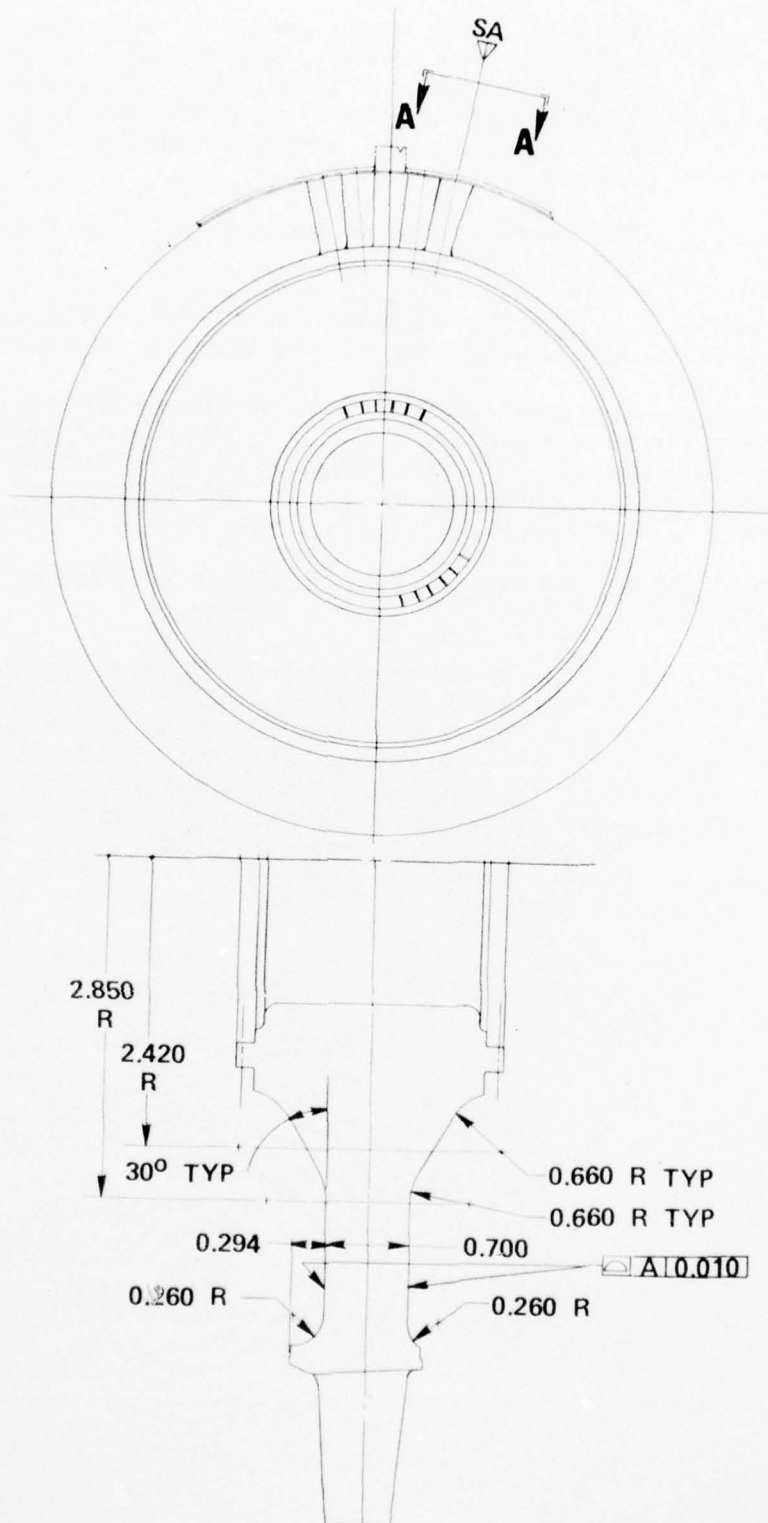
Figure 34. (a) Final Laminated Turbine Rotor Detail Design.

Figure 34. Continued (b)

73

LEADING EDGE

STACKING POINT

– LAMINATES

+ LAMINATES

TRAILING EDGE

0.0629 CENTER OF LAMINATE +1 VENT PASSAGE AT R=5.5750

STACKING PLANE

TOOLING AID FOR BLADE POSITIONING

AFT SIDE OF ROTOR
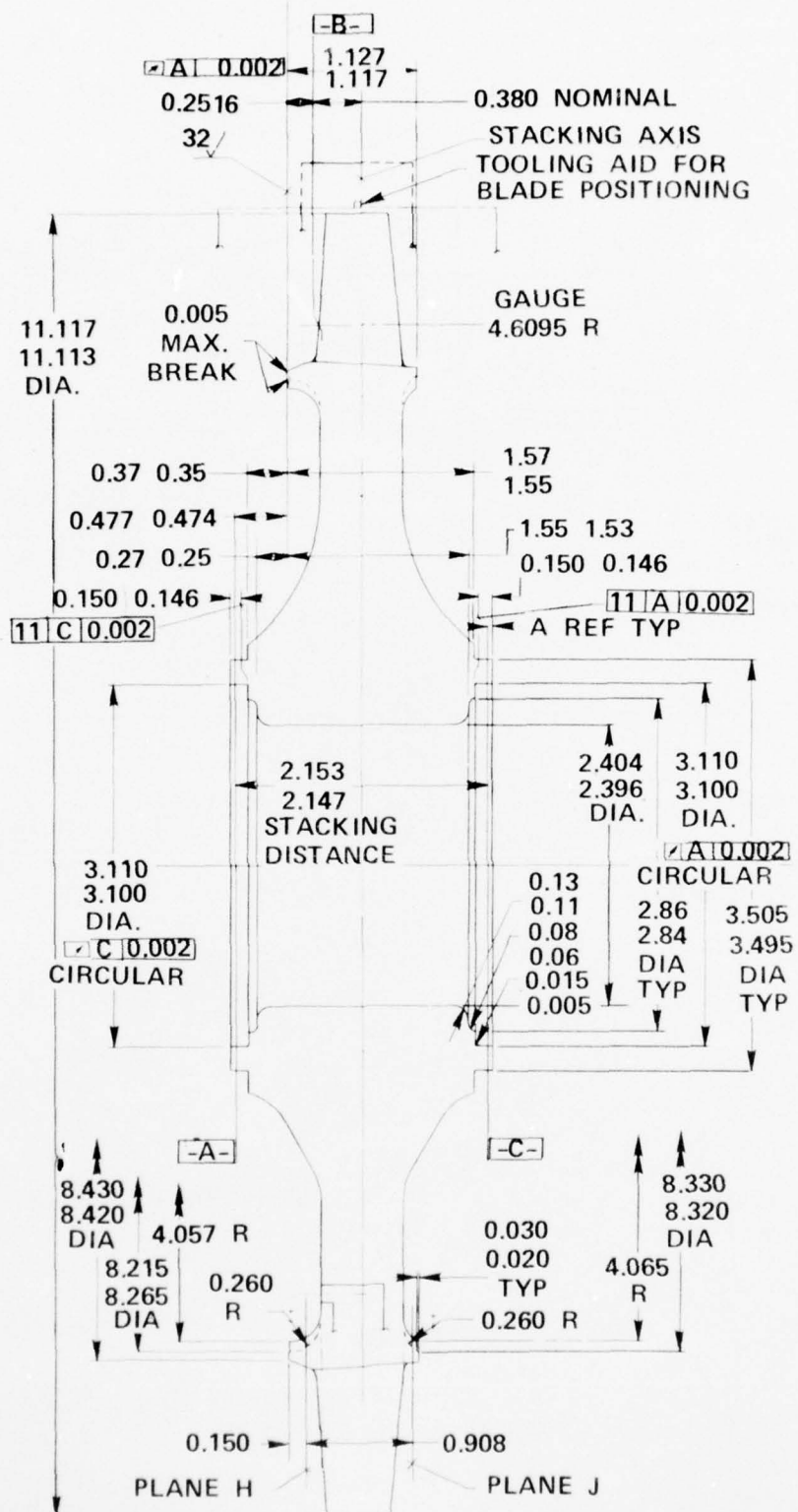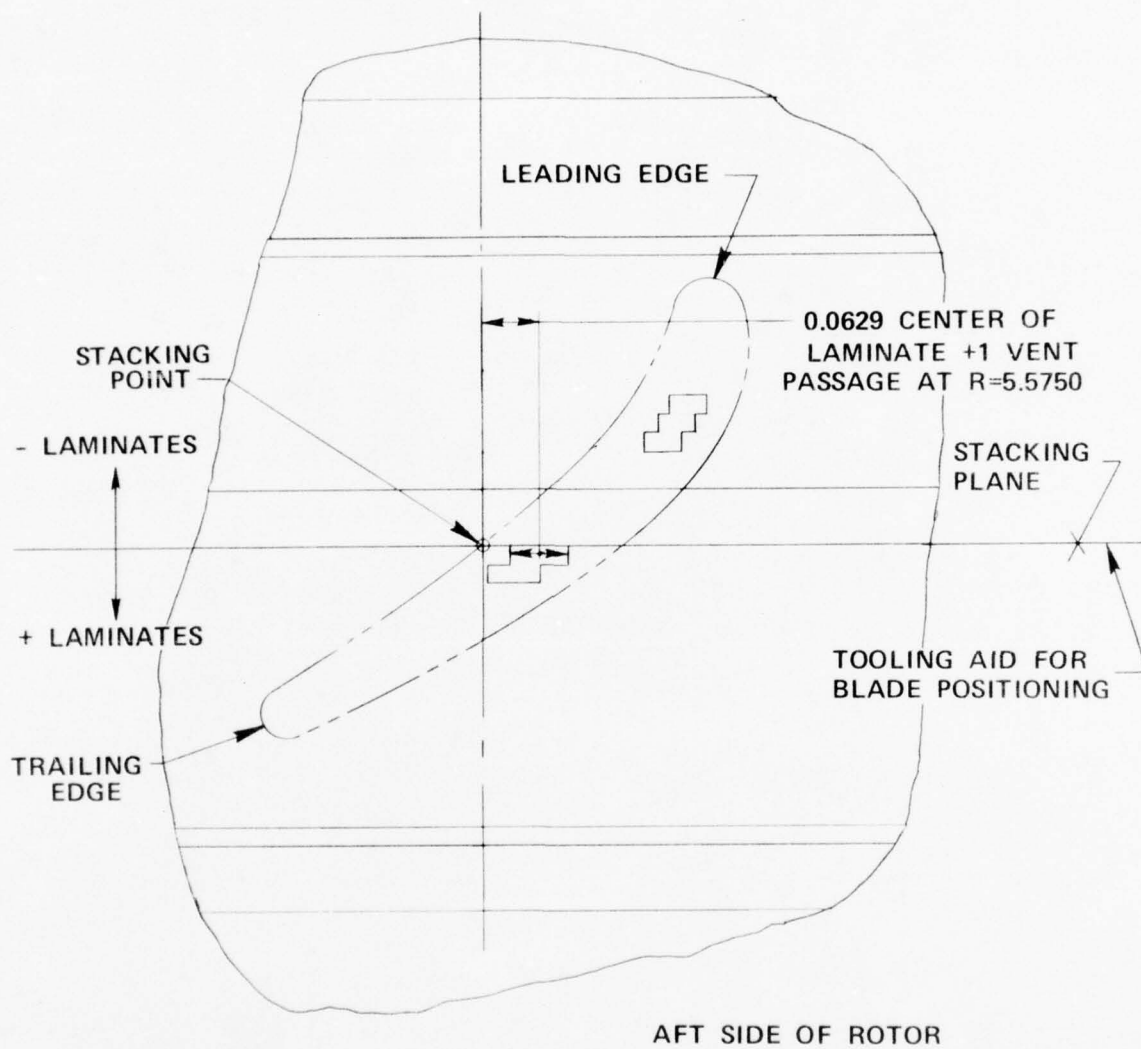
SECTION A-A

TYPICAL BLADE LOCATION

Figure 34. Continued (c)

74

Figure 34. Continued (d)

0.500

STACKING
AXIS

0.250

0.100

30°

LAMINATE NUMBER TO BE READ
WITH "V" NOTCH AT BOTTOM OF
NUMBER

6.000

0.100

11.320-INCH DIAMETER
REFERENCE FOR
LAMINATES NUMBER:
-1, -2, -3, -22, -23,
+25 AND +26 ONLY

11.200-INCH DIAMETER
REFERENCE FOR
ALL LAMINATES OTHER
THAN THOSE
NOTED ABOVE

TYPICAL LAMINATE
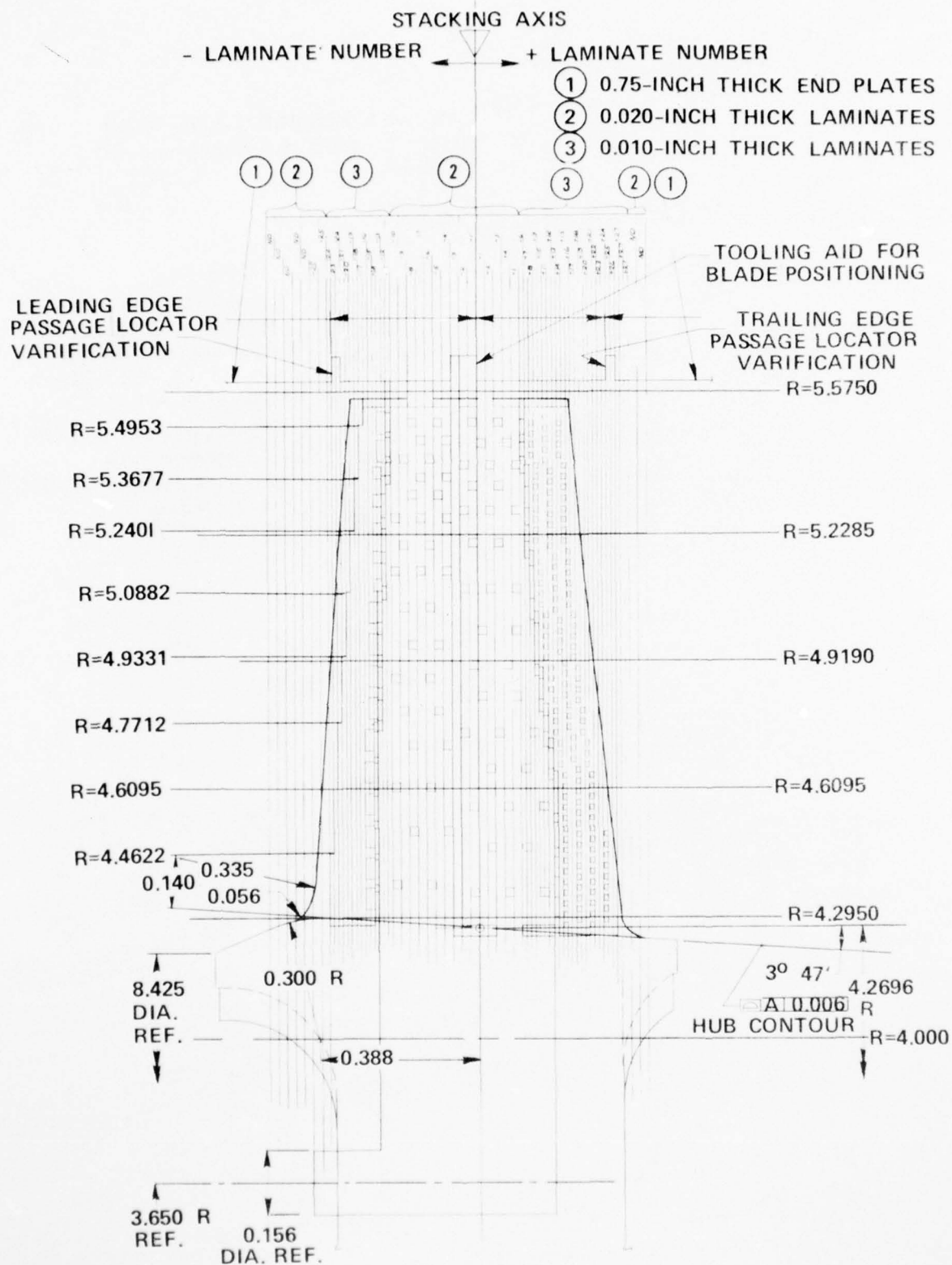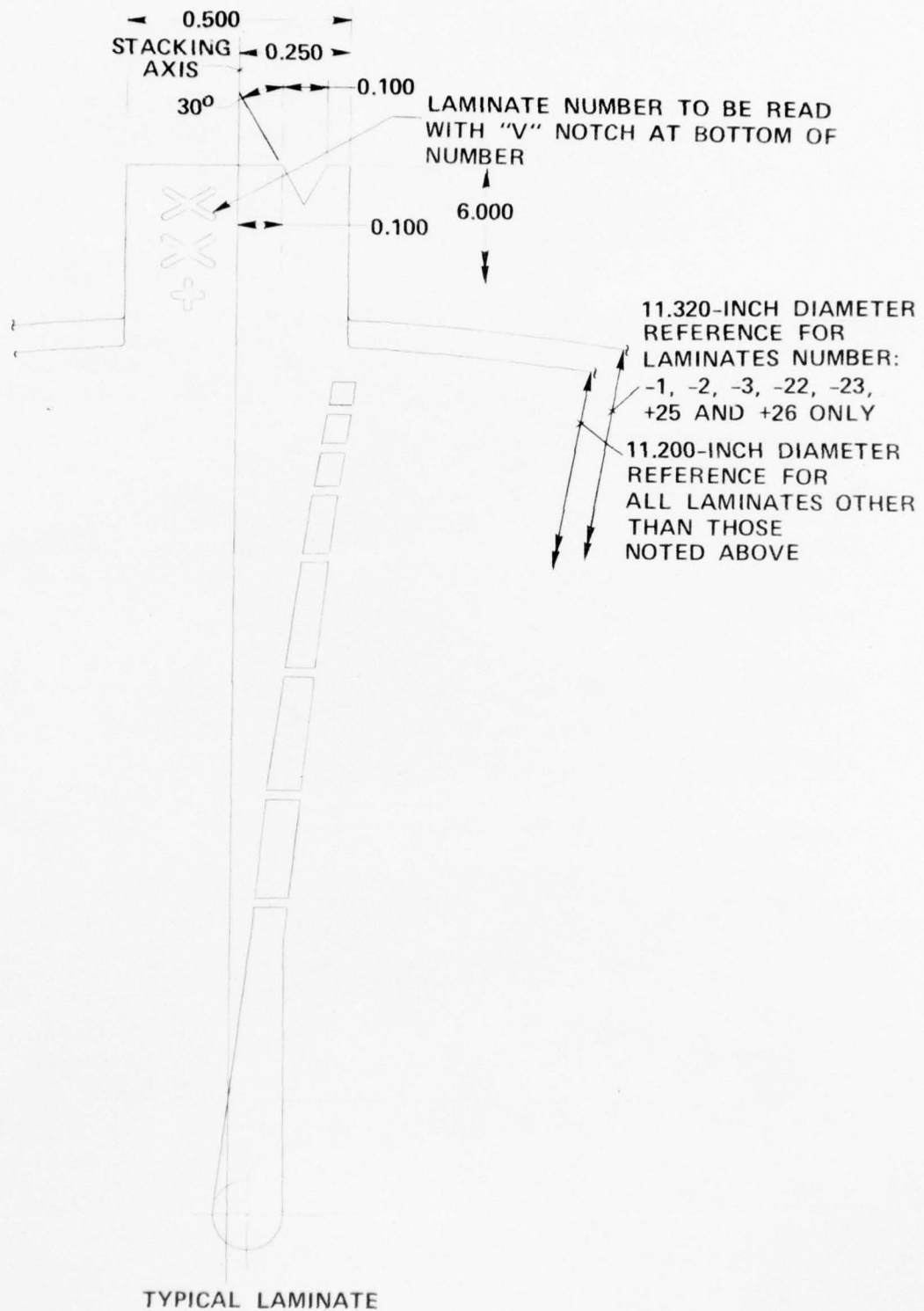
Figure 34. Concluded (e)

SECTION IV

MANUFACTURING METHODS TASK

The manufacturing methods task consisted of optimizing
photoetching and bonding parameters to an extent that would
permit fabrication of an integral-cooled laminated turbine
wheel. This task included the evaluation of photoetching
Waspaloy laminations, bonding processes, and bond alloys utiliz-
ing a number of small test stacks and one large stack (simulating
the thermal mass and dimensions of a full-size wheel blank).
This task included mechanical property testing of the small test
stacks, development of the full-size wheel blank bonding tool,
and of an ultrasonic nondestructive testing method to verify
the soundness of bonds in the turbine wheel blank. The task
was concluded with the finish machining of a bonded laminated
turbine wheel.

1.   BONDING OPTIMIZATION

   a.   Laboratory Evaluation of Activated-Diffusion Bonding
        Alloys

Candidate commercial brazing alloys were obtained as argon-
atomized powder from Alloy Metals Inc., Troy, Michigan in
-100 to +325 mesh fraction. Three alloys designated AMI-914,
AMI-915, and AMI-915E were evaluated on the basis of flow and
bond interface characteristics. The nominal composition of these
alloys is given in Table 5.

Tests were conducted with T-joint specimens prepared from
0.020-inch Waspaloy sheet to determine the liquidus temperatures
of the three alloys. The liquidus temperatures determined for
these alloys are shown in Table 6 as compared to the alloy
producers published liquidus temperatures.

   b.   Bond Property Determination

   (1)   Stacks 1, 2, and 3

A quantity of 12-inch by 18-inch by 0.020-inch thick
Waspaloy sheet was photoetched to provide rectangular laminates
1.4-inches wide by 2.2-inches long. The photoetched laminates
were cleaned prior to bond-alloy application as specified in the
sequence listed below:

   (a)   Vapor degrease for 4 to 5 minutes

   (b)   Having previously laid the sheets flat to prevent
         warpage, vapor-hone at 40- to 60-psig pressure while
         holding the nozzle 6 to 8 inches from the surface

   (c)   Cold-water rinse (tap water)

77
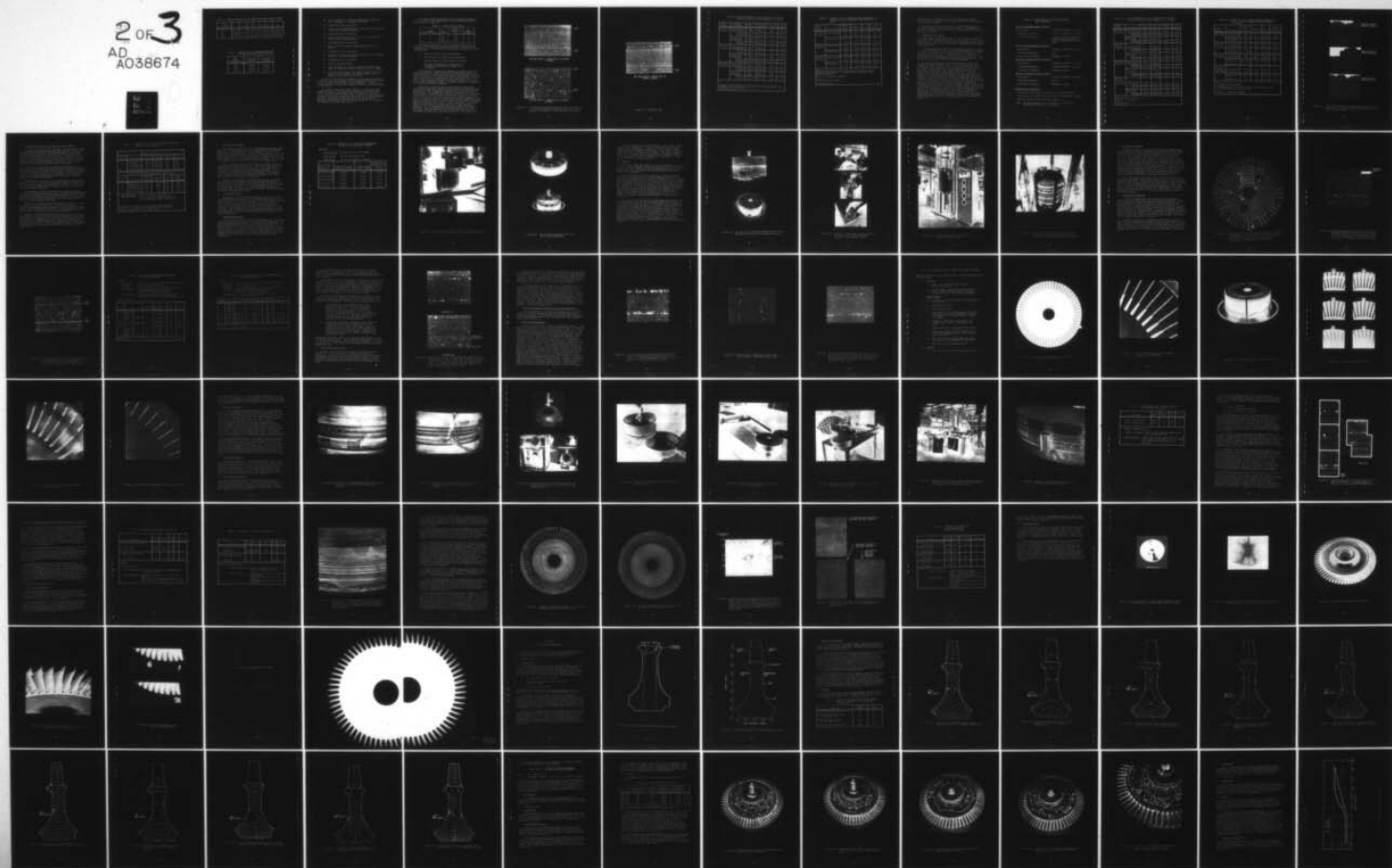
TABLE 5. NOMINAL COMPOSITION OF THREE CANDIDATE BRAZING ALLOYS.

AMI Alloy Designation	C	Cr	Si	B	Fe	Co	Ni
914	0.03	---	4.5	3.5	---	20.0	Balance
915	0.02	13.0	4.0	3.0	4.0	---	Balance
915E	0.03	15.1	3.1	2.6	---	22.4	Balance

TABLE 6. COMPARISON OF LIQUIDUS TEMPERATURES OF THREE CANDIDATE BRAZING ALLOYS.

AMI Alloy Designation	Published Liquidus	Determined Liquidus
914	1940°F	1975°F
915	2150°F	2130°F
915E	2112°F	2025°F

(d) Apply Wyndote F.S. alkaline commercial cleaner for 4 to 5 minutes (no current, only soak)

(e) Cold-water rinse (tap water)

(f) Pickle in 50-percent Muriatic acid for 4 to 5 minutes (Fresh acid is not necessary)

(g) Cold-water rinse (tap water)

(h) Place in 50-percent nitric acid for 4 to 5 minutes (Fresh acid is not necessary)

(i) Cold-water rinse (tap water)

(j) Apply alkaline cleaner (same as above) for 4 to 5 minutes

(k) Cold-water rinse (tap water)

(l) Pickle in 50-percent Muriatic acid for 4 to 5 minutes (Fresh acid is not necessary)

(m) Cold-water rinse (tap water)

(n) Rinse in dionized water

(o) Vapor degrease for 10 to 15 minutes with the sheet held in a vertical position (spray at least 3 times)

(p) Stack the clean superalloy sheets between individual sheets of brown paper. The sheets should only be handled using clean white gloves.

Bond alloy application consisted of hand spraying the ADB powder and an acrylic binder with an appropriate solvent to form a uniform layer on one side of each lamination. Sufficient coated laminations were then stacked to yield an unbonded height of 2.1 inches.

All small sheet stacks were bonded in a laboratory ABAR Vacuum Hot Press. This equipment provides a hot zone three-inches square by eight-inches high. The stack is centered within the hot zone on rigidly-mounted vertical rams that can be adjusted to apply a controlled axial force to the stack during bonding. The press is equipped with up to eight type-K sheathed thermocouples that can be positioned at any location in the furnace or on the bond tooling.

The three stacks were bonded with an applied pressure of 15 psi normal to the laminations utilizing the bond thermal cycles shown in Table 7.

TABLE 7. BOND THERMAL CYCLES.

Stack Designation No.	Bond Alloy	Bond Temperature (°F)	Time (Hours)
1	914	1975	2
2	915	2130	2
3	915E	2025	2

The three stacks were given a post-bond diffusion heat treatment of three hours at 2000°F in order to improve joint homogenization. This cycle was followed by a three-cycle heat treatment of:

1. 4 hours at 1975°F with air cooling*

2. Plus 4 hours at 1550°F with air cooling*

3. Plus 16 hours at 1400°F with air cooling*

    *All heat treatment was conducted in a
     protective atmosphere of argon or in
     a vacuum.

Metallographic samples were removed from each stack after bonding and prior to the three-hour diffusion-heat treatment. Considerable grain growth was observed in these stacks, particularly in Stack 2, as a result of heating the Waspaloy above the gamma-prime solvus; approximately 1925° [see Figure 35 (a) and (b)]. Metallographic sections from these stacks (after post-bond thermal treatment) showed no observed change as a result of the post-bond thermal treatments.

Mechanical properties were established for these three stacks using specimens taken parallel (longitudinal orientation) and perpendicular (transverse orientation) to the plane of the laminations. Room-temperature tensile properties and 1500°F stress-rupture properties were obtained in these two orientations (see Tables 8 and 9). Examination of these properties showed Stack 1 to have the best room-temperature tensile properties in both orientations, with the longitudinal values similar to forged Waspaloy given the 1825°F solution treatment per AMS (AiResearch Materials Specification) 5544B. Stack 1 provided longitudinal 1500°F stress-rupture strength approaching the base-metal strength, but the transverse orientation showed low-rupture strength. The room-temperature tensile properties of Stack 2 and 3 were approximately the same in both orientations, but considerably lower than the Stack 1 material. At 1500°F, the

80
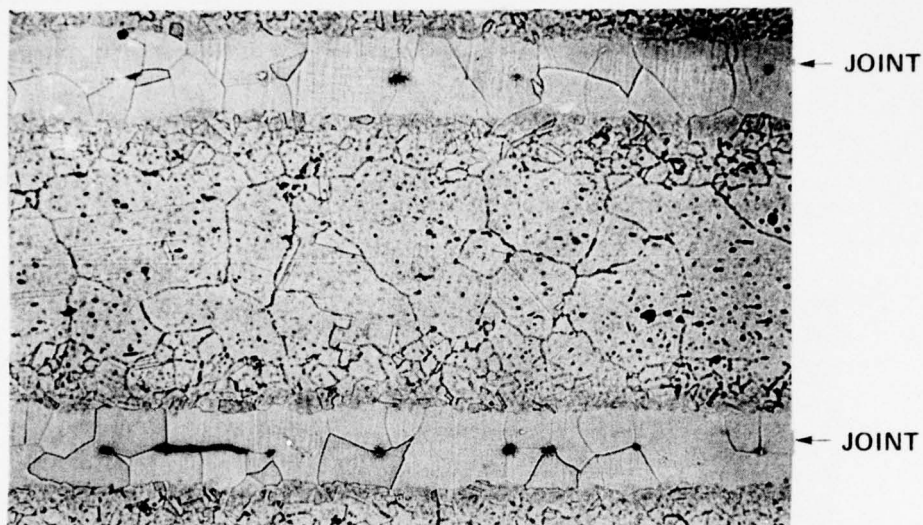
→ JOINT

→ JOINT

**AMI 914, STACK 1 - BOND CYCLE OF 2 HOURS
AT 1975°F**
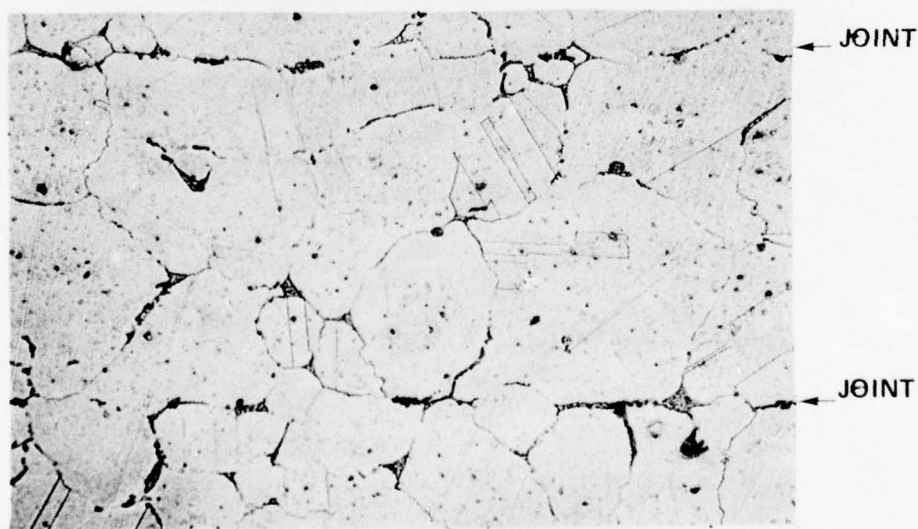
→ JOINT

→ JOINT

**AMI 915, STACK 2 - BOND CYCLE OF 2 HOURS
AT 2130°F**

Figure 35.   (a) Optical Micrographs Showing Bond-Joint Regions
            in 0.020-inch Waspaloy Sheet Stacks (1, 2, and 3)
            Bonded as Indicated. (Kallings etch) (Mag.:100X)

81

← JOINT

← JOINT
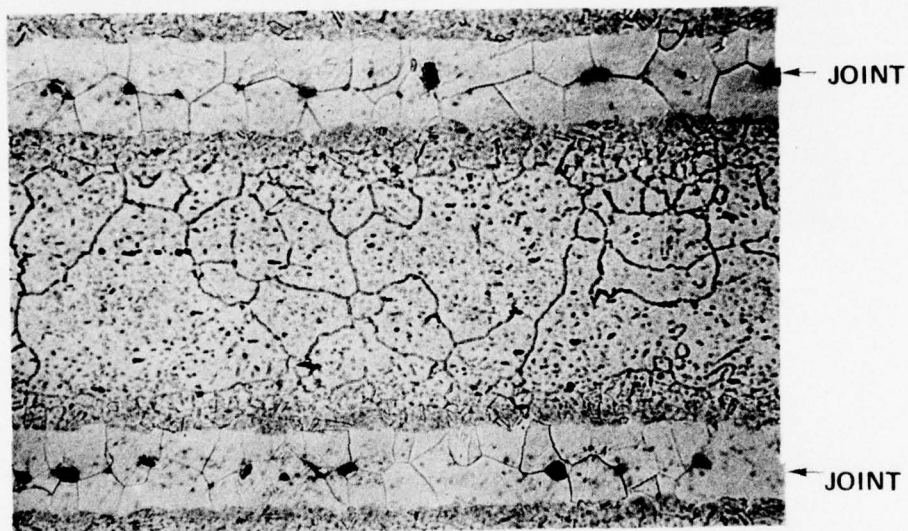
**AMI 915E, STACK 3 – BOND CYCLE OF
2 HOURS AT 2025°F**

Figure 35.   Concluded (b).

82

TABLE 8. ROOM-TEMPERATURE TENSILE PROPERTIES OF BONDED
0.020-INCH WASPALOY SHEET STACKS 1, 2, AND 3.

Bond Alloy	Specimen Orientation	0.2% Y.S. (ksi)	U.T.S. (ksi)	Elongation (%)	R of A (%)
AMI 914 (Stack 1)	Longitudinal Longitudinal	128.0 127.0	184.5 180.2	14.5 12.0	11.5 11.5
	Average	127.5	182.2	13.3	11.5
	Transverse Transverse	124.5 125.0	147.5 143.8	4.5 3.0	4.5 2.5
	Average	124.8	145.6	3.8	3.5
AMI 915 (Stack 2)	Longitudinal Longitudinal	112.8 111.5	135.0 128.2	3.5 3.5	1.5 1.5
	Average	112.2	131.6	3.5	1.5
	Transverse Transverse	110.0 110.6	115.0 117.5	2.0 1.5	<1.0 <1.0
	Average	110.3	116.3	1.8	<1.0
AMI 915E (Stack 3)	Longitudinal Longitudinal	116.1 117.0	136.1 133.8	3.5 3.5	2.0 2.5
	Average	116.6	135.0	3.5	2.3
	Transverse Transverse	113.1 116.2	119.5 130.0	2.0 3.0	<1.0 1.0
	Average	114.7	124.8	2.5	<1.0

Typical forged Waspaloy room-temperature tensile properties
(1950°F solution temperature) 122 0.2% Y.S., 188 U.T.S., 25.5%
elongation, 26.3% R of A.

TABLE 9. 1500°F/47.5 KSI STRESS-RUPTURE PROPERTIES OF
BONDED 0.020-INCH WASPALOY SHEET STACKS 1, 2,
AND 3.

Bond Alloy	Orientation	Rupture Life (Hours)	Elongation (%)	R of A (%)	L-M[3] Parameters
AMI 914 (Stack 1)	Longitudinal	25.0	40.0	33.1	41.9
		24.0	29.5	37.0	41.8
	Transverse	F.O.L.[1]	<1.0	1.0	---
		0.6	<1.5	1.0	38.7
AMI 915 (Stack 2)	Longitudinal	56.0	19.0	25.4	42.6
		42.5	26.0	27.2	42.4
	Transverse	36.0	3.5	3.2	42.3
		49.0	10.5	11.0	42.5
AMI 915E (Stack 3)	Longitudinal	25.0[2]	---	---	42.0
		25.0	25.0	29.2	42.0
	Transverse	0.4	0.5	<1.0	38.4
		0.1	0.0	0.0	37.5

Typical forged Waspaloy stress-rupture properties (1950°F solution temperature), 47.5 ksi/1500°F: 54 hours, 28.0-percent elongation

[1] F.O.L. - failed on loading.

[2] Furnace malfunction.

[3] Larson-Miller

84

stress-rupture strength of Stack 2 was excellent in both orientations, and considerably higher than was provided by the other two bond alloys.

Based upon these observations, a second bond cycle and post-bond thermal treatment was selected for investigation. This was to achieve a better balance between tensile and stress-rupture properties.

(2) Stacks 4, 5, 6, and 7

Three sheet stacks (Stacks 4, 5, and 6) were prepared for bonding by the same process as the previous stacks. A fourth stack (Stack 7) was also prepared using 0.002-inch nominal thickness AMI 915 bond alloy in tape form as the bond-alloy application technique.

Bonding procedures were the same as those noted for Stacks 1, 2 and 3; however, the axial load during bonding was reduced to 12 psi. The bond thermal cycle for each of the four stacks is described in Table 10. Stacks 4 and 6 were post-bond diffusion cycled to promote joint ductility, and then all four stacks were given the Waspaloy three-cycle heat treatment. All but Stack 4 received a 1975°F solution treatment.

Mechanical properties were established for these four stacks, as shown in Tables 11 and 12, in order to provide a comparison to the previous stacks as shown in Tables 8 and 9. Stack 4 again exhibited the highest-tensile properties in both test orientations. The lowest tensile strength was exhibited by the 915E bonded stack, (Stack 6). This is attributed to the increased void formation in the bond joint. Comparison of the two AMI 915 stacks, the sprayed-alloy powder (Stack 5), and the tape alloy (Stack 7) showed that the tape provided a definite advantage in tensile strength and ductility in both orientations. This is attributed to a reduction of the apparent joint width by 50 percent, as seen in Figure 36. Comparison of the two AMI 915-sprayed-alloy stacks (Stacks 2 and 5) bonded, respectively, at 2130° and 2090°F showed that lowering the bond temperature reduced the transverse-rupture life and ductility 50 percent, but had little effect on the tensile properties. A further comparison of Stack 2 and Stack 7 showed that the lower bond temperature gave three times less transverse-rupture life and ductility while gaining 20-percent better transverse-tensile strength, and double the tensile ductility.

85

TABLE 10. BOND THERMAL CYCLE AND POST-BOND
HEAT TREATMENT.

AMI 914 (sprayed powder), Stack 4

Bond cycle: 6 hours at 2000°F (in vacuum)

Post-bond diffusion: 3 hours at 2000°F (in vacuum)

Final heat treatment: 4 hours at 1900°F solution
treatment (in air), plus bal-
ance of Waspaloy heat treat-
ment*

AMI 915 (sprayed powder), Stack 5

Bond cycle: 6 hours at 2090°F (in vacuum)

Post-bond diffusion: None

Final heat treatment: Waspaloy 3 cycle*

AMI 915E (sprayed powder), Stack 6

Bond cycle: 6 hours at 2050°F (in vacuum)

Post-bond diffusion: 6 hours at 2070°F (in vacuum)

Final heat treatment: Waspaloy 3 cycle*

AMI 915 (0.002-inch tape), Stack 7

Bond cycle: 6 hours at 2090°F (in vacuum)

Post-bond diffusion: None

Final heat treatment: Waspaloy 3 cycle*

*Waspaloy heat treatment:

4 hours at 1975°F with air cooling - solution treatment

plus 4 hours at 1550°F with air cooling - double-age treatment

plus 16 hours at 1400°F with air cooling

NOTE: All heat treatment was conducted in a protective
atmosphere of argon or in a vacuum.

86

TABLE 11. ROOM-TEMPERATURE TENSILE PROPERTIES OF BONDED 0.020-INCH WASPALOY SHEET STACKS 4, 5, 6, AND 7.

Bond Alloy	Orientation	0.2% Y.S. (ksi)	U.T.S. (ksi)	Elongation (%)	R of A (%)
AMI 914 (Stack 4)	Longitudinal	129.2	184.0	14.0	13.5
	Longitudinal	126.8	173.0	10.0	7.8
	Average	128.0	178.5	12.0	10.7
	Transverse	126.5	165.5	8.0	5.5
	Transverse	--(1)	107.0	1.0	1.0
	Average	126.5	165.5	8.0	5.5
AMI 915 (powder) (Stack 5)	Longitudinal	---	141.0	4.0	4.0
	Longitudinal	---	144.0	5.0	4.3
	Average	---	142.5	4.5	4.2
	Transverse	---	109.0	1.0	1.0
	Transverse	---	122.0	1.0	1.0
	Average	---	115.5	1.0	1.0
AMI 915E (Stack 6)	Longitudinal	117.0	131.0	3.5	1.1
	Longitudinal	---	134.0	1.5	1.0
	Average	117.0	132.5	2.5	1.1
	Transverse	--- (2)	69.2	1.0	1.0
	Transverse	--- (3)	3.05	1.0	1.0
	Average	---	69.2	1.0	1.0
AMI 915 (0.002-inch tape) (Stack 7)	Longitudinal	117.5	151.5	6.0	6.6
	Longitudinal	116.8	153.5	7.0	5.9
	Average	117.2	152.5	6.5	6.3
	Transverse	115.8	141.0	3.0	1.9
	Transverse	118.6	146.0	4.0	4.3
	Average	117.2	143.5	3.5	3.1

(1) Bond defect present
(2) Broke in threads
(3) Bond defect

TABLE 12. 1500°F/47.5 KSI STRESS-RUPTURE PROPERTIES OF
BONDED 0.020-INCH WASPALOY SHEET STACKS, 4,
5, 6, AND 7.

Bond Alloy	Orientation	Rupture Life (Hours)	Elongation (%)	R of A (%)	Larson-Miller Parameters
AMI 914 (Stack 4)	Longitudinal	20.9	28.0	32.0	41.8
	Longitudinal	41.3	21.0	23.0	42.4
	Transverse	0.0	0.5	<0.5	---
	Transverse	0.2	0.8	0.7	---
AMI 915 (spray) (Stack 5)	Longitudinal	44.0	24.0	20.1	42.4
	Longitudinal	33.0	20.0	26.0	42.2
	Transverse	22.1	3.0	3.6	41.9
	Transverse	3.5[1]	1.0	<0.5	40.3
AMI 915E (Stack 6)	Longitudinal	20.9	12.0	16.0	41.8
	Longitudinal	29.5	19.0	19.0	42.1
	Transverse	F.O.L. [3]	<0.5	<0.5	---
	Transverse	F.O.L. [3]	<0.5	<0.5	---
AMI 915 (0.002-inch tape) (Stack 7)	Longitudinal	39.0	22.5	23.0	42.3
	Longitudinal	33.2[2]	17.0	23.3	42.2
	Transverse	16.0	2.0	2.3	41.5
	Transverse	16.0	2.0	<0.5	41.5

[1] Suspected gauge defect

[2] Temperature control malfunction. Total specimen time 64.2 hours with 31 hours at 14°F

[3] F.O.L. - failed on loading

88
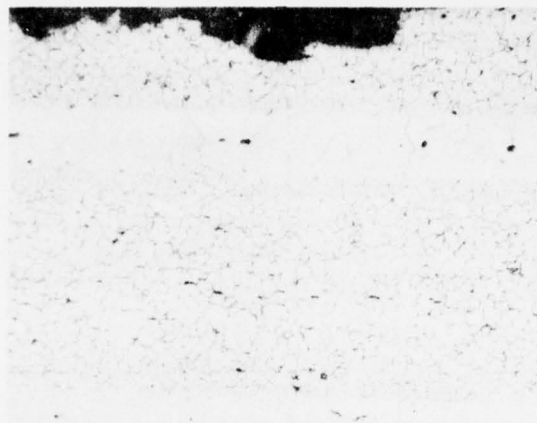
AMI 914, STACK 4
(SPRAYED POWDER)

AMI 915, STACK 5
(SPRAYED POWDER)

AMI 915, STACK 7
(0.002-INCH TAPE)

Figure 36.   Optical Micrographs of Traverse-Orientation Tensile
             Specimens of 0.020-Inch Waspaloy Sheet Stacks 4, 5,
             and 7.   (Mag.: 100X)

89

c.   Bond-Process Selection - Stacks 8, 9, 10, and 11

With the information then available, the bond alloy, application technique, and the tentative bond thermal cycle were selected that would provide the best balance of tensile and stress-rupture properties for Waspaloy. Evaluation of the mechanical properties of Stacks 1 through 7 indicated that AMI 915 was the most suitable bond alloy. While AMI 915 does not offer as high tensile properties as AMI 914, it does provide superior stress-rupture strength in both test orientations together with higher transverse-rupture ductility.

Use of tape as the alloy application technique was also selected, since this will provide improved process control while potentially offering somewhat higher tensile properties resulting from the reduced amount of bond alloy at the bond interface. In order to define optimum bond temperature, four additional small sheet stacks were prepared for bonding for 6 hours at 2110°, 2115°, 2140°, and 2150°F.

Four stacks were prepared for bonding by the same process used for Stack 7. Stack 8 was bonded at 2140°F, and was given the same Waspaloy heat treatment used for Stacks 1 through 7, while the other three stacks (Stacks 9, 10, and 11) were left in the as-bonded condition.

Metallographic sections removed from these four stacks revealed that temperatures below 2140°F resulted in some porosity at the bond interface. At bond temperatures above 2115°F, the Waspaloy grain boundarys were found to contain a eutectic phase with the simultaneous elimination of the thin layer of bond material at the original bond line.

Mechanical properties were established for Stack 8 bonded at 2140°F (as shown in Table 13). This stack exhibited tensile and stress-rupture properties that were slightly higher in both test orientations than Stack 2, which was also bonded at 2140°F, but with sprayed ADB alloy (see Tables 8 and 9).

Based on the results of the last four stacks, the six-hour 2140°F bond cycle was selected for use in bonding a large wheel blank stack. A temperature variation of +20°F was anticipated in bonding this large blank stack. Based upon the previous metallographic evidence, defect-free joints were produced when bonding in the 2120° to 2160°F temperature range, and therefore, the 2140°F bond temperature was expected to produce a sound wheel blank.

TABLE 13.   MECHANICAL PROPERTIES OF BONDED 0.020-INCH
            WASPALOY SHEET STACK 8.

Tensile Properties					
Specimen No.	Orientation	0.2% Y.S. (ksi)	U.T.S. (ksi)	Elongation (%)	R of A (%)
1	Transverse	112.5	117.5	1.5	1.9
2	Transverse	112.5	125.0	2.0	4.0
5	Longitudinal	113.3	132.5	2.5	4.0
6	Longitudinal	113.3	138.0	3.0	1.2
*	Longitudinal	116.5	175.3	13.5	---

1500°F Stress-Rupture Properties - 47.5 ksi					
Specimen No.	Orientation	Rupture Life (Hours)	Elongation (%)	R of A (%)	Larson-Miller Parameter
3	Transverse	54.1	6.0	5.9	42.6
4	Transverse	47.4	4.0	4.3	42.5
7	Longitudinal	63.1	19.0	8.2	42.7
8	Longitudinal	47.0	17.5	12.4	42.5
*	Longitudinal	67.8	7.4	---	39.5

Heat Treatment: 2 hours at 1975°F with air cool
                  plus 4 hours at 1550°F with air cool
                  plus 16 hours at 1400°F with air cool

*0.020-inch Waspaloy sheet to specification AMS 5544B
 (62.5 ksi at 1350°F) for comparison to the bonded
 Waspaloy using AMI 915 transfer tape.

91

2.   AIRFLOW-STACK BONDING

The purpose of this task was to provide early design feedback for the optimization of flow passage shape, and to determine axial stack compression during bonding. This activity was required prior to bonding full-size wheel blanks in order to define the Z-section element locations for detail design of the wheel laminations. The program timetable required this input at a very early stage in the bond-process development task in order to accommodate the long-lead design and procurement times.

Five stacks were prepared and bonded utilizing the same processes as employed for Stack 7. Thickness of the individual laminations was measured before and after tape application to determine the average sprayed bond-joint thickness. After bonding, the bonded-stack height was determined for the five stacks before preparation for airflow testing. The average joint thickness for the five stacks was determined to range from 0.0009 to 0.0012 inch (see Table 14).

Figure 37 illustrates the airflow test setup. During airflow testing, all the stacks exhibited leakage through the laminate interfaces--negating the validity of the airflow data. The leakage was a result of joint porosity due to the low bonding temperature of 2090°F. No further airflow testing was conducted since any additional data would have occurred too late to assist the design activities.

3.   LARGE-STACK BONDING

The purpose of the large-stack bonding task was to verify the laboratory bond process on a full-scale wheel blank. The large stack simulated the approximate thermal mass and dimensions of the wheel blank, as shown in Figure 38. The photoetched laminates used in construction of this stack incorporated simplified slots and holes to simulate the wheel blank cooling passages. The chemical-milling techniques utilized to prepare the small stack laminates were appropriately refined to provide the required accuracy of laminate reproduction required in the large wheel blank.

a.   Laminate Preparation

The large stack consisted of 29 laminations, 11.2 inches in diameter by 0.020-inch thick, that were placed between two 0.75-inch thick Waspaloy end plates. Prior to tape application, the above laminate details were cleaned by the method noted in Section IV.1.b.(1) of this report. Following lamination cleaning, one layer of 12-inch wide bond tape was properly positioned on one face of each laminate. The tape overlaying the cooling passages was removed prior to bonding. Two layers of tape were applied to the interfaces between the end plates and the laminates.

TABLE 14. WASPALOY JOINT THICKNESS MEASUREMENTS
FOR THE FIVE AIRFLOW TEST STACKS.

Material:

Specification: 0.020-inch sheet, AMS 5544B

Bond Alloy: AMI 915 0.002-inch tape

Bond Cycle: 6 hours at 2090°F in vacuum

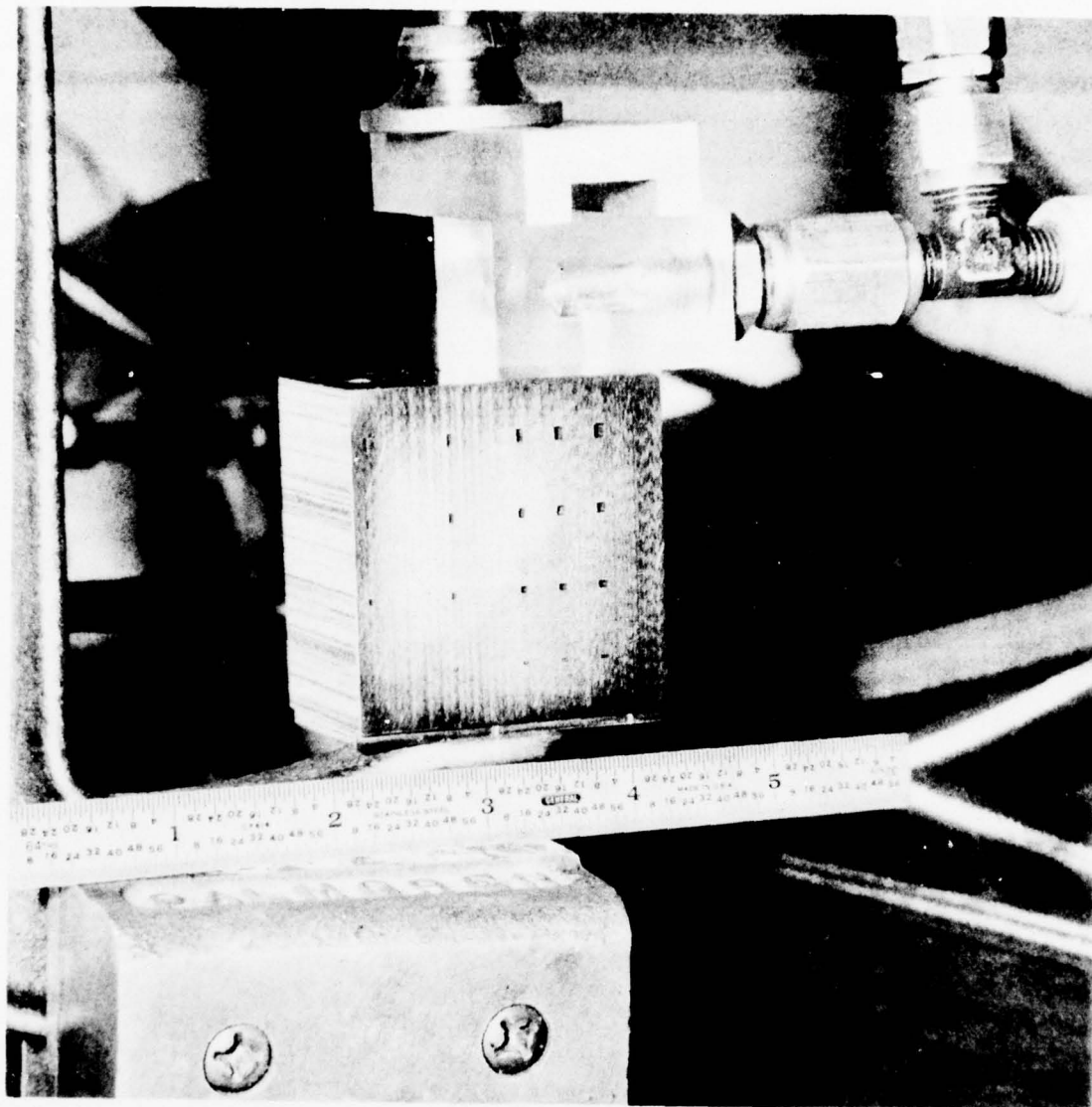| Sheet Stack I.D./No. of Laminates	Average Lamination Thickness (inch)	Average Stack Height (inch)	Calculated Average Joint Thickness (inch)
915(TPE)-A/109	0.0192	0.190	0.0009
915(TPE)-B/109	0.0191	2.210	0.0011
915(TPE)-C/109	0.0191	2.210	0.0012
915 S-1/110	0.0197	2.230	0.0011
915 S-2/110	0.0192	2.216	0.0010

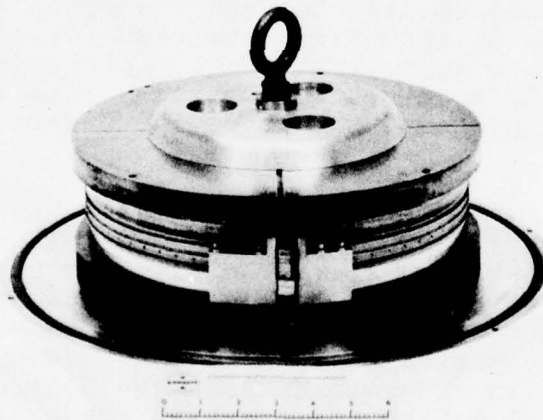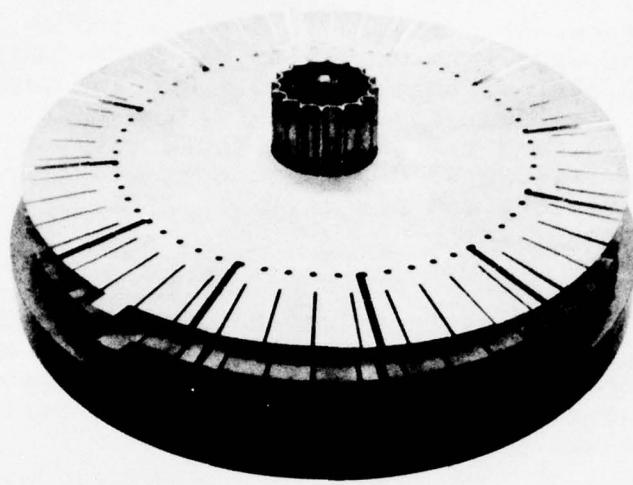Figure 37.   Test Setup for Laminate Sheet Stack Airflow Tests.

Figure 38.   Large Stack Laminates, End Plates,
and the Bonding Fixture.

The laminate and the end plates were then stacked on the bonding tool (Figure 38). Figure 39 depicts the 16 type-K thermocouples that were tack welded to the bore and outside diameter of the 0.75-inch thick plates. Two locating pins were then inserted in the lower tooling plate, the upper tooling plate was installed, and the entire fixture was then placed in the shipping box. Figure 40 depicts the stacking and crating of the laminates and the end plates.

b.   Bonding

The large stack was shipped to the bonding vendor for bonding in a 75-ton capacity vacuum hot-press furnace, as shown in Figure 41. The press design minimized bending moments introduced during axial loading, and the bonding was performed at 50-psi axial pressure.

The furnace was induction heated by a 14-inch diameter four-turn coil with directly induced assembly heating. Two plates, 4-inches thick by 12 inches in diameter, of ATJ graphite were used to provide flat tooling support to the top and bottom of the assembly, as well as, a radial heat path with minimal-heat capacity. Following placement of the lower graphite plate and assembly in the furnace, Fiberfrax-Felt was placed between the induction coil inside diameter and the assembly outside diameter to insulate against excessive heat (Figure 42). The press was evacuated to approximately 165 Pa before heating began. During the 72-hour prebond-outgass cycle at 750° to 1200°F, the chamber pressure was observed to vary from 0.1 to 3.3 Pa.

An axial load of 50 psi was applied when the assembly temperature reached 1800°F. This load was maintained throughout the remainder of the bond cycle. The assembly temperature was stabilized at 2140°F, and held for 6 hours. The steady-state temperature distribution achieved during the 6-hour hold required that the temperature of the stack outside diameter be increased to 2195°F in order to achieve the desired 2140°F minimum at the bore. As the temperature rose above 1800°F, the vacuum chamber experienced a rapid increase in pressure. This pressure increased from approximately 1.3 Pa at 1800°F to a maximum of 20 Pa at 2140°F. This pressure rise was later attributed to a leak in an instrumentation fitting in the vacuum chamber.
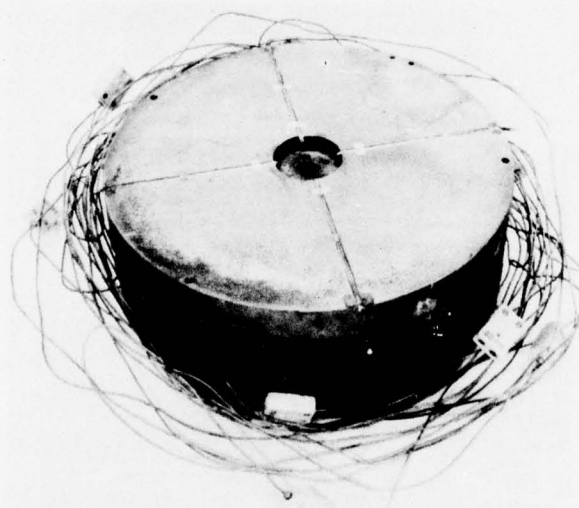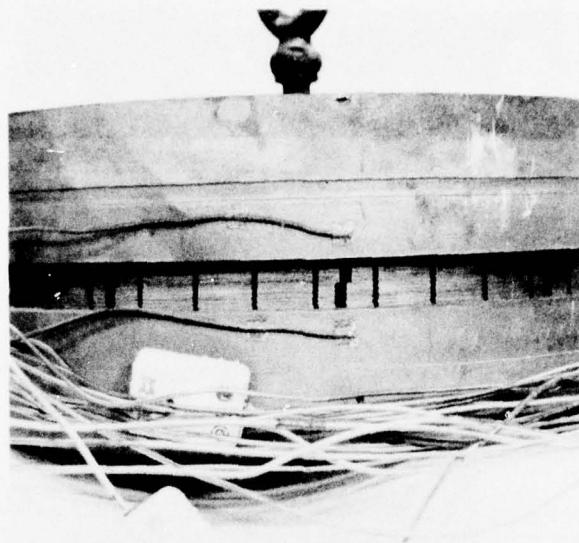
Figure 39.   The Large Stack Laminated Wheel Blank, and the Waspaloy End Plates on the Bonding Fixture.
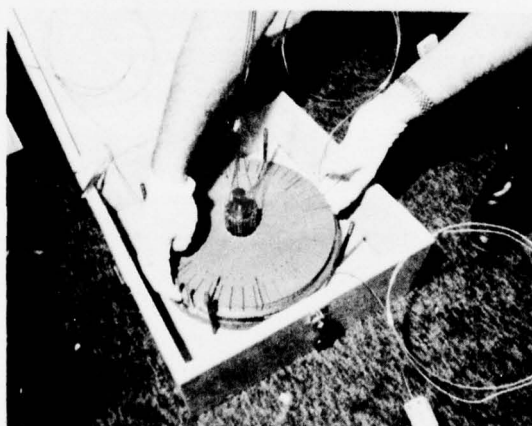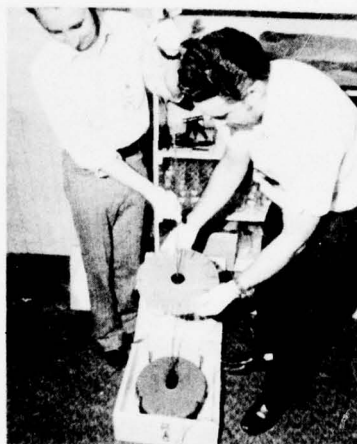
97

Figure 40.   Assembly of the Large Stack Laminates,
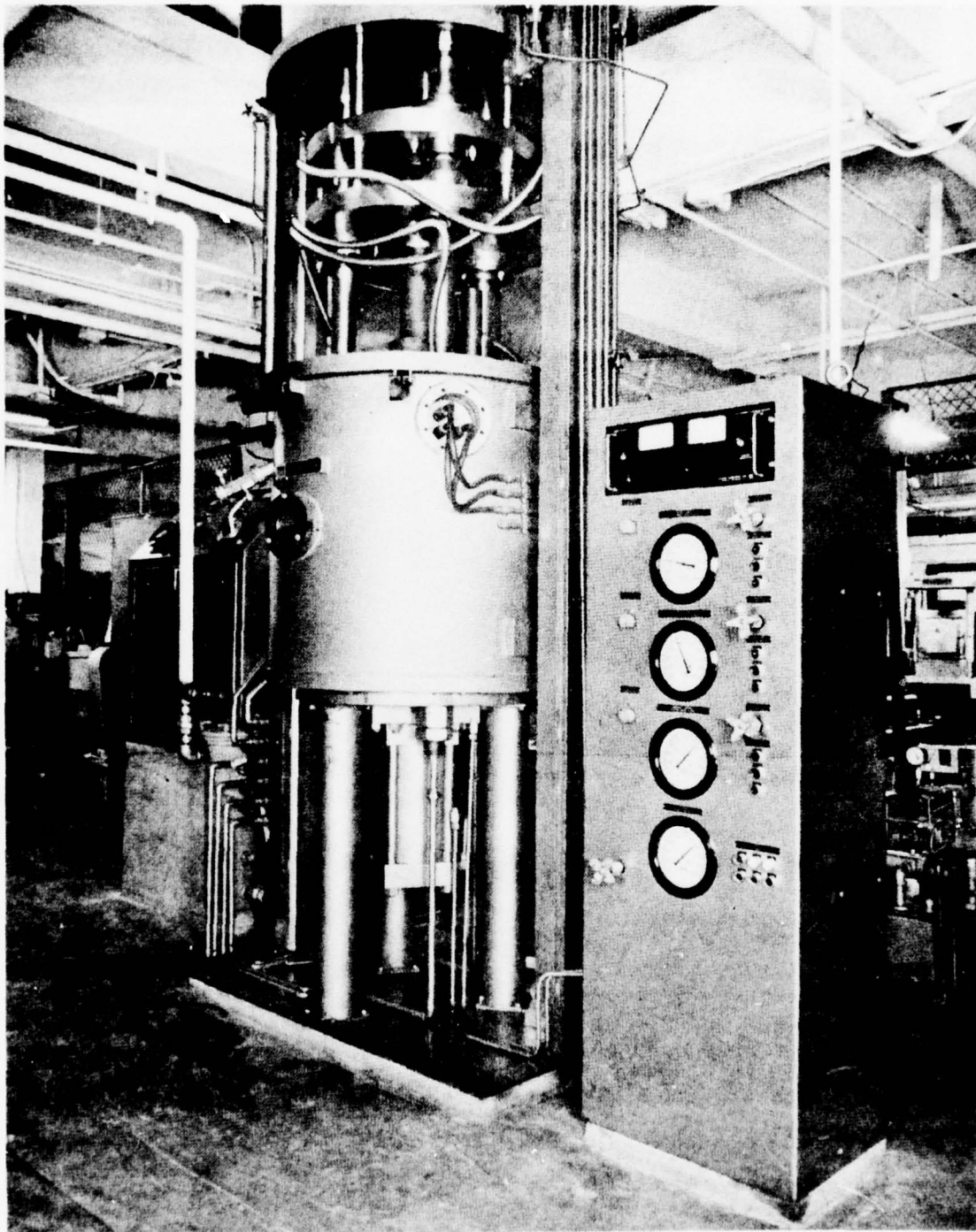the End Plates, and the Bonding
Fixture in the Shipping Crate.

Figure 41. Bonding Facility - 75-Ton Capacity
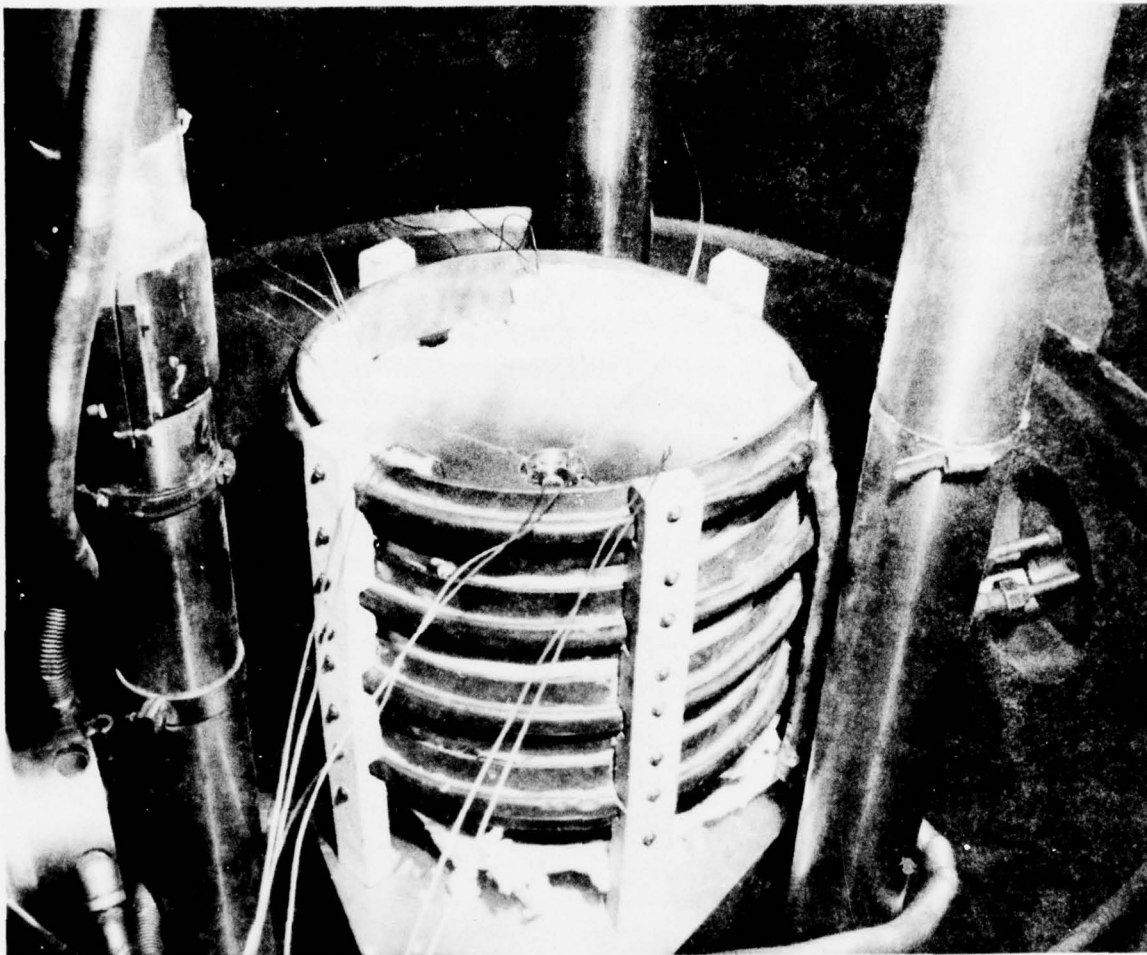Vacuum Hot-Press Furnace.

Figure 42. View of the Furnace Induction Coil with the
Bonding Assembly Placed Inside, and the
Placement of the Fiberfrax-Felt Insulation.

100

c.   Post-Bond Processing

Following bonding, the large as-bonded stack was examined ultrasonically utilizing an Automation Industries US-450 Series Laboratory System. This system incorporates a water immersion tank that has a motorized scanning bridge with a transducer attached. The immersion testing method, with water as the couplant, was employed in all tests. A polar plotter is connected to the unit, and is used to obtain a graphic record of the test data. This inspection proved to be valuable in locating two unbonded regions midway between the bore and the outer perimeter, with both regions located on the same diameter. Several much smaller indications were also detected, and the majority of those were adjacent to the bore, as seen in Figure 43. The ultrasonic inspection also established that the two unbonded areas were located close to the upper and lower 0.75-inch plate/laminate interfaces rather than within the main laminated region.

At the perimeter of the blank, the inspection capability was negated by the cooling slots and holes that interfered with the scanning resolution. Comparison of the ultrasonic records before and after heat treatment showed that there were no new indications, and the existing indications had remained the same. The stack was given almost the same Waspaloy heat treatment as the small stacks. The one exception was that the 4-hour 1975°F cycle was reduced to 1900°F in order to minimize any potential cracking from quench stresses.

d.   Evaluation and Testing

In order to assess the microstructure as a function of location in the large stack, and to determine the nature of the sonic indications, three cylinders were removed from the heat-treated stack in an axial orientation (normal to laminates). The locations of these cylinders are shown in Figure 43. Defects were identified at the interface between the end plates and the laminations in all three cylinders. A typical unbonded region is shown in Figure 44. Examination of cylinder M-3 from the periphery of the large stack revealed an unusual joint microstructure as shown in Figure 45. This unusual microstructure was later determined to exist throughout the stack.

A total of ten 0.5-inch diameter cylinders were removed in the axial and tangential orientations from the heat-treated large sheet stack for mechanical property determinations (see Figure 43). These cylinders were located in regions the ultrasonic inspection showed to be free of indications. The results of the tensile and stress-rupture testing of these specimens are shown in Tables 15 and 16.
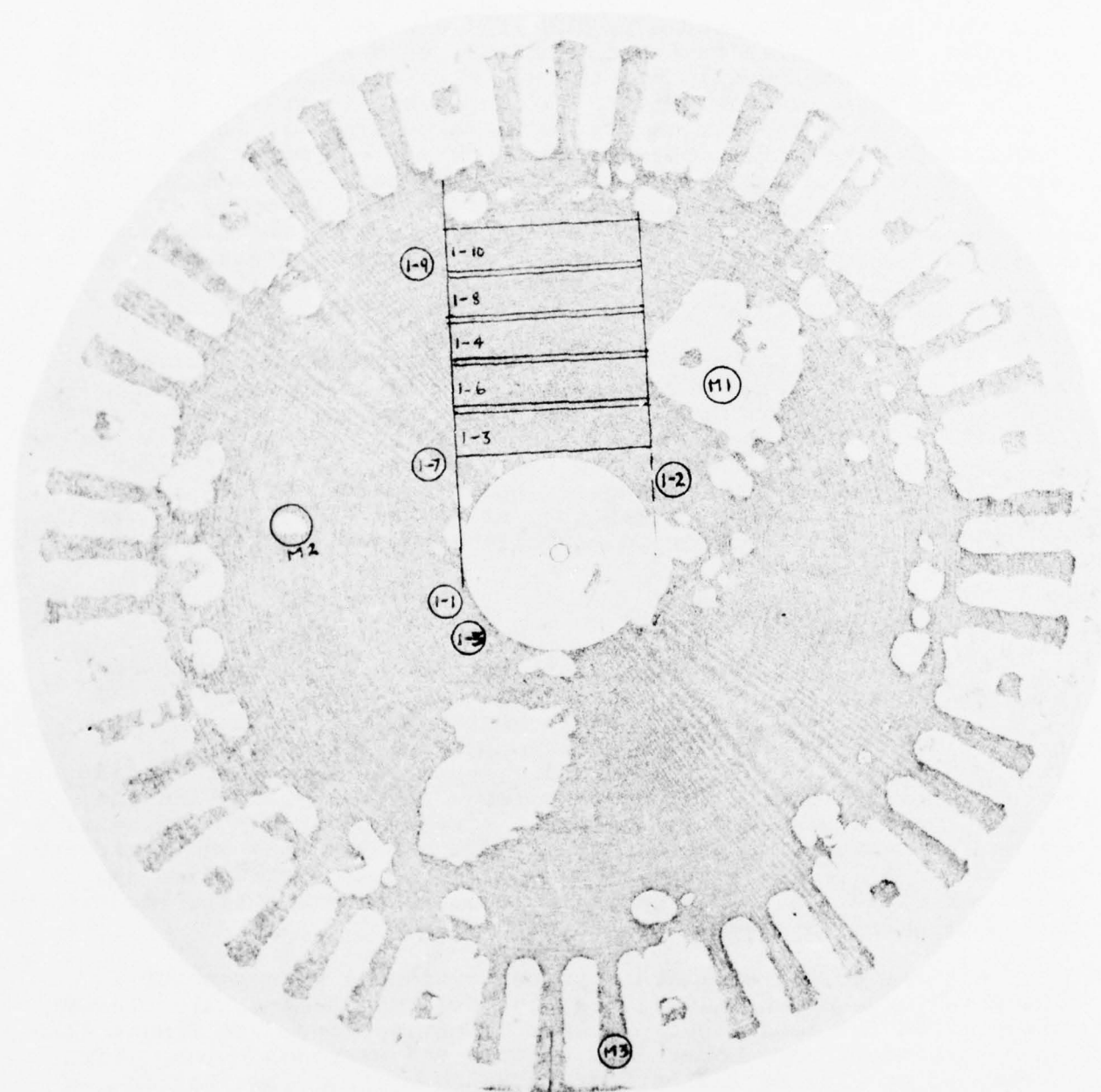
101

Figure 43. Ultrasonic C-scan Chart Showing Location of Axially-
and Tangentially-Oriented Tensile and Stress-Rupture
Specimens Within Sound Regions of the Heat-Treated
Large Stack. Also Shown are Locations of
Metallographic Specimens M1, M2, and M3.
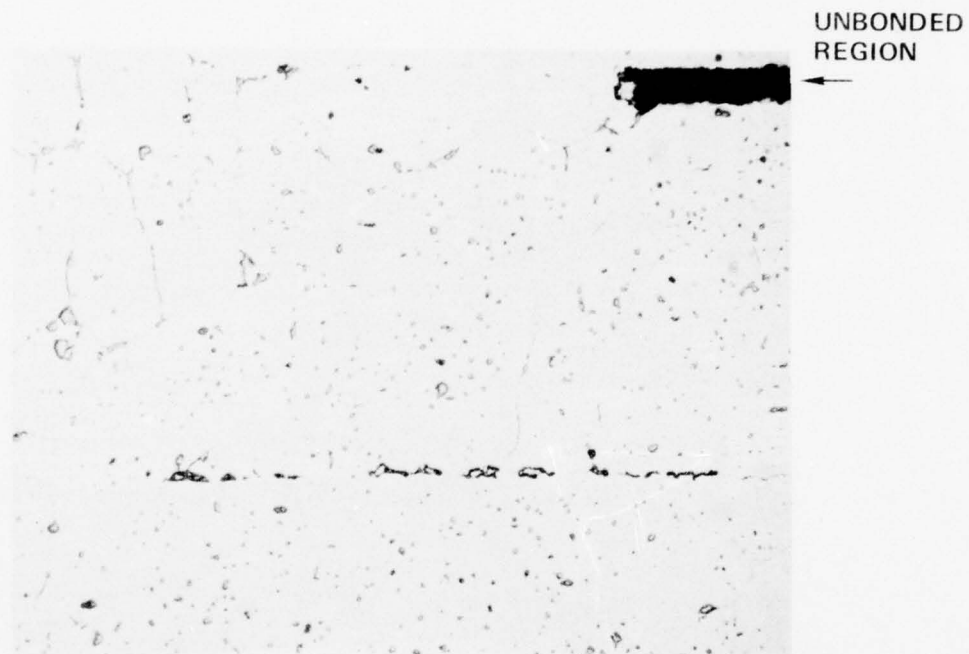
UNBONDED
REGION

Figure 44. Optical Micrograph of Cylinder M1 Showing an
            Unbonded Region Between the End Plate and the
            Adjacent Lamination. This Region Appeared
            as a Sonic Indication on the C-Scan Recording
            in Figure 43. (Kallings Etch) (Mag.: 100X)

103

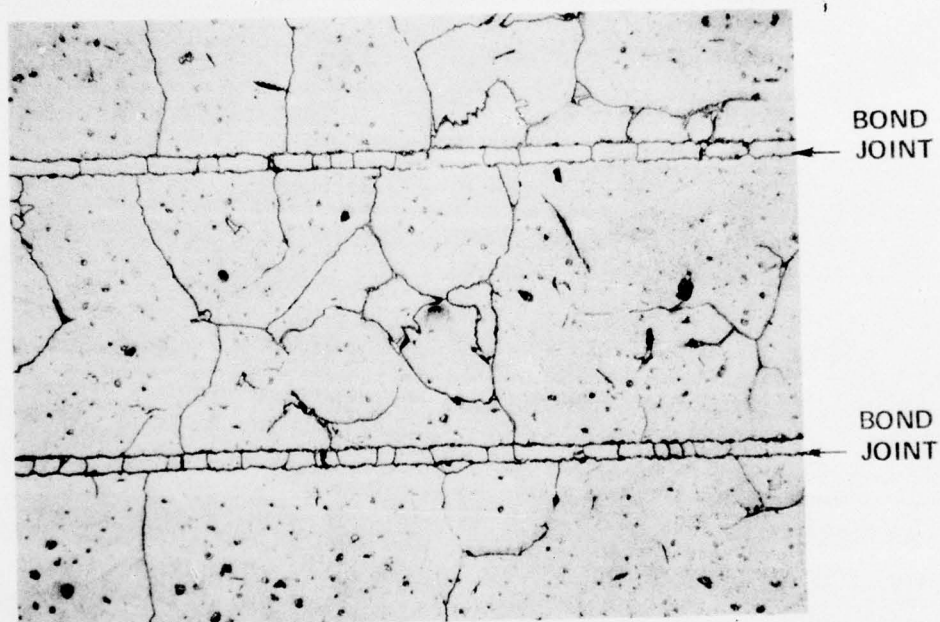MP-56519

BOND
JOINT

BOND
JOINT

Figure 45. Optical Micrograph of Cylinder M3 Showing
Laminate Joint Irregularity at the Periphery
of the Large Stack in the As-Bonded
Condition. (Kallings Etch) (Mag.: 100X)

104

TABLE 15.   TENSILE PROPERTIES FOR THE LARGE SHEET STACK
FOLLOWING HEAT TREATMENT.

MATERIAL

Specification:	0.020-inch sheet, 0.25-inch, and 0.6-inch plate, AMS 5544B
Bond Alloy:	AMI 915 0.002-inch Transfer Tape
Bond Cycle:	6 hours at 2140°F to 2200°F in vacuum with vacuum cool
Heat Treatment:	4 hours at 1900°F with vacuum/argon fan cooling Plus 4 hours at 1550°F with air cooling Plus 16 hours at 1400°F with air cooling
Specimen Geometry:	Tensile and stress-rupture bars, MSC 1106 drawing, 0.25-inch gauge diameter, 1.0-inch gauge length; all specimens $K_t \approx 1$ other than notch-combo bar $K_t = 3.7$.

TENSILE PROPERTIES

Specimen No.	Location	Orientation	Temperature (°F)	0.2 % Y.S. (ksi)	U.T.S. (ksi)	Elongation (%)	R of A (%)
1-1	Lamina-tions and end-plates	Axial	R.T.	N.Y.*	73.3	0.0	0.0
1-2				N.Y.*	81.5	0.0	0.0
1-3	Lamina-tions	Tangential	R.T.	103.0	112.9	2.0	0.0
1-4				102.8	113.2	1.5	0.0
10-1	End-plate	Tangential	R.T.	102.4	167.6	17.0	10.9
10-2				101.8	169.0	16.5	14.6
1-5	Lamina-tions and end-plates	Axial	1400	N.Y.*	70.3	0.0	0.0
1-6	Lamina-tions	Tangential	1400	62.5	102.5	2.0	0.0
*N.Y. no yield							

105

TABLE 16. STRESS-RUPTURE PROPERTIES FOR THE LARGE SHEET STACK
FOLLOWING HEAT TREATMENT.

MATERIAL:

Specification: 0.020-inch sheet, 0.25-inch, and 0.60-inch plate, AMS 5544B

Bond Alloy: AMI 915 0.002-inch Transfer Tape

Bond Cycle: 6 hours at 2140°F to 2200°F in vacuum with vacuum cooling

Heat Treatment: 4 hours at 1900°F with vacuum/argon fan cooling
plus 4 hours at 1550°F with air cooling
plus 16 hours at 1400°F with air cooling

Specimen Geometry: 0.25-inch gauge diameter, 1.0-inch gauge length, $K_t = 1$; notch-combination bar $K_r = 3.7$.

Specimen Number	Location	Orientation	Stress (ksi)	Temp. (°F)	Life (hrs)	Elong. (%)	R of A (%)	Comments
1-7	Laminations and end-plate	Axial	47.5	1500	0.1	<0.5	0.0	S Smooth Bar
1-9	Laminations and end-plate	Axial	47.5	1500	0.1	<0.5	0.0	Smooth Bar
1-8	Laminations	Tangential	47.5	1500	55.2[1]	5.0	19.3	Smooth Bar
1-10	Laminations	Tangential	47.5	1500	63.6	16.5	18.0	Smooth Bar
B-3	End-plate	Tangential	100.0	1350	0.7	---	---	Notch-combination
B-3	End-plate	Tangential	80.0	1350	8.0	10.7	11.5	Notch-combination

[1] Total of 55.2 hours at 1500°F

Stress-rupture and tensile properties were low in both orientations for specimens located in the laminate region. These values were noticeably lower than those previously exhibited in small sheet stacks using a similar bond temperature and heat treatment.

Examination of the fractured test specimens revealed further evidence of typical joint microstructure conditions. Figure 46 shows the traces of a double interface delineating the adjacent sheets in the bore and peripheral regions of the large sheet stack. This condition appeared to consist of two lines of particles. A similar microstructure had not been observed with the small sheet stacks, and is believed to be associated with the poor mechanical properties of the large sheet stack.

Analysis of the bond cycle experienced by the large sheet stack disclosed that a number of potentially important differences were encountered when compared to the small sheet stacks bonded in the laboratory. The most noteable differences were:

o   The heating rate from below the bond alloy solidus, approximately 1700°F, to the bond temperature (2140°F). The rate achieved in laboratory bonding, although not precisely controlled, was approximately 25°F per minute. The rate experienced by the large stack was 1.5°F per minute. This lower rate was imposed by the physical restraints of induction heating the large stack in the bonding facility.

o   The vacuum environment achieved in the laboratory bonding was significantly improved over that encountered by the large sheet stack. A 72-hour outgassing of the acrylic bond alloy binder and graphite plates was required due to the low pumping speed of the vacuum equipment. Further compromise was incurred when a leak developed during the heating cycle.

Subsequent laboratory tests were conducted based on the results of the large sheet stack. These tests were designed to evaluate the effect of the heating rate and bonding atmosphere on mechanical properties. These tests were conducted as part of the wheel fabrication task.

4.   FIRST WHEEL BLANK BONDING

A survey was initiated to identify an alternative bond facility due to the limitations in the heating rate and atmospheric control exhibited by the bonding vendors equipment. Subsequently, Rockwell International Corporation, Los Angeles Aircraft Division, was chosen because they succeeded in demonstrating an acceptable heating rate using an instrumented test part.
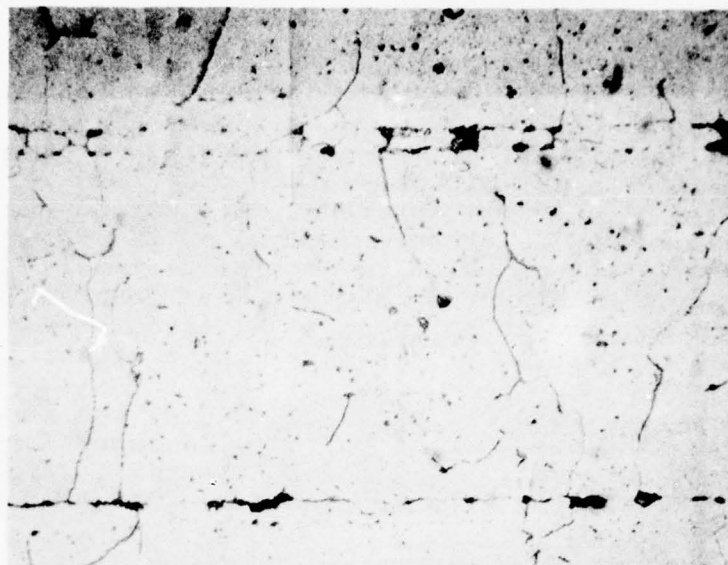
SPECIMEN 1-2
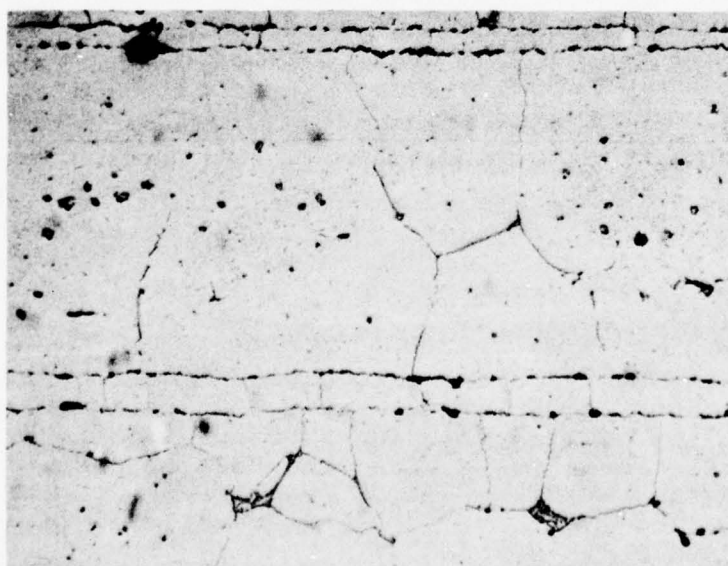
0.020-INCH
LAMINATES

END PLATE

SPECIMEN M-4

Figure 46. Optical Micrographs Showing Joint Microstructure in the Large Sheet Stack. Specimen 1-2 (Upper View) was Removed From the Bore Region, and Contained Isolated Traces of a Double Interface, Whereas Specimen M-4 (Lower View) Showed Almost Continuous Double Interface. (Kallings Etch) (Mag.: 100X)

Two small stacks were subsequently bonded in order to verify the heating rate as the predominant cause of poor bond properties in the large stack. These stacks were prepared and bonded identically to Stack 8 (approximately 25°F/min), except for the heating rate. Stack 9 was bonded using the 1.5°F per minute rate achieved with the large stack, and Stack 10 was bonded using 7°F per minute (anticipated rate for the Rockwell facility).

A metallographic section from Stack 9 (see Figure 47) disclosed a joint microstructure identical to the large stack. Initial metallographic examination of the outside surface of Stack 10 indicated a good bond line, as shown in Figure 48. Based on this examination, the bonding proceeded on the initial wheel blank using the same 7°F per minute heating rate as used on Stack 10. However, subsequent metallographic examination of the internal joint interfaces exhibited excessive porosity, as shown in Figure 49. This interior porosity is related to the preferential loss of the liquid phase to grain boundaries during bonding. This phenomenon is modified at the stack exterior to exhibit a continuous liquid film.

a.   Laminate Photoetch Process Definition and Optimization

During development of the Waspaloy photoetching process, a number of important considerations in attaining consistant dimensional quality of the photoetched features were determined. These considerations established the basis for the processing steps noted in Table 17.

b.   Wheel Blank Preparation

Figures 50 and 51 show a typical photoetched laminate. The photoetched laminations and end plates were cleaned, as specified in Section IV.1.b.(1) of this report, prior to tape application. Laminations exhibiting a mat finish were not vapor honed. The cleaned sheet laminations then had the bond-alloy tape applied. Tape application consisted of cooling the tape preforms below 20°F to facilitate removal of the polyethylene backing. The tape preforms were then placed in position on the individual laminates. These individual laminates were then exposed to a saturated vapor of ethyl ether. The ethyl-ether vapor partially liquifies the acrylic tape binder, and promoted adhesion of the tape to the laminate. The laminates were then removed from the vapor, and were racked on the outgass tooling, as shown in Figure 52. The tooling was then sealed, evacuated to less than 0.01 Pa, and heated to 450°F for 50 hours. This outgass cycle removed approximately 75 percent of the acrylic binder, and rendered the tape brittle so that it could be readily removed from the blade cooling passage areas. The laminates were then sequentially assembled on the bond fixture. Figure 53 shows six laminates typical of the 62 laminates used. Figures 54 and 55 show close-ups of laminates of leading- and trailing-edge portions of laminates from the assembly stack. Twelve type-K sheathed thermocouples were then installed on the bond fixture

Figure 47. Optical Micrograph Showing Joint Microstructure
in Stack 9 Following the Standard 2140°F Bond
Cycle. The Double-Interface Condition is Clearly
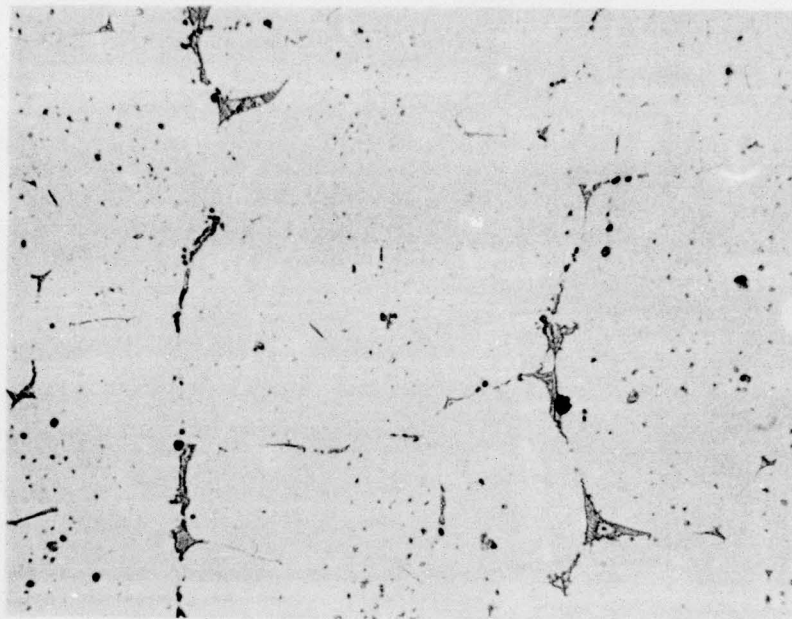Evident. (Kallings Etch) (Mag.: 100X).

Figure 48. Metallographic Examination of the Stack 10
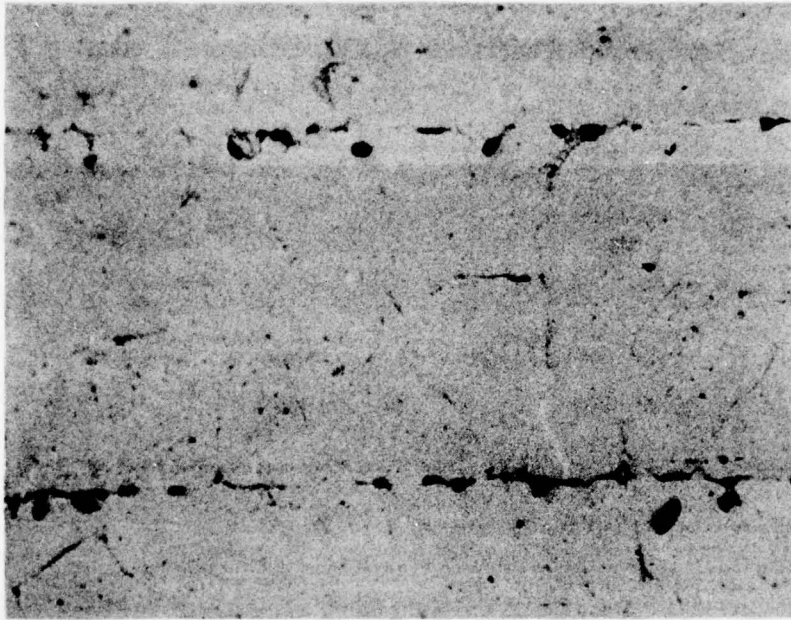Outer Surface. (Unetched) (Mag.: 200X)

111

Figure 49.   Photomicrograph Showing the Microstructure Near
to the Bottom Edge of Stack 10. Note the Eutectic
Film at the Lamination Interfaces and Along the
Grain Boundaries. The Bonds are Quite Porous.
(Unetched) (Mag.: 100X)

MP-56743

112

TABLE 17.   WASPALOY LAMINATE CHEMICAL-MILLING PROCEDURE.

Extreme care must be used in all steps to insure maximum quality with all parts.

1. Cleaning

    a. Sheets will be precleaned as noted in Section IV.I.b(1).

    b. Vapor degrease just prior to Photo Process steps. Sheets should be photo processed within 24 hours of the cleaning operation.

2. Photo Process

    a. Pre-etch in ferric chloride for approximately five seconds

    b. Rinse with tap water

    c. Squeege and air dry

    d. Dip in 18.0 to 18.5 Zahn seconds (No. 2 cup) viscosity photo resist (KTFR), and withdraw at a rate of 8 inches per minute. (Gyrex dip coater).

    e. Prebake at 210°F for 2.5 minutes in an infrared (I.R.) oven. (Glo-quartz I.R. oven).

    f. Rotate sheet 90°, and repeat Steps d and e.

    g. Expose the sheets for 1.75 minutes on the Gyrex 905 exposure system. (Two passes at No. 30 setting).

    h. Develop for 2.0 minutes (KTFR) developer, and spray rinse thoroughly for one minute.

    i. Post bake for 20 minutes at 250°F

3. Etching

    a. Use fresh 46° Be Ferric Cloride as etchant.
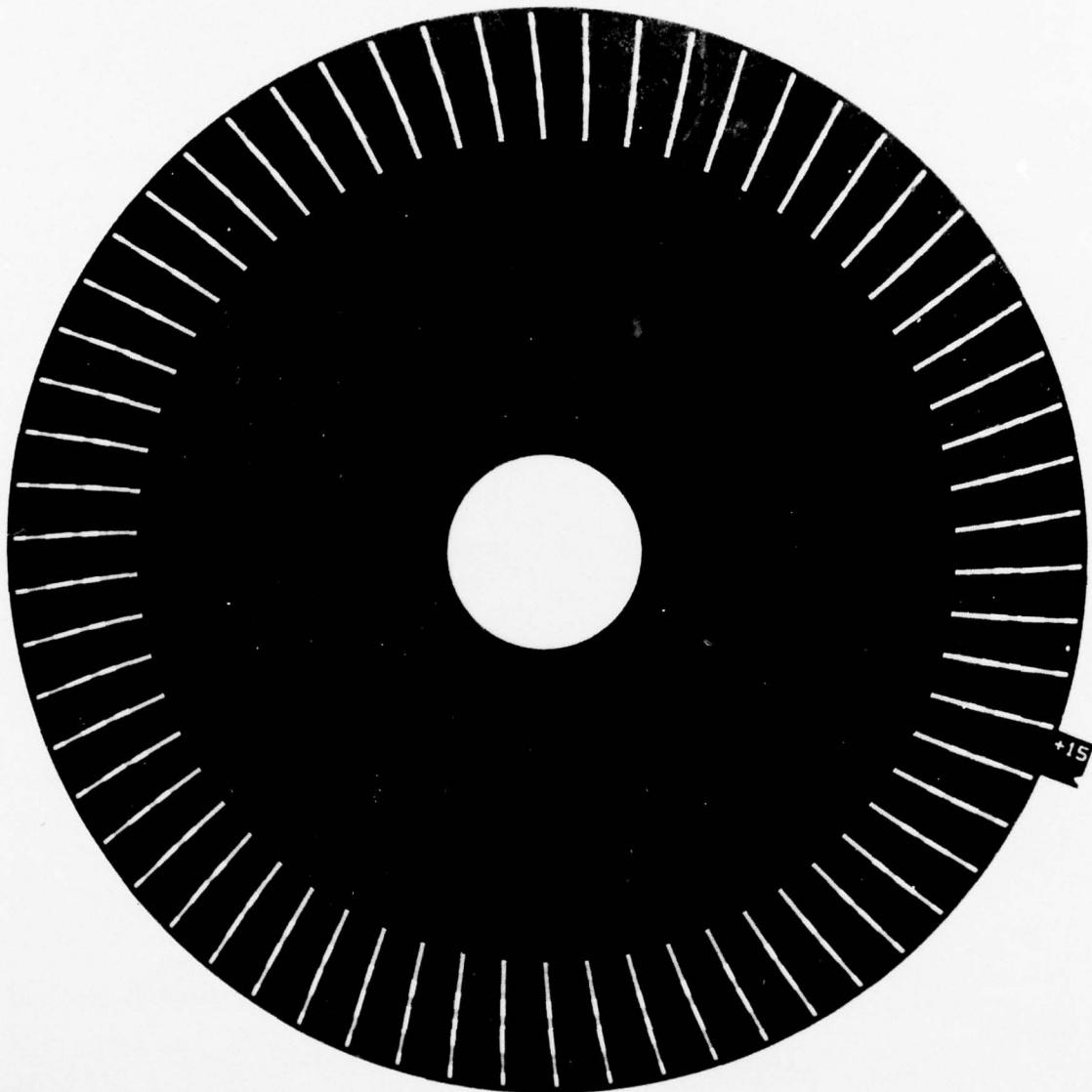
Figure 50. Completed Final Wheel Blank Laminate
Showing Cooling Passages.

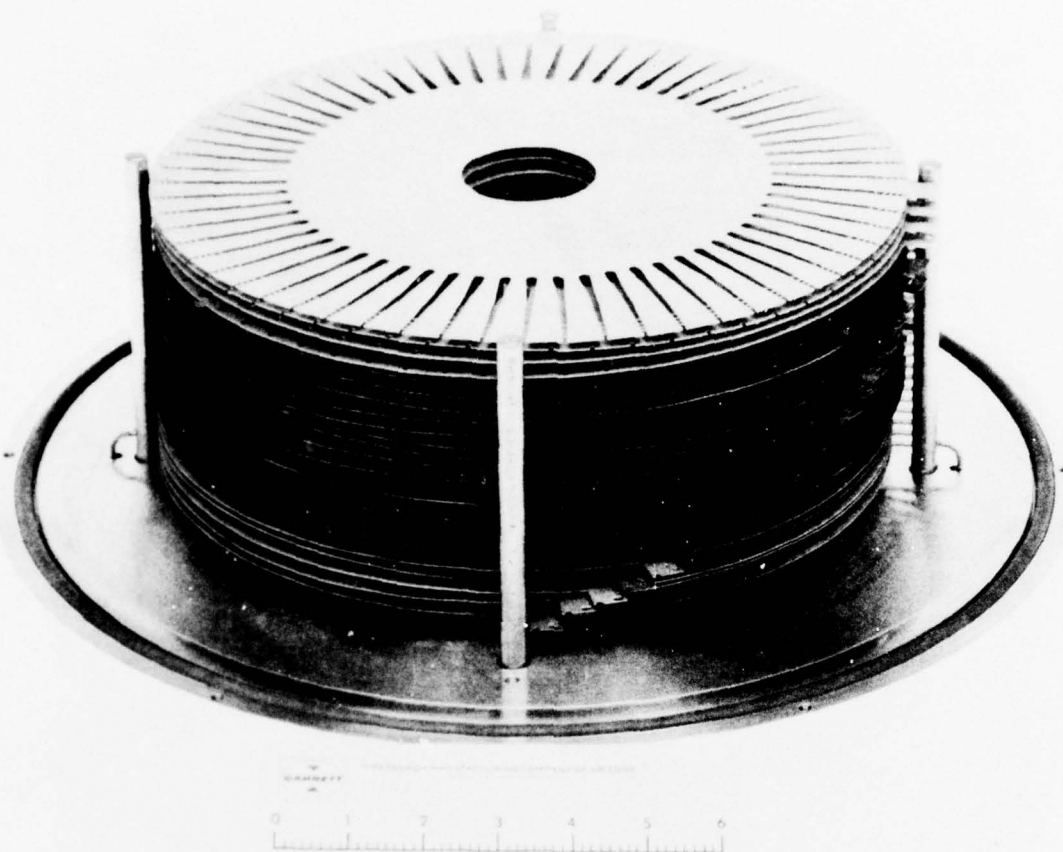Figure 51.   Completed Final Wheel Blank Laminate
            Showing Cooling Passages.

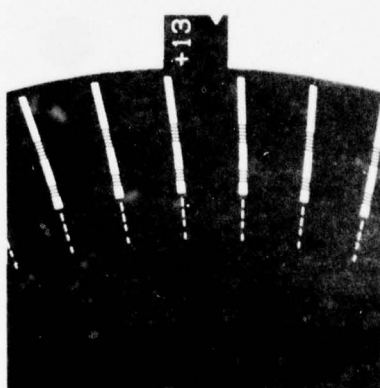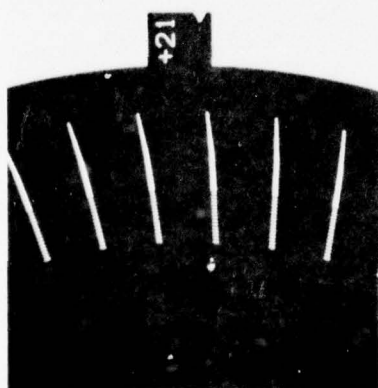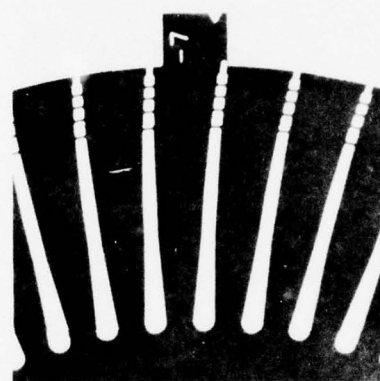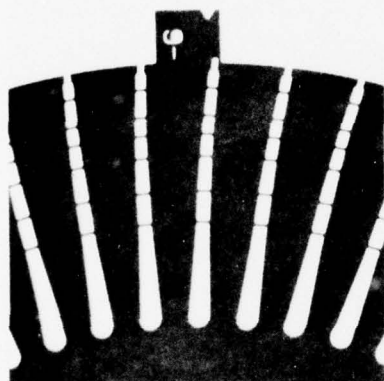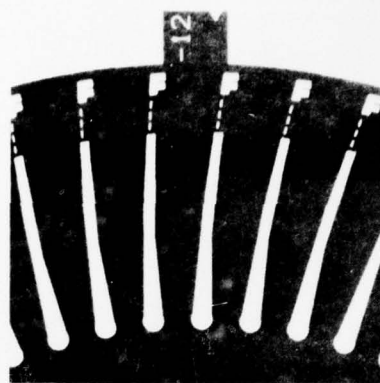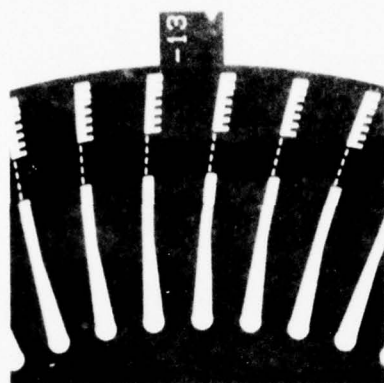Figure 52. Laminates Racked on the Outgass Tooling.
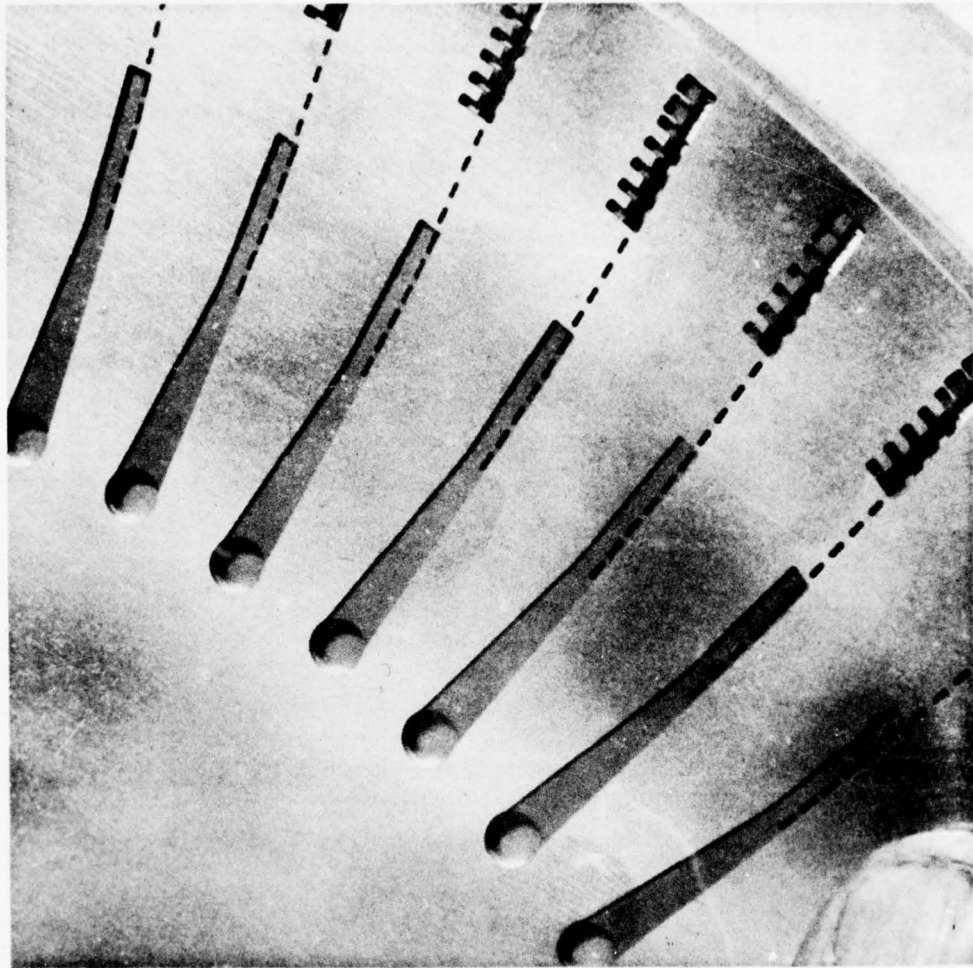
Figure 53.   Six Typical Laminate Sheets.

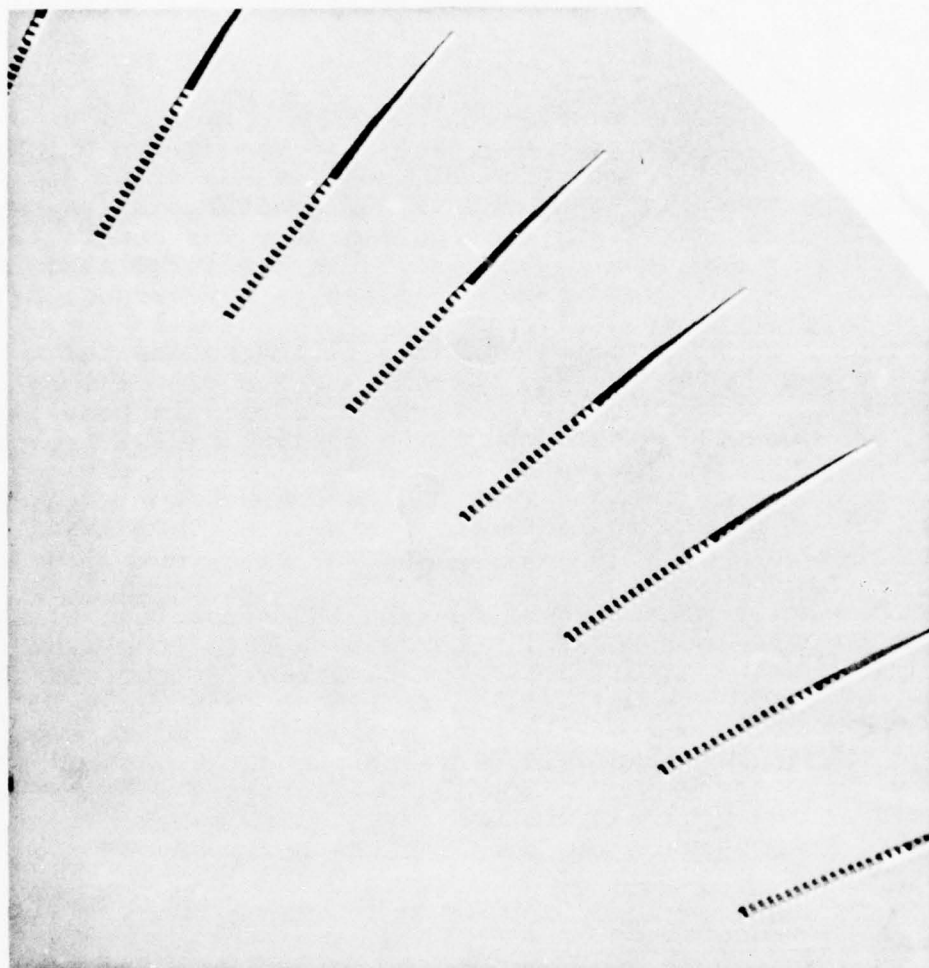Figure 54. Laminate Leading-Edge Area Impingement
Plus Film Cooling.

118

Figure 55. Laminate Trailing-Edge Orifices, and Pin Fins.

119

(see Figures 56 and 57), and the completed assembly was bolted
in place in the outgass tool for shipping. The outgass tool was
evacuated and filled with pressurized argon to preclude contami-
nation, and the wheel blank was shipped to Rockwell International
(see Figure 58).

c.   Bonding Procedures

     The wheel blank assembly was placed in the vacuum bonding
retort at the Rockwell International facility, as shown in
Figure 59. Thermocouple leads and vacuum feedthrough (as shown
in Figure 60) were installed, and the assembly was backfilled
with argon and welded (see Figure 61). The completed assembly
was placed in the hot press, and connected to the vacuum
pumping system, as shown in Figure 62. The Rockwell
International bonding facility utilizes resistance-heated
ceramic plattens on the top and bottom surfaces of the wheel
blank assembly. Temperature uniformity of these plattens is
monitored and controlled throughout the bonding cycle. Tempera-
ture variation was controlled to within $\pm5°F$ for the area of
the heaters in direct contact with the retort. After evacu-
ation to below 0.01 Pa, the assembly was helium leak tested and
sealed, as necessary, prior to initiating the bond thermal cycle.

     The bond cycle consisted of heating the retort and blank to
2140°F and holding for 6 hours. The heating rate from 1700°F
through 2140°F was controlled to approximately 7°F per minute.
An axial load of 50 psi was applied at 1950°F, and was maintained
throughout the remainder of the bond cycle. The vacuum system
maintained the pressure below 0.01 Pa throughout the bond cycle.
The steady-state temperature distribution achieved during the
6-hour hold at the bond temperature resulted in a maximum dif-
ferential of 10°F between the bore and the periphery of the wheel
blank.

d.   Post-Bond Processing

     Visual examination of the bonded wheel blank (see Figure
63) indicated limited bond-alloy flow had been achieved. The
as-bonded blank was examined ultrasonically, and then the blank
was given the same heat treatment as the large sheet stack.
Following heat treatment, the blank was again ultrasonically
inspected. The ultrasonic results were indicative of a high
degree of porosity throughout the wheel blank laminated section,
which was present before and after heat treatment.

e.   Evaluation and Testing

     Several 0.16-inch diameter cylinders were removed by
electrical discharge machining (EDM) from the heat-treated blank.
One of the axial cylinders removed from the bore area was
prepared for metallurgical analysis. The remaining cylinders
were prepared for mechanical-property testing. Table 18 shows
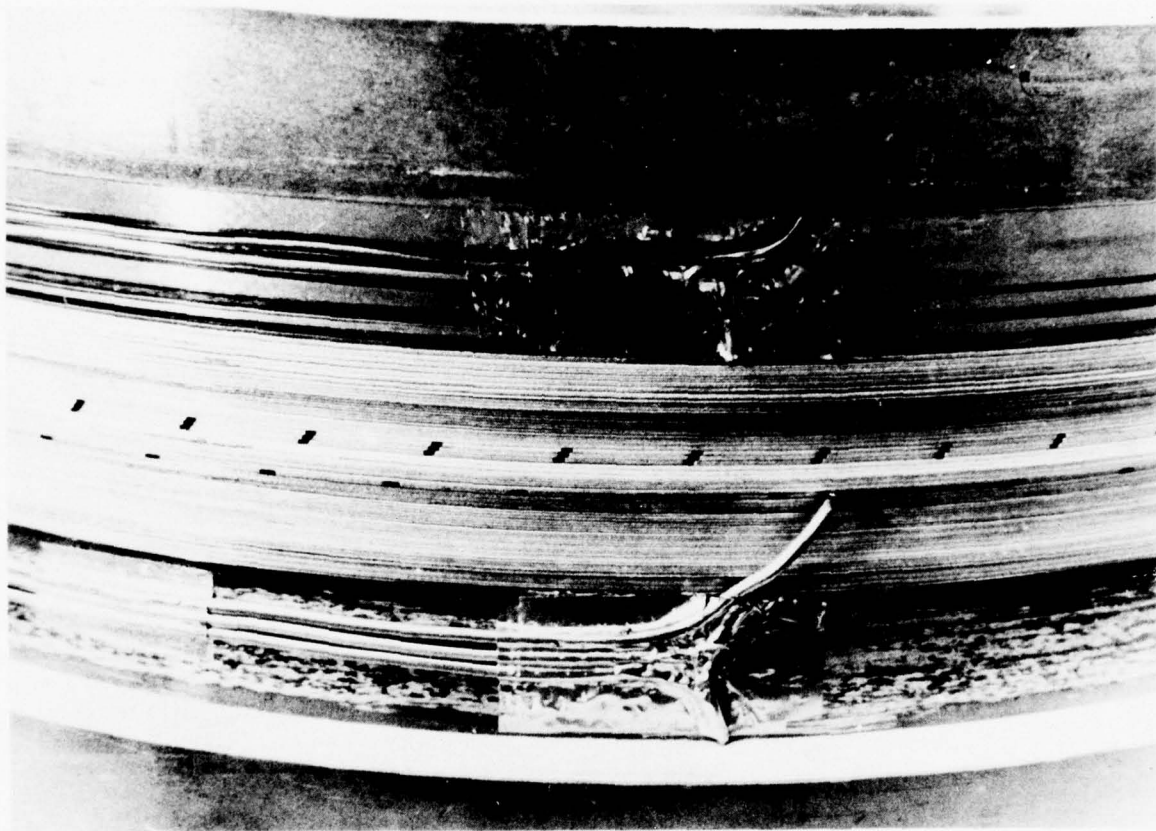the mechanical properties obtained.

Figure 56. Sequentially Assembled Wheel Blank Laminates on the Bond Fixture with the Thermocouples Installed.
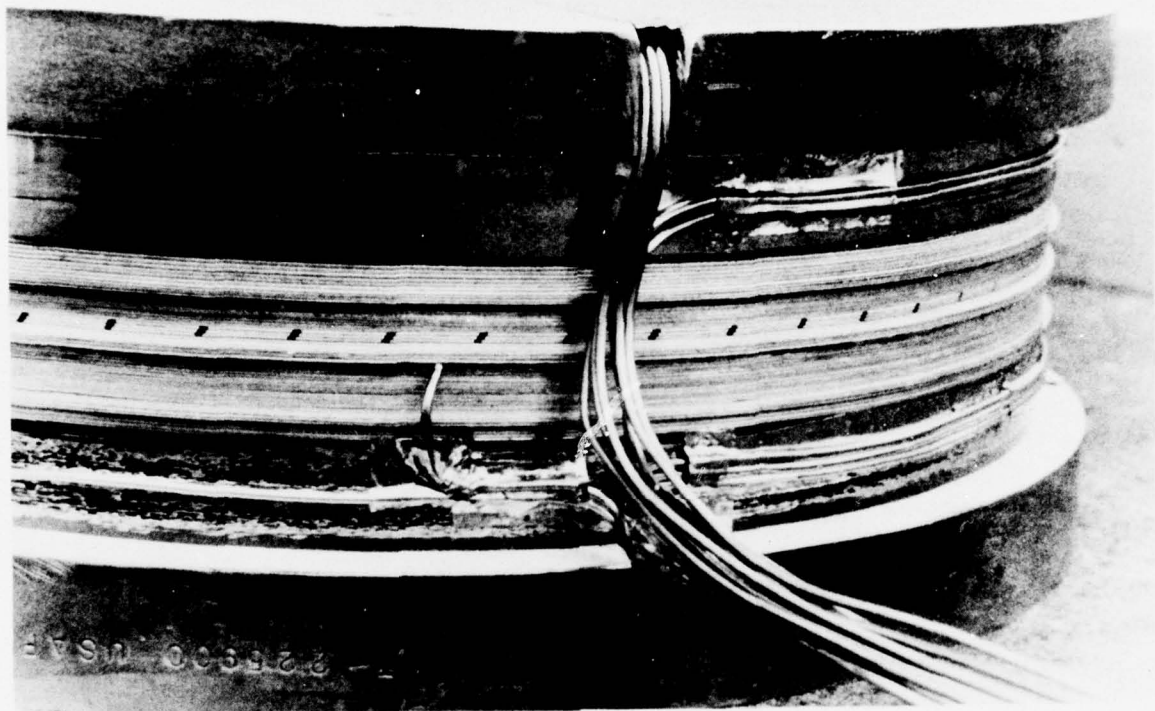
Figure 57. Sequentially Assembled Wheel Blank Laminates on
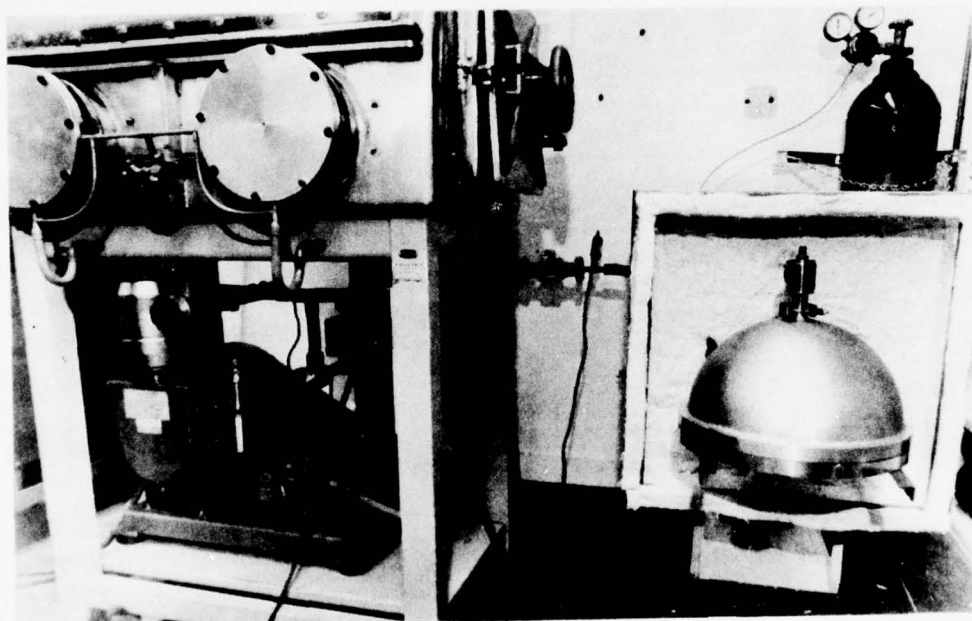the Bond Fixture with the Thermocouples
Installed.

Figure 58.   Outgass Tooling Fixture Before Shipping and
During Vacuum Evacuation to Below 0.1µ, and
Heating to 450°F.

123

Figure 59.   Unbonded Laminated Wheel Blank Being Placed
             Into the Retort.

Figure 60.   Thermocouple Leads and the Feedthrough
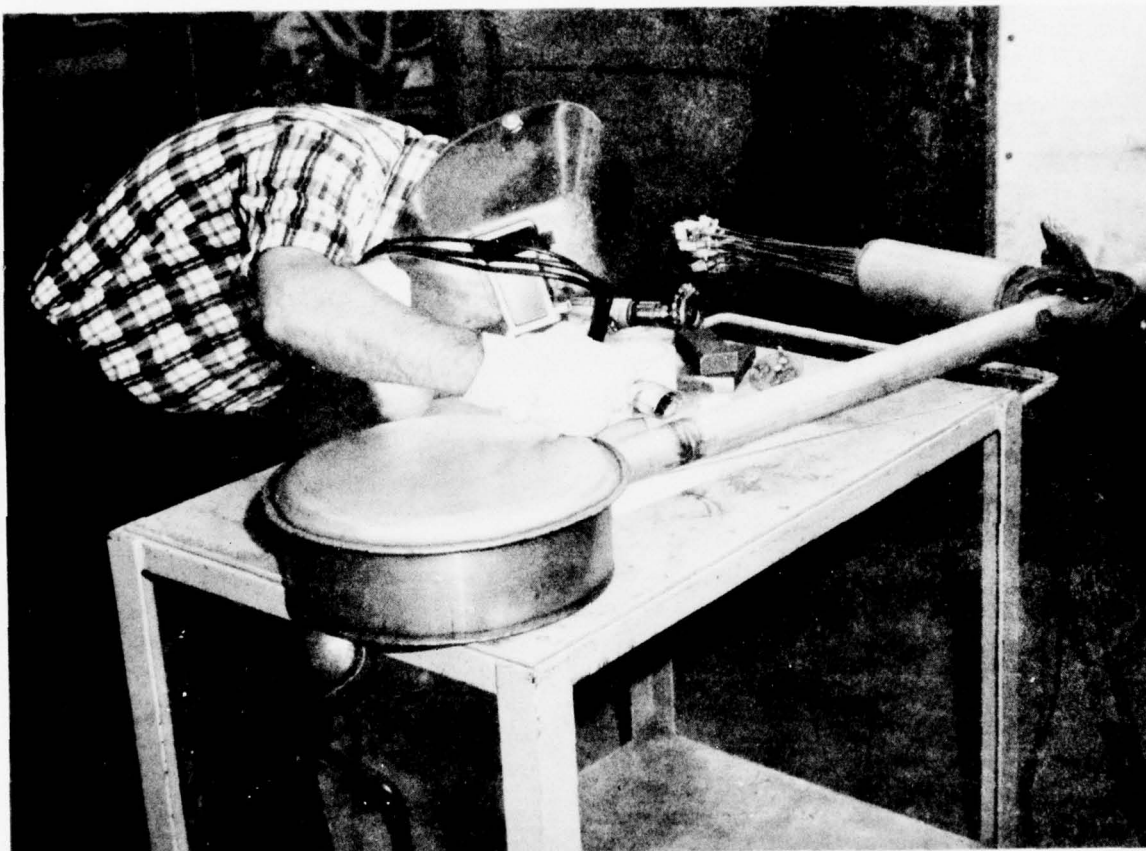   for the Bonding Retort.

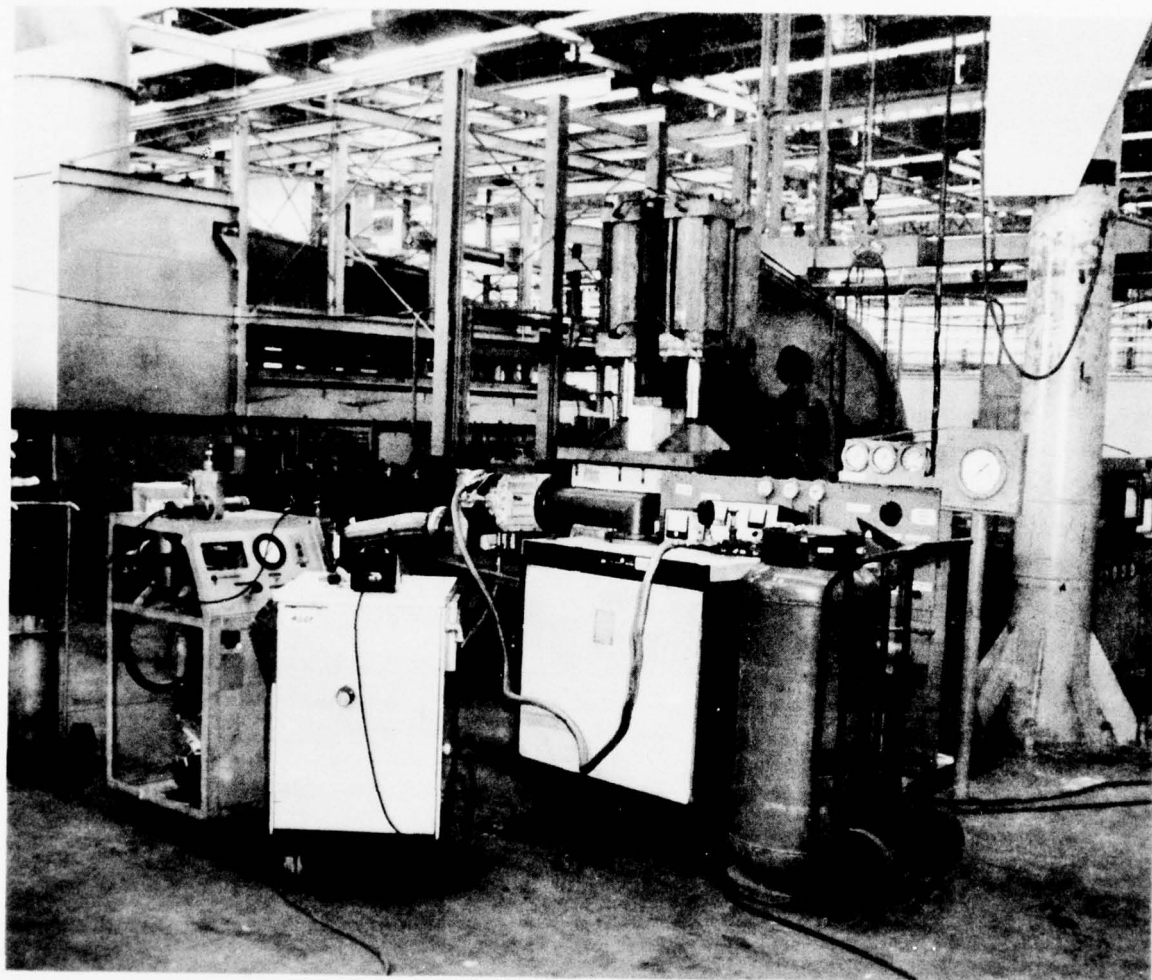Figure 61. Laminated Wheel Blank Retort Being Welded After
Backfilling with Argon.

Figure 62. Completed Laminate Wheel Blank Bonding Assembly in the Hot Press, and Connected to the Vacuum System of the Rockwell International Facility.
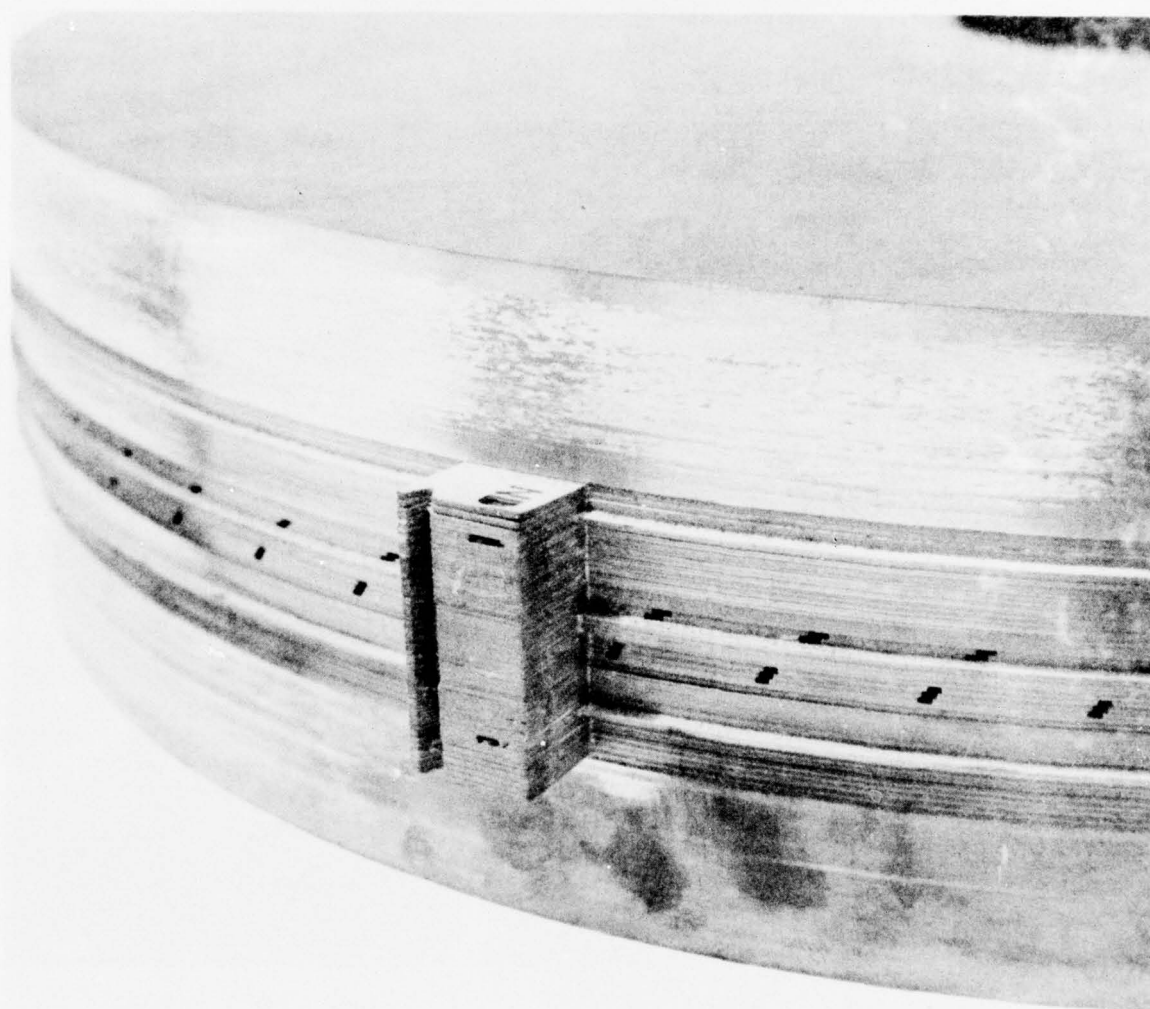
MP-50505

Figure 63.   Completed Laminated Wheel Stack at the
            Blank Outer Diameter Tab Area.

TABLE 18.   ROOM-TEMPERATURE TENSILE PROPERTIES
OF THE FIRST WHEEL BLANK.

Specimen	U.T.S. (ksi)	0.2% Y.S. (ksi)	EL. (%)	R of A (%)
Radial (longitudinal)	150.2	---	9.2	---
Axial (transverse)	61.7	---	4.0	---

NOTES: Thermal History

Diffusion Bonding - heat at 7°F/minute to 2140°F, hold
for 6 hours, air cool

Heat Treatment - 1900°F for 4 hours, argon gas fan cooled
Plus 1550°F for 4 hours with air cooling
Plus 1400°F for 16 hours with air
cooling

Figure 64 illustrates the typical microstructural appearance of bonds observed in the cross section of the wheel blank. Gross porosity was observed at each of the laminate interfaces with the following three types of bond-joint micro-structures:

(1)   Type A, nonbonded

(2)   Type B, single-bond interface

(3)   Type C, double-bond interface

The nonbonded joint (Type A) was characterized by a solid-state diffusion bond at the interface that created a zone of fine-grained material essentially free of carbides, and without detectable eutectic structure. The single-bond interface (Type B) exhibited a similar eutectic-free, fine-grained diffusion-bonded structure on one side of the interface, but diffusion appeared to have been inhibited on the other side by a continuous film of precipitates. On the double-bond interface (Type C), bonding had been inhibited by a film of precipitates on both surfaces.

Examination of the entire stack thickness revealed a pre-dictable pattern for the three types of interfaces. Type A occurred if both surfaces of the mating laminates had been pre-pared by chemical milling, or if the cleaned laminate surface had been matt-white in appearance. Type B was produced by joints between chemical-milled or matt-white and vapor-honed laminate surfaces. Type C bonds were the result of vapor honing laminates on both sides of the joint.

In addition to the cleaning procedures outlined in Section IV.1.b.(1) of this report, vapor honing was selected as a probable means of removing the translucent brown film present on the 0.010-inch thick laminations. All the laminations of this type that were not chemically milled exhibited Type C joints. On a laboratory scale, the vapor-honing technique had been effective with small sheet stacks; however, none of these stacks utilized the contaminated 0.010-inch thick material. Use of this contaminated sheet in the wheel blank demonstrated that vapor honing is not completely acceptable. Consequently, future laminations were cleaned by a technique of alternate ferric-chloride solution immersion and mechanical scrubbing.

The mechanical properties of the wheel blank, as shown in Table 18, were very poor, indicating that the heating rate of 7°F per minute also contributed to less than optimum results. It was determined that loss of the low-melting constituent to the laminate grain boundaries could be modified by achieving a higher heating rate through the critical liquidus range. Dis-cussions with the bonding vendor indicated that a higher heating rate was obtainable, but at the risk of damage to the bonding equipment. Subsequently, a heating rate varying from 15°F per
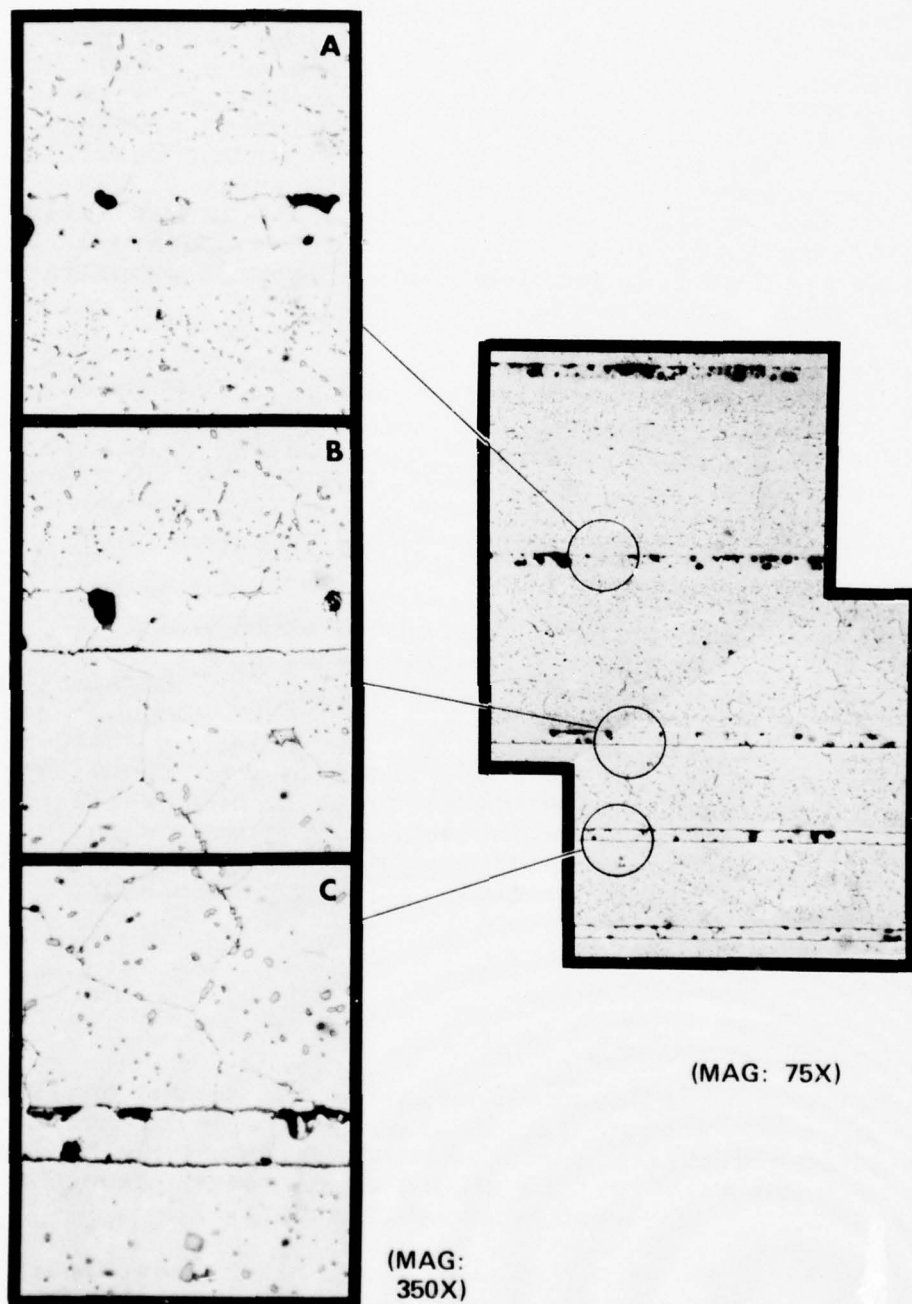
(MAG: 75X)

(MAG: 350X)

Figure 64. Typical Appearance of a Cross Section of the First Wheel Blank. The Photos Show the Three Types of Bond Joint Microstructures.

minute up to 1700°F, followed by 10°F per minute up to 2140°F was successfully demonstrated using an instrumented test specimen.

Prior to fabrication of the second wheel blank, two specimen sheet stacks (Stacks 11 and 12) were prepared to verify the improved cleaning technique and faster heating rate. The stacks were prepared and bonded similarly to specimen Stack 8. Stacks 11 and 12 both incorporated the contaminated 0.010-inch thick material. This material was cleaned in ferric chloride followed by the standard cleaning procedure. Stack 11 was heated at 11°F per minute to 2140°F, while Stack 12 was heated at 11°F per minute to 2175°F. The higher bond temperature of Stack 12 was selected to provide a comparison of properties at a range of bond temperatures.

The mechanical properties exhibited by these two stacks, as shown in Tables 19 and 20, were below those exhibited by Stack 8. The apparent cause was the reduced heating rate imposed by limitations in the vendors bonding equipment heaters. The bond joint microstructure of both stacks was similar to Stack 8, and showed complete interdiffusion across the interfaces. Stack 11 did not exhibit the grain-boundary eutectic found in Stacks 8 and 12.

The bond cycle selected for the second wheel blank incorporated the 11°F per minute heating rate, and a slightly higher bond temperature of 2160°F +20°F. Although the results of mechanical property tests of Stack 8 indicated somewhat higher properties than those achieved in Stack 12, it is not anticipated that the same degree of process temperature control could be achieved at the Rockwell International facility on a wheel blank. Therefore, the process temperature cycle approximating that utilized for Stack 12 was selected on the basis of a realistic cycle that could be obtained on full-scale, non-laboratory equipment.

5.   SECOND WHEEL BLANK BONDING

a.   Wheel Blank Preparation

Wheel blank preparation procedures for the second wheel blank were the same as those for the first, except for the previously noted cleaning procedure modifications. The bonding procedures were the same for the second wheel blank, except for the increased heating rate and bond temperature.

Visual examination of the bonded wheel blank (see Figure 65) indicated that liquation of the bond alloy was achieved. The extent of flow was similar to that observed on small stacks bonded with the same parameters. This blank was also given the same post-bond heat treatment as Stack 8. Following heat treatment, the blank was ultrasonically inspected.

132

TABLE 19.   MECHANICAL PROPERTIES OF STACK 11.

Specimen	U.T.S. (ksi)	0.2% Y.S. (ksi)	EL. (%)	R of A (%)	Life (hr)
Room-Temperature Tensile					
Transverse	103.3	---	0	---	---
Transverse	107.1	105.1	1.0	---	---
1500°F Stress Rupture, 47.5 ksi					
Transverse	---	---	3.5	---	47.1

NOTES:

Thermal history:

  Diffusion bonding = heated at 25°F/min to 2140°F, held for 6 hours, cooled

  Heat treatment = 1900°F for 4 hours with argon gas fan cooling
               Plus 1550°F for 4 hours with air cooling
   Plus 1400°F for 16 hours with air cooling

TABLE 20. MECHANICAL PROPERTIES OF STACK 12.

Specimen	U.T.S. (ksi)	0.2%Y.S. (ksi)	Elongation (%)	R of A (%)	Life (hr)
Room-Temperature Tensile					
Transverse	114.3	104.1	2.5	---	---
Transverse	110.0	101.8	2.3	---	---
1500°F Stress Rupture, 47.5 ksi					
Transverse	---	---	4.0	11.6	23.0

NOTES: Thermal History

    Diffusion Bonding - heat at 11°F/minute to 2175°F, hold for 6 hours, air cool

    Heat Treatment - 1975°F for 4 hours with argon gas fan cooling
Plus 1550°F for 4 hours with air cooling
Plus 1400°F for 16 hours with air cooling
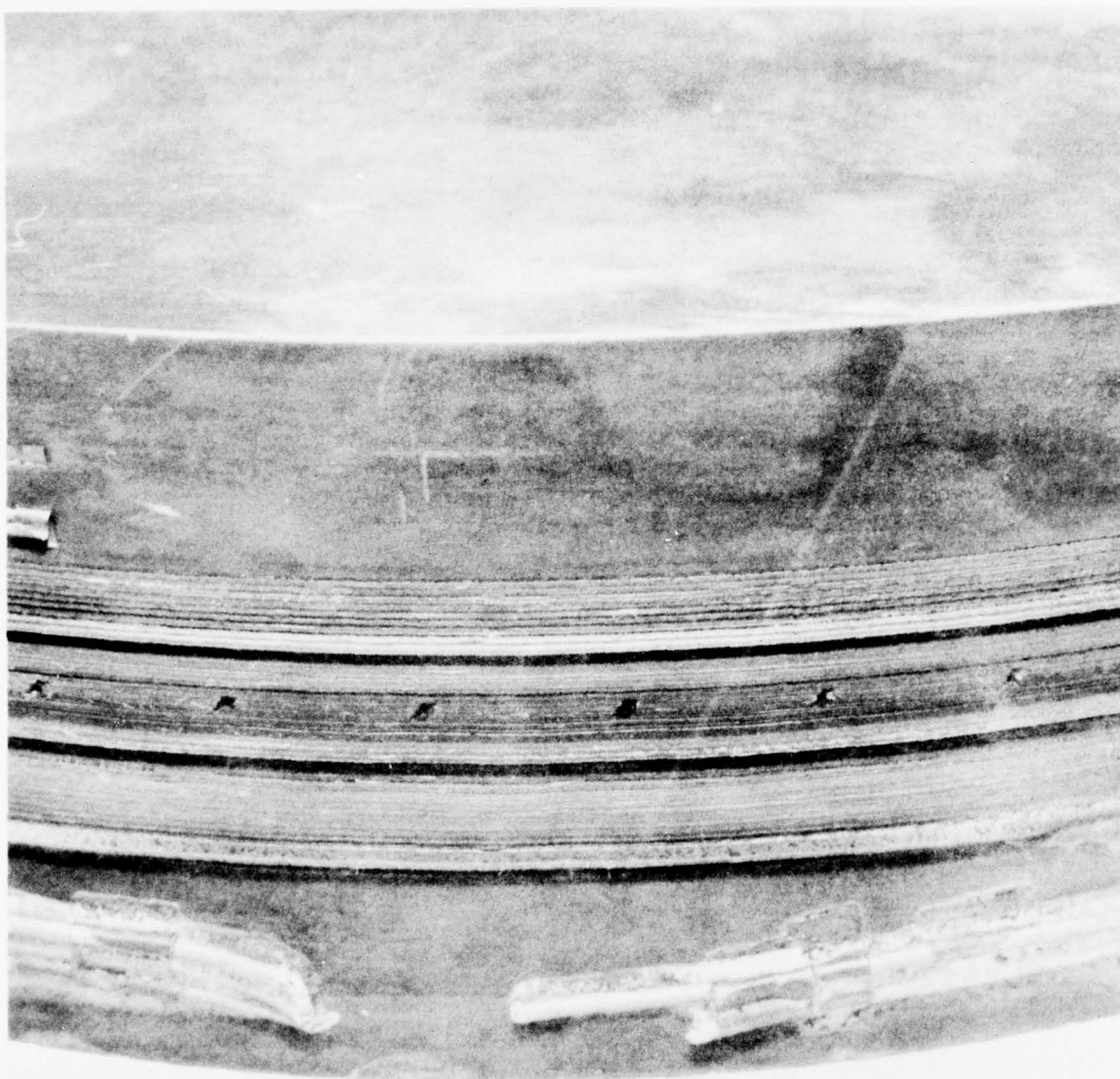
Figure 65. View of the As-Bonded Second Wheel Blank. Flow of
the Bond Alloy is Visable as Fillets on Thermo-
couples and on the Lower Trailing-Edge Dimension
Land. Note Erosion of the Land at the Far Right of
the Photograph.

135

Figures 66 and 67 show the ultrasonic inspection results for each side of the second wheel blank. These results indicated that there were no detectable unbonded areas in the hub section. This inspection technique did not yield results in the blade area because of the disrupted resolution caused by the internal blade cooling passages.

Excess flow of the bond alloy was observed to have occurred due to an over-temperature condition to 2200°F that occurred for approximately 15 minutes during initial heating to 2160°F. Liquid flow was also observed in the small capillary passages in most of the blades. Figure 68 depicts the extent of liquid flow that resulted in closure of most of the blade tip discharge ports.

In order to avoid breaking through the blade walls during airfoil finish machining, it was necessary to accurately determine the location of the interior cooling passages. Measurement of axial positions representing laminate interfaces was utilized to determine the average-joint thickness and cooling-passage positions. This data indicated that the average-joint thickness in the 0.020-inch thick laminates was 0.0008 inch, while in the 0.010-inch thick laminates it was minus 0.00031 inch. This negative interface thickness is the result of the greater ratio of bond alloy to Waspaloy volume in the 0.010-inch thick laminations. The overall average joint thickness was established as 0.00015 inch, which was below the small stack thickness of 0.00065 inch, and was probably due to the temperature excursion encountered during bonding.

Cylinders 0.16-inch in diameter were again removed by EDM in an axial orientation to the wheel laminates adjacent to the bore, and radially at the outside diameter. These samples were used for metallographic evaluation and mechanical property testing of the second wheel blank.

Figure 69 shows the bond-joint microstructure at various locations in a cylinder removed from the bore of the wheel blank. These structures are similar to those exhibited by specimens from Stack 11 that was bonded in the laboratory. Complete inter-diffusion occured at the interfaces with very little eutectic or porosity. A sample removed radially at the outside diameter exhibited similar structures.

The remaining cylinders were prepared for mechanical property testing. The results of these tests, (refer to Table 20 for Stack 12) are shown in Table 21. Due to the small diameter of the specimens removed from the wheel blank, these mechanical properties also reflect the variations expected in properties that are often associated with sub-size mechanical test specimens. A comparison of the data indicates that the wheel-blank tensile properties are 10-percent lower than those achieved in the small stack, and that the stress-rupture properties are 20-percent higher. This trend of lower tensile and increasing stress-rupture properties is
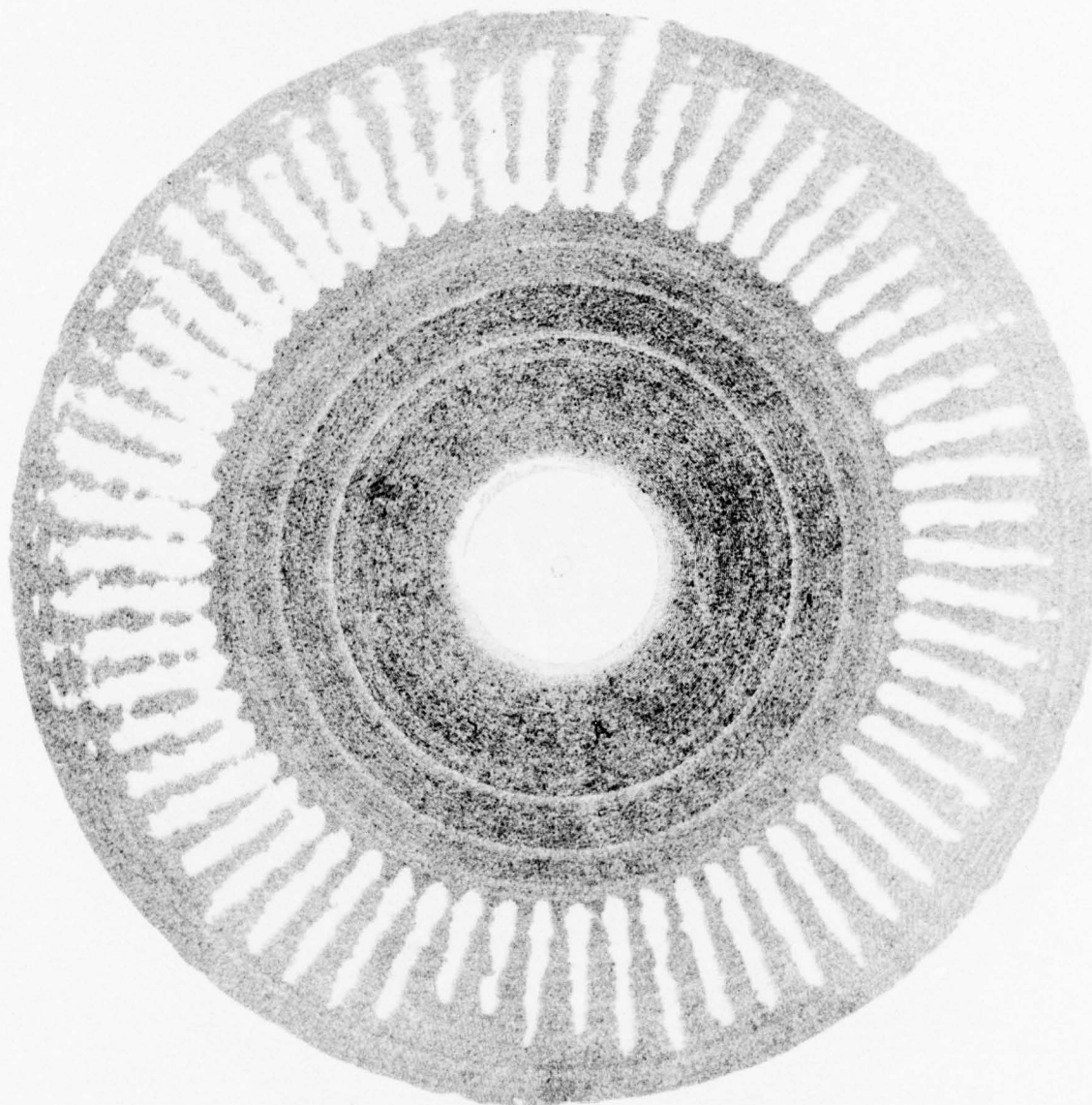
136

Figure 66. Ultrasonic Inspection Results of the Second
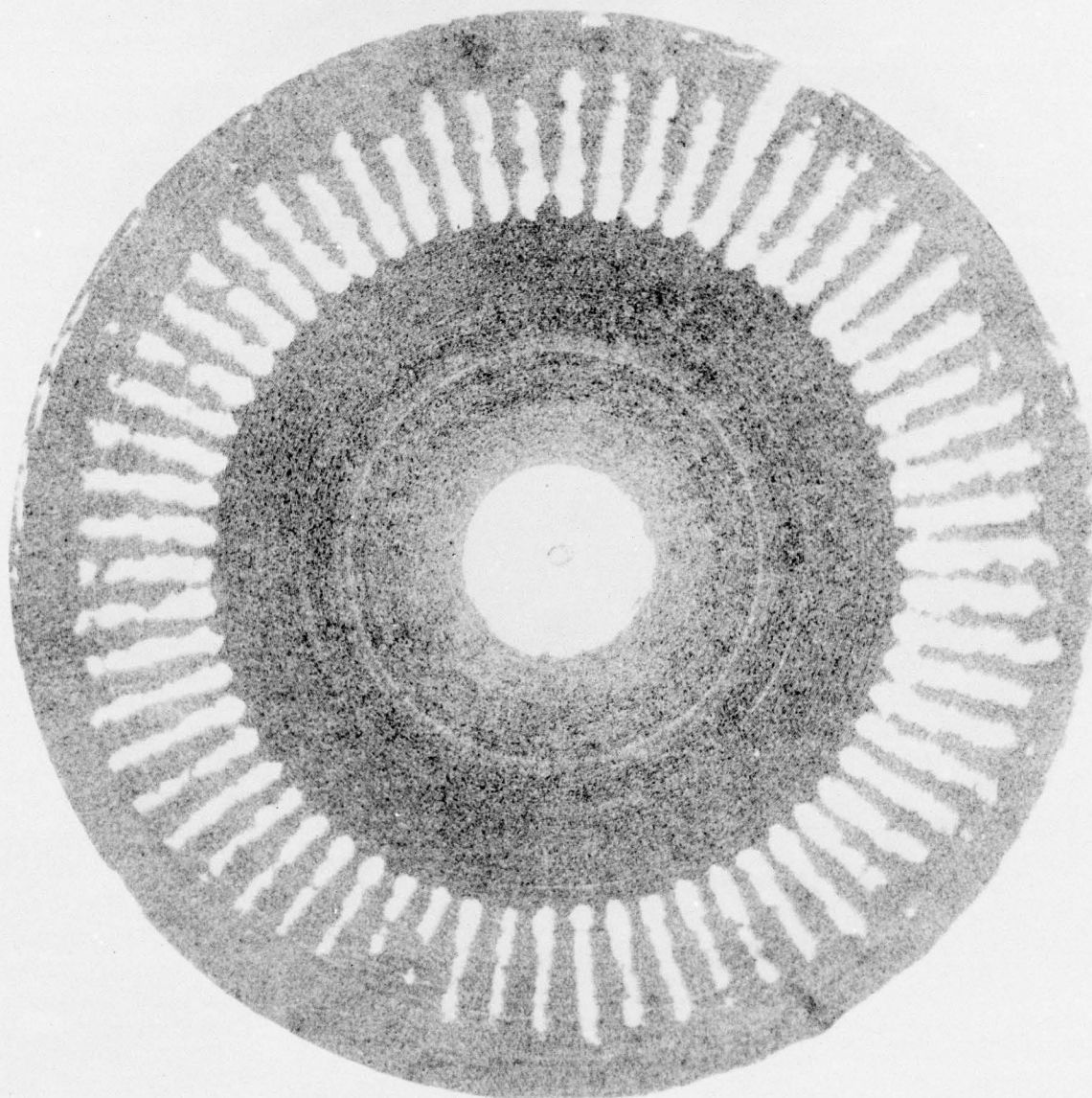Laminated Wheel Blank (Top View).

137

Figure 67. Ultrasonic Inspection Results of the Second
Laminated Wheel Blank (Bottom View).

MP-52409

Figure 68. Metallographically Prepared Surface of the Second
Wheel Blank Outside Diameter Showing the Extent of
Flow of Bond Alloy Liquid into the Tip Passages.
Dotted Lines Show the Approximate Passage True Size.
Numbers at Left Edge Give Locations of Some of the
Axial Points Used in the Dimensional Analysis.
(Mag.: 10X)

139

A. INTERFACE OF END PLATE TO FIRST 0.020-INCH LAMINATE.
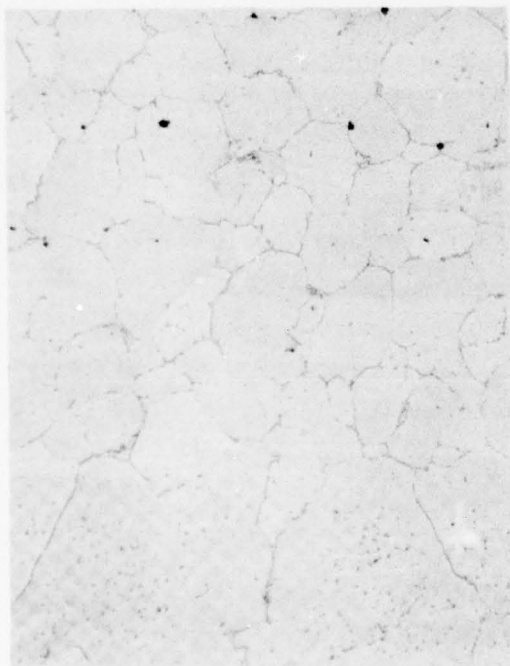
B. INTERFACE OF 0.020- TO 0.010-INCH LAMINATE.
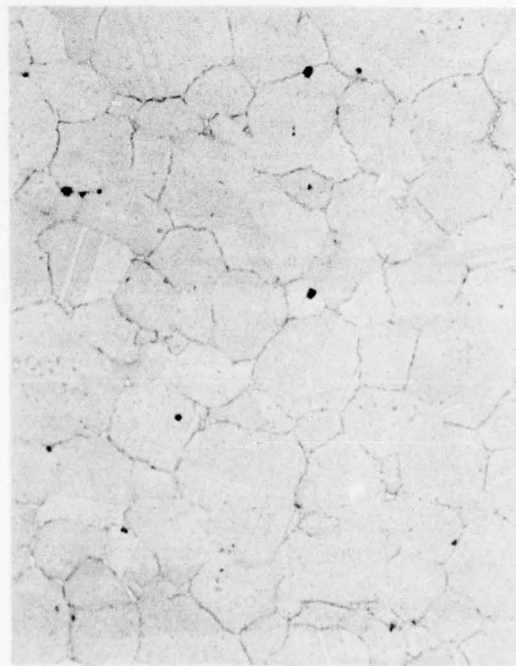
C. INTERFACE OF 0.010- TO 0.010-INCH LAMINATE.

Figure 69. Interfaces of Laminates at the Leading-Edge End of the Bore Specimen from the Second Wheel Blank. (Mag.: 80X)

MP-56464

TABLE 21. MECHANICAL PROPERTIES OF
SPECIMENS FROM THE
SECOND WHEEL BLANK.

Specimen	UTS (ksi)	0.2% YS (ksi)	Elongation (%)	Life (Hours)
Room-Temperature Tensile				
Longitudinal	110.8	---	3.4	---
1400°F Tensile				
Longitudinal	107.9	---	2.8	---
Longitudinal	112.2	---	3.0	---
1400°F Tensile				
Transverse	96.0	---	0.6	---
Transverse	97.3	---	0.2	---
1500°F Stress Rupture, 47.5 ksi	---	---	---	---
Transverse	---	---	---	---

NOTES: Thermal History

    Diffusion Bonding – heat at 11°F per minute to 2165°F, hold for 6 hours, and air cool. Initial excursion to 2200°F for 15 minutes on heating.

    Heat Treatment – 1975°F for 4 hours with argon gas fan cooling
    Plus 1500°F for 4 hours with air cooling
    Plus 1400°F for 16 hours with air cooling

believed to result from the higher bond temperature used in the wheel blank stack, and this trend was also observed with previous stacks bonded in the laboratory.

b.   Finish Machining

After the bonding and heat treatment, the second wheel blank was sent to the profile-machining vendor. The vendor machined the laminated wheel blank to the required shape prior to final blade/disk machining. Figure 70 shows a picture of the rough machined rotor assembly prior to blade machining. Figure 71 is a photograph of the wheel blank after the machining of two sample blades.

The machining task was completed without any difficulties, and Figure 72 shows the machined rotor. Figure 73 is a close-up of the blade tip area. As seen from Figure 73, the blade-tips exhibit varying degrees of plugging. Radiographic inspection was conducted to further define the plugging. Figures 74 and 75 show radiographic results in the blade areas, indicating the variability of internal plugging. As previously determined, the plugging resulted from excess bonding material flow associated with the temperature excursion experienced during bonding. This plugging effect is not expected to occur after the bonding methods for the laminated wheel fabrication process are optimized.

Figure 70. Second Bonded Wheel Blank Rotor Assembly Prior to
Final Machining. Leading-Edge Side of the Wheel.

143
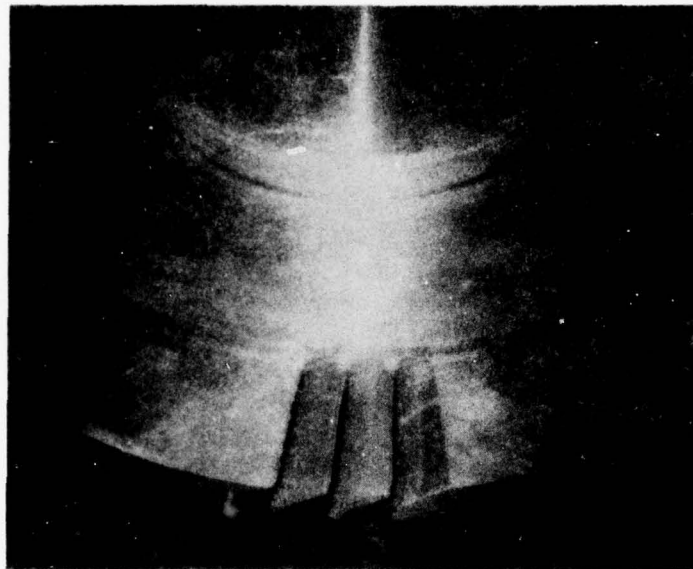
Figure 71. Second Bonded Wheel Blank Rotor Assembly with Sample
Machined Blades. Trailing-Edge Side of the Wheel.

144
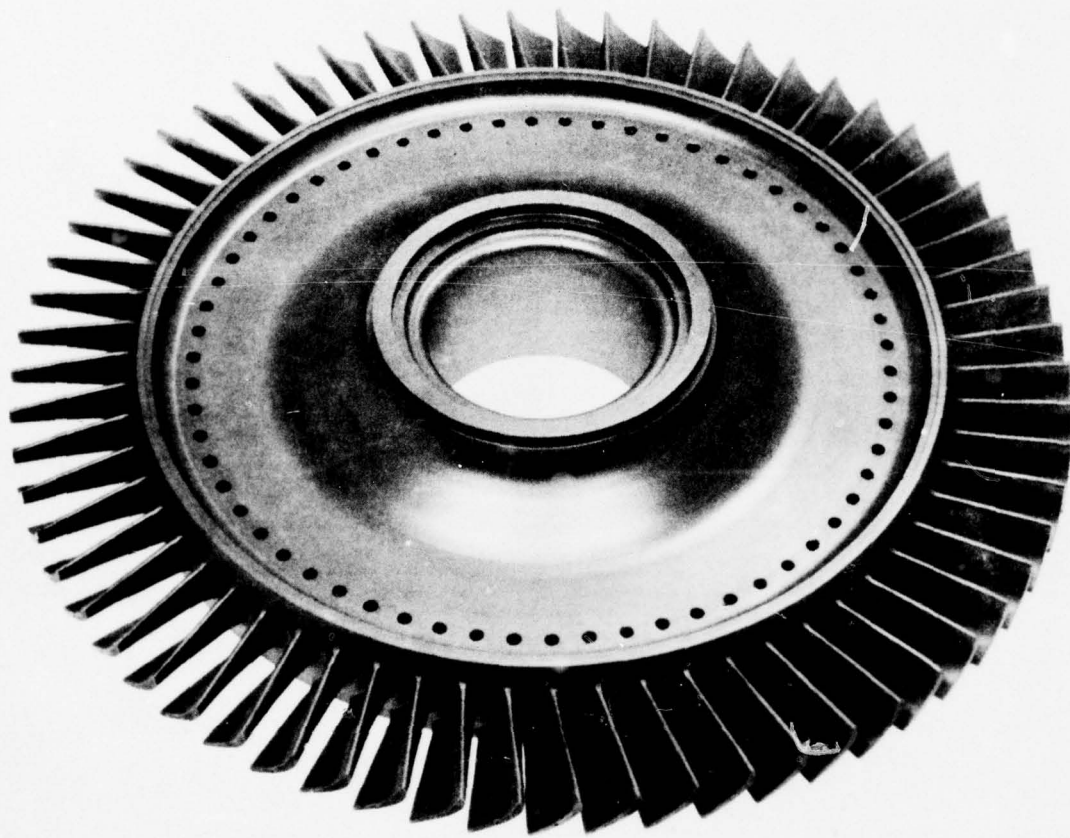
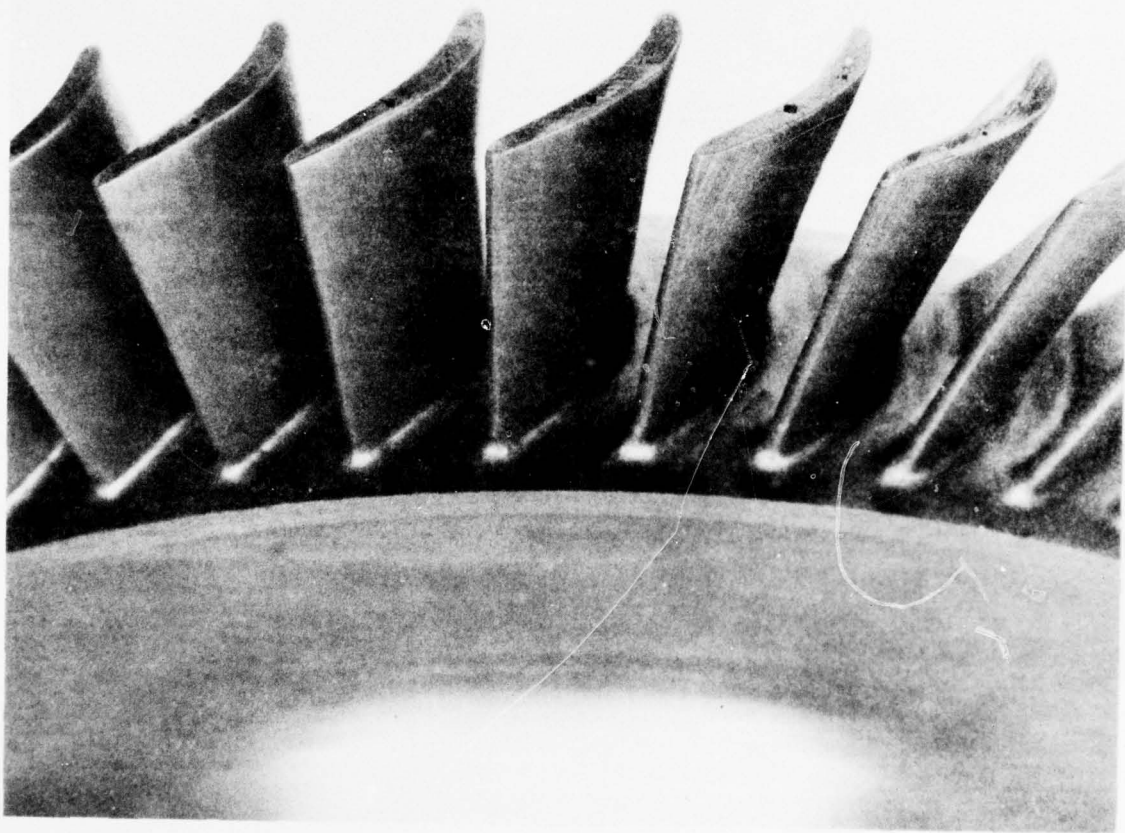Figure 72. Fully-Machined Laminated Turbine Wheel.

145

Figure 73. Close-up of the Blade Tips on the Finish-Machined Laminated Turbine Wheel.
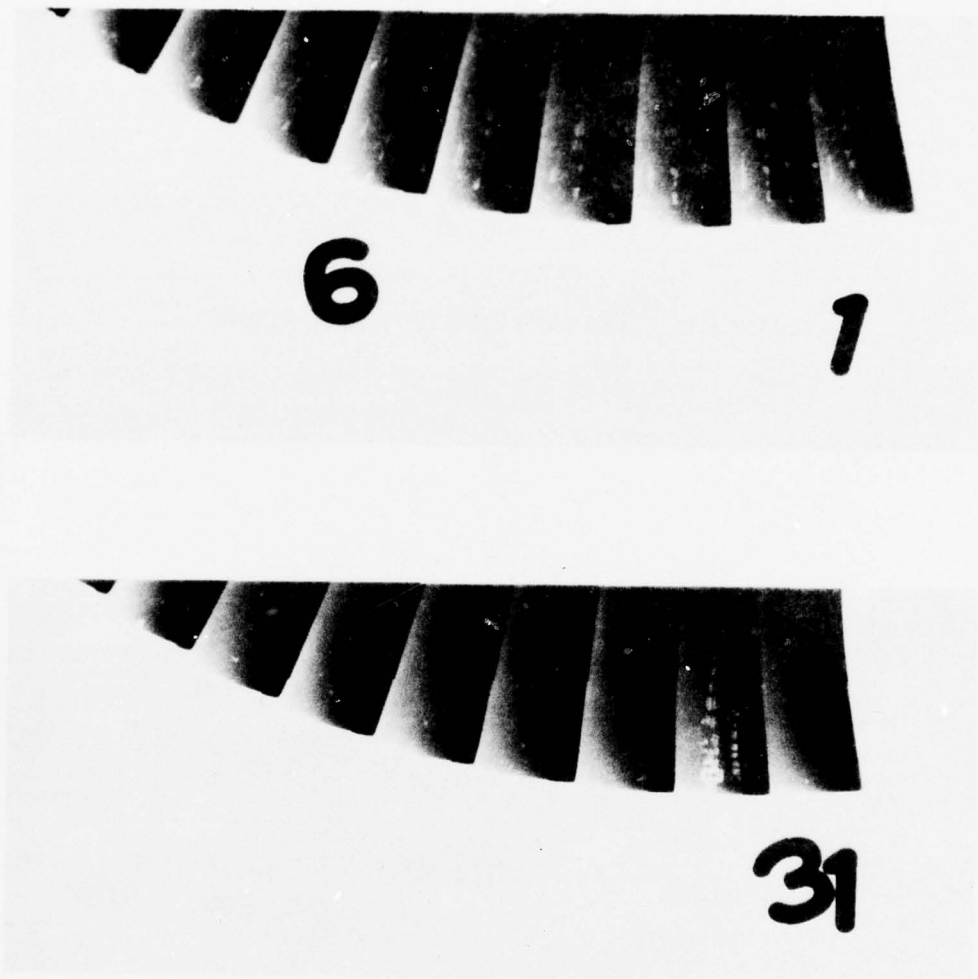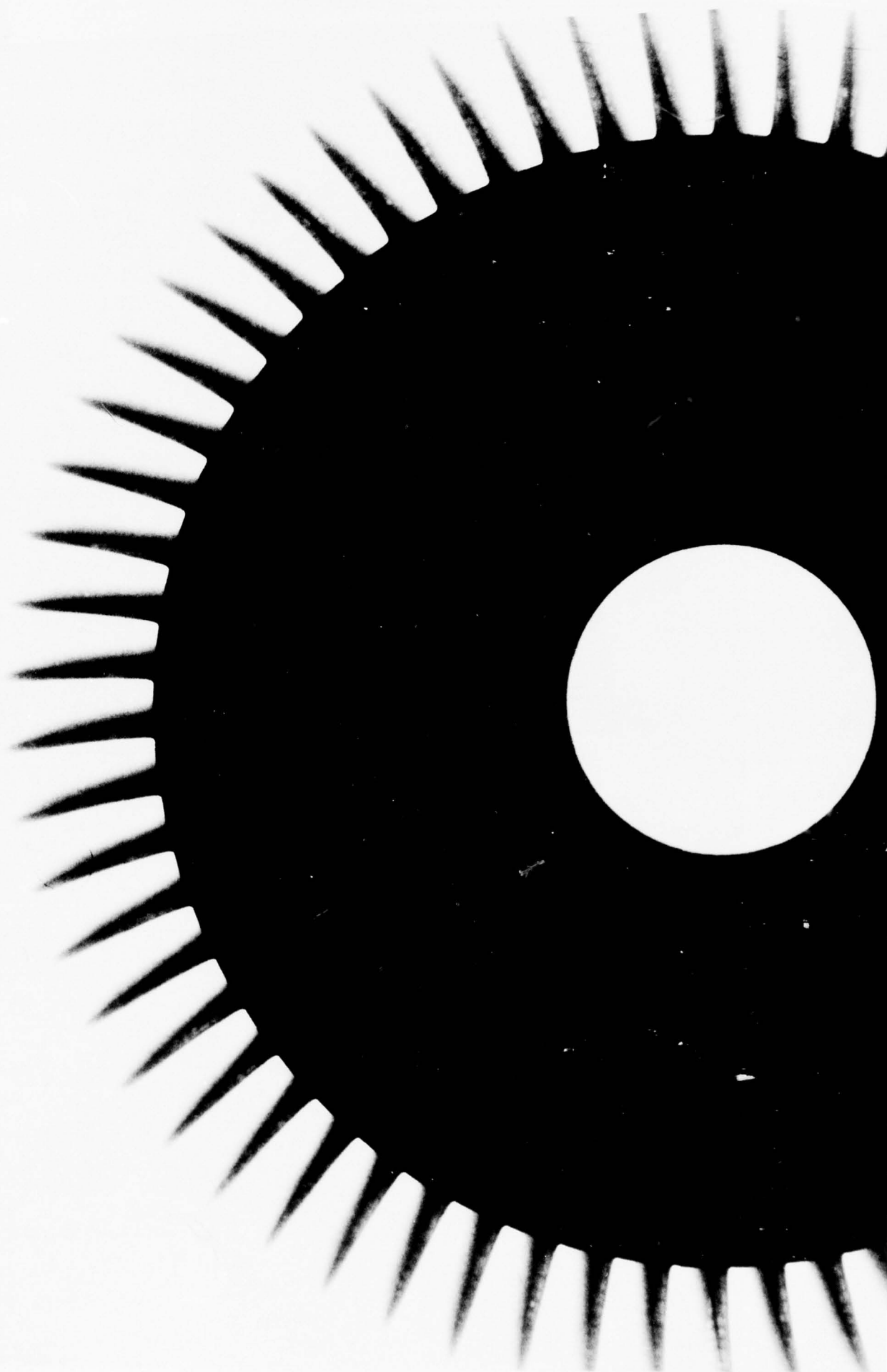
Figure 74.   Radiographic Results from the
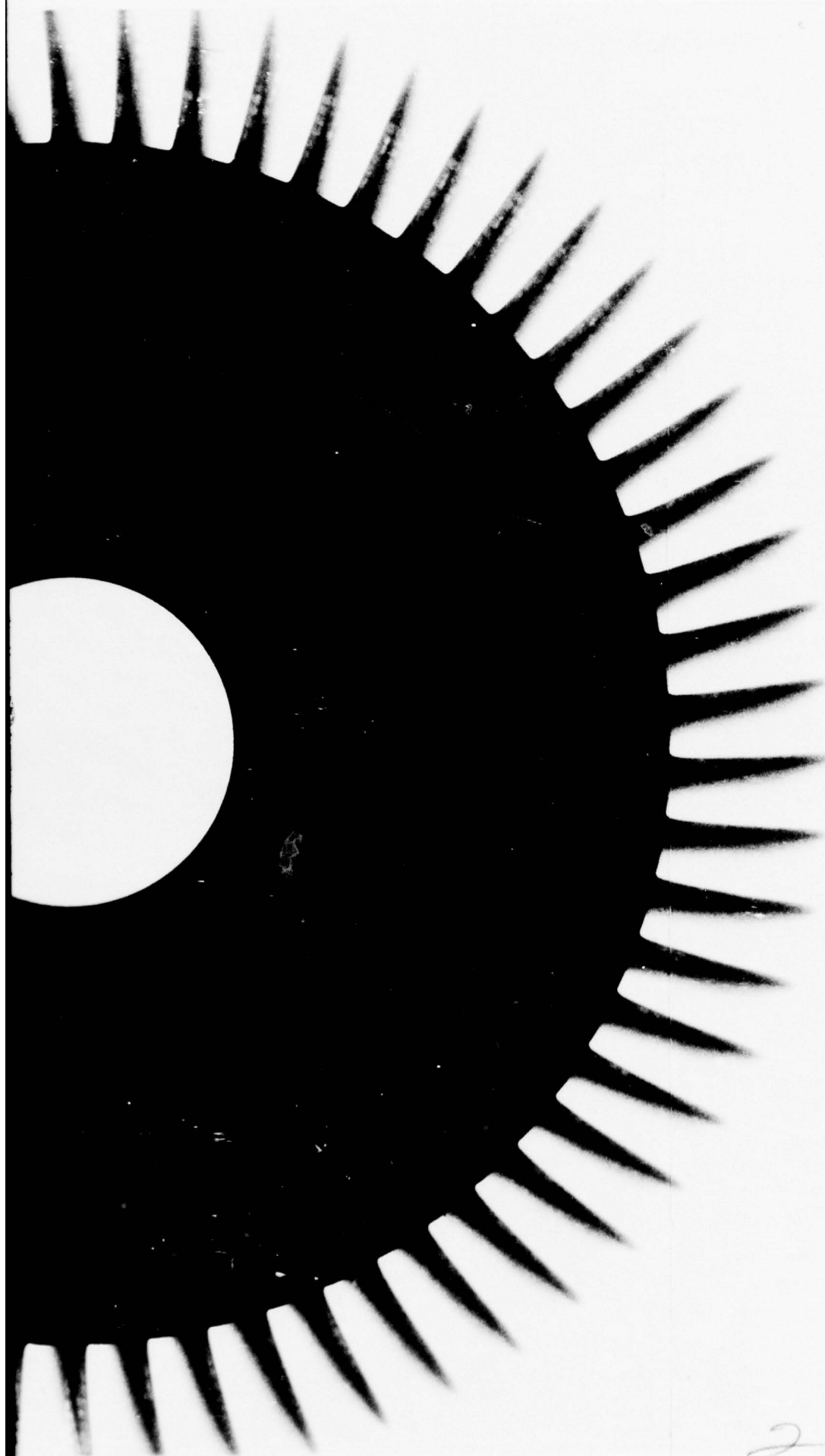Laminated Turbine Wheel.

147

THIS PAGE INTENTIONALLY LEFT BLANK

Figure 75. Radiographic
Results from
the Laminated
Turbine Wheel.

SECTION V

EVALUATION AND TESTING

The evaluation and testing of the fully-machined laminated turbine wheel consisted of an additional stress analysis, Stresscoat testing, and cold spin-pit growth tests.

1. STRESS ANALYSIS

a. Introduction

A second stress analysis of the laminated turbine wheel was performed before growth testing was initiated. The second analysis was deemed necessary because the geometry used in the original stress analysis was altered considerably during fabrication and machining, as can be seen by comparing Figures 76 and 77. The wheel configuration changed in three basic areas:

o   The hub geometry near the bore

o   The transition area from the hub to the
     web of the wheel

o   The blade platform area

The second stress model was constructed utilizing the final layout drawings, giving the most accurate geometry available.

In addition to the geometric differences between the initial and second stress models, a more sophisticated analytical model was used. The analytical model initially used evaluated only two-dimensional stresses induced by rotation. The computer program is limited in that it solves for radial, tangential, and equivalent stresses only. Blade loading was accounted for by specification of a uniformly distributed load at the rim, which in reality is not the case.

The analytical model used in the second stress analysis does utilize a true three-dimensional finite-element stress analysis for an axisymmetric body. Loading due to the blades is calculated internally in the program from the specified geometry. Radial, axial, tangential, shear, and equivalent stresses are calculated, as are blade stresses. In addition, this program evaluates the complete state of stress at each node point in the model grid.
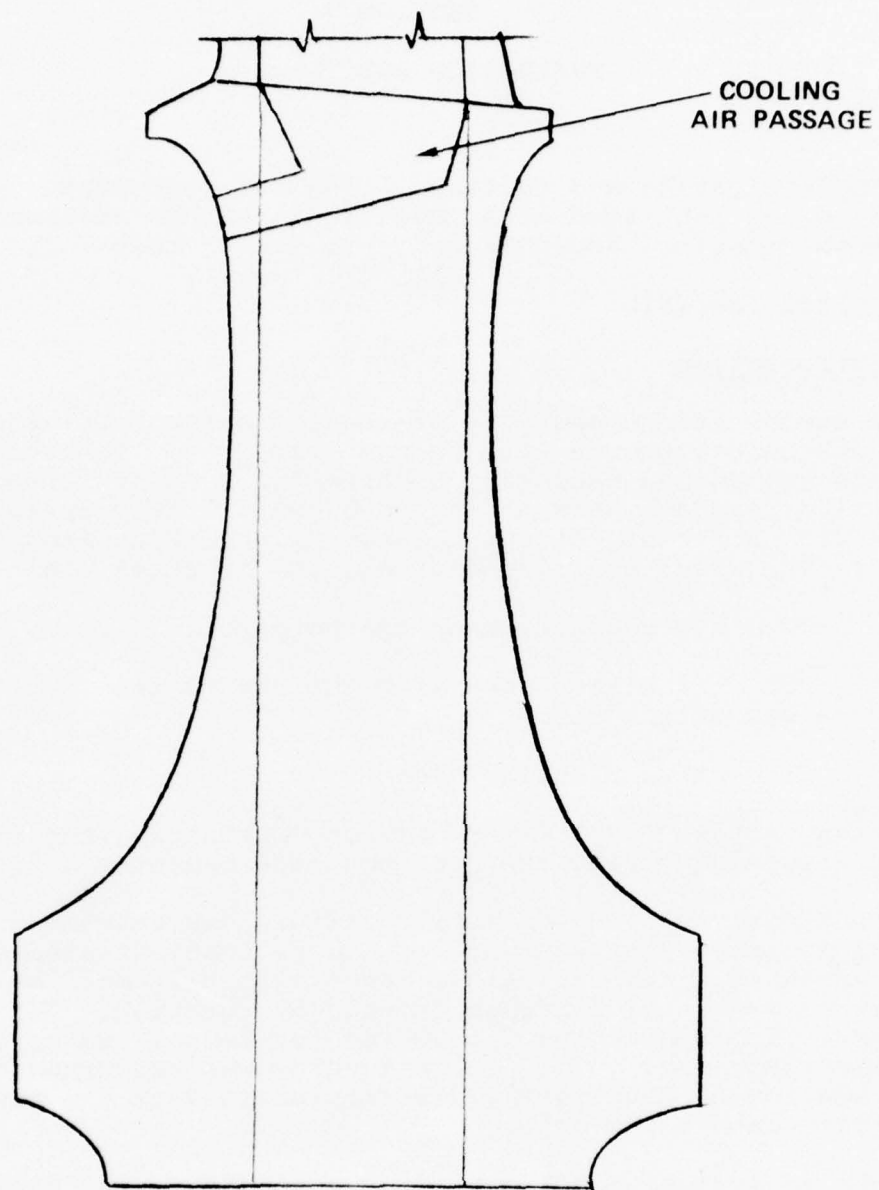
151

COOLING
AIR PASSAGE

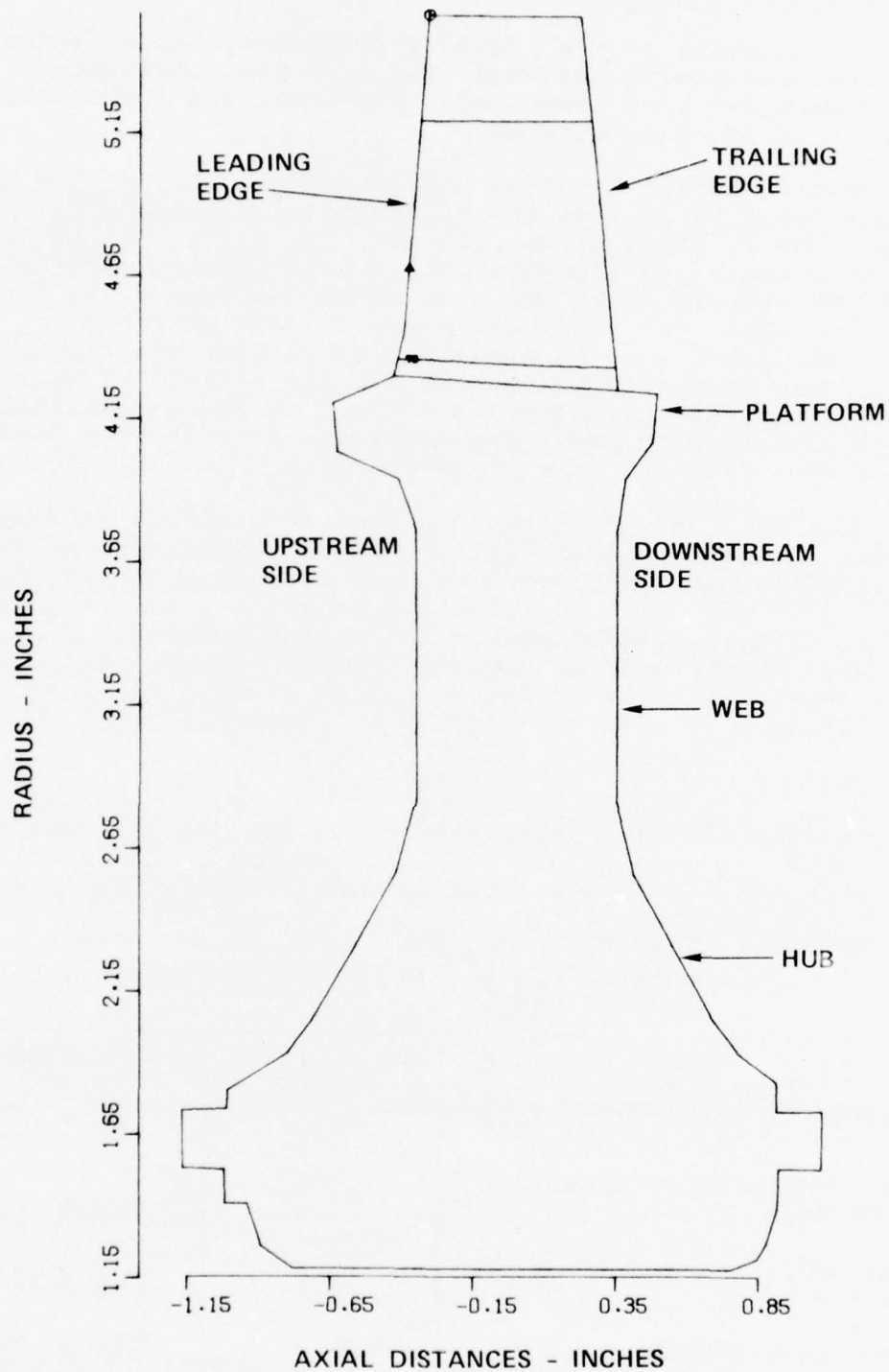Figure 76.   Preliminary Laminated Turbine Disk Geometry.

152

Figure 77.   Laminated Turbine Disk Stress Analysis Geometry.

b. Approach and Analysis

At the beginning of the second stress analysis, a finite-element model describing the wheel geometry was constructed, and a nodal network was then generated. The model was fixed axially at the front or upstream curvic.

In order to better simulate the actual geometry of the wheel, two further modifications to the blade/wheel geometry were necessary. Due to fabrication problems, the blade cooling-air passages near the blade tip were filled with bonding material, and the blade stacking axis had been moved upstream 0.010 inch. To accomodate this, the blade was moved forward on the disk model by 0.010 inch, and the blade thickness near the tip of the blade model was increased to account for the additional mass due to the filled cooling passages. After all of these modifications to the wheel model were made, the model was evaluated to determine the stress levels in the blade and disk.

The disk was assumed to have no thermal gradient imposed on it, and was assumed to have a uniform metal temperature of 70°F. This is in agreement with actual test conditions to which the wheel was to be exposed. Additionally, the wheel was assumed to undergo centrifugal loading only. The stress model was evaluated at two different speeds. Figures 78 through 82 show predicted stress at 100-percent speed (29,692 rpm). Figures 83 through 87 show the stress levels at 120-percent speed (35,630 rpm).

c. Results

The results of this analysis describe the complete state of stress in the laminated wheel. A brief summary of the results of the analytical stress model can be seen in Table 22.

TABLE 22. SUMMARY OF RESULTS OF THE SECOND STRESS ANALYSIS PERFORMED ON THE LAMINATED TURBINE WHEEL.

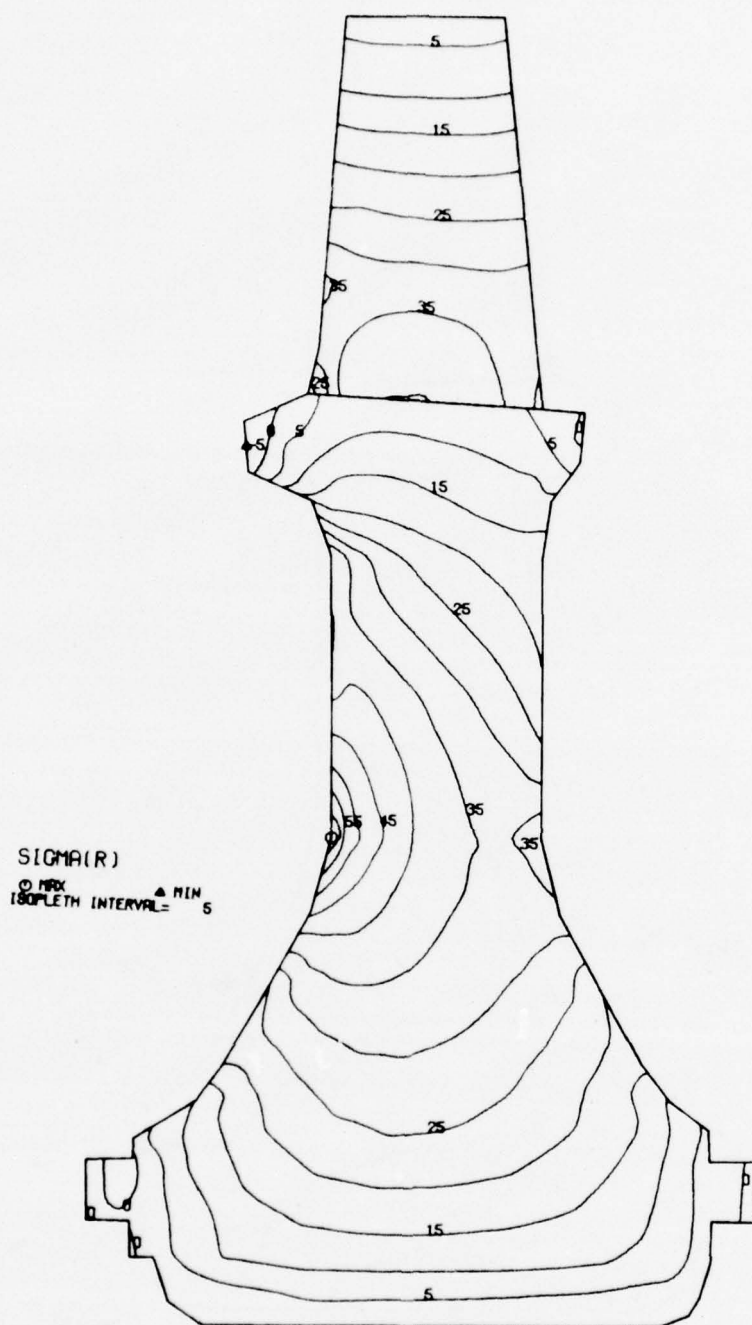| Parameter	100-Percent Speed	120-Percent Speed
Average Tangential Stress (KSI)	56.2	80.8
Maximum Tangential Stress at the Bore (KSI)	85.3	122.9
Maximum Radial Stress at the Web (KSI)	66.5	95.7
Maximum Shear Stress (KSI)	31.9	45.9

154

Figure 78. Laminated Turbine Wheel Radial Stress
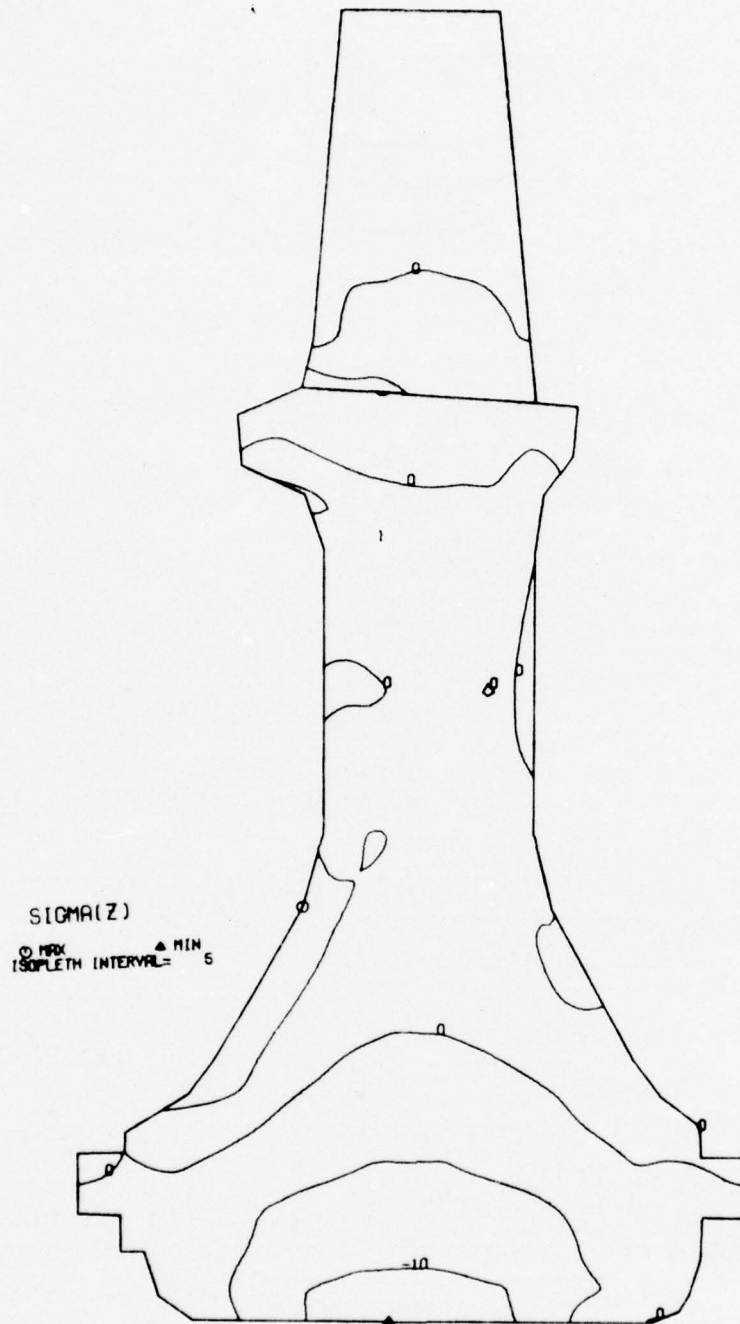Distribution (KSI) at a Speed of 29,692 RPM.

155

Figure 79. Laminated Turbine Wheel Axial Stress
Distribution (KSI) at a Speed of
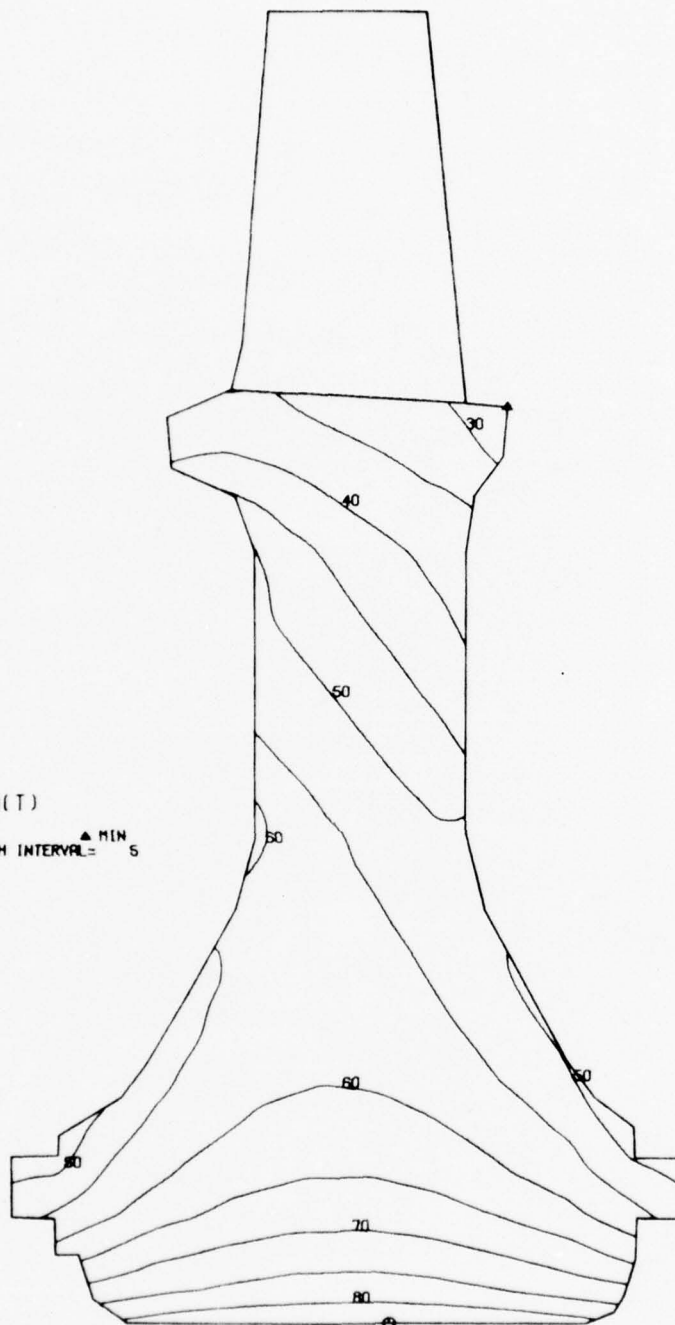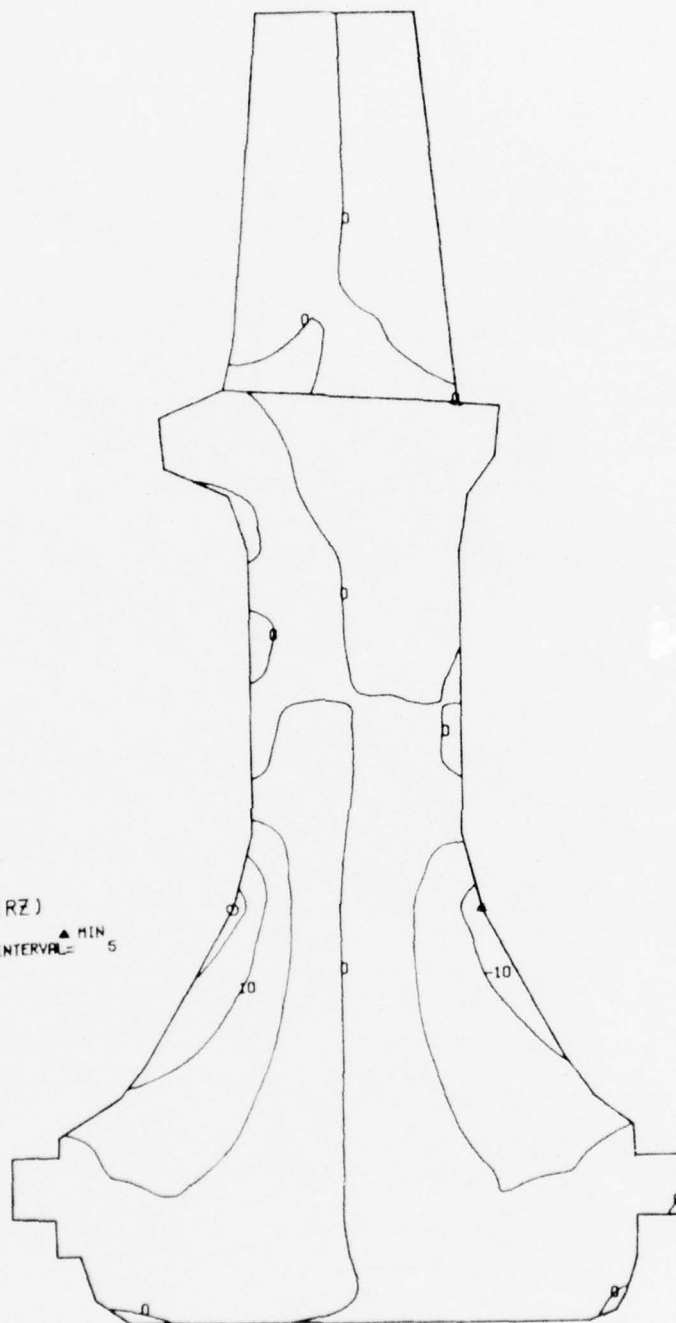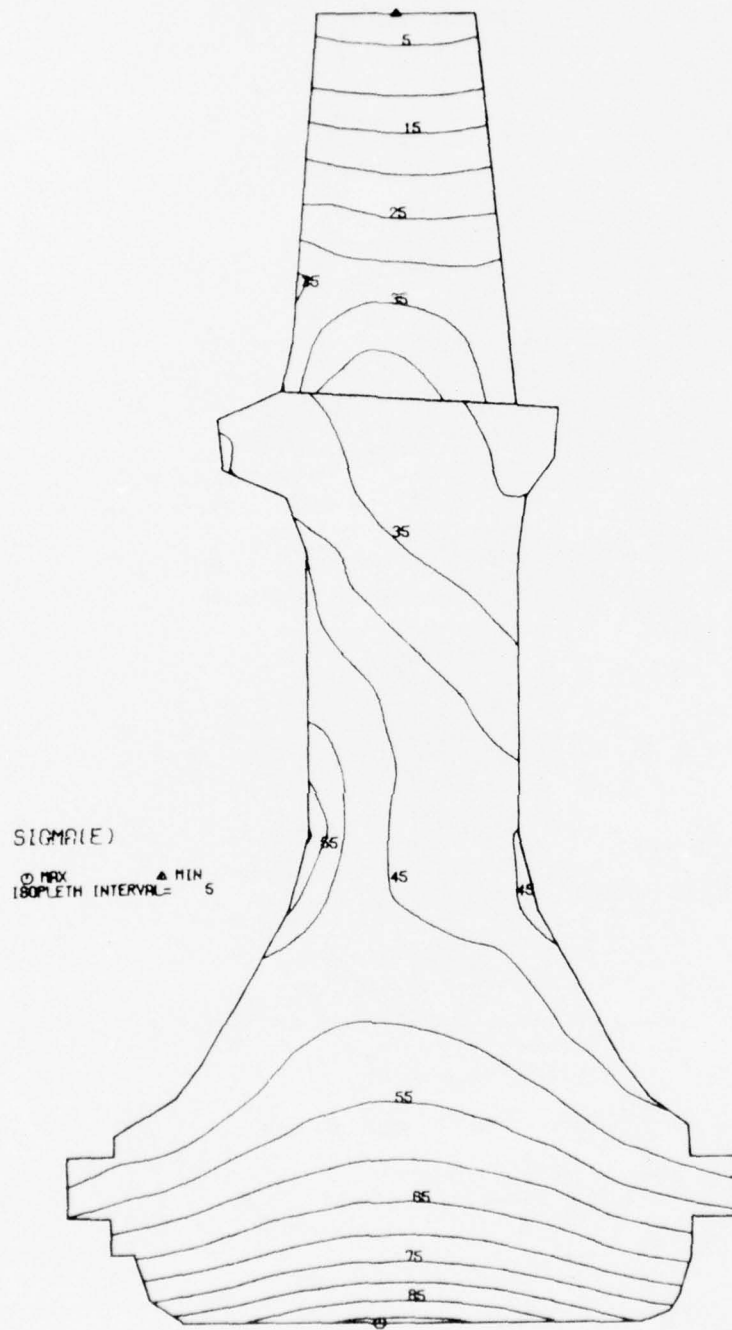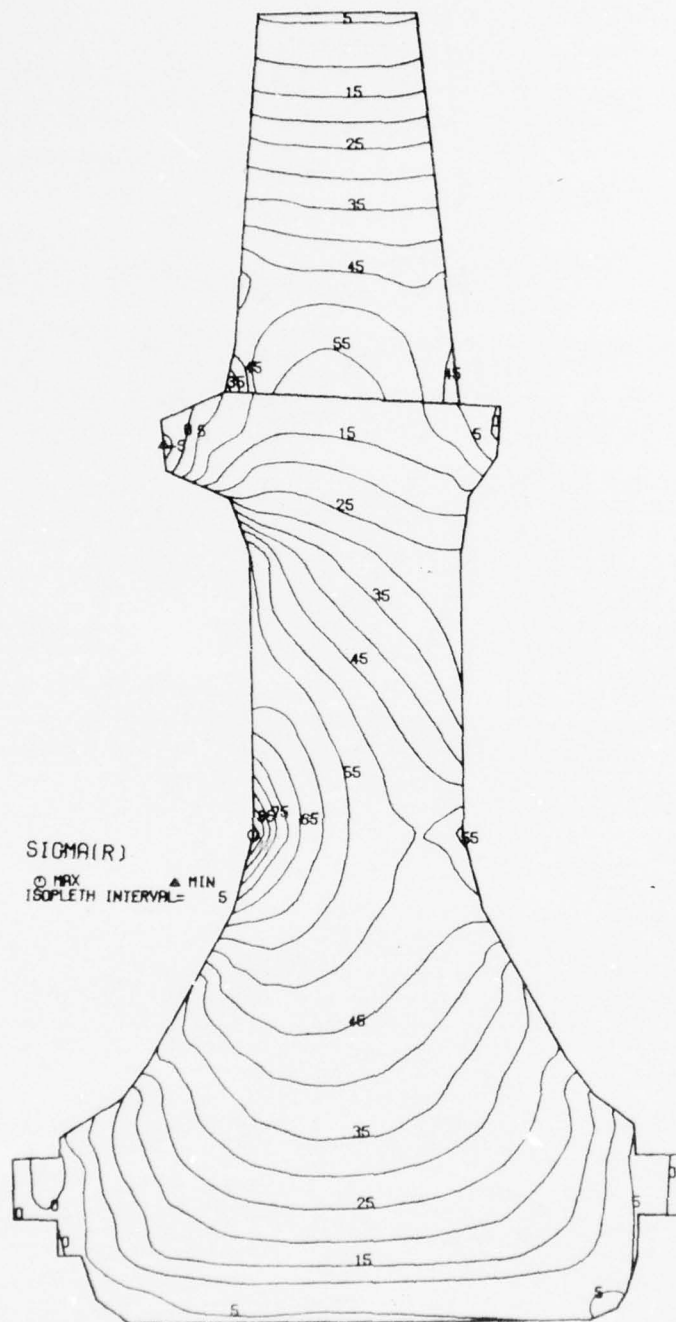29,692 RPM.

156

SIGMA(T)

⊙ MAX   ▲ MIN
ISOPLETH INTERVAL= 5

Figure 80. Laminated Turbine Wheel Tangential Stress
Distribution (KSI) at a Speed of 29,692 RPM.

157

Figure 81. Laminated Turbine Wheel Shear Stress
Distribution (KSI) at a Speed of
29,692 RPM.

Figure 82. Laminated Turbine Wheel Equivalent Stress
Distribution (KSI) at a Speed of 29,692 RPM.

159

Figure 83. Laminated Turbine Wheel Radial Stress Distribution (KSI) at a Speed of 35,630 RPM.
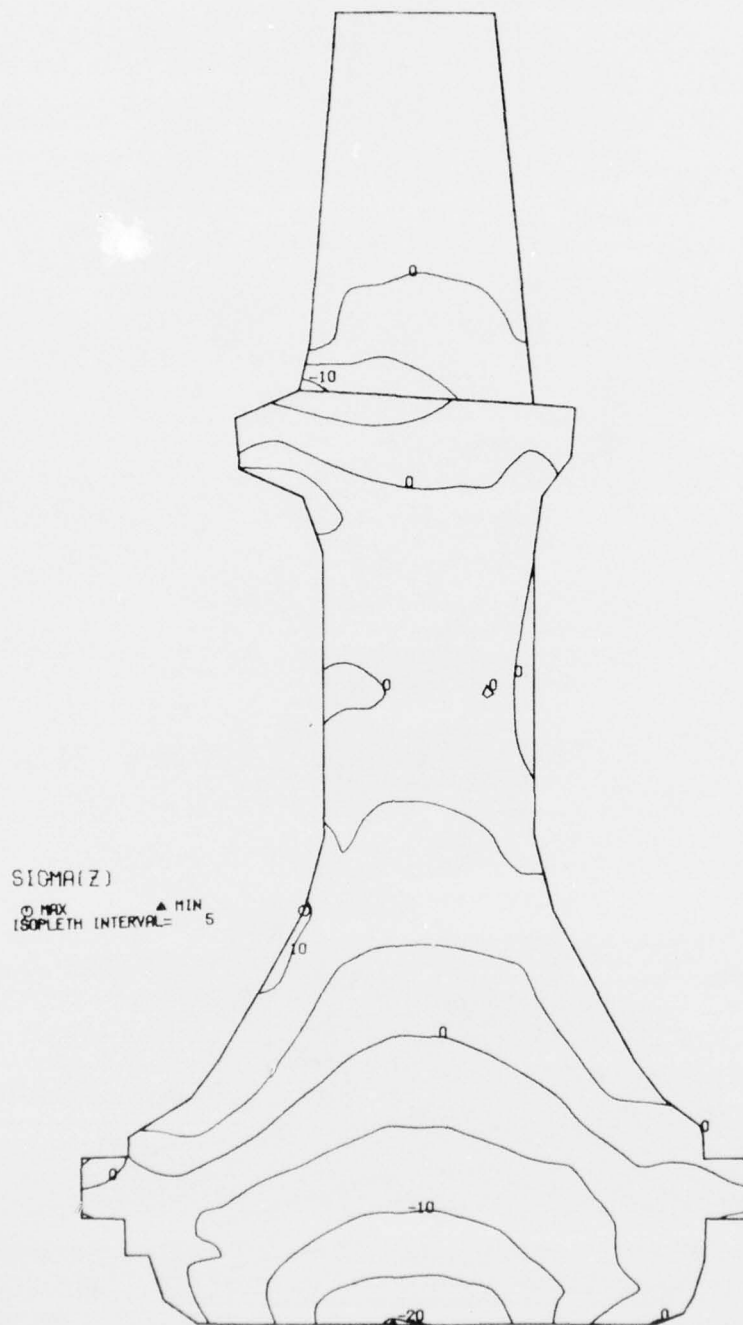
Figure 84. Laminated Turbine Wheel Axial Stress
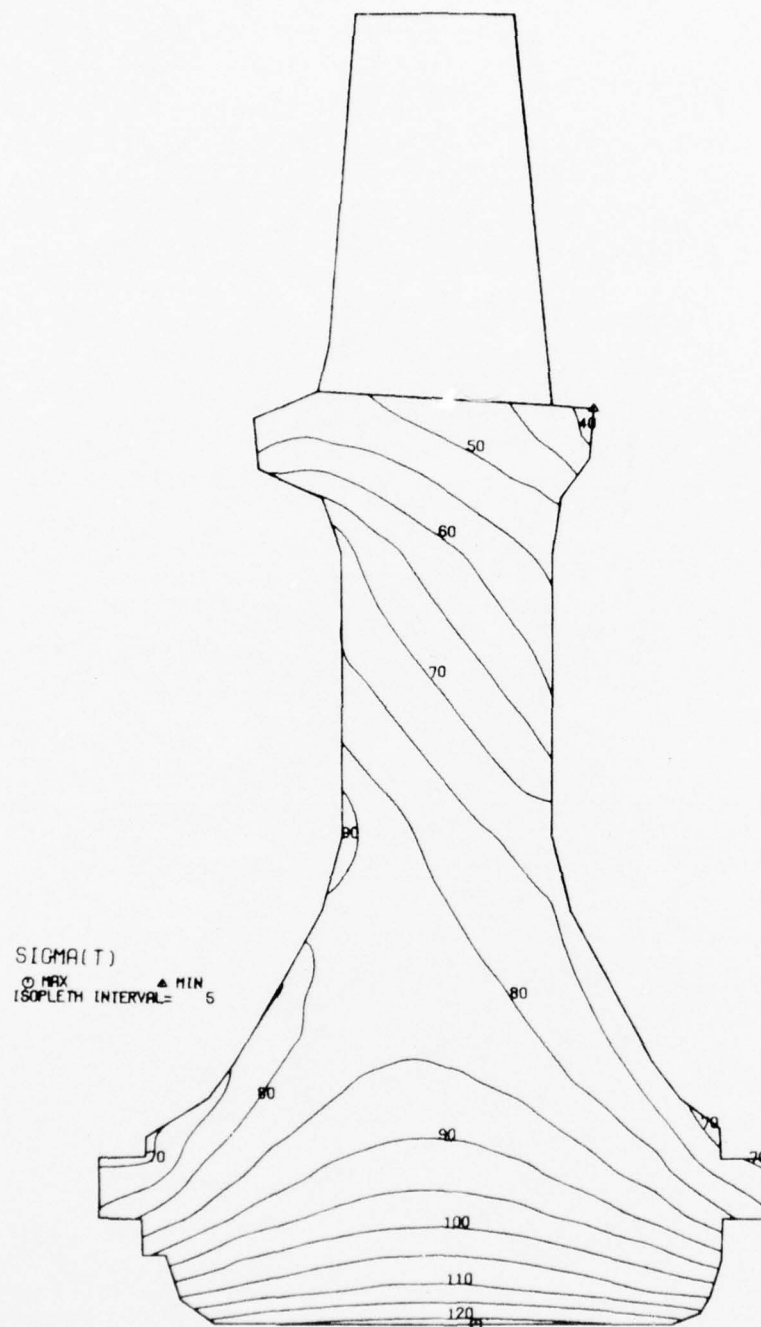Distribution (KSI) at a Speed of
35,630 RPM.

161

Figure 85.   Laminated Turbine Wheel Tangential Stress
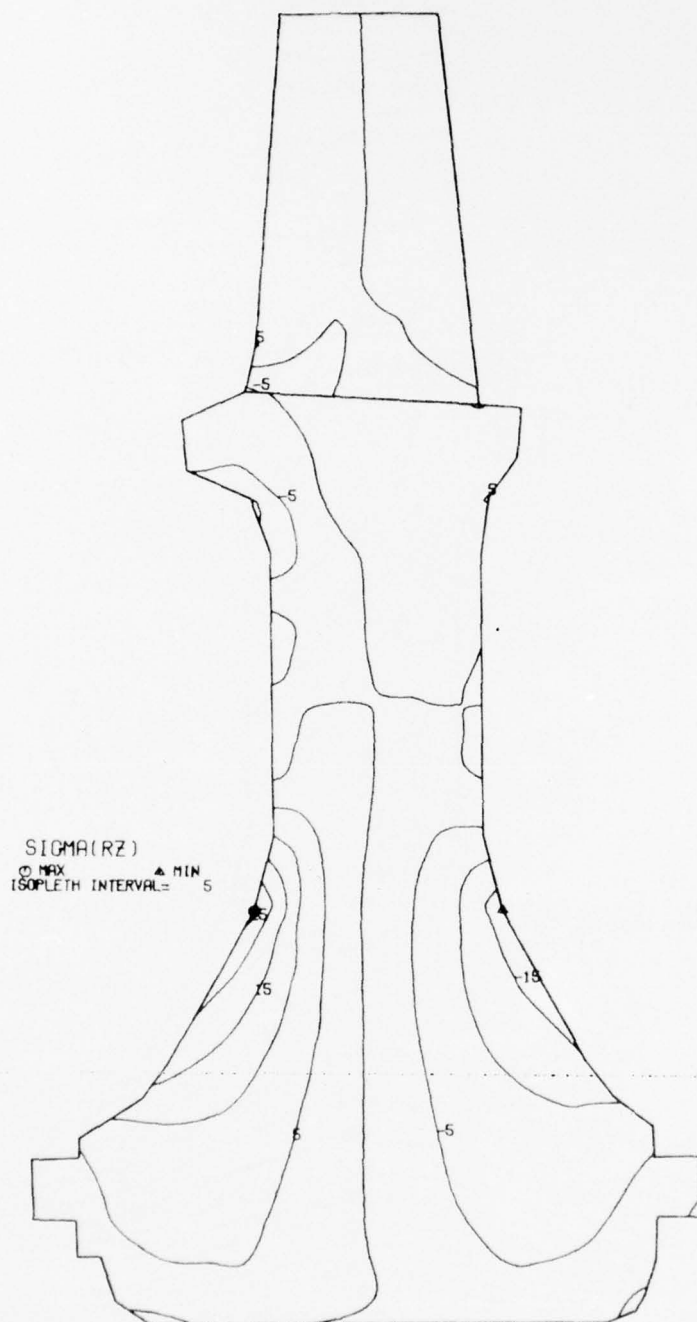   Distribution (KSI) at a Speed of 35,630 RPM.

162

Figure 86.   Laminated Turbine Wheel Shear Stress
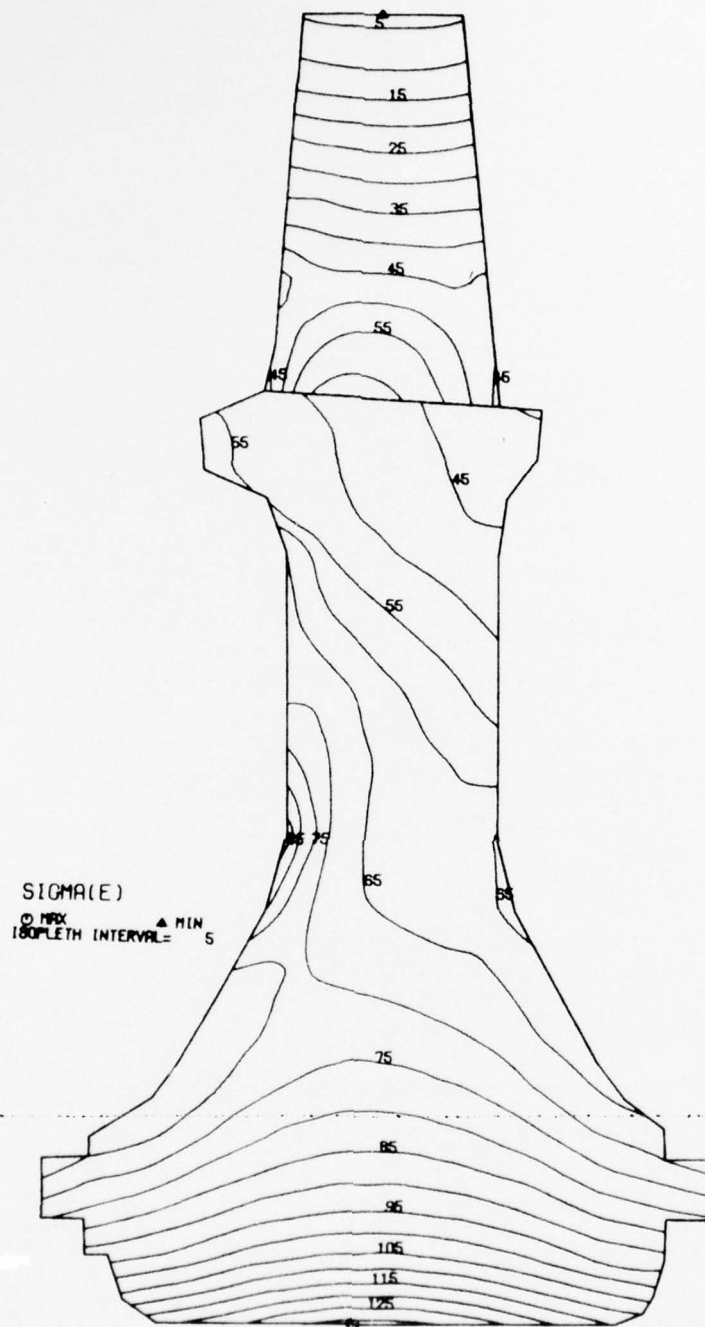Distribution (KSI) at a Speed of
35,630 RPM.

163

Figure 87. Laminated Turbine Wheel Equivalent Stress
Distribution (KSI) at a Speed of 35,630 RPM.

164

From these results, it is possible to calculate the burst margin of this wheel using the equation:

$$\text{Burst Margin} = \sqrt{\frac{(BF) \ X \ (\text{Ultimate Strength})}{\text{Average Tangential Stress}}};$$

where: BF = Burst factor

Ultimate Strength = 110.8 ksi (for laminated Waspaloy)

The value given for ultimate strength was arrived at experimentally at AiResearch, and represents nominal material properties. Use of the above equation and the assumption that the burst factor falls between 0.8 and 1.0 yields a burst margin between 1.26 and 1.40 at full speed (29,692 rpm). Theoretically, a nominal wheel should burst at a speed somewhere between 37,289 rpm and 41,691 rpm.

d.   Conclusions

The analytical stress model, in conjunction with the available material properties for laminated Waspaloy, indicated that little risk is involved in testing to 115-percent overspeed condition.

2.   STRESSCOAT TEST

a.   Introduction

The Stresscoat testing on the laminated turbine wheel was conducted in conjunction with the stress analysis of the wheel, and to assess possible areas of stress concentration. The effect of nonuniform plugging of the blade cooling passages was of particular interest.

b.   Configuration and Test

For this test, the laminated wheel and calibration bar specimens were coated with the strain-sensitive Stresscoat. After coating, the wheel and calibration bars were dried under controlled conditions, and were allowed to thermally stabilize before testing was initiated.

The wheel was mounted on the drive arbor of the spin pit, and at the same time, a calibration bar was placed in the pit at a location in the proximity of the wheel. The pit was then sealed, and the pressure was slowly reduced so as not to adversely affect wheel temperature, and therefore, the Stresscoat sensitivity.

165

The wheel was then accelerated to the desired speed, then decelerated to a complete stop. The spin-pit vacuum was slowly released to minimize or prevent a temperature rise that could close cracks in the Stresscoat. The procedure described above was utilized for each of the four tests performed.

c. Results

The results of the Stresscoat testing are summarized in Table 23.

TABLE 23. STRESSCOAT TEST RESULTS.

Speed	Calibration Bar Sensitivity (μ in./in.)	Nominal Stress (psi)	Indicated Stress at 100-Percent Speed (ksi)	Indicated Stress at 120-Percent Speed (ksi)	Zone
10,750	525	16.0	$\geq$122	$\geq$175	1
12,000	525	16.0	122-98	175-141	2
14,100	495	15.1	98-67	141-96	3
16,050	550	16.8	67-57	96-83	4

The location of the stress zones may be seen in the post-test photographs (see Figures 88 through 92).

The results of the testing indicated that any non-uniform plugging of the blades had not resulted in any excessive stress concentrations on the blade or disk. Good qualitative agreement can be seen by comparing the photographs of the Stresscoat test results (Figures 88 through 92) to the illustrations of equivalent stresses obtained from the second stress analysis (Figures 77 and 87). The stress model indicates high stress levels on the upstream side of the wheel at the transition area between the hub and web, and at the blade root on the leading-edge side of the blade. Results from the Stresscoat testing compare favorably at these locations.

Additionally, the stress model shows an area of high stress just below the hub-web transition area on the downstream side, which is again in agreement with the Stresscoat test results. The location of those high stress areas produced by the Stress-coat test compares very well with the location of highly stressed areas predicted by the stress model.
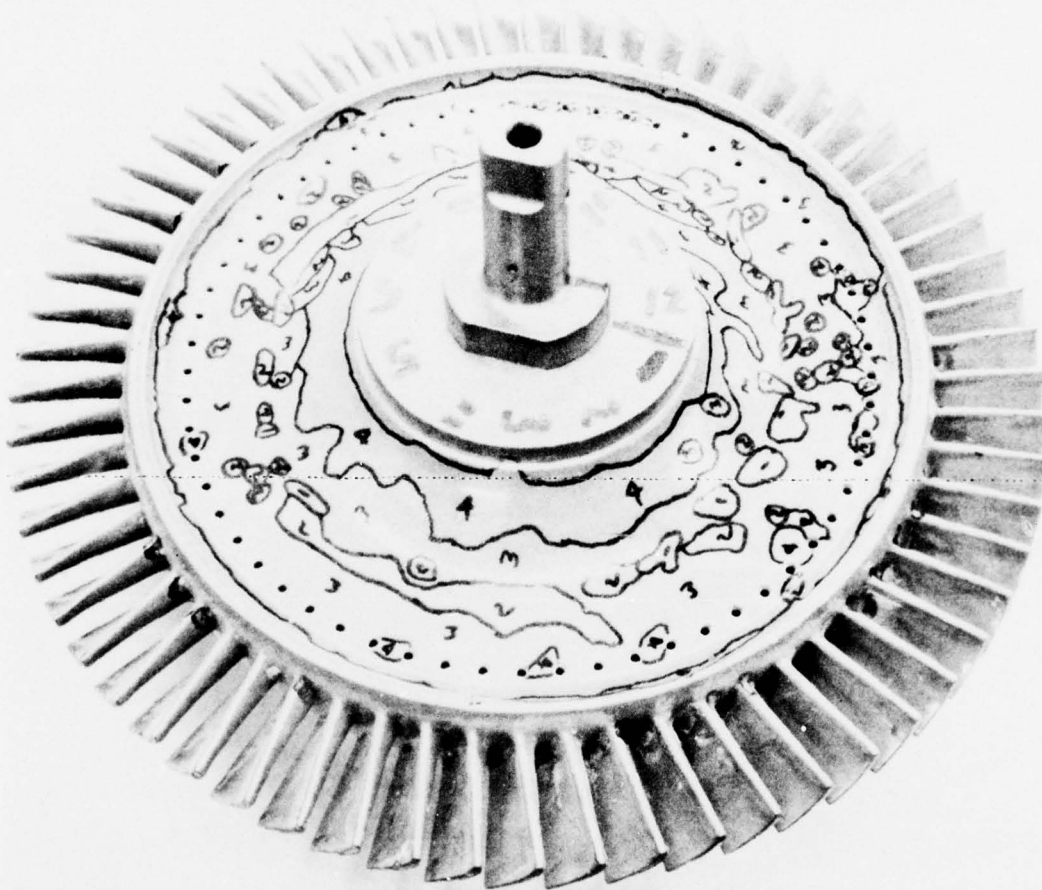
Figure 88. Laminated Turbine Wheel Leading-Edge Side
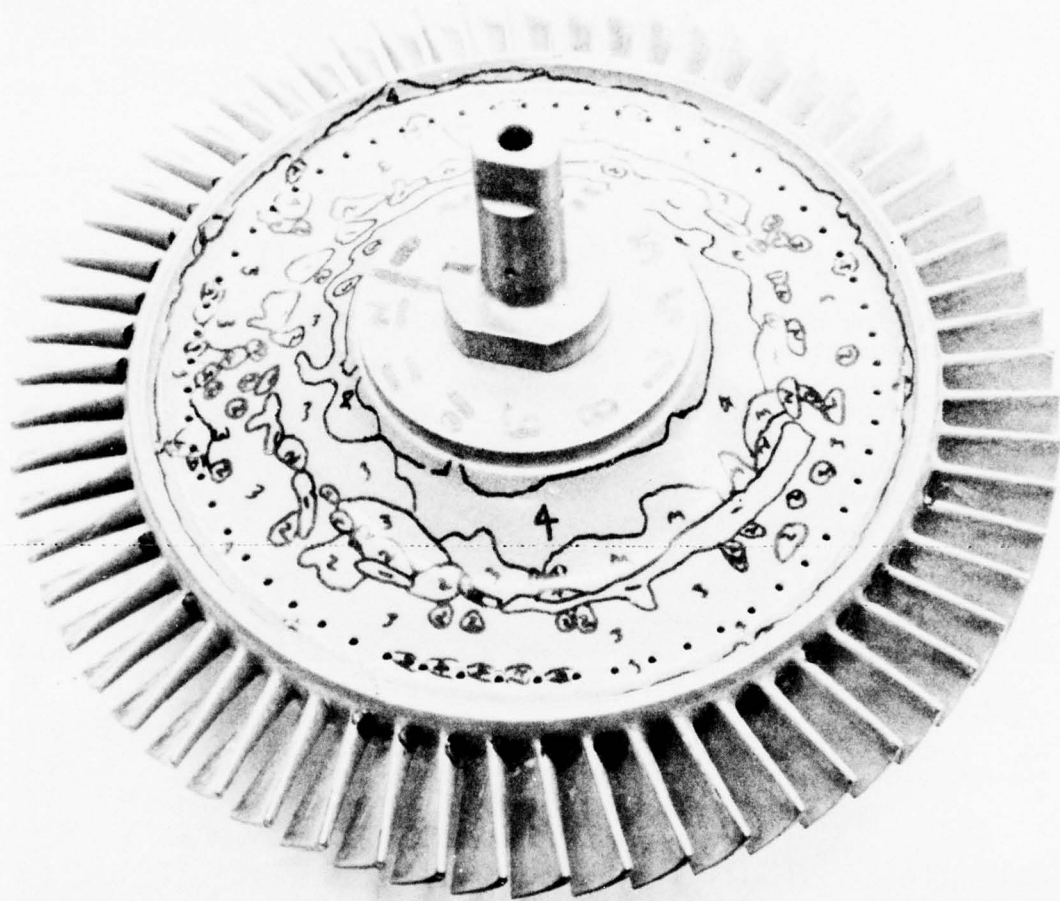After Stresscoat Testing.

Figure 89. Laminated Turbine Wheel Leading-Edge Side
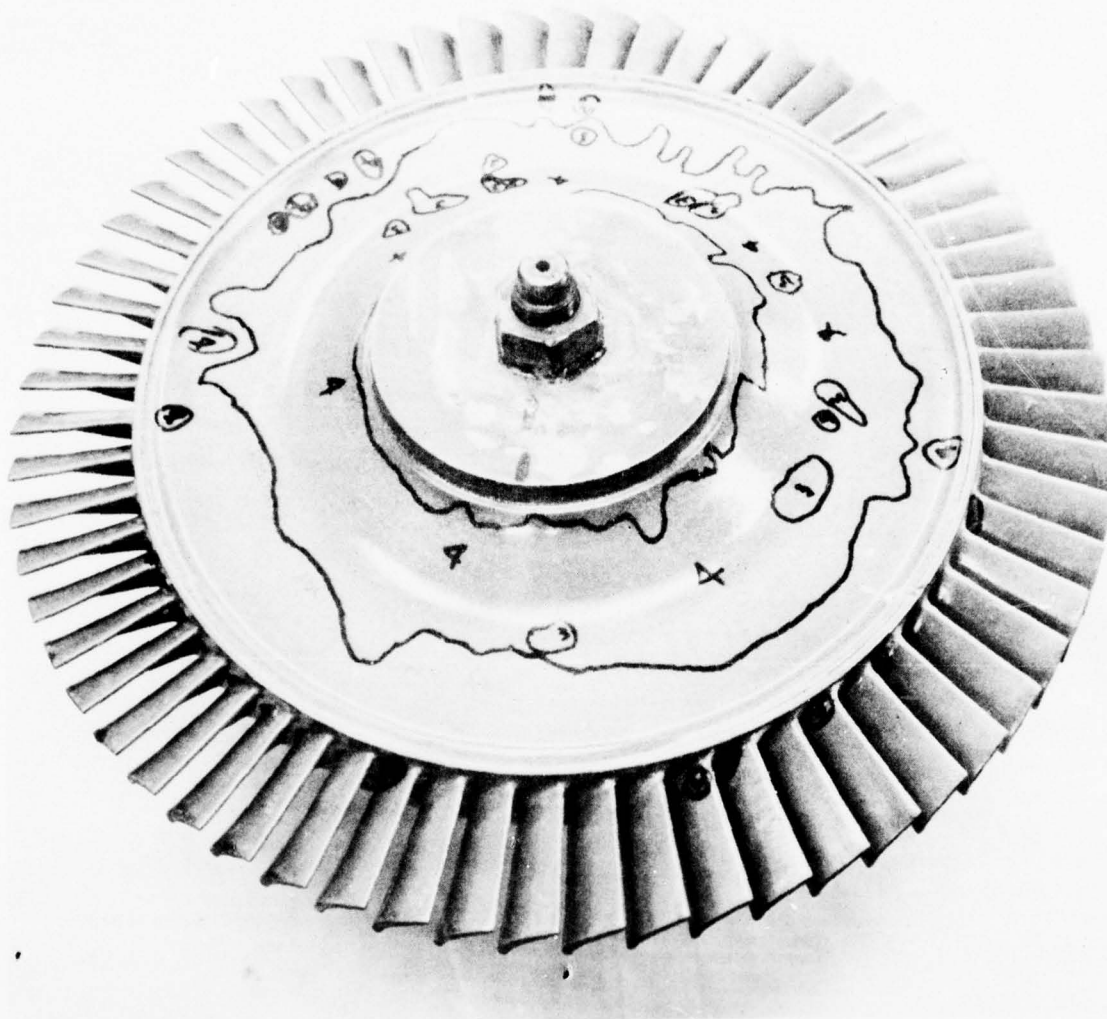After Stresscoat Testing (Wheel Rotated
180°).

168

Figure 90.   Laminated Turbine Wheel Trailing-Edge Side
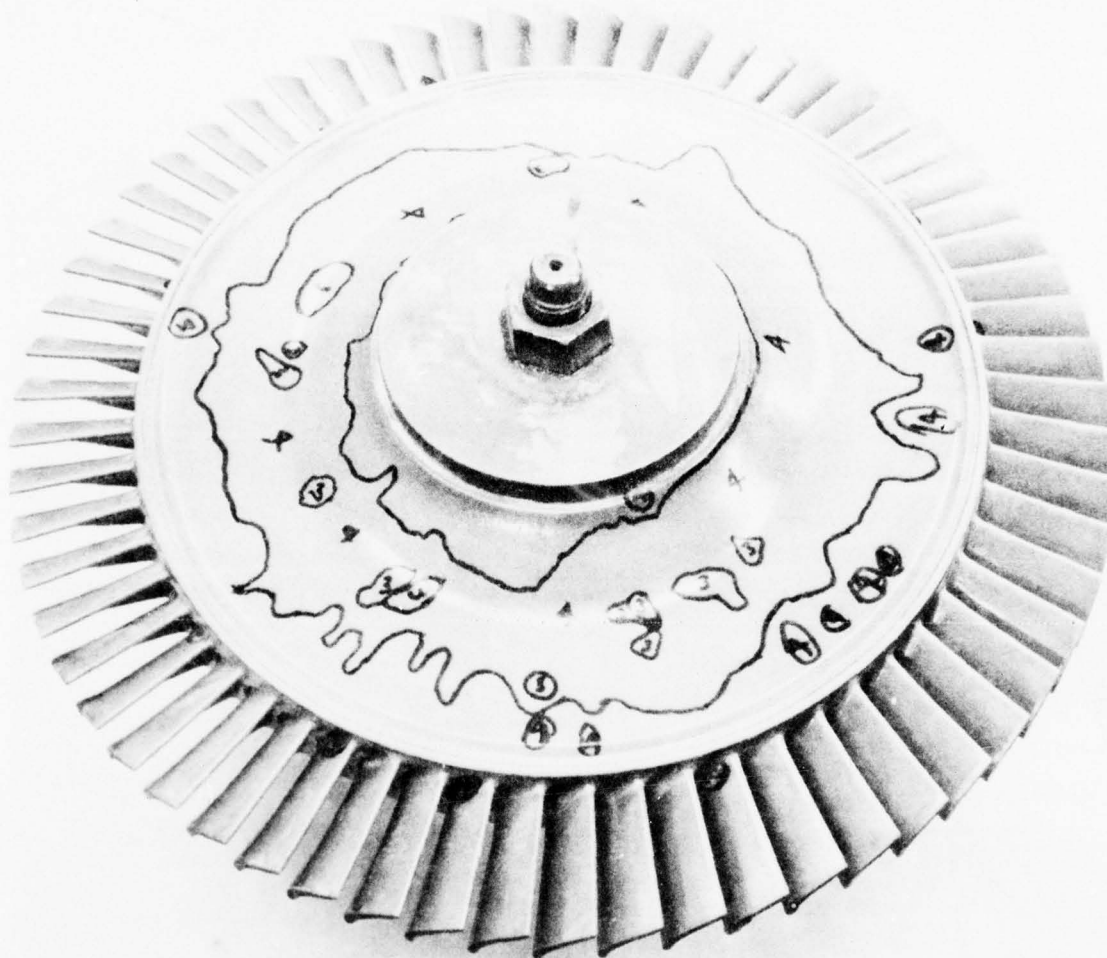After Stresscoat Testing.

Figure 91. Laminated Turbine Wheel Trailing-Edge Side
After Stresscoat Testing (Wheel Rotated
180°).
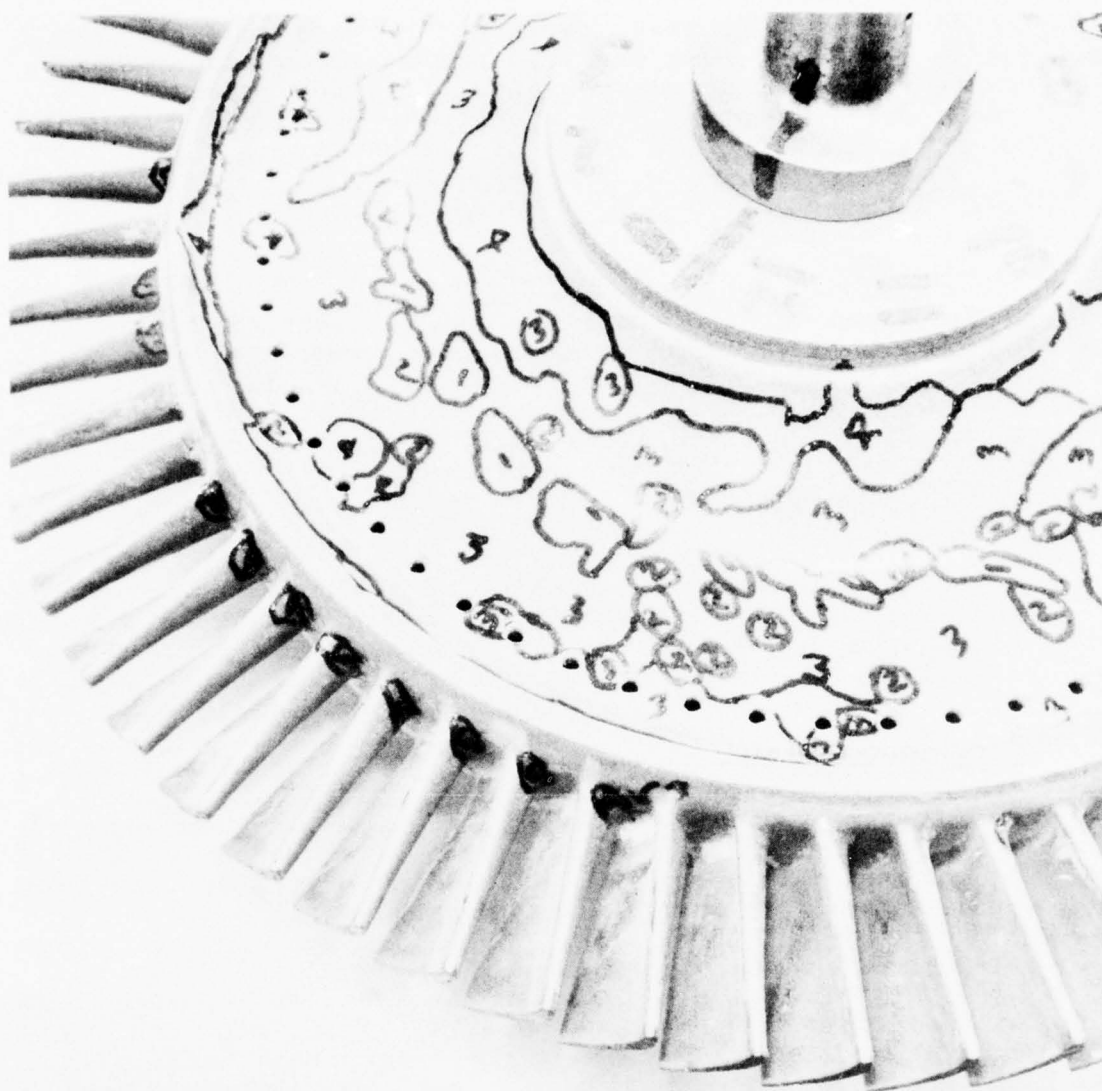
Figure 92.   Laminated Turbine Wheel Leading-Edge Side
             After Stresscoat Testing.   Close-up
             Showing Stressed Blade Root Areas.

d. Conclusions

There is good qualitative agreement between the Stresscoat test results and the stress analysis performed on the wheel. No unexpected areas of stress concentrations were discovered during testing. The second stress analysis performed is valid, and adequately describes the state of stress in the wheel.

3. GROWTH TEST

a. Introduction

The laminated turbine wheel was growth tested in order to determine the wheel response to exposure to overspeed conditions, and to verify the wheel integrity. In addition, it was desirable to learn as much as possible about the effect of laminate construction on ductility, and its ability to yield and redistribute loading in regions of stress concentration.

b. Results

The results of the growth testing is shown in Figures 93 and 94, where total growth has been plotted as a function of speed. As can be seen from the test results, a total maximum growth of only 0.001 inch occurred in the bore after the wheel was run at a speed of 34,100 rpm (approximately 115-percent design speed).

At the completion of the overspeed testing, a Zyglo inspection was conducted. Small voids, with accompanying microscopic cracks on the blade-tip lands appeared to have opened during overspeed testing. No delamination or joint cracks were noted, and the severity of the void and crack propagation was not excessive. The small cracks were generally perpendicular to the joints, and thus not associated with the bonded joint. It is believed that the cracks are a result of excessive loading of the thin tips due to residual bonding material in the tip area. The small voids are a result of some of the excess bond material in the tip orifices falling out as a result of the overspeed testing. Ultrasonic inspection was also conducted, and is shown in Figure 95. No unbonding occurred in the disk section as a result of the overspeed test.

c. Summary and Conclusions

The maximum growth occurred at the bore of the wheel and amounted to a total change of 0.042 percent of the bore diameter, which is somewhat less than that of another AiResearch integral turbine wheel in production for long-life commercial and military applications.
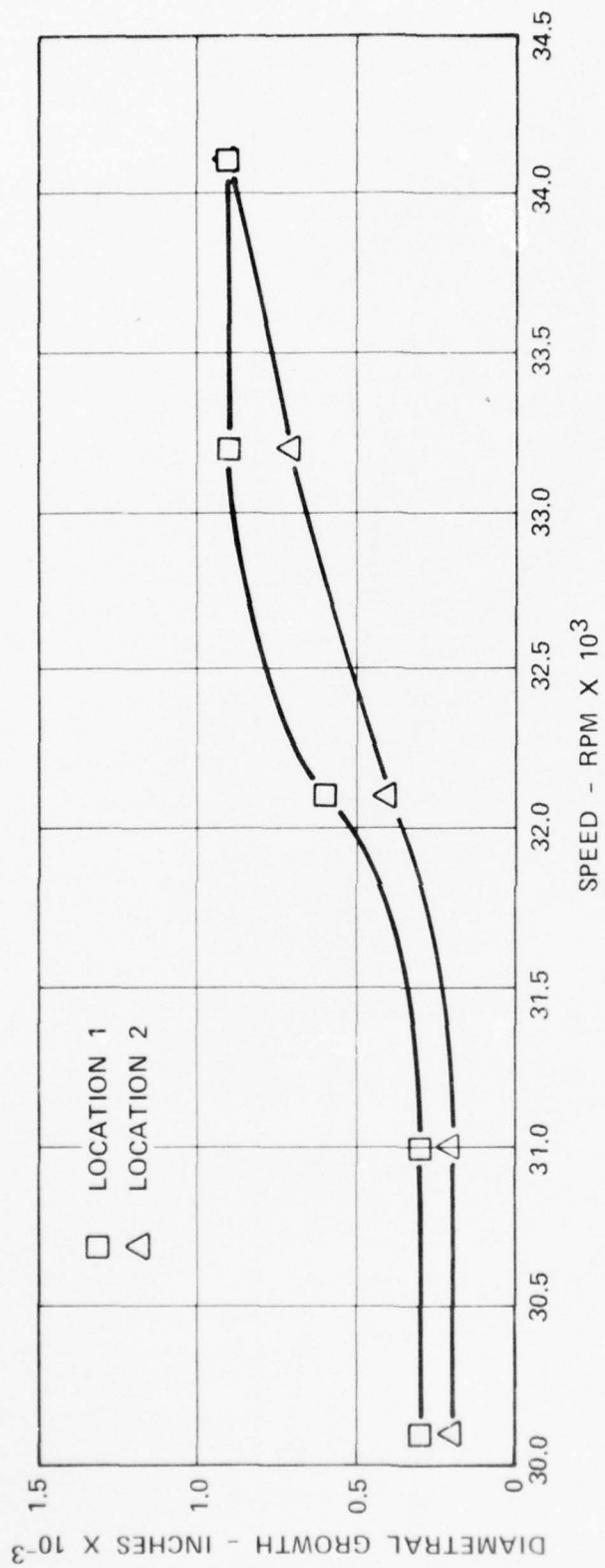
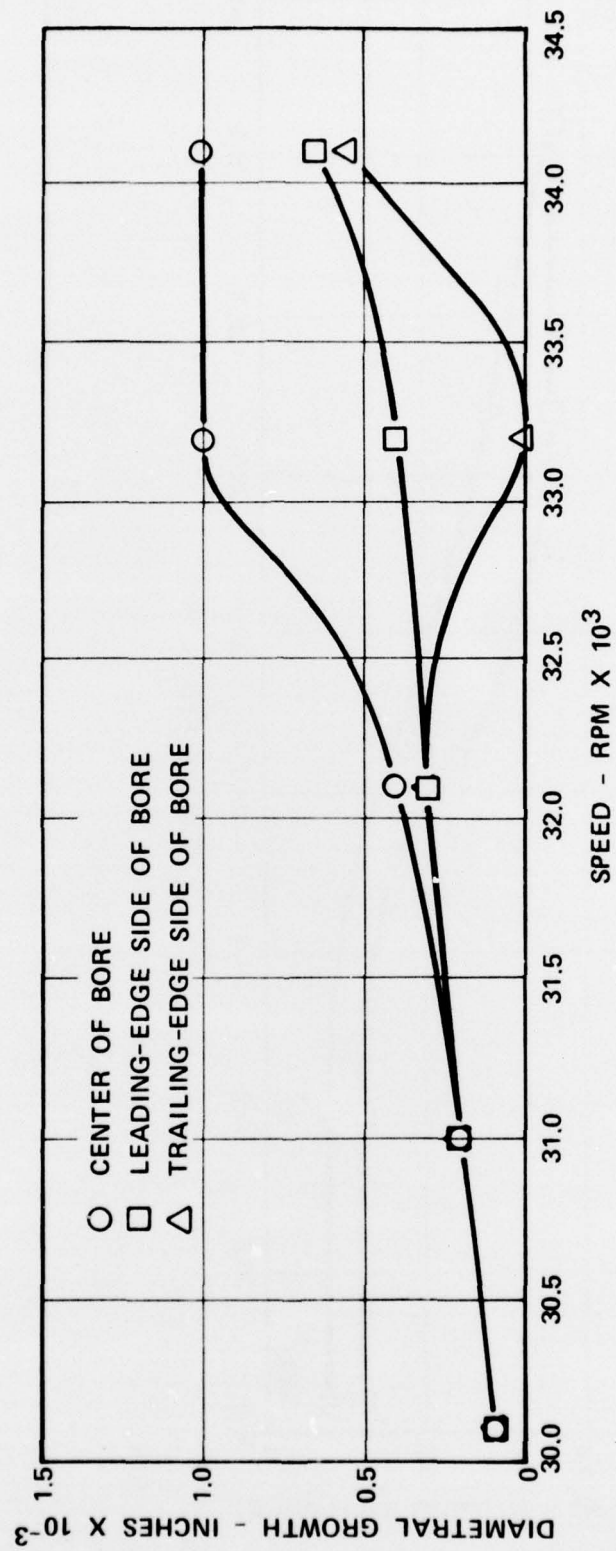Figure 93. Laminated Turbine Wheel Tip Growth.

Figure 94. Laminated Turbine Wheel Bore Growth.
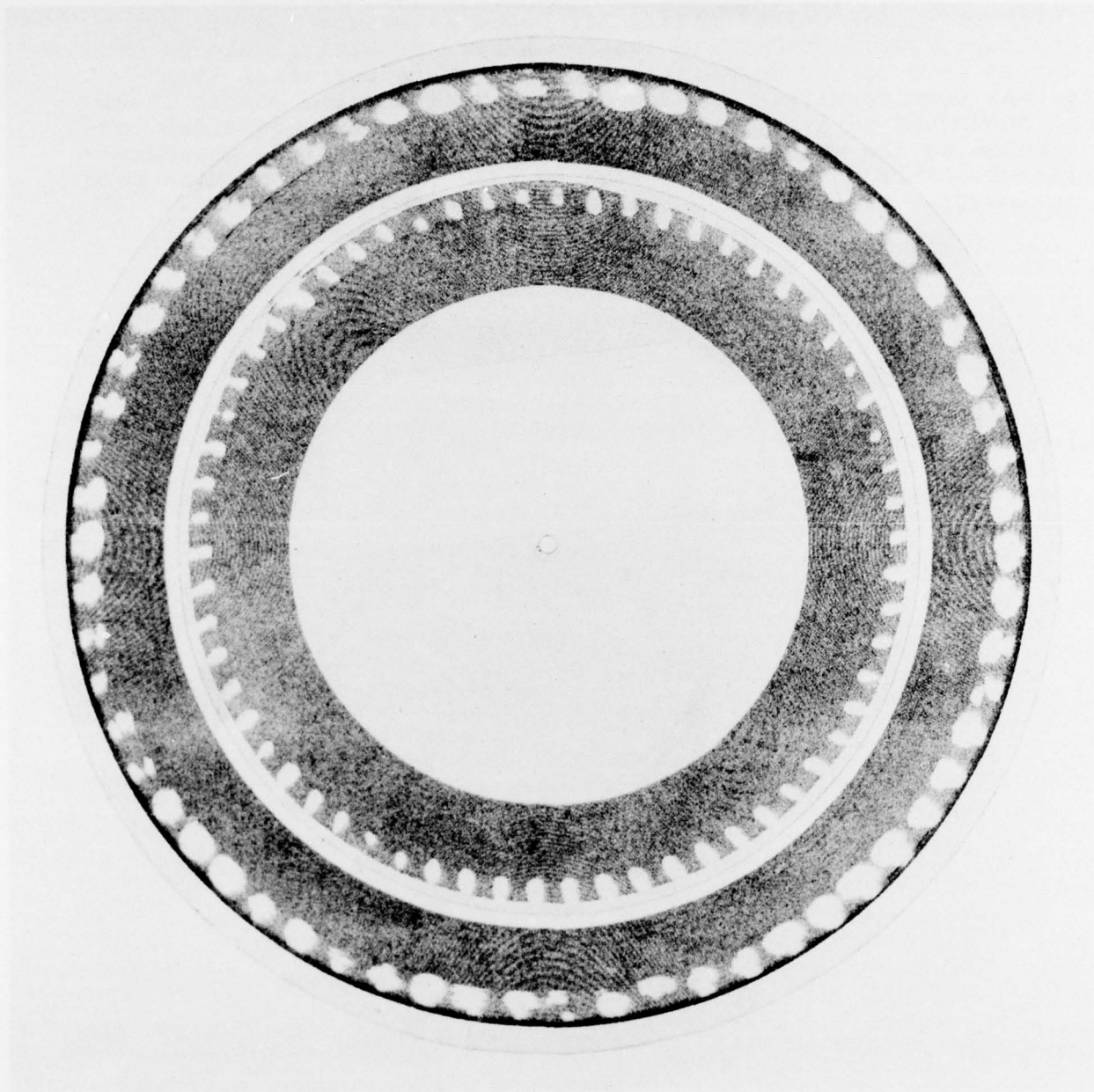
174

Figure 95.   Ultrasonic C-Scan of the Laminated
              Turbine Wheel after Spin-Pit Testing.

175

MP-56804

The program established the feasibility of designing and manufacturing an integral, cooled, laminated turbine wheel incorporating complex cooling passages. It was also proven that the turbine wheel possessed good integrity.

It is recommended that this concept be further developed incorporating more advanced bonding processes and materials developed under United States Air Force Materials Laboratory Contract F33615-75-C-5211. Heat-transfer testing should be conducted in order to correlate predicted characteristics with actual test results. Testing of laminated turbine wheels should be conducted in a high-temperature rig to further establish confidence in the wheel integrity, and to determine life characteristics. This should be followed by redesign of the turbine rotor and testing in a gas generator or turbine engine.